

IntechOpen

Cytotoxicity

Edited by Tülay Aşkin Çelik



CYTOTOXICITY

Edited by **Tülay Aşkin Çelik**

Cytotoxicity

<http://dx.doi.org/10.5772/intechopen.69919>

Edited by Tülay Aşkin Çelik

Contributors

Joanna Kurek, Johannes Wentzel, Angélique Lewies, Lissinda Du Plessis, Omid Gholami, Larissa Fonseca Andrade Vieira, Graciele Lurdes Silveira, Ildikó Bácskay, Dániel Nemes, Zoltán Ujhelyi, Ferenc Fenyvesi, Judit Váradi, Gábor Vasvári, Pálma Fehér, Miklós Vecsernyés, Yasumitsu Nishimura, Takemi Otsuki, Hidenori Matsuzaki, Suni Lee, Naoko Kumagai-Takei, Yu Min, Nagisa Sada, Megumi Maeda, Kei Yoshitome, Magdalena Jedrzejczak-Silicka, Ewa Mijowska, Tülay Askin Celik, Abdelmajid Zyad, Hassan Ait Mouse, Inass Leouifoudi, Mouna Khouchani, Anielle Silva, Fernanda Van Petten Vasconcelos Azevedo, Mariana Alves Pereira Zóia, Lucas Ian Veloso Correia, Aline Teodoro De Paula, Maria Paula Camargo Costa, Layssa Carrilho Giarretta, Renata Santos Rodrigues, Veridiana De Melo Ávila, Luiz Ricardo Goulart, Noelio Oliveira Dantas, Jurgen Kosel, Jose Perez, Nouf Alsharif, Aldo Martinez Banderas, Jasmineen Merzaban, Timothy Ravasi

© The Editor(s) and the Author(s) 2018

The rights of the editor(s) and the author(s) have been asserted in accordance with the Copyright, Designs and Patents Act 1988. All rights to the book as a whole are reserved by INTECHOPEN LIMITED. The book as a whole (compilation) cannot be reproduced, distributed or used for commercial or non-commercial purposes without INTECHOPEN LIMITED's written permission. Enquiries concerning the use of the book should be directed to INTECHOPEN LIMITED rights and permissions department (permissions@intechopen.com). Violations are liable to prosecution under the governing Copyright Law.



Individual chapters of this publication are distributed under the terms of the Creative Commons Attribution 3.0 Unported License which permits commercial use, distribution and reproduction of the individual chapters, provided the original author(s) and source publication are appropriately acknowledged. If so indicated, certain images may not be included under the Creative Commons license. In such cases users will need to obtain permission from the license holder to reproduce the material. More details and guidelines concerning content reuse and adaptation can be found at <http://www.intechopen.com/copyright-policy.html>.

Notice

Statements and opinions expressed in the chapters are those of the individual contributors and not necessarily those of the editors or publisher. No responsibility is accepted for the accuracy of information contained in the published chapters. The publisher assumes no responsibility for any damage or injury to persons or property arising out of the use of any materials, instructions, methods or ideas contained in the book.

First published in London, United Kingdom, 2018 by IntechOpen

eBook (PDF) Published by IntechOpen, 2019

IntechOpen is the global imprint of INTECHOPEN LIMITED, registered in England and Wales, registration number: 11086078, The Shard, 25th floor, 32 London Bridge Street
London, SE19SG – United Kingdom

Printed in Croatia

British Library Cataloguing-in-Publication Data

A catalogue record for this book is available from the British Library

Additional hard and PDF copies can be obtained from orders@intechopen.com

Cytotoxicity

Edited by Tülay Aşkin Çelik

p. cm.

Print ISBN 978-1-78923-430-5

Online ISBN 978-1-78923-431-2

eBook (PDF) ISBN 978-1-83881-443-4

We are IntechOpen, the world's leading publisher of Open Access books Built by scientists, for scientists

3,650+

Open access books available

114,000+

International authors and editors

118M+

Downloads

151

Countries delivered to

Our authors are among the
Top 1%

most cited scientists

12.2%

Contributors from top 500 universities



WEB OF SCIENCE™

Selection of our books indexed in the Book Citation Index
in Web of Science™ Core Collection (BKCI)

Interested in publishing with us?
Contact book.department@intechopen.com

Numbers displayed above are based on latest data collected.
For more information visit www.intechopen.com



Meet the editor



Tülay Aşkin Çelik is an associate professor with a Doctor of Biology degree from the Department of Faculty of Science and Art, Adnan Menderes University. She received her master degree in Biology from the University of Fırat, Elazığ, Turkey. She also completed her PhD degree in Biology from the University of Fırat in 1997. She is a member of the European Association for Cancer Research (EACR) and Molecular Cancer Research Association (MOKAD). Currently, her scientific interests are bioactive phytochemicals and plant extracts on their functional role in cancer cells and *in vitro/in vivo* biological activities. Furthermore, she is also investigating the genotoxic and cytotoxic effects of medicinal plant extracts and environmental pollutants and pesticides.

Contents

Preface XI

Section 1 Introductory Chapter 1

Chapter 1 **Introductory Chapter: Cytotoxicity 3**
Tülay Aşkin Çelik

Section 2 Cytotoxicity of Chemicals 7

Chapter 2 **Cytotoxicity Caused by Asbestos Fibers and Acquisition of Resistance by Continuous Exposure in Human T Cells 9**
Hidenori Matsuzaki, Suni Lee, Naoko Kumagai-Takei, Yu Min, Nagisa Sada, Kei Yoshitome, Yasumitsu Nishimura, Megumi Maeda and Takemi Otsuki

Chapter 3 **The Cytotoxic, Antimicrobial and Anticancer Properties of the Antimicrobial Peptide Nisin Z Alone and in Combination with Conventional Treatments 21**
Angélique Lewies, Lissinda H. Du Plessis and Johannes F. Wentzel

Section 3 Cytotoxic Effects of Natural Substance 43

Chapter 4 **Cytotoxic Colchicine Alkaloids: From Plants to Drugs 45**
Joanna Kurek

Chapter 5 **Natural Products as Cytotoxic Agents in Chemotherapy against Cancer 65**
Abdelmajid Zyad, Inass Leouifoudi, Mounir Tilaoui, Hassan Ait Mouse, Mouna Khouchani and Abdeslam Jaafari

Chapter 6 **Cytotoxicity and Apoptosis Induction by Coumarins in CLL 89**
Omid Gholami

- Section 4 Cytotoxic Endpoints 115**
- Chapter 7 **Cyto(Geno)Toxic Endpoints Assessed via Cell Cycle Bioassays in Plant Models 117**
Larissa Fonseca Andrade Vieira and Graciele Lurdes Silveira
- Chapter 8 **Role of Cytotoxicity Experiments in Pharmaceutical Development 131**
Ildikó Bácskay, Dániel Nemes, Ferenc Fenyvesi, Judit Váradi, Gábor Vasvári, Pálma Fehér, Miklós Vecsernyés and Zoltán Ujhelyi
- Section 5 Nanomaterials and Nanoparticles and Nanocrystals 147**
- Chapter 9 **Biocompatibility of Doped Semiconductors Nanocrystals and Nanocomposites 149**
Anielle Christine Almeida Silva, Mariana Alves Pereira Zóia, Lucas Ian Veloso Correia, Fernanda Van Petten Vasconcelos Azevedo, Aline Teodoro de Paula, Larissa Prado Maia, Layara Santana de Carvalho, Loyna Nobile Carvalho, Maria Paula Camargo Costa, Layssa Carrilho Giaretta, Renata Santos Rodrigues, Veridiana de Melo Ávila, Luiz Ricardo Goulart and Noelio Oliveira Dantas
- Chapter 10 **Toxicity of Titanate Nanosheets on Human Immune Cells 163**
Yasumitsu Nishimura, Daisuke Yoshioka, Naoko Kumagai-Takei, Suni Lee, Hidenori Matsuzaki, Kei Yoshitome and Takemi Otsuki
- Chapter 11 **General Cytotoxicity and Its Application in Nanomaterial Analysis 177**
Magdalena Jedrzejczak-Silicka and Ewa Mijowska
- Chapter 12 **Review of In vitro Toxicity of Nanoparticles and Nanorods: Part 1 209**
Jose Efrain Perez, Nouf Alsharif, Aldo Isaac Martínez Banderas, Basmah Othman, Jasmeen Merzaban, Timothy Ravasi and Jürgen Kosel
- Chapter 13 **Review of In Vitro Toxicity of Nanoparticles and Nanorods—Part 2 233**
Jose E. Perez, Nouf Alsharif, Aldo I. Martínez-Banderas, Basmah Othman, Jasmeen Merzaban, Timothy Ravasi and Jürgen Kosel

Preface

The book “Cytotoxicity” is a web-based resource, encompassing some of the natural cytotoxicity and different chemical substances, such as natural coumarins, colchicine alkaloids, titanate nanosheets, asbestos fiber, nanomaterials, nanocrystals and composites, and curcumin-loaded copolymer encapsulated ZnO nanocomposites. This e-resource comprises four different parts:

- Cytotoxicity of chemicals
- Cytotoxic effects of natural substance
- Cytotoxic endpoints
- Nanomaterials, nanoparticles, and nanocrystals

The first chapter, by Dr. Takemi Otsuki et al. from Japan, describes the different perspectives of “cytotoxicity caused by asbestos fiber and acquisition of resistance by continuous exposure in human T cell.” Considering the most important issue of asbestos-exposed population, such as malignancies, namely, mesothelioma and lung cancer after the long-term latent period, the mechanisms should be explored as well as be prevented. This issue is important for human health.

The second chapter “The Cytotoxic, Antimicrobial, and Anticancer Properties of Antimicrobial Nisin Z Alone and in Combination with Conventional Treatments,” by Dr. Johannes Wentzel et al. from North-West University, South Africa, highlights the cytotoxic, antimicrobial, and anticancer properties of antimicrobial nisin Z alone and in combination with conventional treatments, and they discussed the anticancer potential of nisin Z toward cultured melanoma cells, hence advocating safety and caution regarding their indiscriminate use by the population.

The third chapter “Cytotoxic Colchicine Alkaloids: From Plants to Drug,” by Dr. Joanna Kurek, Chemistry Department, Adam Mickiewicz University, Poznań, Poland, deals with the plants of Liliaceae family that contains colchicine; colchinoids; natural, semisynthetic, and synthetic colchicines; and C-10 sulfur-containing derivatives as a main alkaloid, which has cytotoxic activity and cytotoxic activity of colchicine and its derivatives. Furthermore, we have provided information on the pharmacological use of colchicine, drugs with colchicine derivatives, and docking studies.

The fourth chapter, by Abdelmajid Ziyad et al. from Morocco, discusses some examples of carvacrol, thymol, carveol, carvone, eugenol, isopulegol, and artemisinin as well as polyphenol extracts that have been studied in their laboratory. It is clear that if we understand the

molecular mechanisms of the various interactions between these cytotoxic molecules on the one hand and the tumor cells in their tumoral environments on the other hand, we can develop new therapeutic modalities to overcome the side effects of these molecules and to fight.

The fifth chapter, by Dr. Omid Gholami from Iran, summarizes “Natural Coumarins and Cytotoxicity, Apoptosis Induction and Mcl-1 Regulation in Chronic Lymphocytic Leukemia (CLL).” Coumarins are one of the important cytotoxic agents. They could induce apoptosis and regulate Mcl-1 expression in CLL cell lines. He says that in future, they hope that the coumarins can be used in the treatment of cancer and that detailed studies are needed in this regard.

The sixth chapter, by Dr. Larissa Fonseca Andrade Vieira and Dr. Graciele Lurdes Silveira from the Biology Department, Federal University of Lavras, Lavras, MG, Brazil, describes at cellular level the cytotoxicity, genotoxicity, and mutagenicity in the parameters determined by the cyto(genoto)xic endpoints as mitotic index, DNA fragmentation, induction of cell death, and malfunction of cellular structures leading to chromosome and cell cycle alterations. Each of these endpoints discussed presents details in this chapter.

The seventh chapter outlines a way of understanding “Role of Cytotoxicity Experiments in Pharmaceutical Development” by Dr. Ildikó Bácskay et al. from the Department of Pharmaceutical Technology, Faculty of Pharmacy, University of Debrecen, Hungary, and discusses in detail some of the cytotoxicity experiments that are a crucial part of a modern pharmaceutical development process in the chapter.

The recent increasing interest in the use of different nanoparticles in biological and medical applications encouraged scientists to analyze their potential impact on biological systems. *The application of different nanomaterials in biological environment is strongly limited due to the agglomeration problem.* The present overview describes and compares widely used biocompatibility/cytotoxicity assays in nanomaterial studies. Due to the type of nanoparticles and their properties, applicability of popular assays used for screening of engineered nanomaterials might be limited.

The eighth chapter “Biocompatibility of Doped Semiconductor Nanocrystals and Composites,” by Dr. Anielle Christine Almeida Silva et al. from Brazil, looks at doped semiconductor nanocrystals and composites of their potential toxicity and uses. This chapter summarizes the characterization of doped nanocrystals and composites; Ca-doped ZnO, Ag- and Eu-doped ZnO, and Ni-doped ZnO NCs; their biocompatibility; and applications and uncovers how these nanocrystals present desirable biocompatible properties, which can be useful as antitumoral and antimicrobial inducing agents, which differ markedly from toxic properties observed in other general nanocrystals.

The ninth chapter outlines a way of understanding “Toxicity of Titanate Nanosheets on Human Immune Cells,” which deals with the salient aspects of the influence of titanate nanosheets in promoting well-being and health for human. Dr. Yasumitsu Nishimura and colleagues from Japan discussed the critical TiNS₅ material, which has the harmful potential to cause caspase-dependent apoptosis of human immune cells to the same degree as asbestos.

The 10th chapter, by Dr. Magdalena Jedrzejczak-Silicka and Ewa Mijowska from the Laboratory of Cytogenetics, West Pomeranian University of Technology, Poland, describes the “General Toxicity and Its Application in the Nanomaterials Analysis.”

Finally, Dr. Jurgen Kosel et al. from Kingdom of Saudi Arabia summarize “Cytotoxicity of Nanoparticles: Part 1 and Part 2.” This chapter on toxicological effects of nanostructures focuses mostly on the cytotoxicity of nanoparticles and their internalization, activated signaling pathways, and cellular response.

The book *Cytotoxicity* is an essential reading to all medical students, biologists, biochemists, and professionals involved in the field of toxicology. This book is a useful and ideal guide for novice researchers interested in learning research methods to study cytotoxic bioactive compounds.

Assoc. Prof. Dr. Tülay Aşkin Çelik

Adnan Menderes University, Art and Science Faculty
Aydın, Turkey

Introductory Chapter

Introductory Chapter: Cytotoxicity

Tülay Aşkin Çelik

Additional information is available at the end of the chapter

<http://dx.doi.org/10.5772/intechopen.77244>

1. Introduction

Cell cytotoxicity refers to the ability of certain chemicals or mediator cells to destroy living cells. The cytotoxicity is a very important aspect, as destruction of healthy living cells around the wound will have a negative impact on the healing process. Cytotoxicity is the general quality of being toxic to cells, and can be caused by chemical stimuli, exposure to other cells (NK or T cells for example), or physical/environmental conditions (radiation exposure, temperature or pressure extremes, etc.) [1]. Chemical toxicity can occur in many ways, but we hypothesize that it can be broadly classified into two major categories: disruption of specific biomolecular targets or pathways (e.g., receptor agonist/antagonist effects and enzyme activation/inhibition), or generalized disruption of cellular machinery that can lead to cell stress and cytotoxicity [2]. Chemical toxicity can arise from disruption of specific biomolecular functions or through more generalized cell stress and cytotoxicity-mediated processes. Chemical toxicity can occur in disruption of specific biomolecular targets or pathways (e.g., receptor agonist/antagonist effects and enzyme activation/inhibition), or generalized disruption of cellular machinery that can lead to cell stress and cytotoxicity. Cell-disruptive processes include protein, DNA, or lipid reactivity; physicochemical disruption of proteins or membranes (e.g., by surfactants); or processes such as apoptosis, oxidative stress response, mitochondrial disruption, endoplasmic reticulum (ER) stress, microtubule disruption, or heat shock response [2]. Treating cells with a cytotoxic compound can result in a variety of cell fates. By using a cytotoxic compound, healthy living cells can either be induced to undergo necrosis (accidental cell death) or apoptosis (programmed cell death). Whereas apoptotic cell death is slower, more orderly, and is genetically controlled, the cells may undergo necrosis, in which they rapidly lose membrane integrity and die rapidly as a result of cell lysis. The cells can stop actively growing and dividing (a decrease in cell viability). Cytostasis is a special category of cytotoxicity, wherein cells remain alive but fail to grow and divide [1]. Cell death/cytotoxicity cannot be the sole causal driver of this phenomenon. Some cytotoxicity may be driven by physicochemical factors, such

as protein denaturation or reactivity, which would affect both the cell-free and cell-based assays. Another possibility is very low-affinity non-covalent binding to receptors, enzymes, etc. that only occurs at very high concentrations [2].

1.1. Cytotoxicity

Cytotoxicity is one of the most important methods for biological evaluation as it has a series of advantages, along with the preferred and mandatory items. Given this information, the ability to accurately measure cytotoxicity can prove to be a very valuable tool in identifying compounds that might pose certain health risks in humans [3]. The cytotoxicity test is one of the most important indicators of the biological evaluation system *in vitro* to observe the cell growth, reproduction and morphological effects by chemicals, and with the progress of modern cell biology; experimental methods to evaluate cytotoxicity are also continuously being developed and improved [3].

1.2. Cytotoxicity studies

Cytotoxicity studies are a useful initial step in determining the potential toxicity of a test substance, including plant extracts or biologically active compounds isolated from plants. Minimal to no toxicity is essential for the successful development of a pharmaceutical or cosmetic preparation and in this regard, cellular toxicity studies play a crucial role. The concept of basal cytotoxicity, where deleterious effects are noted on structures and functions common to all human cells, is relevant when considering the relationship between acute toxicity and cytotoxicity. The selectivity index is an important measure to identify substances with promising biological activity and negligible cytotoxicity. Various bioassays and a number of different cell lines have been used to assess cytotoxicity of chemicals. Regulations of cytotoxicity *in vitro*, countries have to make the relevant provisions of the corresponding cytotoxicity tests according to their actual situation [4]. With the continuous development of cytotoxicity tests, methods, such as detection of cell damage by morphological changes, determination of cell damage, measuring cell growth and metabolic properties, have appeared and have gradually been developed from qualitative evaluation to quantitative [5–8]. The ability to measure early indicators of toxicity is an essential part of drug discovery. *In vitro* cytotoxicity assays involving tissue specific cell cultures are considered as valuable predictors of human drug toxicity. However, there are no uniform cytotoxicity test methods and all these existing methods have particular problems. Measuring cell cytotoxicity also proves to be quite indispensable in the process of developing therapeutic anti-cancer drugs. By determining the cytotoxicity levels of cancer cells, anti-cancer medications can hinder the proliferation of target cells either by messing with their genetic material or by blocking the nutrients that the cells needs to survive. Additionally, understanding the mechanisms involved in cytotoxicity can likewise give researchers a more in-depth knowledge on the biological processes (both normal and abnormal) governing cell growth, cell proliferation, and death.

Identification of cytotoxic chemicals may be crucial in helping to explain target cells, and organ toxicity and species differences. Understanding the consequences of the induced natural

or chemical substances should be helpful in creating proper different models for extrapolation to low doses. In addition, biomarkers of exposure are gaining importance as tolls in the cytotoxicity research. The detection of the cytotoxic chemicals in humans may be useful in assessing human exposure or cellular injury. Also, understanding specific mechanisms may be useful in identifying the potential target tissues *in vivo* because cell types have different capacities to handle different types of chemicals.

Today, we need to understand the cytotoxicity that particular cells, organs, and organism are facing and identifying specific treatment interventions to address their unique needs both at macro- and micro-levels. The scope of this book goes precisely toward this direction. Each chapter offers the ways of intervention to address some of the most pressing cytotoxic chemicals of our time.

Cytotoxicity book is a web based resource, encompassing some of the cytotoxicity natural and different chemical substance, such as natural coumarins, colchicine alkaloids, tannin nanosheets, asbestos fiber, nanomaterials, nanocrystals, and composites, and curcumin loaded copolymer encapsulated ZnO nanocomposites.

“Cytotoxicity” is an essential reading to all medical students, biologist, biochemist, and professionals involved in the field of toxicology. The book is an useful and ideal guide for novice researchers interested in learning research methods to study cytotoxic bioactive compounds.

Author details

Tülay Aşkin Çelik

Address all correspondence to: tcelik@adu.edu.tr

Department of Biology, Art and Science Faculty, Adnan Menderes University, Central Campus, Aydın, Turkey

References

- [1] ACEA Biosciences Inc. 2015. Available from: <https://www.aceabio.com/applications/cytotoxicity/27.02.2018>
- [2] Judson R, Houck K, Martin M, Richard AM, Knudsen TB, Shah I, Little S, Wambaugh J, Setzer RW, Kothya P, Phuong J, Filer D, Smith D, Reif D, Rotroff D, Kleinstreuer N, Sioes N, Xia M, Huang R, Crofton K, Thomas RS. Analysis of the effects of cell stress and cytotoxicity on *in vitro* assay activity across a diverse chemical and assay space. *Toxicological Sciences*. 2016;**152**(2):323-339
- [3] Li W, Zhou J, Xu Y. Study of the *in vitro* cytotoxicity testing of medical devices (review). *Biomedical Reports*. 2015;**3**:617-620

- [4] Osthues RM, da Silva SN, Zavaglia CA, Fialho SL. Study of the release potential of the antibiotic gentamicin from microspheres of BCP. *Key Engineering Materials*. **493**:269-274
- [5] Piao MJ, Kang KA, Lee IK, Kim HS, Kim S, Choi JY, Choi J, Hyun JW. Silver nanoparticles induce oxidative cell damage in human liver cells through inhibition of reduced glutathione and induction of mitochondria-involved apoptosis. *Toxicology Letters*. 2011;**201**:92-100
- [6] Damas BA, Wheeler MA, Bringas JS, Hoen MM. Cytotoxicity comparison of mineral trioxide aggregates and EndoSequence bioceramic root repair materials. *Journal of Endodontia*. 2011;**37**:372-375
- [7] Kasper J, Hermanns MI, Bantz C, Maskos M, Stauber R, Pohl C, Unger RE, Kirkpatrick JC. Inflammatory and cytotoxic responses of an alveolar-capillary coculture model to silica nanoparticles: Comparison with conventional monocultures. *Particle and Fibre Toxicology*. **8**(1):6. DOI: 10.1186/1743-8977-8-6
- [8] Uboldi C, Giudetti G, Broggi F, Gilliland D, Ponti J, Rossi F. Amorphous silica nanoparticles do not induce cytotoxicity, cell transformation or genotoxicity in Balb/3T3 mouse fibroblasts. *Mutation Research*. **745**:11-20

Cytotoxicity of Chemicals

Cytotoxicity Caused by Asbestos Fibers and Acquisition of Resistance by Continuous Exposure in Human T Cells

Hidenori Matsuzaki, Suni Lee,
Naoko Kumagai-Takei, Yu Min, Nagisa Sada,
Kei Yoshitome, Yasumitsu Nishimura,
Megumi Maeda and Takemi Otsuki

Additional information is available at the end of the chapter

<http://dx.doi.org/10.5772/intechopen.72064>

Abstract

The cytotoxic effects of asbestos fibers on human T cells and the acquisition of resistance against asbestos-induced apoptosis have been studied. These analyses are based on the establishment of a continuous and relatively low-dose exposure model of human immune cells exposed to asbestos that resembles actual exposure in the human body. The MT-2 T cell line was selected as the candidate for the investigations. A transient and high-dose exposure to chrysotile resulted in apoptosis with production of reactive oxygen species (ROS) and activation of the mitochondrial apoptotic pathway. However, sublines continuously exposed to low dose of asbestos exhibited resistance to asbestos-induced apoptosis. The mechanism of resistance acquisition involved excess production of IL-10, activation of STAT3, and enhanced expression of Bcl-2 located downstream of STAT3. These changes were also found in a subline continuously exposed to crocidolite. Furthermore, sublines showed a marked decrease in the expression of forkhead box O1 (FoxO1) transcription factor. FoxO1 is known to regulate apoptosis and various other cellular processes. Regarding apoptosis, sublines continuously exposed to asbestos showed reduction of FoxP1-driven proapoptotic genes. This pathway is also considered one of the mechanisms that result in resistance to asbestos-induced apoptosis in sublines. These sublines also exhibited several characteristics suggesting reduction of antitumor immunity.

Keywords: cytotoxicity, asbestos, T cell, apoptosis, reactive oxygen species, FoxO1, antitumor immunity

1. Introduction

It is well known that asbestos fibers cause lung fibrosis as well as certain malignant diseases such as malignant mesothelioma, lung cancer, and other diseases (the International Agency for Research on Cancer (IARC) indicated that asbestos exposure results in a significant increased risk for ovarian and laryngeal cancers) [1–4]. A consideration of the carcinogenic mechanisms of asbestos suggests that various factors may be related. One factor involves DNA damage caused by reactive oxygen species (ROS) produced by asbestos fibers, especially iron-containing fibers such as crocidolite (CR) and amosite [5–7]. In addition to this aspect, ROS are also produced by alveolar macrophages which handle asbestos fibers as a foreign substance. However, they are not able to completely process the fibers because of the rigid and long morphological features of the fibers [8, 9]. Thus, these cells fail as a “frustrated macrophage” and begin to produce ROS [8, 9]. Another mechanism is the direct damage to DNA in cells located near the fibers since the cells possess a tendency to incorporate these foreign fibers into their interiors, but the fibers reach and damage cellular DNA directly because of the physiological features of the fibers [10, 11]. Furthermore, inhaled asbestos fibers may be found in the lung, related lymph nodes, and other pulmonary areas for a long time since they are not removed easily from the human body. Various carcinogenic substances existing in inspired air such as tobacco smoke and air pollutants are adsorbed onto the surface of the asbestos fibers. These additional substances also cause DNA damage to cells surrounding fibers [12, 13].

Cytotoxicity caused by asbestos fibers, particularly DNA damage caused by fibers, has been investigated in alveolar epithelial cells and pleural mesothelial cells since these cells are the targets of asbestos-induced cancers [14–17]. DNA damage was found when asbestos fibers were exposed to these cells using transient and relatively high doses, which cause apoptosis of cells. Subsequently, the accumulation of relatively small DNA damage that does not cause a quick cell death and/or escape from the apoptotic pathway by continuous or recurrent and relatively low-dose exposure which may exist in the bodies of asbestos-exposed populations is thought to represent the mechanism by which cancers occur in these populations.

2. Immunological effects of asbestos fibers regarding cytotoxicity

Asbestos is a mineral silicate [18]. Silica is known to affect the human immune system since silicosis patients who are chronically and recurrently exposed to silica particles by relatively low doses (inhaled as well as cells exposed to intrabody remnant silica particles) often exhibit disorders of autoimmunity [19–21]. Complications of various autoimmune diseases include rheumatoid arthritis (known as Caplan’s syndrome [22]), systemic sclerosis [23, 24], and antineutrophil cytoplasmic antibody (ANCA)-related vasculitis/nephritis [25, 26]. Our investigations indicate that silica particles disturb the balance of responder T cells (Tresp), which react with antigens including foreign nonself as well as self-antigens and regulatory T cells (Treg) that control the reaction of Tresp stimulated by antigens. Silica particles can reduce Treg through Fas-mediated apoptosis by enhancing Fas expression and long-term survival of Tresp by increasing inhibitors of Fas-mediated apoptosis such as soluble Fas and decoy receptor 3 molecules [27–29].

Asbestos fibers may, therefore, affect human immune cells. To investigate the effects of asbestos fibers on human immune cells, especially T cells, a human T-cell leukemia virus 1 (HTLV-1) immortalized human polyclonal T cell line, MT-2 [30], was selected for use in the establishment of a cell line model of asbestos exposure to immune cells. To choose an MT-2 cell line, various human T or B cell-derived tumorous or virus immortalized cell lines were transiently exposed to asbestos fibers, namely, chrysotile (CH) [31]. We selected chrysotile because of its wide use around the world, and the most exposed populations are thought to have resulted mainly through inhaled chrysotile fibers, although other iron-containing fibers such as crocidolite and amosite are known to possess a much higher potential for carcinogenic activity. Among the various cell lines, MT-2 was the most sensitive (growth inhibition was the strongest). The MT-2 cell line was then used to investigate the mechanisms of cell death in MT-2 cells exposed to asbestos fibers using transient and relatively high doses (doses causing cell death in at least half of the cells) [31, 32]. Thereafter, changes of cell death in MT-2 cells by a continuous and relatively low dose (doses causing cell death in less than half of cells) were investigated to explore cellular and molecular alterations in T cells by long-term exposure to asbestos. Exposure to asbestos in a human population is thought to involve a continuous, recurrent, and low-dose exposure, even for immune cells, because the existence of asbestos fibers in the lung and related lymph nodes can cause repeated encounters between immune cells and fibers [32].

3. Transient and high-dose exposure to asbestos fibers in MT-2 cells: Cytotoxicity

The left side of **Figure 1** shows findings concerning the transient and high-dose exposure to asbestos fibers in MT-2 cells. The cells proceed to apoptosis just as alveolar epithelial cells and pleural mesothelial cells were previously reported [14–17].

Asbestos exposure caused production of ROS. **Figure 1** shows the production of superoxide anion (O_2^-) as positive for hydroethidine analyzed by flow cytometry. Proapoptotic signaling molecules in the mitogen-activated protein kinase (MAPK) pathway such as JNK and p38 were then phosphorylated. Cytochrome c in mitochondria was then released into the cytoplasm. As a result, the proapoptotic molecule BAX was upregulated in the cells. These findings indicated that the mitochondrial apoptotic pathway was activated by asbestos exposure. Caspase 9 and 3 were then truncated into active forms to cause apoptosis of cells [31, 32].

In addition, cellular phenomena such as growth inhibition, appearance of apoptosis analyzed by annexin V staining (as an early event), activation of caspase 3, positivity of Tunel staining (a late event), and ROS production were compared between MT-2 cells exposed to fibers of chrysotile and crocidolite (CH and CR, respectively in **Figure 1**). Since CR contains a massive level of iron compared with CH, ROS production was higher in MT-2 cells exposed to CR. However, other events (the degree of growth inhibition, appearance of apoptosis assayed by different methods) were stronger in MT-2 cells exposed to CH compared to CR, although these were just comparisons between these two fibers and apoptosis was certainly caused by asbestos exposure on MT-2 cells [31–33].

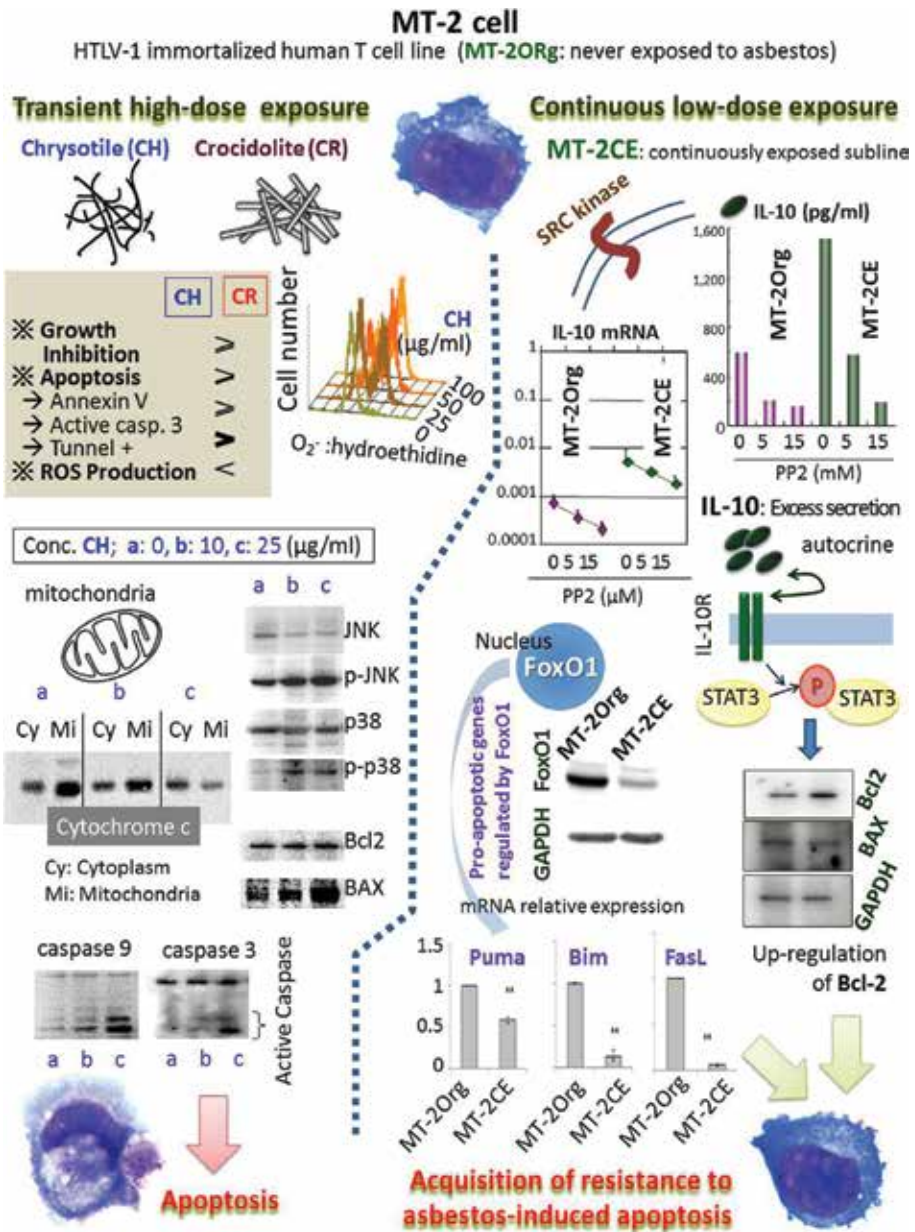


Figure 1. Schematic representation of the effects of the asbestos fibers chrysotile (CH) and crocidolite (CR) on MT-2 cells, a human T cell leukemia virus (HTLV)-1 immortalized human polyclonal T cell line [44–46]. Left side: Cellular and molecular alterations in MT-2 cells following transient and relatively high-dose exposure to CH or CR are summarized [32, 33]. Cells produced O₂⁻, proapoptotic signaling molecules such as JNK and p38 were phosphorylated, cytochrome c was released from mitochondria to the cytoplasm, and caspases 9 and 3 were truncated into active forms. Cells then proceeded to apoptosis. A comparison of the effects caused by CH or CR showed that reactive oxygen species (ROS) production was greater with CR exposure, whereas growth inhibition and the level of apoptosis were greater following CH exposure. Right side: The effects of continuous and relatively low-dose exposure are summarized. MT-2 CE (a continuously exposed subline) revealed excess IL-10 production via Src kinase and phosphorylation of STAT3 resulting in upregulation of Bcl-2 [34]. In addition, the transcription factor FoxO1 was reduced in MT-2 CE, causing a reduction of proapoptotic molecules such as puma, bim, and FasL [36]. Both exposures contributed to the development of resistance to asbestos-induced apoptosis in MT-2 CE cells [44–46].

Taken together, the cytotoxicity of asbestos fibers on human T cells was caused by a mechanism similar to that demonstrated for alveolar epithelial and pleural mesothelial cells.

4. Continuous low-dose exposure to asbestos fibers in MT-2 cells: Resistance to cytotoxicity

The initial aim of asbestos exposure on the MT-2 cell line was to establish a model of continuous, recurrent, and relatively low-dose exposure on human T cells and observe which kind of alterations occur under conditions of continuous and low-dose exposure as found with human populations exposed to asbestos, such as the occurrence of cancers.

Exposed doses for continuous exposure were then determined as doses which caused apoptosis in less than half of MT-2 cells. Doses included 5 or 10 $\mu\text{g/ml}$ in culture flasks, as shown on the left side of **Figure 1**. A dose of 10 $\mu\text{g/ml}$ of chrysotile caused various apoptotic cellular events, although the degrees of these events were less than those resulting from exposure to 25 $\mu\text{g/ml}$ of chrysotile [31, 34]. Since MT-2 cells were derived from T cells, they were grown by floating in the culture. Thus, the concentration of asbestos fibers was determined using $\mu\text{g/ml}$, although various adherent cells such as epithelial and mesothelial cells were measured using $\mu\text{g/cm}^2$ in the culture. The MT-2 cell culture was continued with a subculture twice a week and substitute asbestos fibers according to the determined concentrations. To monitor cellular alteration, the asbestos fibers were removed from continuous culture by density gradient centrifugation using LymphoPrep (gradient = 1.077) and continuously exposed cells were analyzed for the occurrence of apoptosis after transient exposure to high-dose asbestos fibers (which caused apoptosis in most of the MT-2 cells such as 25–50 $\mu\text{g/ml}$) [31, 32, 34]. After 8 months of continuous exposure, the appearance of apoptosis was reduced in the continuously exposed subline. This acquisition of resistance to asbestos-induced apoptosis was sustained in long-term cultures (until now, the sublines were cultured with asbestos fibers) [31, 34].

After 1 year of continuous exposure, the cellular features of the continuously exposed subline (MT-2 CE) were compared to those of the original MT-2 cells (MT-2Org, which were never exposed to asbestos fibers) as shown on the right side of **Figure 1**. A consideration of cytokine production showed that there was an excess production of interleukin (IL)-10 in MT-2 CE relative to MT-2Org. The regulation of IL-10 production was mediated by Src kinase, since PPT, the Src inhibitor, reduced IL-10 production in both MT-2Org and MT-2 CE cells. The excessively produced IL-10 was then utilized by the autocrine mechanism, since MT-2 possesses the IL-10 receptor (R) at its surface. As a result of IL-10 utilization, the signaling molecule, signal transducers, and the activator of transcription (STAT)-3, located downstream of IL-10R, were phosphorylated to a higher level in MT-2 CE compared to MT-2Org. Since the antiapoptotic molecule Bcl-2 is located downstream of STAT3, the expression of Bcl2 was upregulated in MT-2 CE compared to that in MT-2Org. The Bax/Bcl2 ratio was lower in MT-2 CE than in MT-2Org, as shown on the right side of **Figure 1**. In order to investigate the importance of Bcl-2 in MT-2 CE concerning acquisition of resistance to asbestos-induced apoptosis, siRNA for Bcl-2 was introduced into MT-2 CE cells and the occurrence of apoptosis and growth inhibition following transient and high-dose exposure to asbestos fibers were examined. As

suspected, Bcl-2 silenced cells exhibited much higher apoptosis and growth inhibition. Thus, the Src → IL-10 → STAT3 → Bcl-2 axis was considered important for the acquisition of resistance to asbestos-induced apoptosis in MT-2 CE [31, 34]. Additionally, CD4-positive peripheral blood cells from asbestos-exposed patients exhibiting pleural plaque (PP) or malignant mesothelioma (MM) showed enhanced expression of Bcl-2 compared with that of healthy volunteers (HV). Thus, the MT-2 CE model may express events occurring within T cells of asbestos-exposed patients [31, 34].

Sublines continuously exposed to asbestos were established independently and comprised six sublines exposed to CH and three sublines exposed to CR. The profiles of cytokine production in these MT-2 CEs (exposed to CH or CR) were similar [31, 33, 35]. Continuous exposure caused excess production of IL-10 (as mentioned earlier) and transforming growth factor (TGF)- β , whereas interferon (IFN)- γ production was reduced in MT-2 CEs compared to that in MT-2Org. In addition, Bcl-2 upregulation was found in all MT-2 CEs and there were no differences between exposure to CH and CR [31, 33, 35]. In fact, a cDNA microarray assay using MT-2 CEs and MT-2org indicated that most of the upregulated and downregulated genes were similar in MT-2 CEs. Therefore, these MT-2 CEs could be used as a continuously asbestos-exposed immune T cell model.

The cDNA microarray assay revealed that the transcription factor forkhead box O1 (FoxO1) was expressed to a lesser degree in MT-2 CE compared to MT-2Org [36]. FoxO1 is known to regulate various genes in apoptosis, metabolism, cell growth and differentiation, and so on. In particular, FoxO1 controls various proapoptotic genes such as the p53 upregulated modulator of apoptosis (Puma), bcl-2 interacting mediator of cell death (Bim), and the Fas ligand (FasL) [36, 37]. The message expression of these proapoptotic molecules was reduced in MT-2 CE compared with that in MT-2Org (shown on the right side of **Figure 1**). In addition, following knockdown of the FoxO1 gene in MT-2Org, the level of apoptotic cells caused by transient and high-dose exposure to asbestos was reduced. Furthermore, when the expression of FoxO1 was forced in MT-2 CE, the ratio of apoptosis increased following transient and high-dose exposure to asbestos and the expression of Puma was recovered [36].

These results indicated that acquisition of resistance to asbestos-induced apoptosis by continuous and low-dose exposure to asbestos was regulated by the FoxO1 transcription factor in addition to the Src → IL-10 → STAT3 → Bcl-2 axis [31–36].

5. Findings in MT-2CEs regarding antitumor immunity

The purpose of establishing a cell line model involving continuous and relatively low-dose exposure of human T cells to asbestos fibers was to investigate cellular and molecular alterations that may reflect the immune function in human populations exposed to asbestos as well as patients exhibiting PP or MM.

A consideration of the development of cancer in asbestos-exposed patients suggested that focus within investigations should be placed on antitumor immunity.

Our investigations showed that the CXC chemokine receptor 3 (CXCR3) exhibited reduced expression in MT-2 CEs compared to MT-2Org [38, 39]. CXCR3 is known to play an important role in antitumor immunity because it summons antitumor T cells with IFN- γ . As shown in the cell line model, investigation of freshly isolated CD4-positive T cells revealed decreased expression of CXCR3 when activated *in vitro* with CH fibers. Furthermore, peripheral blood CD4-positive cells from patients with PP or MM showed a reduction of CXCR3 and an inhibited potential for IFN- γ production when stimulated *in vitro* [31, 38, 39]. These investigations indicated that the cell line model for continuous and low-dose exposure to asbestos using the MT-2 cell line was suitable for analysis of immune alteration in asbestos-exposed human populations and patients with PP or MM [31, 38, 39].

As the MT-2 cell line was known to possess a Treg function [40, 41], the Treg function was estimated in MT-2Org and MT-2 CE. In regard to cell-cell contact, MT-2 CE enhanced its suppressive function onto Tresp cells [42]. In addition, MT-2 CE produced higher TGF- β and IL-10 in comparison to MT-2Org as described earlier. These two cytokines are the typical soluble factors for Treg in order to manifest its function. Following the knockdown of each cytokine in MT-2 CE, the suppressive function was reduced relative to that in MT-2 CE [42]. These results indicated that asbestos exposure enhanced Treg function by cell-cell contact and an increase of soluble factors [42]. In addition, FoxO1 reduced its expression in MT-2 CE as described earlier, and is known to regulate the cell cycle to suppress the accelerating genes, such as cyclins, as well as to enhance the breaking genes, such as cyclin-dependent kinase inhibitors (CDK-Is) [43]. As a consequence, cyclins were enhanced and the expression of CDK-I2 was reduced in MT-2 CE because of the reduced expression of FoxO1. Cell cycle progression was, therefore, enhanced in MT-2 CE [43]. These overall results suggest that Treg volume may also be enhanced in asbestos-exposed human populations and patients exhibiting PP or MM [42, 43]. These findings indicated that asbestos exposure causes reduction of antitumor immunity.

6. Conclusion

Investigation of cytotoxicity in human T cells caused by asbestos exposure indicated that the production of ROS and activation of the mitochondrial apoptotic pathway were the main causes for apoptosis of T cells following a transient and relatively high-dose exposure [32], similar to known mechanisms investigated previously using alveolar epithelial and pleural mesothelial cells [5–9, 44–46]. However, the continuous and relatively low-dose exposure of T cells to asbestos altered cellular and molecular events that caused acquisition of resistance against asbestos-induced cytotoxicity. Investigations revealed the importance of the Src \rightarrow IL-10 \rightarrow STAT3 \rightarrow Bcl-2 axis as well as the reduced expression of FoxO1 [31, 33–35]. These changes induce the reduction of antitumor immunity in an asbestos-exposed population and create an increased risk of carcinogenicity due to the transforming activity associated with asbestos fibers [44–46].

Considering the most important issue in asbestos-exposed population, the occurrence of malignancies such as mesothelioma and lung cancer after long-term latent period should be explored the mechanisms as well as be prevented [1–4]. Thus, regarding the cytotoxic effects

of asbestos fibers onto human T cell, the acquisition of reduced antitumor immunity caused by continuous exposure to fibers should be focused, since it may be possible to dissolve or recover this situation. As a result, some preventive ways for asbestos-induced cancers in exposed population will be identified.

Recovery of cellular and molecular changes in asbestos-exposed T cells using certain food constituents or physiologically active substances, including plants or other materials, may support the maintenance of antitumor activity in an asbestos-exposed population and might help to reduce the chances of carcinogenesis caused by asbestos fibers.

Acknowledgements

The authors thank Ms. Tamayo Hatayama, Shoko Yamamoto, and Miho Ikedas for their technical assistance.

Author details

Hidenori Matsuzaki¹, Suni Lee¹, Naoko Kumagai-Takei¹, Yu Min^{1,2,3}, Nagisa Sada^{1,4}, Kei Yoshitome¹, Yasumitsu Nishimura¹, Megumi Maeda⁵ and Takemi Otsuki^{1*}

*Address all correspondence to: takemi@med.kawasaki-m.ac.jp

1 Department of Hygiene, Kawasaki Medical School, Kurashiki, Okayama, Japan

2 Department of Occupational and Environmental Health Science, School of Public Health, Peking University, Beijing, People's Republic of China

3 Department of Occupational Diseases, Zhejiang Academy of Medical Sciences, Zhejiang, People's Republic of China

4 Department of Biophysical Chemistry, Graduate School of Medicine, Dentistry and Pharmaceutical Sciences, Okayama University, Okayama, Japan

5 Department of Biofunctional Chemistry, Division of Bioscience, Okayama University Graduate School of Natural Science and Technology, Okayama, Japan

References

- [1] Myers R. Asbestos-related pleural disease. *Current Opinion in Pulmonary Medicine*. 2012;**18**:377-381. DOI: 10.1097/MCP.0b013e328354acfe
- [2] Lazarus A, Massoumi A, Hostler J, Hostler DC. Asbestos-related pleuropulmonary diseases: Benign and malignant. *Postgraduate Medicine*. 2012;**124**:116-130. DOI: 10.3810/pgm.2012.05.2555

- [3] Markowitz S. Asbestos-related lung cancer and malignant mesothelioma of the pleura: Selected current issues. *Seminars in Respiratory and Critical Care Medicine*. 2015;**36**:334-346. DOI: 10.1055/s-0035-1549449
- [4] IARC Monographs 100c, Asbestos (Chrysotile, Amosite, Crocidolite, Tremolite, Actinolite and Anthophyllite). <http://monographs.iarc.fr/ENG/Monographs/vol100C/mono100C-11.pdf>
- [5] Kamp DW, Graceffa P, Pryor WA, Weitzman SA. The role of free radicals in asbestos-induced diseases. *Free Radical Biology & Medicine*. 1992;**12**:293-315
- [6] Shukla A, Gulumian M, Hei TK, Kamp D, Rahman Q, Mossman BT. Multiple roles of oxidants in the pathogenesis of asbestos-induced diseases. *Free Radical Biology & Medicine*. 2003;**34**:1117-1129
- [7] Upadhyay D, Kamp DW. Asbestos-induced pulmonary toxicity: Role of DNA damage and apoptosis. *Experimental Biology and Medicine (Maywood, N.J.)*. 2003;**228**:650-659
- [8] Simeonova PP, Luster MI. Iron and reactive oxygen species in the asbestos-induced tumor necrosis factor-alpha response from alveolar macrophages. *American Journal of Respiratory Cell and Molecular Biology*. 1995;**12**:676-683
- [9] Murthy S, Adamcakova-Dodd A, Perry SS, Tephly LA, Keller RM, Metwali N, Meyerholz DK, Wang Y, Glogauer M, Thorne PS, Carter AB. Modulation of reactive oxygen species by Rac1 or catalase prevents asbestos-induced pulmonary fibrosis. *American Journal of Physiology. Lung Cellular and Molecular Physiology*. 2009;**297**:L846-L855. DOI: 10.1152/ajplung.90590.2008
- [10] Nagai H, Toyokuni S. Biopersistent fiber-induced inflammation and carcinogenesis: Lessons learned from asbestos toward safety of fibrous nanomaterials. *Archives of Biochemistry and Biophysics*. 2010;**502**:1-7. DOI: 10.1016/j.abb.2010.06.015
- [11] Nagai H, Ishihara T, Lee WH, Ohara H, Okazaki Y, Okawa K, Toyokuni S. Asbestos surface provides a niche for oxidative modification. *Cancer Science*. 2011;**102**:2118-2125. DOI: 10.1111/j.1349-7006.2011.02087.x
- [12] Toyokuni S. Role of iron in carcinogenesis: Cancer as a ferrototoxic disease. *Cancer Science*. 2009;**100**:9-16. DOI: 10.1111/j.1349-7006.2008.01001.x
- [13] Chew SH, Toyokuni S. Malignant mesothelioma as an oxidative stress-induced cancer: An update. *Free Radical Biology & Medicine*. 2015;**86**:166-178. DOI: 10.1016/j.freeradbiomed.2015.05.002
- [14] Aljandali A, Pollack H, Yeldandi A, Li Y, Weitzman SA, Kamp DW. Asbestos causes apoptosis in alveolar epithelial cells: Role of iron-induced free radicals. *The Journal of Laboratory and Clinical Medicine*. 2001;**137**:330-339
- [15] Panduri V, Weitzman SA, Chandel NS, Kamp DW. Mitochondrial-derived free radicals mediate asbestos-induced alveolar epithelial cell apoptosis. *American Journal of Physiology. Lung Cellular and Molecular Physiology*. 2004;**286**:L1220-L1227

- [16] Broaddus VC, Yang L, Scavo LM, Ernst JD, Boylan AM. Asbestos induces apoptosis of human and rabbit pleural mesothelial cells via reactive oxygen species. *The Journal of Clinical Investigation*. 1996;**98**:2050-2059
- [17] Broaddus VC, Yang L, Scavo LM, Ernst JD, Boylan AM. Crocidolite asbestos induces apoptosis of pleural mesothelial cells: Role of reactive oxygen species and poly(ADP-ribose) polymerase. *Environmental Health Perspectives*. 1997;**105**(Suppl 5):1147-1152
- [18] Kohyama N, Shinohara Y, Suzuki Y. Mineral phases and some reexamined characteristics of the International Union against Cancer standard asbestos samples. *American Journal of Industrial Medicine*. 1996;**30**:515-528
- [19] Pollard KM. Silica, silicosis, and autoimmunity. *Frontiers in Immunology*. 2016;**7**:97. DOI: 10.3389/fimmu.2016.00097
- [20] Steenland K, Goldsmith DF. Silica exposure and autoimmune diseases. *American Journal of Industrial Medicine*. 1995;**28**:603-608
- [21] Parks CG, Conrad K, Cooper GS. Occupational exposure to crystalline silica and autoimmune disease. *Environmental Health Perspectives*. 1999;**107**(Suppl 5):793-802
- [22] Caplan A. Certain unusual radiological appearances in the chest of coal-miners suffering from rheumatoid arthritis. *Thorax*. 1953;**8**:29-37
- [23] Rodnan GP, Benedek TG, Medsger TA Jr, Cammarata RJ. The association of progressive systemic sclerosis (scleroderma) with coal miners' pneumoconiosis and other forms of silicosis. *Annals of Internal Medicine*. 1967;**66**:323-334
- [24] Sluis-Cremer GK, Hessel PA, Nizdo EH, Churchill AR, Zeiss EA. Silica, silicosis, and progressive systemic sclerosis. *British Journal of Industrial Medicine*. 1985;**42**:838-843
- [25] Neyer U, Wöss E, Neuweiler J. Wegener's granulomatosis associated with silicosis. *Nephrology, Dialysis, Transplantation*. 1994;**9**:559-561
- [26] Mulloy KB. Silica exposure and systemic vasculitis. *Environmental Health Perspectives*. 2003;**111**:1933-1938
- [27] Otsuki T, Miura Y, Nishimura Y, Hyodoh F, Takata A, Kusaka M, Katsuyama H, Tomita M, Ueki A, Kishimoto T. Alterations of Fas and Fas-related molecules in patients with silicosis. *Experimental Biology and Medicine (Maywood, N.J.)*. 2006;**231**:522-533
- [28] Lee S, Hayashi H, Maeda M, Chen Y, Matsuzaki H, Takei-Kumagai N, Nishimura Y, Fujimoto W, Otsuki T. Environmental factors producing autoimmune dysregulation - chronic activation of T cells caused by silica exposure. *Immunobiology*. 2012;**217**:743-748. DOI: 10.1016/j.imbio.2011.12.009
- [29] Lee S, Hayashi H, Mastuzaki H, Kumagai-Takei N, Otsuki T. Silicosis and autoimmunity. *Current Opinion in Allergy and Clinical Immunology*. 2017;**17**:78-84. DOI: 10.1097/ACI.0000000000000350

- [30] Miyoshi I, Kubonishi I, Yoshimoto S, Shiraishi YA. T-Cell line derived from normal human cord leukocytes by co-culturing with human leukemic T-cells. *Gan*. 1981;**72**:978-981
- [31] Maeda M, Yamamoto S, Hatayama T, Mastuzaki H, Lee S, Kumagai-Takei N, Yoshitome K, Nishimura Y, Kimura Y, Otsuki T. T cell alteration caused by exposure to asbestos. In: Otsuki T, Holian A, Yoshioka Y, editors. *Biological Effects of Fibrous and Particulate Substances*. Japan, Tokyo: Springer; 2015. pp. 195-210
- [32] Hyodoh F, Takata-Tomokuni A, Miura Y, Sakaguchi H, Hatayama T, Hatada S, Katsuyama H, Matsuo Y, Otsuki T. Inhibitory effects of anti-oxidants on apoptosis of a human polyclonal T-cell line, MT-2, induced by an asbestos, chrysotile-a. *Scandinavian Journal of Immunology*. 2005;**61**:442-448
- [33] Maeda M, Yamamoto S, Chen Y, Kumagai-Takei N, Hayashi H, Matsuzaki H, Lee S, Hatayama T, Miyahara N, Katoh M, Hiratsuka J, Nishimura Y, Otsuki T. Resistance to asbestos-induced apoptosis with continuous exposure to crocidolite on a human T cell. *Science Total Environment*. 2012;**429**:174-182. DOI: 10.1016/j.scitotenv.2012.04.043
- [34] Miura Y, Nishimura Y, Katsuyama H, Maeda M, Hayashi H, Dong M, Hyodoh F, Tomita M, Matsuo Y, Uesaka A, Kuribayashi K, Nakano T, Kishimoto T, Otsuki T. Involvement of IL-10 and Bcl-2 in resistance against an asbestos-induced apoptosis of T cells. *Apoptosis*. 2006;**11**:1825-1835
- [35] Maeda M, Chen Y, Hayashi H, Kumagai-Takei N, Matsuzaki H, Lee S, Nishimura Y, Otsuki T. Chronic exposure to asbestos enhances TGF- β 1 production in the human adult T cell leukemia virus-immortalized T cell line MT-2. *International Journal of Oncology*. 2014;**45**:2522-2532. DOI: 10.3892/ijo.2014.2682
- [36] Matsuzaki H, Lee S, Maeda M, Kumagai-Takei N, Nishimura Y, Otsuki T. FoxO1 regulates apoptosis induced by asbestos in the MT-2 human T-cell line. *Journal of Immunotoxicology*. 2016;**13**:620-627. DOI: 10.3109/1547691X.2016.1143539
- [37] Zhang X, Tang N, Hadden TJ, Rishi AK. Akt, FoxO and regulation of apoptosis. *Biochimica et Biophysica Acta*. 2011;**1813**:1978-1986. DOI: 10.1016/j.bbamcr.2011.03.010
- [38] Maeda M, Nishimura Y, Hayashi H, Kumagai N, Chen Y, Murakami S, Miura Y, Hiratsuka J, Kishimoto T, Otsuki T. Reduction of CXC chemokine receptor 3 in an in vitro model of continuous exposure to asbestos in a human T-cell line, MT-2. *American Journal of Respiratory Cell and Molecular Biology*. 2011;**45**:470-479. DOI: 10.1165/rcmb.2010-0213OC
- [39] Maeda M, Nishimura Y, Hayashi H, Kumagai N, Chen Y, Murakami S, Miura Y, Hiratsuka J, Kishimoto T, Otsuki T. Decreased CXCR3 expression in CD4+ T cells exposed to asbestos or derived from asbestos-exposed patients. *American Journal of Respiratory Cell and Molecular Biology*. 2011;**45**:795-803. DOI: 10.1165/rcmb.2010-0435OC
- [40] Chen S, Ishii N, Ine S, Ikeda S, Fujimura T, Ndhlovu LC, Soroosh P, Tada K, Harigae H, Kameoka J, Kasai N, Sasaki T, Sugamura K. Regulatory T cell-like activity of Foxp3+ adult T cell leukemia cells. *International Immunology*. 2006;**18**:269-277

- [41] Hamano R, Wu X, Wang Y, Oppenheim JJ, Chen X. Characterization of MT-2 cells as a human regulatory T cell-like cell line. *Cellular & Molecular Immunology*. 2015;**12**:780-782. DOI: 10.1038/cmi.2014.123
- [42] Ying C, Maeda M, Nishimura Y, Kumagai-Takei N, Hayashi H, Matsuzaki H, Lee S, Yoshitome K, Yamamoto S, Hatayama T, Otsuki T. Enhancement of regulatory T cell-like suppressive function in MT-2 by long-term and low-dose exposure to asbestos. *Toxicology*. 2015;**338**:86-94. DOI: 10.1016/j.tox.2015.10.005
- [43] Lee S, Matsuzaki H, Maeda M, Yamamoto S, Kumagai-Takei N, Hatayama T, Ikeda M, Yoshitome K, Nishimura Y, Otsuki T. Accelerated cell cycle progression of human regulatory T cell-like cell line caused by continuous exposure to asbestos fibers. *International Journal of Oncology*. 2017;**50**:66-74. DOI: 10.3892/ijo.2016.3776
- [44] Otsuki T, Matsuzaki H, Lee S, Kumagai-Takei N, Yamamoto S, Hatayama T, Yoshitome K, Nishimura Y. Environmental factors and human health: Fibrous and particulate substance-induced immunological disorders and construction of a health-promoting living environment. *Environmental Health and Preventive Medicine*. 2016;**21**:71-81. DOI: 10.1007/s12199-015-0499-6
- [45] Matsuzaki H, Maeda M, Lee S, Nishimura Y, Kumagai-Takei N, Hayashi H, Yamamoto S, Hatayama T, Kojima Y, Tabata R, Kishimoto T, Hiratsuka J, Otsuki T. Asbestos-induced cellular and molecular alteration of immunocompetent cells and their relationship with chronic inflammation and carcinogenesis. *Journal of Biomedicine & Biotechnology*. 2012;**2012**:492608. DOI: 10.1155/2012/492608
- [46] Kumagai-Takei N, Maeda M, Chen Y, Matsuzaki H, Lee S, Nishimura Y, Hiratsuka J, Otsuki T. Asbestos induces reduction of tumor immunity. *Clinical & Developmental Immunology*. 2011;**2011**:481439. DOI: 10.1155/2011/481439

The Cytotoxic, Antimicrobial and Anticancer Properties of the Antimicrobial Peptide Nisin Z Alone and in Combination with Conventional Treatments

Angélique Lewies, Lissinda H. Du Plessis and Johannes F. Wentzel

Additional information is available at the end of the chapter

<http://dx.doi.org/10.5772/intechopen.71927>

Abstract

Nisin is an antimicrobial peptide commonly used as a food preservative since 1969. This peptide has potent antimicrobial activity against several Gram-positive bacterial strains, including clinically important and resistant pathogens. The combination of nisin with conventional antibiotics has been shown to improve the antimicrobial activity of these antibiotic agents. Apart from the antimicrobial properties of nisin, this AMP also displays promising anticancer potential towards several types of malignancies. The nisin Z variant is able to induce selective cytotoxicity in melanoma cells compared to non-malignant cells. It was shown that nisin Z disrupts the cell membrane integrity of melanoma cells and that cytotoxicity is likely due to the activation of an apoptotic pathway. In addition, when used in combination with the conventional chemotherapeutic agents, nisin Z has the potential to enhance the cytotoxicity of these chemotherapeutic agents against cultured melanoma cells. Nisin Z has great potential for clinical application considering its low cytotoxicity to non-malignant cells and its effectiveness against Gram-positive bacterial strains and certain cancers.

Keywords: melanoma, antimicrobial peptide nisin Z, combination therapy, selective cancer cytotoxicity, chemotherapeutic agents, antibiotic resistance

1. Introduction

Antimicrobial peptides (AMPs) are produced by all known living species and exhibit direct microbial killing activity while also playing an important role in the innate immune system [1]. This diverse group of peptides is found in all living species and may be promising alternatives

or serves as additives to current antibiotics [2–4]. Many of the more than 2000 known AMPs have been demonstrated to exhibit broad-spectrum antibacterial activity [5], and bacteria are less likely to develop resistance to these peptides compared to conventional antibiotics [6, 7].

The lantibiotic nisin, produced by *Lactococcus lactis*, has promising potential for clinical application with its *Generally Regarded as Safe* (GRAS) status. This AMP was approved by the World Health Organisation (WHO) in 1969 and the US Federal Food and Drug Administration (FDA) in 1988 for the use as a food preservative [8]. Despite being extensively utilised for food preservation for nearly 50 years, there is very little indication of resistant mutants arising in food products treated with this AMP [8, 9].

Nisin is primarily used for its antibacterial activity. However, AMPs, and especially bacteriocins, display selectivity towards cancer cells [10]. Due to the toxicity associated with many conventional chemotherapeutic agents, as well as the development of chemotherapy resistance [11–13], there is a need for the development of novel anti-cancer therapies. Furthermore, to overcome chemotherapy resistance, the efficacy of chemotherapeutic agents can be enhanced by the co-administration of multi-functional agents to achieve synergistic interactions [14, 15]. The ability of nisin to increase the activity of the chemotherapeutic drug doxorubicin was investigated *in vivo* by Preet and co-workers. Nisin, when used in combination with doxorubicin, enhanced the anti-cancer activities of doxorubicin. Apoptosis could be detected upon treatment of mice with induced skin carcinogenesis. However, the exact mechanism by which nisin exerts its anti-cancer activities was not known [16].

2. Antimicrobial properties of the antimicrobial peptide nisin

A report published in 2016 projects that resistance to antibiotics could potentially lead to 10 million deaths per year by 2050 [17]. Moreover, the estimated economic impact of microbial resistance will be massive, costing nearly 100 trillion US dollars while leading to sharp decreases in the gross domestic product. Microbial resistance against conventional antibiotic agents is a serious hazard to the effective treatment of numerous diseases. This upsurge in antibiotic resistance has stimulated research into the development of alternative antimicrobial agents. Antimicrobial peptides are considered promising alternatives to current antibiotics and have the potential to replace certain antibiotics or to be used synergistically in combination with existing antimicrobial agents [2, 18].

2.1. Anti-bacterial effects of Nisin

Nisin was discovered in the same year as penicillin, but was quickly overshadowed by this antibiotic due to penicillin's ease of mass production and low manufacturing costs [19]. Nisin is a 3.5 kDa polycyclic peptide consisting of 34 amino acids and is produced by the non-pathogenic bacteria *Lactococcus lactis* [20]. Two naturally occurring variants of this peptide are nisin A and nisin Z. These two variants are structurally identical with the exception a single amino acid at position 27, where histidine occurs in nisin A while asparagine is found in nisin Z [20]. Both variants display similar antimicrobial activity but nisin Z is more soluble at neutral pH [21, 22].

In Gram-positive bacteria, nisin exhibits a dual mode of action by binding to lipid II on the bacterial membrane resulting in the inhibition of cell wall synthesis and the formation of pores in the bacterial cell membrane [23]. The antimicrobial effects of nisin Z against Gram-negative bacteria are largely inadequate. However, the activity towards Gram-negative bacteria can be improved by using ethylenediaminetetraacetic acid (EDTA) and the non-ionic surfactant Tween®80 [24, 25] (**Figure 1**).

The glycopeptide antibiotic, vancomycin, also binds to lipid II to inhibit cell wall synthesis, albeit at a different amino acid moiety. Vancomycin is one of the last line treatments against several Gram-positive antibiotic-resistant bacteria including methicillin-resistant *Staphylococcus aureus* (MRSA) [26, 27]. Disturbingly, clinical variants of MRSA have been isolated of which the lipid II pentapeptide have mutated to acquire resistant to vancomycin. These strains contain the *vanA*-type gene cluster where the terminal D-Ala has been changed to D-Lactate in the lipid II pentapeptide [28]. Due to its different binding motif, nisin remains active against the *vanA*-type resistant strains [29]. This shows the potential of nisin to bolster the antimicrobial defences against antibiotic-resistant bacterial strains. Nisin has a promising potential for clinical application with its GRAS status and approval by both the FDA and WHO, considering its low cytotoxicity and the fact that it is considered safe for human consumption. Currently, it is employed as a food preservative in nearly 50 countries to guard food against spoilage resulting from pathogens such as *Staphylococcus aureus*, *Listeria monocytogenes*, and *Clostridium botulinum* [30]. In addition, nisin has also been demonstrated to possess antibacterial activity against several clinically

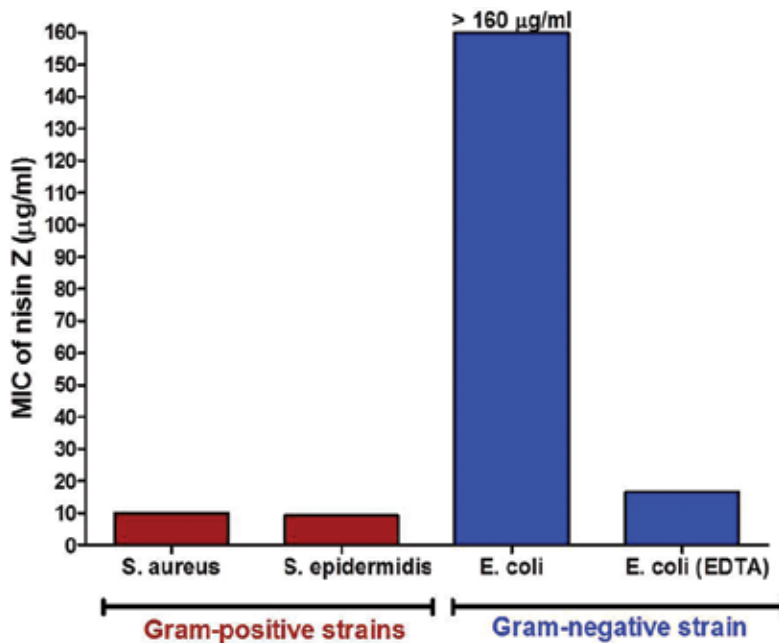


Figure 1. Minimum inhibitory concentrations (MIC) of nisin Z for Gram-positive and Gram-negative bacterial strains. The effect of EDTA (200 µM) on the MIC of *E. coli* is also demonstrated.

relevant pathogens including vancomycin-resistant *Enterococci*, *Streptococcus pneumoniae*, and methicillin-resistant *Staphylococcus aureus* [31, 32].

Mastitis-causing *Staphylococcus* strains have a tendency to develop resistance to antibiotics [33, 34]. Nisin has been successfully applied as a sanitizer against mastitis causing *Staphylococcus* and *Streptococcus* species in lactating cows even when these species are antibiotic resistant [35, 36]. Three nisin-based products were developed for the treatment of bovine mastitis, namely Ambicin N® (Applied Microbiology, Inc., New York) and Mast Out® as well as Wipe Out® Dairy wipes (ImmuCel Corporation, Maine, USA) [30]. *In vivo* nisin has also been shown to be an effective and safe alternative to antibiotics in the treatment of staphylococcal mastitis during lactation in pregnant women [37].

Antibacterial agents possessing various modes of action are particularly of interest in the fight against antimicrobial resistance as it is considered to be more challenging for bacteria to develop resistance against multiple mechanisms concurrently. This has proven true in the case of nisin, as there is very little evidence of transmissible and stable resistance occurring after nearly 50 years of treating food products with this AMP [37–39].

2.2. AMPs as antibiotic adjuvant therapy

The discovery and subsequent development of a wide range of antibiotics have revolutionised modern health care. Over the last century, the introduction of antibiotics drastically reduced morbidity and mortality. Today, antibiotics are readily available to the global population, and effective antibiotic agents have been developed against the majority of illness-causing bacteria. Ironically, the success of antibiotics has resulted in these drugs being misused, leading to the accelerated development of antimicrobial resistance amongst many bacterial species. Antibiotic resistance is making the effective treatment of numerous infections no longer achievable and there is a pressing need for alternative therapeutic approaches.

Antibiotic adjuvant therapy (to achieve synergistic interactions, although additive interactions are also favoured) can be considered as a promising strategy to combat antibiotic resistance. Combination of antibiotics and AMPs that possess different modes of action are valuable in the fight against antimicrobial resistance as it is unlikely for bacteria to develop resistance against multiple mechanisms simultaneously. Several studies have demonstrated synergism between nisin and conventional antibiotics. Nisin displayed synergism with the antibiotics, colistin and clarithromycin, against the common Gram-negative bacteria, *Pseudomonas aeruginosa* [40]. Synergistic effects were also observed with streptomycin, penicillin, rifampicin and lincomycin against *P. fluorescens* as well as the antibiotic-resistant variants of this strain [41]. Daptomycin, teicoplanin and ciprofloxacin displayed synergism against MRSA biofilms [4]. In a study by Dosler and Gerceker, nisin-antibiotic combinations were shown to have synergistic interactions against clinical isolates of methicillin-susceptible *S. aureus* (MSSA), MRSA and *Enterococcus faecalis*. A major finding from their study was that a high incidence of synergistic interactions occurred with a nisin-ampicillin combination against MSSA and nisin-daptomycin combination against *E. faecalis* strains [42]. When nisin is combined with

penicillin, chloramphenicol or ciprofloxacin, biofilm formation of *E. faecalis* was significantly reduced [43].

In a previous study, we also evaluated the interaction of the nisin Z variant with conventional antibiotics [24]. Antibiotic-nisin Z combinations (1:1) were evaluated on *Staphylococcus epidermidis* (ATCC 12228) and *Staphylococcus aureus* (ATCC 12600) seeing as nisin is principally effective against Gram-positive bacterial species. Several conventional antibiotics with different mechanisms of action against Gram-positive bacteria were selected and included methicillin; vancomycin; ampicillin; tetracycline; gentamicin and novobiocin. The minimum inhibitory concentration (MIC) was used as a reflection of the bacterial cytotoxicity following exposure to the antibiotic-nisin Z combinations. The MIC was determined using a modified broth microdilution method [44], where the p-iodonitrophenyltetrazolium violet (INT) was replaced with the yellow tetrazolium salt 3-(4,5-dimethylthiazol-2-yl)-2,5-diphenyltetrazolium bromide (MTT). The interactions between the antibiotics and nisin were determined using the fractional inhibitory concentrations (FIC) [45] and values were interpreted as $\Sigma\text{FIC} \leq 0.5$ synergistic, $\Sigma\text{FIC} > 0.5-1.0$ additive, $\Sigma\text{FIC} > 1.0$ and < 4.0 indifferent and $\Sigma\text{FIC} \geq 4.0$ antagonistic.

Bacterial treatment with nisin Z-antibiotic combinations resulted in the identification of three additive and two synergistic combinations. Nisin Z displayed an additive effect ($\Sigma\text{FIC} > 0.5$ to 1.0) when combined with ampicillin and gentamicin in *S. aureus* (Table 1).

Bacterial strain	MIC of nisin Z (µg/ml)	MIC of antibiotic (µg/ml)	Nisin Z:antibiotic (1:1)
			ΣFIC
<i>S. epidermidis</i>	Nisin Z (9.17)	Methicillin (1.88)	2.68
		Vancomycin (2.50)	2.55
		Ampicillin (16.67)	0.71
		Tetracycline (80.00)	3.65
		Gentamicin (1.04)	2.23
		Novobiocin (1.46)	0.50
<i>S. aureus</i>	Nisin Z (10.00)	Methicillin (1.88)	1.06
		Vancomycin (2.50)	2.50
		Ampicillin (1.04)	0.66
		Tetracycline (0.47)	1.40
		Gentamicin (6.67)	0.94
		Novobiocin (2.29)	0.17

Highlighted values represent ΣFIC values which indicate positive interactions between nisin Z and antibiotics where; ≤ 0.5 synergistic, $> 0.5-1.0$ additive, 1.1–3.9 indifferent and ≥ 4.0 antagonistic.

Table 1. MIC values and ΣFIC values for antibiotic-nisin Z combinations.

Furthermore, *S. epidermidis* treated with ampicillin-nisin Z combination also showed an additive interaction. Novobiocin-nisin Z combinations showed synergistic interactions when used against *S. epidermidis* and *S. aureus*. Novobiocin, as part of the aminocoumarins antibiotic group, is able to indirectly block DNA replication by effectively inhibiting bacterial DNA gyrase. Novobiocin-nisin Z combination was particularly effective in the treatment of *S. aureus* as a dramatic reduction in the Σ FIC was witnessed. This may be due to the different, but complementary, mechanisms of actions of nisin Z and novobiocin. As the lipid II-nisin Z complex forms pores in the bacterial membrane, hydrophobic novobiocin can pass through the cell membrane to interact with the DNA gyrase of *S. aureus*. This is only speculation and the exact synergistic mechanism of should be examined further. This *in vitro* study shows the potential of nisin Z for the use as an adjuvant with conventional antibiotics. AMP-antibiotic combination therapy may aid in reinforcing the defences against resistant organisms by making it more challenging for a bacterial strain to adapt to multiple antimicrobial mechanisms. Furthermore, novobiocin is used for the treatment of mastitis in lactating cows [46]; and as previously mentioned, some nisin-based products have been developed for the treatment of mastitis. The synergistic interactions between nisin and novobiocin make this combination especially of interest for developing novel formulations for the treatment of mastitis.

3. Cytotoxic effects of nisin on non-malignant mammalian cells

It is clear that nisin is an effective antimicrobial agent which can inhibit the growth of/kill several Gram-positive bacterial species, including food-borne pathogens such as *Staphylococcus aureus*, *Listeria monocytogenes* and *Clostridium botulinum* as well as exhibiting activity against many clinical important pathogens such as vancomycin-resistant *Enterococci* (VRE), *Streptococcus pneumonia* and MRSA [32, 47, 48]. Despite having exceptional antimicrobial activity, many AMPs also exhibit high toxicity to mammalian cells. An example of a cytotoxic AMP is melittin, the main active component of apitoxin (bee venom). Melittin has an excellent antibacterial activity and the antimicrobial mechanism of this AMP is most likely the permeabilisation of cell membranes by pore formation resulting in cell lysis and death [49]. Although melittin has effective broad-spectrum antimicrobial activity, this AMP is extremely toxic to mammalian cells even at very low concentrations.

As mentioned before, nisin has a *Generally Regarded as Safe* (GRAS) status and is considered safe for human consumption. The Accepted Daily Intake (ADI) of nisin was determined by the FDA as 2.94 mg/per day (0.049 mg/kg body weight/day) in 1988, prior to receiving GRAS status [50]. In a study by Joo and co-workers, mice were exposed to a concentration of nisin more than $\times 1000$ (150 mg/kg body weight/day) the recommended ADI over a period of 3 weeks with no signs of cytotoxicity [51]. In another study, mice were treated with doses of 800 mg/kg body weight/day (more than 10 000 times higher than the recommended ADI) ultra-pure nisin Z for 3 weeks without any evidence of toxicity [52]. In both these studies, long-term (>3 weeks) treatment with high concentrations of nisin did not result in any observable toxicity.

We also investigated cytotoxicity of nisin Z towards mammalian cells using the MTT assay to measure metabolic activity and the lactate dehydrogenase (LDH) assay to indicate membrane integrity. The non-malignant human immortalised keratinocyte (HaCaT) cells were employed for cytotoxicity testing and cultured under normal conditions [24]. Briefly, HaCaT cells were seeded in a 96-well plate and incubated until ~90% confluent. Synthetic melittin was used ($\geq 97\%$ HPLC from Sigma-Aldrich) as a positive AMP control for cytotoxicity. After 24 h of exposure to nisin Z or melittin (2.5–40 $\mu\text{g/ml}$), the MTT assay was performed as described previously [24]. The ability of NAD(P)H-dependent cellular oxidoreductase enzymes to reduce MTT to formazan is considered a reflection of the number of viable cells present. Cell viability is expressed as a percentage relative to the untreated control, which was set as being 100% viable. For an assay positive control, cells were exposed to 0.01% Triton-X 100 (Sigma-Aldrich, St Louis, MO, USA).

To investigate the effect of the two AMPs on cell membrane integrity, the CytoTox-ONE™ Homogeneous Membrane Integrity Assay (Promega, Madison, WI, USA) was employed. This assay determines the release of lactate dehydrogenase (LDH) into the culture media from cells with impaired cell membranes. HaCaT cells were exposed to melittin and nisin Z as described earlier. A lysis solution (Promega) was used as a maximum LDH release positive control. The LDH release assay was performed as described previously [24]. Results are conveyed relative to the untreated control (set to 0% LDH release) and the maximum release sample (set to 100% LDH release).

Cytotoxicity data (**Figure 2**) shows that nisin Z did not negatively affect the cell viability of HaCaT cells.

The MTT assay indicates that the ability of NAD(P)H-dependent cellular oxidoreductase enzymes to reduce MTT to formazan was not affected by the exposure to the tested nisin

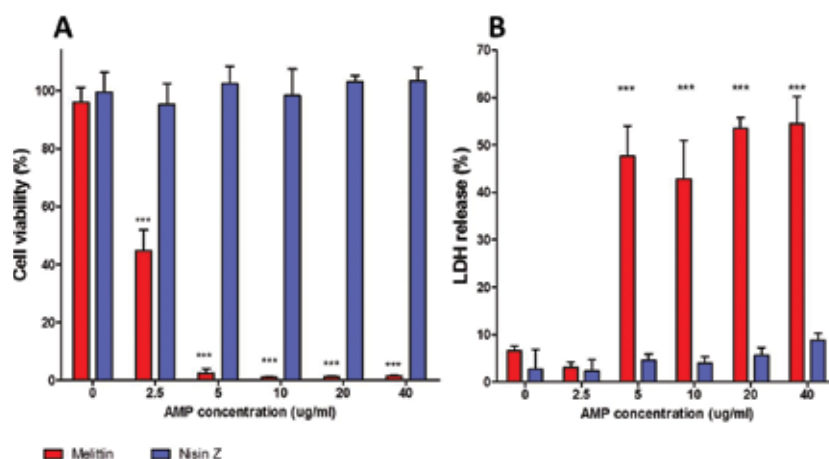


Figure 2. Cytotoxicity assay of HaCaT cells exposed to the AMPs melittin and nisin Z. (A) MTT assay and (B) LDH release assay. Vehicle control groups are represented by 0 mg/ml. Values represent mean stdev $n = 3$. *** $p < 0.001$ compared to the vehicle control group.

Z concentrations. Indicating that nisin Z did not negatively affect the cell viability of HaCat cells. The LDH assay also showed that there was no significant increase in the release of LDH, indicating that nisin Z did not cause any measurable membrane damage. On the other hand, both the MTT and LDH assays showed that relatively low concentrations of melittin led to a considerable increase in cytotoxicity in HaCat cells.

These *in vitro* results echo many of the recent *in vivo* findings, showing that nisin exposure to non-malignant cells has very little to no cytotoxic effects. Even at concentrations of nisin Z that exceeds the MICs for *S. aureus* and *S. epidermidis* (**Figure 1**) no toxicity was observed. Keeping in mind that nisin is an effective antimicrobial agent against several Gram-positive bacterial species, including clinically important and resistant pathogens, this AMP shows promising potential for clinical application.

4. Cytotoxic effect of nisin on malignant cells

Over the last few decades, great strides have been made in cancer treatment and therapies, leading to the steady decline of cancer death rates [53]. Despite these developments, many current cancer therapies are still associated with high cytotoxicity and lack specificity. There is consequently still a need for the development of novel anti-cancer therapies. AMPs, especially bacteriocins, display selectivity towards cancer cells [10]. These AMPs are, therefore, potential alternative candidates to current chemotherapeutic agents. AMPs can also be applied as adjuvants to chemotherapeutic agents to lower the therapeutic doses needed with the intention of quelling the toxicity of these treatments.

Studies have previously investigated the anti-tumour potential of nisin *in vitro* and *in vivo* for head and neck squamous cell carcinoma (HNSCC) [52]. The study by Joo and co-workers indicated that nisin has the ability to selectively induce apoptosis, cell cycle arrest and reduce cell proliferation in HNSCC cells, compared to primary keratinocytes *in vitro* [51]. *In vivo*, nisin treatment reduced the overall tumour burden compared to non-nisin treated groups, in a floor-of-mouth oral cancer xenograft mouse model. Also, to examine the mechanism by which nisin facilitates its anti-proliferative and pro-apoptotic effects on HNSCC cells, the effect of nisin-treatment on the expression of 39,000 genes was examined by using Affymetrix gene arrays. The expression of multiple genes was altered, including those in the apoptotic and cell cycle pathways, membrane physiology, energy and nutrient pathways, ion transport and signal transduction and protein binding pathways. The *CHAC1* gene, a cation transport regulator and apoptosis mediator were dramatically up-regulated. This study was the first to show that the antibacterial food preservative nisin could effectively reduce and prevent tumorigenesis both *in vitro* and *in vivo*.

4.1. Cytotoxic effects of nisin Z on melanoma cells

We also evaluated the potential of nisin Z to induce selective cytotoxicity towards human melanoma cells *in vitro*. Melanoma is the leading cause of skin cancer-related deaths [54, 55].

Contrary to most types of cancer, the frequency of melanoma has been increasing over the last three decades [54]. In addition to a high mortality rate, Melanoma cells also have a sinister tendency to rapidly develop resistance to mainstream chemotherapeutic agents [12, 13]. *In vitro* cytotoxicity of the nisin Z was determined by employing the MTT assay, LDH assay and flow cytometric apoptosis and necrosis analyses. The non-malignant human keratinocyte (HaCat) cell line was used as a control. The MTT and LDH assays were performed, as described previously [56]. The flow cytometric FITV Annexin V apoptosis assay (BD Pharmingen™, BD Biosciences, San Jose, CA, USA) was employed for the detection of apoptotic cytotoxicity. FITC Annexin emits green fluorescence and its presentation indicates early apoptotic events, while propidium iodide (PI) emanates red fluorescence and is associated with late apoptotic or necrotic cells.

The quantitative colourimetric MTT assay was used to investigate the cytotoxic effect of nisin Z on cultured melanoma cells as well as non-malignant keratinocytes. There is a clear concentration-dependent decline in cell viability observed in melanoma cells exposed to nisin Z (**Figure 3A**).

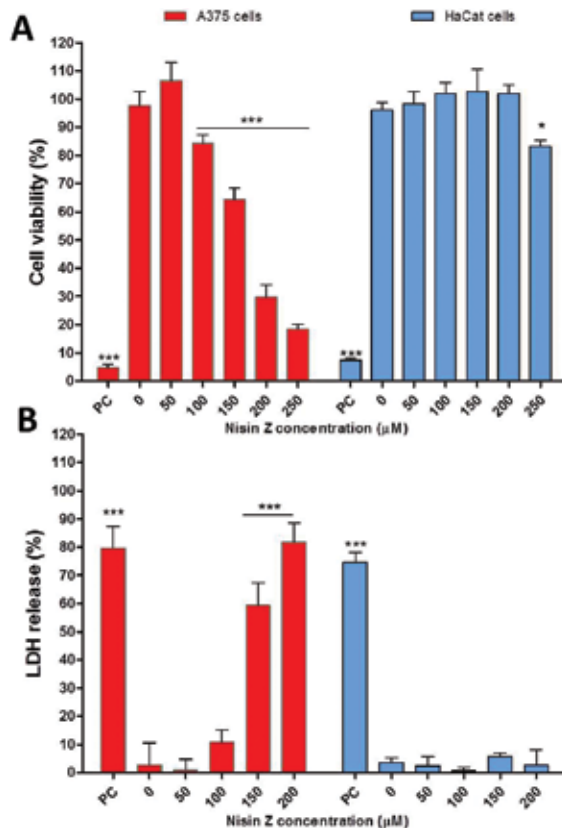


Figure 3. Cytotoxic effects of nisin Z on melanoma (A375) cells. (A) Cell viability was determined using the MTT assay. (B) LDH release from cells following treatment with nisin Z. Keratinocytes (HaCat) were used as a non-malignant control. * $p < 0.05$ and *** $p < 0.001$ compared to the control groups.

A significant increase in cytotoxicity is observed in melanoma cells after exposure to relatively low concentrations of nisin Z. The IC_{50} value of melanoma cells exposed to nisin Z is approximately 180 μM . Conversely, the non-malignant keratinocytes exposed to nisin Z presented with considerably higher cell viability, with an IC_{50} value more than double that of its malignant counterpart. To examine whether the observed cytotoxicity of melanoma cells exposed to nisin Z is the result of membrane damage, the LDH assay was performed. This assay measures the release of lactate dehydrogenase, the cytosolic enzyme, as a result of cellular plasma membrane damage. Results suggest that the exposure of melanoma cells to nisin Z concentrations of 150 μM and higher (**Figure 3B**) lead to in a significant increase in LDH release. No significant LDH release was detected in the non-malignant keratinocytes after nisin Z exposure, indicating very little membrane damage. Both, the basic cytotoxicity assays (MTT and LDH assay) suggest that nisin Z is selectively more toxic towards cultured melanoma cells compared to non-malignant cells.

Flow cytometry was used to investigate whether the cytotoxicity observed in melanoma cells was of apoptotic or necrotic origin. For the non-malignant keratinocyte cells, the flow cytometric analysis indicated that >98% of the cells exposed to 50 μM nisin Z could be considered viable and is comparable to the untreated control (**Figure 4**).

A small increase in cytotoxicity is observed at higher concentration. Melanoma cells exposed to 50 μM nisin Z showed a much larger early apoptosis (>17%) population than their non-malignant counterparts. A significant increase in cytotoxicity is observed in melanoma cells exposed to higher concentrations of nisin Z, resulting in approximately half of the cancer cells undergoing apoptosis/necrosis after being exposed to nisin Z concentrations of 100 μM or higher. These results confirm the basic viability data that nisin Z is more selectively cytotoxic to melanoma cells and give an indication that the cell death observed in these cells is probably due to the activation of an apoptotic pathway.

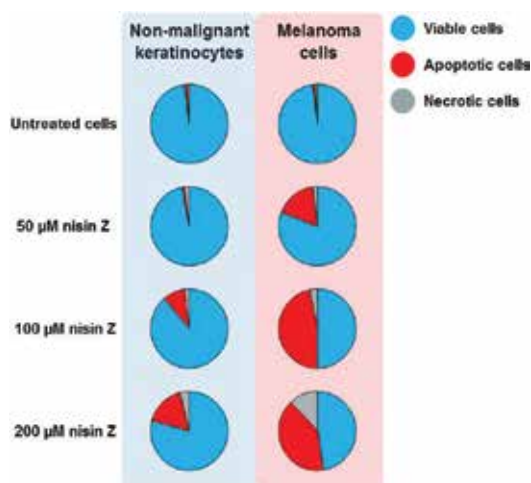


Figure 4. Pie graphs representing the cell population sizes of viable, apoptotic and necrotic non-malignant keratinocyte (HaCat) and melanoma (A375) cells after exposure to 50–200 μM of nisin Z for 24 h.

4.2. The potential of nisin Z to increase the cytotoxicity and selectivity of conventional chemotherapeutic agents

Due to the toxicity associated with some conventional chemotherapeutic agents, as well as the constant threat of malignancies evolving chemotherapy resistance [11–13], there is a necessity for the development of novel anti-cancer therapies. To combat chemotherapy resistance, the efficacy of chemotherapeutic agents can be enhanced by the co-administration of multi-functional agents to achieve synergistic interactions [14, 15].

As stated earlier, there is an abundance of studies which investigated the use of nisin as an adjuvant to conventional antibiotics [4, 40–42, 57]. It has been shown that nisin displays anti-cancer properties; however, inadequate focus has been given to applying nisin as an adjuvant for chemotherapeutic agents. The ability of nisin to increase the activity of the chemotherapeutic drug, doxorubicin, was investigated *in vivo* by Preet and co-workers [16]. Doxorubicin (Adriamycin) is traditionally employed to treat breast cancer, bladder cancer, lymphoma, and acute lymphocytic leukaemia, to name a few. When combining nisin with doxorubicin, enhanced anti-cancer activities were observed and apoptosis could be detected upon treatment of mice with induced skin carcinogenesis as well as a slight increase in oxidative stress. However, the exact mechanism by which nisin exerts its anti-cancer activities was not determined [16]. It is suggested that AMPs, which display anticancer activity, should be used in combination with conventional chemotherapeutic agents to enhance the effectiveness of these treatments, prevent recurrence of cancer following treatment and possibly reduce instances of chemotherapy resistance [58, 59]. Other studies have also shown that AMPs have the potential to enhance the effectiveness of conventional chemotherapeutic agents. The cytotoxicity of etoposide and cisplatin could be enhanced through the combination with magainin A and magainin G, respectively [60]. More recently, it was shown that the combination of melittin and 5-Fluorouracil enhanced cytotoxic effects against squamous skin cancer cells, while simultaneously reducing the toxicity to normal keratinocytes [61]. There are currently no AMPs that have entered into clinical trials or that are in preclinical development as cancer therapeutics. However, peptide-derived therapies are being recognised for the selectivity and anticancer effectiveness and have been investigated in clinical trials [59]. For example, the peptide asparagine-glycine arginine tumour homing peptide (NGR-hTNF) has completed phase 1 clinical trials and is waiting to enter phase 2 clinical trials to test its effectiveness when used in combination with cisplatin for the treatment of several refractory solid tumours including melanomas [62].

Based on the findings that nisin Z is more selectively cytotoxic to melanoma cells, the cytotoxic effect of the combination of nisin Z with conventional chemotherapeutic agents was investigated in cultured melanoma cells. The effect of combinations of nisin Z with conventional chemotherapeutic agents (5-Fluorouracil, etoposide, hydroxyurea) on A375 (melanoma) and HaCat (non-malignant keratinocyte) cells was determined by the MTT assay. Cells were exposed to different concentrations of the respective chemotherapeutic agents independently and in combination with 150 μ M of nisin Z for 24 h. Following exposure, the MTT assay was performed as described earlier. Blank and background measurements were subtracted and cell viability is expressed as a percentage relative to the untreated control, which was set as

100% viable. Possible synergistic interactions were evaluated by comparing the cytotoxicity of combination treatment with mono-treatment on melanoma cells.

The chemotherapeutic agent 5-Fluorouracil can inhibit RNA and DNA synthesis leading to cell death. The combination of nisin Z with 5-Fluorouracil increased the cytotoxicity to melanoma cells over the entire concentration range tested compared to the mono-treatment of 5-Fluorouracil ($p < 0.05$) (**Figure 5A**), with no significant increase in toxicity to non-malignant keratinocytes (**Figure 5B**).

The 5-Fluorouracil treatment is initially cytotoxic at 50 μM ($p < 0.01$ compared to the control), whereas the combination of 5-Fluorouracil and nisin Z only begins to induce toxicity at 200 μM ($p < 0.001$ compared to the control) in the non-malignant keratinocytes. Results indicate that the 5-Fluorouracil-nisin Z combination is more cytotoxic to melanoma cells compared to the mono-treatment. The anti-cancer activity of 5-Fluorouracil may, therefore, be enhanced by combination treatment with nisin Z. Etoposide is a chemotherapeutic agent that is able to induce DNA strand breaks in cancer cells by interfering with type II topoisomerase, ultimately inducing apoptosis. When combining etoposide with nisin Z it was found that the activity towards melanoma cells was enhanced compared to mono-treatment across the entire concentration range ($p < 0.001$) (**Figure 5C**), with no increase in cytotoxicity to non-malignant keratinocytes (**Figure 5D**). In melanoma cells, the combination of nisin Z with etoposide had a higher level of activity at the lowest concentration tested compared to the highest concentration for mono-treatment ($p < 0.001$). The anti-cancer activity of etoposide can, therefore, be significantly enhanced through the combination of nisin Z. Hydroxyurea is able to induce DNA damage and inhibit DNA synthesis. The combination of nisin Z with hydroxyurea was able to increase the cytotoxicity to melanoma cells at concentrations of between 25 and 400 μM compared to the mono-treatment of hydroxyurea ($p < 0.01$) (**Figure 5E**), with no significant increase in toxicity to non-malignant keratinocytes (**Figure 5F**).

To evaluate if possible synergistic interactions occurred between the chemotherapeutic agents and nisin Z, the cytotoxicity of melanoma cells following the mono-treatment of the respective chemotherapeutic agents (50 μM) was compared to that of the mono-treatment of nisin Z (150 μM), followed by that of the combination (50 μM chemotherapeutic agent +150 μM nisin Z). Synergism occurs when the combined effects of the different components are greater than their individual effects. The cell viability of melanoma cells was significantly lower for all combinations compared to mono-treatment with the chemotherapeutic agent alone ($p < 0.05$) (**Figure 6**). However, the only combination that displayed synergism was the combination of nisin Z with etoposide.

The AMP nisin, which is considered safe for human consumption, not only displays antibacterial properties, but also anti-cancer activities. Although the use of nisin as an adjuvant for conventional antibiotics has been investigated extensively, there are few studies investigating nisin as an adjuvant for conventional chemotherapeutic agents. Nisin also exhibits immune-modulatory properties. We have shown that nisin Z induces selective cytotoxicity towards melanoma cells through an apoptotic pathway. These properties make nisin Z an attractive anti-cancer agent to be used alone or in combination with current chemotherapeutic agents to enhance anti-cancer properties of these agents, while also potentially combatting chemotherapy resistance. Here,

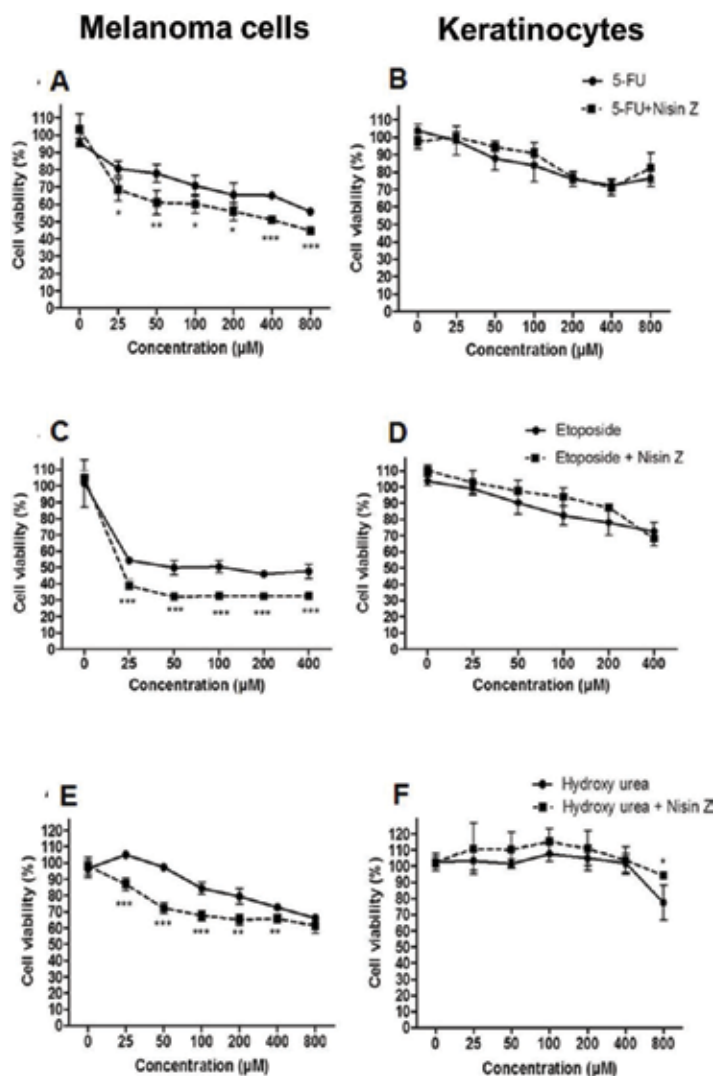


Figure 5. Cytotoxicity of chemotherapeutic agents in combination with nisin Z on melanoma (A375) cells and non-malignant keratinocytes (HaCat) as determined by the MTT assay. (A) Melanoma cells exposed to 5-Fluorouracil (FU) combinations. (B) HaCat exposed to 5-FU combinations. (C) Melanoma cells exposed to etoposide combinations. (D) HaCat exposed to etoposide combinations. (E) Melanoma cells exposed to hydroxyurea combinations. (F) HaCat exposed to hydroxyurea combinations. Vehicle control groups were included and are represented by 0 µM. Results are expressed relative to the untreated controls which were set as being 100% viable. Bars represent the standard deviation, n = 4. *p < 0.05, **p < 0.01 and *** p < 0.001 for combination compared to chemotherapeutic agent alone.

it was shown that combinations of nisin Z with 5-Fluorouracil, hydroxyurea and etoposide was able to enhance the cytotoxicity to melanoma cells, while no significant increase in toxicity toward non-malignant keratinocytes were observed. Especially of interest is the consequence of nisin Z on the effectiveness of etoposide, seeing as etoposide resistance is known in melanoma [63, 64]. The combination of nisin Z with etoposide was able to significantly and selectively

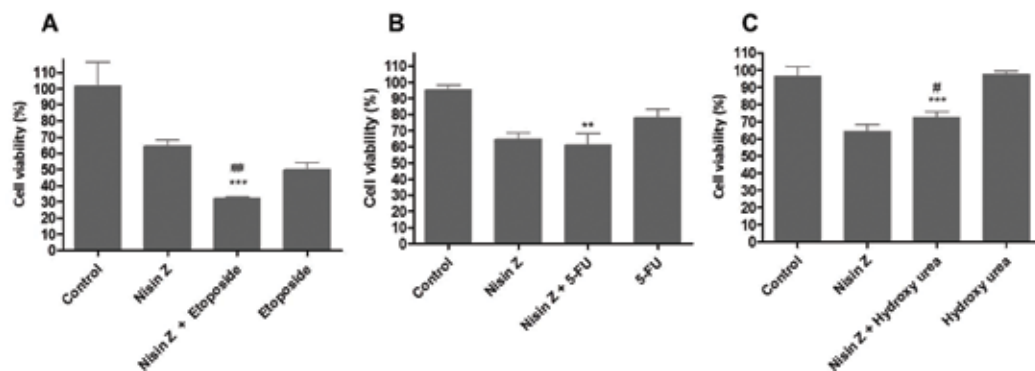


Figure 6. Cytotoxicity results for mono-treatment and combinations of chemotherapeutic agents (50 μ M) and nisin Z (150 μ M) as determined by the MTT assay. Nisin Z was combined with (A) etoposide, (B) 5-Fluorouracil and (C) hydroxyurea. Bars represent the average and error bars the standard deviation, $n = 4$. ** $p < 0.01$ and *** $p < 0.001$ for combination compared to chemotherapeutic agent alone. # $p < 0.05$ and ## $p < 0.01$ for combination compared to nisin Z alone.

enhance the cytotoxic effect etoposide to melanoma cells. Synergism was also observed when combining nisin Z and etoposide with regards to the cytotoxic effect in melanoma cells. Based on all the properties of nisin Z and its GRAS status it could, therefore, be considered as an adjuvant for conventional chemotherapeutic agents.

5. Conclusion

The majority of AMPs exhibit direct microbial killing activity and occur in all living species as an important part of their innate immune system. Due to the co-evolution of AMPs and bacteria, bacterial species are less likely to develop resistance to these peptides compared to conventional antibiotics. The lantibiotic, nisin, has a promising potential for clinical application as it exhibits very low cytotoxicity to mammalian cells, while displaying potent antimicrobial activity against several common foodborne and clinically important Gram-positive bacteria. The use of nisin against Gram-negative bacteria still remains limited. Nisin can be considered as a promising adjuvant for antibiotics in the treatment of Gram-positive bacteria. Antibiotic-nisin combinations can potentially be used to lower the therapeutic dose of antibiotic treatments, while also enhancing the antimicrobial activity by employing multiple modes of action. With multiple antimicrobial mechanisms concurrently in play, these combinations can hinder the development of antibiotic resistance. We have demonstrated that nisin Z displays synergism when combined with novobiocin against *S. aureus*. This bacterial species is associated with mastitis. Both nisin-based products and novobiocin are used for the treatment of mastitis. The synergistic interactions between nisin and novobiocin make this combination, especially of interest for developing novel formulations for the treatment of mastitis (**Figure 7A**).

Apart from the antimicrobial properties of nisin, this AMP also displays promising anticancer potential towards several types of malignancies. This chapter discussed the anti-cancer potential of nisin Z towards cultured melanoma cells. Results showed that this AMP is more

cytotoxic to melanoma cells compared to non-malignant keratinocytes. It was shown that nisin Z disrupts the cell membrane integrity of melanoma cells, while also inducing apoptosis in the majority of exposed malignant cells (**Figure 7B**). Taking into account these anticancer properties of nisin Z, the cytotoxicity of nisin Z-chemotherapeutic agent combinations to melanoma cells was compared to the mono-treatment with selected conventional chemotherapeutic agents. This study indicated that when used in combination with the conventional chemotherapeutic agents (5-Fluorouracil, hydroxyurea and etoposide), nisin Z has the potential to enhance the cytotoxicity of these conventional chemotherapeutic agents against cultured melanoma cells. Synergism was observed between the nisin Z and etoposide combination. However, this study was only limited to the *in vitro* effect in melanoma cells with regards to cytotoxicity as measured by the MTT assay. For future *in vitro* studies, it is suggested that more cancer cell lines be included. The mechanistic interaction between nisin Z and the chemotherapeutic agents should also be investigated. It is also suggested that *in vivo* studies be conducted similarly to that by Preet and co-workers to assess whether the combination of nisin Z with these conventional chemotherapeutic agents are able to reduce melanoma tumorigenesis *in vivo* [16]. The effective dosages also need to be determined with *in vivo* assays. Nisin Z has great potential for clinical application considering its low cytotoxicity to non-malignant cells and the effectiveness of this AMP against Gram-positive bacterial strains and certain cancers. However, detailed antimicrobial and anticancer mechanistic interaction studies analysis are lacking and many *in vitro* results must still be confirmed within *in vivo* systems.

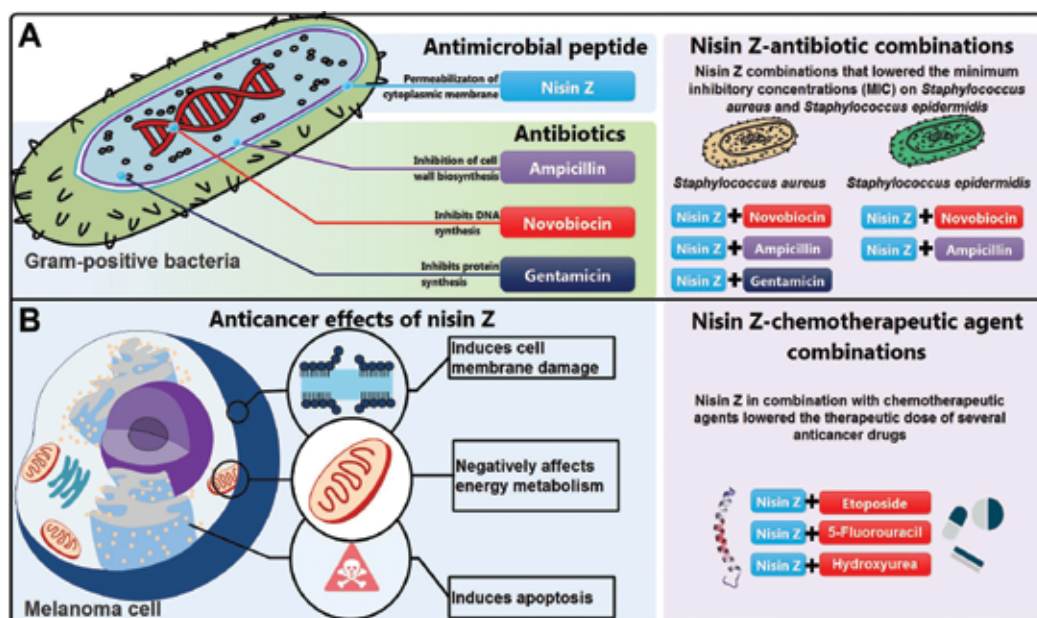


Figure 7. Summary of the antimicrobial and anticancer properties of nisin Z alone and in combination with conventional therapies. (A) The antimicrobial effects and mechanisms of action of nisin Z and selected antibiotics alone and in combination on gram-positive bacteria. (B) The cytotoxic effect of nisin Z on cultured melanoma cells and combinations of this AMP with conventional chemotherapeutic agents.

Acknowledgements

AL is grateful for financial assistance from the National Research Foundation (NRF) of South Africa (Grant Number 94942). Opinions expressed and conclusions arrived at are those of the authors and are not to be attributed to the NRF.

Author details

Angélique Lewies, Lissinda H. Du Plessis and Johannes F. Wentzel*

*Address all correspondence to: 20134045@nwu.ac.za

Centre of Excellence for Pharmaceutical Sciences (PHARMACEN), North-West University, Potchefstroom, South Africa

References

- [1] Hancock RE, Diamond G. The role of cationic antimicrobial peptides in innate host defences. *Trends in Microbiology*. 2000;**8**:402-410
- [2] Fox JL. Antimicrobial peptides stage a comeback. *Nature Biotechnology*. 2013;**31**:379-382. DOI: 10.1038/nbt.2572
- [3] Lewies A, Wentzel JF, Jacobs G, Du Plessis LH. The potential use of natural and structural analogues of antimicrobial peptides in the fight against neglected tropical diseases. *Molecules*. 2015;**20**:15392-15433. DOI: 10.3390/molecules200815392
- [4] Mataraci E, Dosler S. *In vitro* activities of antibiotics and antimicrobial cationic peptides alone and in combination against methicillin-resistant *Staphylococcus aureus* biofilms. *Antimicrobial Agents and Chemotherapy*. 2012;**56**:6366-6371. DOI: 10.1128/AAC.01180-12
- [5] Wang G, Li X, Wang Z. APD3: The antimicrobial peptide database as a tool for research and education. *Nucleic Acids Research*. 2016;**44**:D1087-D1093. DOI: 10.1093/nar/gkv1278
- [6] Marr AK, Gooderham WJ, Hancock REW. Antibacterial peptides for therapeutic use: Obstacles and realistic outlook. *Current Opinion in Pharmacology*. 2006;**6**:468-472. DOI: <http://dx.doi.org/10.1016/j.coph.2006.04.006>
- [7] Peschel A, Sahl HG. The co-evolution of host cationic antimicrobial peptides and microbial resistance. *Nature Reviews Microbiology*. 2006;**4**:529-536. DOI: 10.1038/nrmicro1441
- [8] Shin JM, Gwak JW, Kamarajan P, Fenno JC, Rickard AH, Kapila YL. Biomedical applications of nisin. *Journal of Applied Microbiology*. 2016;**120**:1449-1465. DOI: 10.1111/jam.13033

- [9] Cleveland J, Montville TJ, Nes IF, Chikindas ML. Bacteriocins: Safe, natural antimicrobials for food preservation. *International Journal of Food Microbiology*. 2001;**71**:1-20
- [10] Kaur S, Kaur S. Bacteriocins as potential anticancer agents. *Frontiers in Pharmacology*. 2015;**6**:272. DOI: 10.3389/fphar.2015.00272
- [11] Luqmani YA. Mechanisms of drug resistance in cancer chemotherapy. *Medical Principles and Practice: International Journal of the Kuwait University, Health Science Centre*. 2005;**14**(Suppl 1):35-48. DOI: 10.1159/000086183
- [12] Soengas MS, Lowe SW. Apoptosis and melanoma chemoresistance. *Oncogene*. 2003;**22**:3138-3151. DOI: 10.1038/sj.onc.1206454
- [13] Wellbrock C. MAPK pathway inhibition in melanoma: Resistance three ways. *Biochemical Society Transactions*. 2014;**42**:727-732. DOI: 10.1042/BST20140020
- [14] Sylvester PW, Wali VB, Bachawal SV, Shirode AB, Ayoub NM, Akl MR. Tocotrienol combination therapy results in synergistic anticancer response. *Frontiers in Bioscience*. 2011;**16**:3183-3195
- [15] Wei XQ, Ma HQ, Liu AH, Zhang YZ. Synergistic anticancer activity of 5-aminolevulinic acid photodynamic therapy in combination with low-dose cisplatin on Hela cells. *Asian Pacific Journal of Cancer Prevention: APJCP*. 2013;**14**:3023-3028
- [16] Preet S, Bharati S, Panjeta A, Tewari R, Rishi P. Effect of nisin and doxorubicin on DMBA-induced skin carcinogenesis— A possible adjunct therapy. *Tumour Biology: The Journal of the International Society for Oncodevelopmental Biology and Medicine*. 2015;**36**:8301-8308. DOI: 10.1007/s13277-015-3571-3
- [17] O'Neill J. The review on antimicrobial resistances. *Tackling Drug-Resistant Infections Globally: Final Report and Recommendations*. [Online]. 2016. Available: https://amr-review.org/sites/default/files/160518_Final%20paper_with%20cover.pdf [Accessed: 16 January 2017]
- [18] Hancock RE, Sahl HG. Antimicrobial and host-defense peptides as new anti-infective therapeutic strategies. *Nature Biotechnology*. 2006;**24**:1551-1557. DOI: 10.1038/nbt1267
- [19] Rogers LA, Whittier EO. Limiting factors in the lactic fermentation. *Journal of Bacteriology*. 1928;**16**:211-229
- [20] Mulders JW, Boerrigter IJ, Rollema HS, Siezen RJ, de Vos WM. Identification and characterization of the lantibiotic nisin Z, a natural nisin variant. *European Journal of Biochemistry*. 1991;**201**:581-584
- [21] De Vos WM, Mulders JW, Siezen RJ, Hugenholtz J, Kuipers OP. Properties of nisin Z and distribution of its gene, *nisZ*, in *Lactococcus lactis*. *Applied and Environmental Microbiology*. 1993;**59**:213-218
- [22] De VWM, Kuipers OP, Siezen RJ. Lantibiotics similar to nisin a, lactic acid bacteria which produce such lantibiotics, method for constructing such lactic acid bacteria and method

for preserving foodstuffs with the aid of these lantibiotics and these lactic acid bacteria producing lantibiotics. Google Patents; 2003

- [23] Pag U, Sahl HG. Multiple activities in lantibiotics—Models for the design of novel antibiotics? *Current Pharmaceutical Design*. 2002;**8**:815-833
- [24] Lewies A, Wentzel JF, Jordaan A, Bezuidenhout C, Du Plessis LH. Interactions of the antimicrobial peptide nisin Z with conventional antibiotics and the use of nanostructured lipid carriers to enhance antimicrobial activity. *International Journal of Pharmaceutics*. 2017;**526**:244-253. DOI: 10.1016/j.ijpharm.2017.04.071
- [25] Natrajan N, Sheldon BW. Efficacy of nisin-coated polymer films to inactivate *Salmonella Typhimurium* on fresh broiler skin. *Journal of Food Protection*. 2000;**63**:1189-1196
- [26] Liu C, Bayer A, Cosgrove SE, Daum RS, Fridkin SK, Gorwitz RJ, et al. Clinical practice guidelines by the infectious diseases society of america for the treatment of methicillin-resistant *Staphylococcus aureus* infections in adults and children. *Clinical Infectious Diseases: An Official Publication of the Infectious Diseases Society of America*. 2011;**52**:e18-e55. DOI: 10.1093/cid/ciq146
- [27] Tarai B, Das P, Kumar D. Recurrent challenges for clinicians: Emergence of methicillin-resistant *Staphylococcus aureus*, vancomycin resistance, and current treatment options. *Journal of Laboratory Physicians*. 2013;**5**:71-78. DOI: 10.4103/0974-2727.119843
- [28] Perichon B, Courvalin P. VanA-type vancomycin-resistant *Staphylococcus aureus*. *Antimicrobial Agents and Chemotherapy*. 2009;**53**:4580-4587. DOI: 10.1128/AAC.00346-09
- [29] Hsu ST, Breukink E, Tischenko E, Lutters MA, de Kruijff B, Kaptein R, et al. The nisin-lipid II complex reveals a pyrophosphate cage that provides a blueprint for novel antibiotics. *Nature Structural & Molecular Biology*. 2004;**11**:963-967. DOI: 10.1038/nsmb830
- [30] Cotter PD, Hill C, Ross RP. Bacteriocins: Developing innate immunity for food. *Nature Reviews Microbiology*. 2005;**3**:777-788. DOI: 10.1038/nrmicro1273
- [31] Bartoloni A, Mantella A, Goldstein BP, Dei R, Benedetti M, Sbaragli S, et al. In-vitro activity of nisin against clinical isolates of *Clostridium difficile*. *Journal of Chemotherapy*. 2004;**16**:119-121. DOI: 10.1179/joc.2004.16.2.119
- [32] Dosler S, Gerceker AA. In vitro activities of nisin alone or in combination with vancomycin and ciprofloxacin against methicillin-resistant and methicillin-susceptible *Staphylococcus aureus* strains. *Chemotherapy*. 2011;**57**:511-516. DOI: 10.1159/000335598
- [33] Gill SR, Fouts DE, Archer GL, Mongodin EF, Deboy RT, Ravel J, et al. Insights on evolution of virulence and resistance from the complete genome analysis of an early methicillin-resistant *Staphylococcus aureus* strain and a biofilm-producing methicillin-resistant *Staphylococcus epidermidis* strain. *Journal of Bacteriology*. 2005;**187**:2426-2438. DOI: 10.1128/JB.187.7.2426-2438.2005
- [34] Melchior MB, Vaarkamp H, Fink-Gremmels J. Biofilms: A role in recurrent mastitis infections? *Veterinary Journal*. 2006;**171**:398-407. DOI: 10.1016/j.tvjl.2005.01.006

- [35] Cao LT, Wu JQ, Xie F, Hu SH, Mo Y. Efficacy of nisin in treatment of clinical mastitis in lactating dairy cows. *Journal of Dairy Science*. 2007;**90**:3980-3985. DOI: 10.3168/jds.2007-0153
- [36] Wu J, Hu S, Cao L. Therapeutic effect of nisin Z on subclinical mastitis in lactating cows. *Antimicrobial Agents and Chemotherapy*. 2007;**51**:3131-3135. DOI: 10.1128/AAC.00629-07
- [37] Fernandez L, Delgado S, Herrero H, Maldonado A, Rodriguez JM. The bacteriocin nisin, an effective agent for the treatment of staphylococcal mastitis during lactation. *Journal of Human Lactation: Official Journal of International Lactation Consultant Association*. 2008;**24**:311-316. DOI: 10.1177/0890334408317435
- [38] Gravesen A, Jydegaard Axelsen AM, Mendes da Silva J, Hansen TB, Knochel S. Frequency of bacteriocin resistance development and associated fitness costs in *Listeria monocytogenes*. *Applied and Environmental Microbiology*. 2002;**68**:756-764
- [39] Willey JM, van der Donk WA. Lantibiotics: Peptides of diverse structure and function. *Annual Review of Microbiology*. 2007;**61**:477-501. DOI: 10.1146/annurev.micro.61.080706.093501
- [40] Giacometti A, Cirioni O, Barchiesi F, Scalise G. In-vitro activity and killing effect of polycationic peptides on methicillin-resistant *Staphylococcus aureus* and interactions with clinically used antibiotics. *Diagnostic Microbiology and Infectious Disease*. 2000;**38**:115-118
- [41] Naghmouchi K, Le Lay C, Baah J, Drider D. Antibiotic and antimicrobial peptide combinations: Synergistic inhibition of *Pseudomonas fluorescens* and antibiotic-resistant variants. *Research in Microbiology*. 2012;**163**:101-108. DOI: 10.1016/j.resmic.2011.11.002
- [42] Dosler S, Gerceker AA. In vitro activities of antimicrobial cationic peptides; melittin and nisin, alone or in combination with antibiotics against Gram-positive bacteria. *Journal of Chemotherapy*. 2012;**24**:137-143. DOI: 10.1179/1973947812Y.0000000007
- [43] Tong Z, Zhang Y, Ling J, Ma J, Huang L, Zhang L. An in vitro study on the effects of nisin on the antibacterial activities of 18 antibiotics against *Enterococcus faecalis*. *PLoS One*. 2014;**9**:e89209. DOI: 10.1371/journal.pone.0089209
- [44] Van Vuuren SF, Nkwanyana MN, de Wet H. Antimicrobial evaluation of plants used for the treatment of diarrhoea in a rural community in northern Maputaland, KwaZulu-Natal, South Africa. *BMC Complementary and Alternative Medicine*. 2015;**15**:53. DOI: 10.1186/s12906-015-0570-2
- [45] Van Vuuren SF, Suliman S, Viljoen AM. The antimicrobial activity of four commercial essential oils in combination with conventional antimicrobials. *Letters in Applied Microbiology*. 2009;**48**:440-446. DOI: 10.1111/j.1472-765X.2008.02548.x
- [46] Brunton LA, Duncan D, Coldham NG, Snow LC, Jones JR. A survey of antimicrobial usage on dairy farms and waste milk feeding practices in England and Wales. *Veterinary Record*. 2012;**171**:296. DOI: 10.1136/vr.100924

- [47] Brumfitt W, Salton MR, Hamilton-Miller JM. Nisin, alone and combined with peptidoglycan-modulating antibiotics: Activity against methicillin-resistant *Staphylococcus aureus* and vancomycin-resistant enterococci. *The Journal of Antimicrobial Chemotherapy*. 2002;**50**:731-734
- [48] Goldstein BP, Wei J, Greenberg K, Novick R. Activity of nisin against *Streptococcus pneumoniae*, *in vitro*, and in a mouse infection model. *The Journal of Antimicrobial Chemotherapy*. 1998;**42**:277-278
- [49] Dempsey CE. The actions of melittin on membranes. *Biochimica et Biophysica Acta*. 1990;**1031**:143-161
- [50] Müller-Auffermann K, Grijalva F, Jacob F, Hutzler M. Nisin and its usage in breweries: A review and discussion. *Journal of the Institute of Brewing*. 2015;**121**:309-319
- [51] Joo NE, Ritchie K, Kamarajan P, Miao D, Kapila YL. Nisin, an apoptogenic bacteriocin and food preservative, attenuates HNSCC tumorigenesis via CHAC1. *Cancer Medicine*. 2012;**1**:295-305. DOI: 10.1002/cam4.35
- [52] Kamarajan P, Hayami T, Matte B, Liu Y, Danciu T, Ramamoorthy A, et al. Nisin ZP, a bacteriocin and food preservative, inhibits head and neck cancer tumorigenesis and prolongs survival. *PLoS One*. 2015;**10**:e0131008. DOI: 10.1371/journal.pone.0131008
- [53] Siegel RL, Miller KD, Jemal A. Cancer statistics, 2017. *CA: A Cancer Journal for Clinicians*. 2017;**67**:7-30. DOI: 10.3322/caac.21387
- [54] National Institute of Health (NIH). Surveillance, Epidemiology and End Results (SEER). [Online]. 2017. Available: <https://seer.cancer.gov/statfacts/html/melan.html> [Accessed: 18 August 2017]
- [55] American Cancer Society (ACS) — Key Statistics for Melanoma Skin Cancer [Online]. 2017. Available: <https://www.cancer.org/cancer/melanoma-skin-cancer/about/key-statistics.html> [Accessed: 13 April 2017]
- [56] Wentzel JF, Lombard MJ, Du Plessis LH, Zandberg L. Evaluation of the cytotoxic properties, gene expression profiles and secondary signalling responses of cultured cells exposed to fumonisin B1, deoxynivalenol and zearalenone mycotoxins. *Archives of Toxicology*. 2017;**91**:2265-2282. DOI: 10.1007/s00204-016-1872-y
- [57] Rishi P, Preet Singh A, Garg N, Rishi M. Evaluation of nisin-beta-lactam antibiotics against clinical strains of *Salmonella enterica* serovar Typhi. *The Journal of Antibiotics*. 2014;**67**:807-811. DOI: 10.1038/ja.2014.75
- [58] Gaspar D, Veiga AS, Castanho MA. From antimicrobial to anticancer peptides. A review. *Frontiers in Microbiology*. 2013;**4**:294. DOI: 10.3389/fmicb.2013.00294
- [59] Swithenbank L, Morgan M. The role of antimicrobial peptides in lung cancer therapy. *Journal of Antimicrobial Agents*. 2017;**3**:134. DOI: 10.4172/2472-1212.1000134
- [60] Ohsaki Y, Gazdar AF, Chen HC, Johnson BE. Antitumor activity of magainin analogues against human lung cancer cell lines. *Cancer Research*. 1992;**52**:3534-3538

- [61] Do N, Weindl G, Grohmann L, Salwiczek M, Koksich B, Korting HC, et al. Cationic membrane-active peptides—Anticancer and antifungal activity as well as penetration into human skin. *Experimental Dermatology*. 2014;**23**:326-331. DOI: 10.1111/exd.12384
- [62] Gregorc V, De Braud FG, De Pas TM, Scalamogna R, Citterio G, Milani A, et al. Phase I study of NGR-hTNF, a selective vascular targeting agent, in combination with cisplatin in refractory solid tumors. *Clinical Cancer Research: An Official Journal of the American Association for Cancer Research*. 2011;**17**:1964-1972. DOI: 10.1158/1078-0432.CCR-10-1376
- [63] Helmbach H, Kern MA, Rossmann E, Renz K, Kissel C, Gschwendt B, et al. Drug resistance towards etoposide and cisplatin in human melanoma cells is associated with drug-dependent apoptosis deficiency. *The Journal of Investigative Dermatology*. 2002;**118**:923-932. DOI: 10.1046/j.1523-1747.2002.01786.x
- [64] Kalal BS, Upadhya D, Pai VR. Chemotherapy resistance mechanisms in advanced skin cancer. *Oncology Reviews*. 2017;**11**:326. DOI: 10.4081/oncol.2017.326

Cytotoxic Effects of Natural Substance

Cytotoxic Colchicine Alkaloids: From Plants to Drugs

Joanna Kurek

Additional information is available at the end of the chapter

<http://dx.doi.org/10.5772/intechopen.72622>

Abstract

Plants produce and store many organic compounds like amino acids, proteins, carbohydrates, fats, and alkaloids, which are usually treated as secondary metabolites. Many alkaloids are biologically active for humans. For thousand years, extracts from plants containing alkaloids had medicinal use as drugs and they owe their powerful effects thanks to presence of alkaloids. Alkaloids have anti-inflammatory, antibacterial, analgesic, local anesthetic, hypnotic, psychotropic, antimutagenic, and antitumor activity. Nowadays, alkaloids from plants are still of great interest to organic chemists, pharmacologists, biologists, biochemists, and pharmacists. Plants of *Liliaceae* family contain colchicine as the main alkaloid, which has cytotoxic activity. Colchicine has limited pharmacological application because of its toxicity, but many derivatives have been synthesized and their cytotoxic activity and tubulin-binding properties have been tested. Many of the synthetic derivatives showed good cytotoxic activity.

Keywords: colchicine, colchinoids, plants containing colchicine alkaloids, cytotoxic compounds, cancer cell lines, cytotoxic activity

1. Introduction

One of the best known biologically active compounds from ancient times is colchicine (**Figure 1**), an alkaloid naturally occurring in *Colchicum autumnale* a plant of *Liliaceae* family and also in *Gloriosa superba*. In the past, extracts from these plants containing colchicine were useful in gout therapy and still are [1]. The anti-gout action of colchicine could be explained by its powerful spindle toxicity [2, 3]. Moreover, colchicine is a useful medicine in the treatment of familial Mediterranean fever (FMF), liver cirrhosis, chronic myelocytic leukemia, Behçet disease, chondrocalcinosis and other microcrystalline arthritis also more recently in cardiovascular diseases, Sweet's syndrome, and hepatic disorders (HCC hepatocellular carcinoma) [4–12].

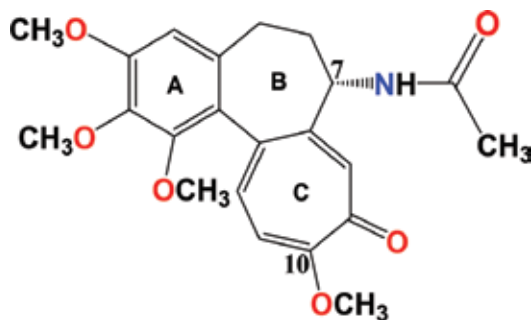


Figure 1. Colchicine molecule (color version available on the online version).

In 2009, the FDA approved colchicine for the treatment of gout and familial Mediterranean fever (FMF) [1]. Recent investigations utilizing large cohorts of gout patients who have been taking colchicine for years have demonstrated novel applications within oncology, immunology, cardiology, and dermatology [4, 13–16]. Some emerging dermatologic uses include the treatment of epidermolysis bullosa acquisita, leukocytoclastic vasculitis, and aphthous stomatitis. Colchicine has also anti-inflammatory and anticancer properties. Colchicine has been proven to have a fairly narrow range of effectiveness as a chemotherapy agent though it is also occasionally used in veterinary medicine to treat cancers in some animals. Nowadays, colchicine is very useful as an antimetabolic agent in cancer research involving cell culture [17]. Colchicine has limited medical usage because of its high toxicity [18]. Because of this reason, many attempts have been made to design, synthesize new colchicine derivative and to screen them as cytotoxic agents to search more biologically active/effective compounds with lower toxicity.

2. Cytotoxic colchinoids in plants

Colchicine **1** and related alkaloids were isolated from many plants of *Liliaceae* family. The *Colchicum* species are most known plants in which colchicine exists in majority and other colchicine-like derivatives are in minority. Unripe seeds of *Colchicum* plants were found to contain 40% less colchicine **1** than fully ripe one [19]. Colchicine occurs in all parts of *Colchicum* plants but especially in seeds and bulbs. One of the most known plants which contain colchicine **1** is meadow saffron (*C. autumnale*, **Figure 2**). The other plants of *Colchicum* sp. are: *C. crocifolium*, *C. turicum*, *C. kesselvoingii*, *C. luteum*, *C. byzantinum*, *C. crocifolium*, *C. szovitsii*, *C. soboliferum*, and many more [20]. Beside **1** in these plants of *Colchicum* species also are present: 2-demethylcolchicine **2**, 3-demethylcolchicine **3**, demecolcine **4**, 2-demethylcolchicine **5**, 3-demethylcolchicine **6**, *N*-methyl-demecolcine **7**, 3-demethyl-*N*-methyl-demecolcine **8**, *N*-formyl-*N*-deacetylcolchicine **9** [19], *N*-deacetylcolchicine **10**, *N*-deacetylcolchicine **11**, and colchicine **12**. Many of colchicine alkaloids exist in plants in glycoside form [21, 22]. Colchicine and its derivatives are also present in other plants like: *Gloriosa superba*, *Merendera* species (*M. kurdica*, *M. sobolifera*, *M. vaddeana*, *M. robusta*, and many more), *Bulbocodium vernum*, *Androcymbium palaestinum*, and *Kreysigia multiflora* [20, 23]. In *Gloriosa superba* plants were found



Figure 2. Meadow saffron *Colchicum autumnale*: bulb, flowers, and leaves (color version available on the online version). (*author's own photos).

alkaloids: **1**, **2**, **5**, **6**, 2,3-*O*-didemethylcolchicine **13**, 2,3-*O*-didemethyl-*N*-deacetylcolchicine **14**, and 2,3-*O*-didemethyl-*N*-formyl-*N*-deacetylcolchicine **15** [22]. More recently, a new colchicine glycoside, 3-*O*-demethylcolchicine-3-*O*- α -*D*-glucopyranoside **41** has been isolated from *Gloriosa superba* seeds [22]. Moreover, in plants extracts were also isolated photolysis products of colchicine like α -lumicolchicine, β -lumicolchicine, γ -lumicolchicine, and their 3-*O*-demethyl derivatives [24, 25].

3. Unusual chemical structure of colchinoids

Colchicine (**1**) is an alkaloid with unusual structure and has the whole family of structural relations. This alkaloid was isolated in 1820 by Pelletier and Caventou [26]. Although listed at this point, colchicines are biogenetically very close to the isoquinoline alkaloids. Colchicines possess exocyclic N-atoms [15]. Corrected structure of colchicine molecule with seven-membered C ring proposed Dewar in 1945 [27]. Colchicine possesses both one stereogenic center at C7 and chirality axis, since the two rings A and C are not positioned in coplanar fashion (atropisomerism). In naturally occurring (-)-*aR*,7*S*-colchicine, the two rings (A and C) are oriented in a clockwise manner [15].

4. Natural, semi-synthetic, and synthetic colchicines

Many naturally occurring colchicine alkaloids (some of them are listed in **Figures 3** and **4**) have been converted into semi-synthetic compounds and have been prepared as potential antitumor agents. Usually starting with colchicine **1** hundreds of semi-synthetic and synthetic colchicine derivatives have been synthesized [28–30].

Starting compound was 1,2-*O*-didemethylcolchicine **16** converted into 1,2,3-*O*-tridemethylcolchicine **17** [28–30], 1,2,3-*O*-tridemethyl-*N*-deacetylcolchicine **18** [28–30], 1,2,3-*O*-tridemethyl-*N*-deacetyl-*N*-trifluoroacetylcolchicine **19** [28–30], and 1,2,3-*O*-tridemethyl-*N*-deace

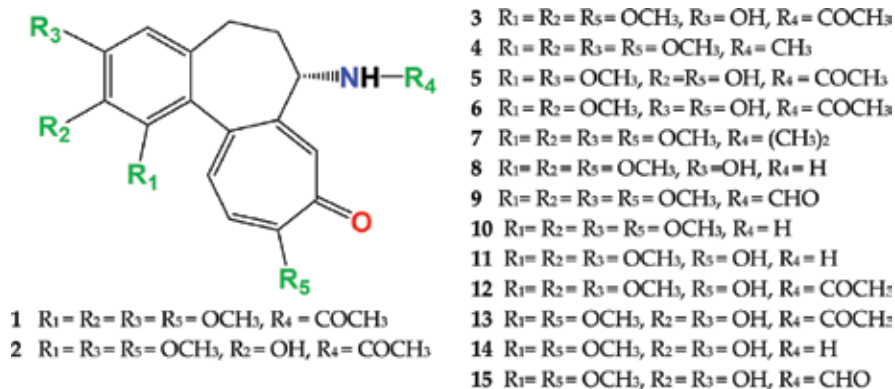


Figure 3. Naturally occurring colchicine derivatives (color version available on the online version).

tyl-*N*-formyl(2,4,6-trihydroxyphenyl)colchicine **20** [28–30]. 1,2-didemethyl-*N*-deacetylcolchicine **21** was converted into: 1,2-didemethyl-*N*-deacetyl-*N*-(propane-2,3-diol)colchicine **22** [31] and 1,2-didemethyl-*N*-deacetyl-*N*-(propane-2,3-diacetyl)colchicine **23** [31]. Derivatives **24** with halogen substituent and with alkyl, aryl, or hydrogen **25** at C-10 position have also been obtained [32]. 10-demethoxy-10-azido-colchicine **26** [33] and 10-demethoxy-10-amino-colchicine = colchiceinamide **27** [34]. 2-Demethyl-*N*-benzylidemecolchicine = speciocolchicine **28** [35] has been prepared from 2-demethylidemecolchicine. 10-*O*-*p*-tosylsulfonylcolchicine **29** can be converted into compound **24** [36]. One of the interesting derivatives modified at C-7 position by –sulfur-containing substituent is *N*-deacetyl-*N*-(2merkaptoacetyl)-colchicine **30** (DAMAcolchicine) [37]. Glycopeptide dendrimer conjugates of colchicine modified at C-7 have been synthesized and tested as mitosis inhibitors [38]. *N*-substituted derivatives colchicine-lipids with different length of alkyl chain of olenyl and stearyl groups have been obtained and their interaction with lipid membrane has been studied [39]. Ring-C-modified colchicine analogs with different nitroso substituents in Diels-Alder reaction have been obtained [40]. 3-Demethyl derivative of colchicine and 10-methylthiocolchicine have been obtained also by regioselective bioconversion of **1** and **31** by microorganisms *Bacillus* IND-B 375 and strain of *Bacillus megaterium* ACBT03 [41, 42].

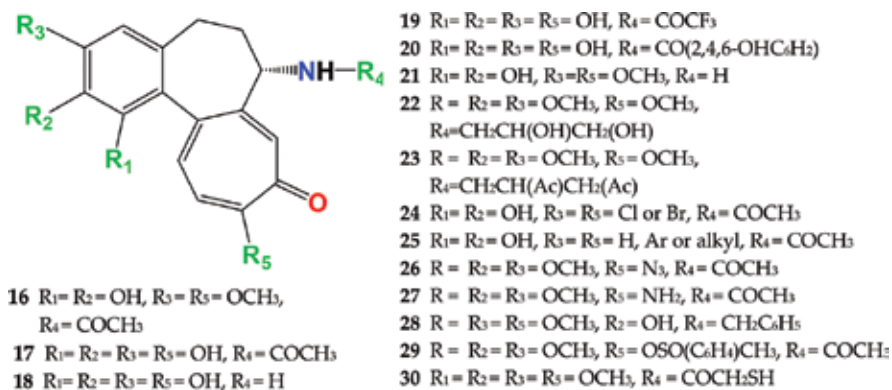
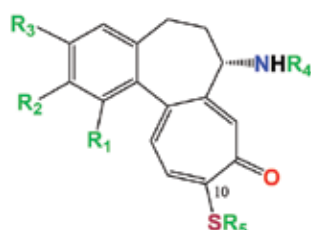


Figure 4. Natural, seminatural and synthetic colchicines (chosen examples).

4.1. C-10 sulfur-containing derivatives

After many years of searching colchicine derivatives as good cytotoxic agents, it was established that exchange of methoxyl substituent $-\text{OCH}_3$ at C-10 position to amino group (NH_2 , NHR_1 , or NR_1R_2) and especially to methylthio ($\text{CH}_3\text{S}-$) or alkylthio increases cytotoxic activity. Thiocolchicine **31** is a colchicine **1** derivative used in the therapy of some diseases [43] and extensively studied in the field of oncological research as antimetabolic agent [44–46]. There were mentioned some of wide range of synthesized colchicine compounds with thio substituent at C-10 position during last 60 years. Derivatives with alkylthio substituent at C-10 position have been synthesized from colchicine **31–35** (Figure 5) [47]. *N*-deacetyl-10-methylthiocolchicine **36** was converted into compounds: **37** [44], **38** and **39** [44]. 10-Methylthiocolchicine was modified at C-3 position to compound 3-demethoxy-3-amino-10-methylthiocolchicine **40** and then to 3-demethoxy-3-glycosylaminothiocolchicines **41–47** (Figure 5) [48]. From derivatives **48–52**



- 31** $\text{R}_1 = \text{R}_2 = \text{R}_3 = \text{OCH}_3$, $\text{R}_5 = \text{CH}_3$,
 $\text{R}_4 = \text{COCH}_3$
32 $\text{R}_1 = \text{R}_2 = \text{R}_3 = \text{OCH}_3$, $\text{R}_5 = \text{C}_2\text{H}_5$,
 $\text{R}_4 = \text{COCH}_3$
33 $\text{R}_1 = \text{R}_2 = \text{R}_3 = \text{OCH}_3$, $\text{R}_5 = n\text{C}_3\text{H}_7$,
 $\text{R}_4 = \text{COCH}_3$
34 $\text{R}_1 = \text{R}_2 = \text{R}_3 = \text{OCH}_3$, $\text{R}_5 = i\text{C}_3\text{H}_7$,
 $\text{R}_4 = \text{COCH}_3$
35 $\text{R}_1 = \text{R}_2 = \text{R}_3 = \text{OCH}_3$, $\text{R}_5 = n\text{C}_4\text{H}_9$,
 $\text{R}_4 = \text{COCH}_3$
36 $\text{R}_1 = \text{R}_2 = \text{R}_3 = \text{OCH}_3$, $\text{R}_5 = \text{CH}_3$, $\text{R}_4 = \text{H}$
37 $\text{R}_1 = \text{R}_2 = \text{R}_3 = \text{OCH}_3$, $\text{R}_5 = \text{CH}_3$,
 $\text{R}_4 = \text{CO}(\text{CH}_2)_n\text{CH}_3$, $n = 0-8$
38 $\text{R}_1 = \text{R}_2 = \text{R}_3 = \text{OCH}_3$, $\text{R}_5 = \text{CH}_3$,
 $\text{R}_4 = \text{CO}(\text{Ph or Ar})$
39 $\text{R}_1 = \text{R}_2 = \text{R}_3 = \text{OH}$, $\text{R}_5 = \text{CH}_3$,
 $\text{R}_4 = \text{CH}_2\text{C}_6\text{H}_4\text{-}p\text{NO}_2$
40 $\text{R}_1 = \text{R}_2 = \text{OCH}_3$, $\text{R}_3 = \text{NH}_2$, $\text{R}_5 = \text{CH}_3$,
 $\text{R}_4 = \text{COCH}_3$
41 $\text{R}_1 = \text{R}_2 = \text{OCH}_3$, $\text{R}_5 = \text{CH}_3$,
 $\text{R}_4 = \text{COCH}_3$, $\text{R}_3 = D\text{-glucopyranosyl}$,
42 $\text{R}_1 = \text{R}_2 = \text{OCH}_3$, $\text{R}_5 = \text{CH}_3$,
 $\text{R}_4 = \text{COCH}_3$, $\text{R}_3 = D\text{-arabinopyranosyl}$,
43 $\text{R}_1 = \text{R}_2 = \text{OCH}_3$, $\text{R}_3 = \text{CH}_3$, $\text{R}_4 = \text{COCH}_3$,
 $\text{R}_5 = D\text{-lyxopyranosyl}$,
44 $\text{R}_1 = \text{R}_2 = \text{OCH}_3$, $\text{R}_3 = D\text{-xylopyranosyl}$,
 $\text{R}_5 = \text{CH}_3$, $\text{R}_4 = \text{COCH}_3$
45 $\text{R}_1 = \text{R}_2 = \text{OCH}_3$, $\text{R}_5 = \text{CH}_3$, $\text{R}_4 = \text{COCH}_3$,
 $\text{R}_3 = L\text{-rhamnopyranosyl}$
46 $\text{R}_1 = \text{R}_2 = \text{OCH}_3$, $\text{R}_3 = D\text{-manopyranosyl}$,
 $\text{R}_5 = \text{CH}_3$, $\text{R}_4 = \text{COCH}_3$

- 47** $\text{R}_1 = \text{R}_2 = \text{OCH}_3$, $\text{R}_3 = L\text{-fucopyranosyl}$,
 $\text{R}_5 = \text{CH}_3$, $\text{R}_4 = \text{COCH}_3$
48 $\text{R}_1 = \text{R}_2 = \text{OCH}_3$, $\text{R}_3 = \text{OH}$, $\text{R}_5 = \text{CH}_3$, $\text{R}_4 = \text{COCH}_3$
49 $\text{R}_1 = \text{R}_3 = \text{OH}$, $\text{R}_2 = \text{OCH}_3$, $\text{R}_5 = \text{CH}_3$, $\text{R}_4 = \text{COCH}_3$
50 $\text{R}_1 = \text{OCH}_3$, $\text{R}_2 = \text{R}_3 = \text{OH}$, $\text{R}_5 = \text{CH}_3$, $\text{R}_4 = \text{COCH}_3$
51 $\text{R}_1 = \text{R}_3 = \text{OCH}_3$, $\text{R}_2 = \text{OH}$, $\text{R}_5 = \text{CH}_3$, $\text{R}_4 = \text{COCH}_3$
52 $\text{R}_1 = \text{R}_2 = \text{OH}$, $\text{R}_3 = \text{OCH}_3$, $\text{R}_5 = \text{CH}_3$, $\text{R}_4 = \text{COCH}_3$
53 $\text{R}_1 = \text{R}_3 = \text{Ac}$, $\text{R}_2 = \text{OCH}_3$, $\text{R}_5 = \text{CH}_3$, $\text{R}_4 = \text{COCH}_3$
54 $\text{R}_1 = \text{OCH}_3$, $\text{R}_2 = \text{R}_3 = \text{Ac}$, $\text{R}_5 = \text{CH}_3$, $\text{R}_4 = \text{COCH}_3$
55 $\text{R}_1 = \text{R}_3 = \text{OCH}_3$, $\text{R}_2 = \text{Ac}$, $\text{R}_5 = \text{CH}_3$, $\text{R}_4 = \text{COCH}_3$
56 $\text{R}_1 = \text{R}_2 = \text{OCH}_3$, $\text{R}_3 = \text{Ac}$, $\text{R}_5 = \text{CH}_3$, $\text{R}_4 = \text{COCH}_3$
57 $\text{R}_1 = \text{R}_2 = \text{Bz}$, $\text{R}_3 = \text{OCH}_3$, $\text{R}_5 = \text{CH}_3$, $\text{R}_4 = \text{COCH}_3$
58 $\text{R}_1 = \text{OH}$, $\text{R}_2 = \text{R}_3 = \text{OCH}_3$, $\text{R}_5 = \text{CH}_3$, $\text{R}_4 = \text{COCH}_3$
59 $\text{R}_1 = \text{R}_3 = \text{OCH}_3$, $\text{R}_2 = \text{OH}$, $\text{R}_5 = \text{CH}_3$, $\text{R}_4 = \text{COCH}_3$
62 $\text{R}_1 = \text{R}_2 = \text{OCH}_3$, $\text{R}_3 = \text{OCH}_2\text{CH}(\text{OH})\text{CH}_2\text{OH}$,
 $\text{R}_5 = \text{CH}_3$, $\text{R}_4 = \text{COCH}_3$
63 $\text{R}_1 = \text{R}_2 = \text{OCH}_3$, $\text{R}_3 = \text{OCH}_2\text{CH}(\text{OH})\text{CH}_2\text{NH}_2$,
 $\text{R}_5 = \text{CH}_3$, $\text{R}_4 = \text{COCH}_3$
64 $\text{R}_1 = \text{R}_2 = \text{OCH}_3$, $\text{R}_3 = \text{OCH}_2\text{CO}_2\text{H}$, $\text{R}_5 = \text{CH}_3$,
 $\text{R}_4 = \text{COCH}_3$
65 $\text{R}_1 = \text{R}_2 = \text{OCH}_3$, $\text{R}_3 = \text{OCH}_2\text{CH}(\text{Cl})\text{CH}_2\text{OH}$,
 $\text{R}_5 = \text{CH}_3$, $\text{R}_4 = \text{COCH}_3$
66 $\text{R}_1 = \text{R}_2 = \text{R}_3 = \text{OCH}_3$, $\text{R}_5 = \text{CH}_3$,

 $\text{R}_4 =$
67 $\text{R}_1 = \text{R}_2 = \text{R}_3 = \text{OCH}_3$, $\text{R}_5 = \text{CH}_3$,

 $\text{R}_4 =$
68 $\text{R}_1 = \text{R}_2 = \text{R}_3 = \text{OCH}_3$, $\text{R}_5 = \text{CH}_3$,

 $\text{R}_4 =$
69 $\text{R}_1 = \text{R}_3 = \text{OCH}_3$, $\text{R}_4 = \text{COCH}_3$, $\text{R}_5 = \text{CH}_3$,
 $\text{R}_2 = -\text{OCOCH}_2\text{NCH}_3$
70 $\text{R}_1 = \text{R}_3 = \text{OCH}_3$, $\text{R}_4 = \text{COCH}_3$, $\text{R}_5 = \text{CH}_3$,
 $\text{R}_2 = -\text{OCOCH}_2\text{NCH}_3\text{-L-tartrate}$
71 $\text{R}_1 = \text{R}_2 = \text{R}_3 = \text{OCOCH}_3$, $\text{R}_5 = \text{SCH}_3$,
 $\text{R}_4 = \text{CO}_2\text{C}_6\text{H}_4\text{-}p\text{NO}_2$

Figure 5. Seminal and synthetic thiocolchicines (chosen examples).

esters of 1-*O*-demethyl, 2-*O*-demethyl and 3-*O*-demethylthiocolchicine were also obtained **53–57** (**Figure 5**) [49]. 10-methylthiocolchicine has been demethylated to 1-demethyl-10-methylthiocolchicine **58**, 2-demethyl-10-methylthiocolchicine **59**, and 1,2-*O*-didemethylthiocolchicine **52** then **58** and **59** have been oxidized to quinine (**Figure 6**) [50]. Complex ethers of 3-demethyl-10-methylthiocolchicine **62–65** have been prepared as potential pharmaceuticals [51]. The C-7 amide group of ring B with (*R*)-configuration [15] is also one of the crucial factors which decide of molecule's anticancer activity. Eight synthetic derivatives of *N*-deacetylthiocolchicine have been obtained and tested against cancer cell lines and 3 of them showed good activity **66**, **67**, **68** [52]. Thiocolchicine derivative **69** has been modified at C-2 carbon atom and then converted into salt **70** [53]. Among 37 thiocolchicine derivatives tested, compound **71** showed good activity as inhibitor of topoisomerases *in vitro* [54]. *N*-substituted thiocolchicine derivatives and their water-soluble phosphate salts **72–78** (and 5 others) have been obtained and their activity have been tested against cancer cell lines [55] (**Figure 7**).

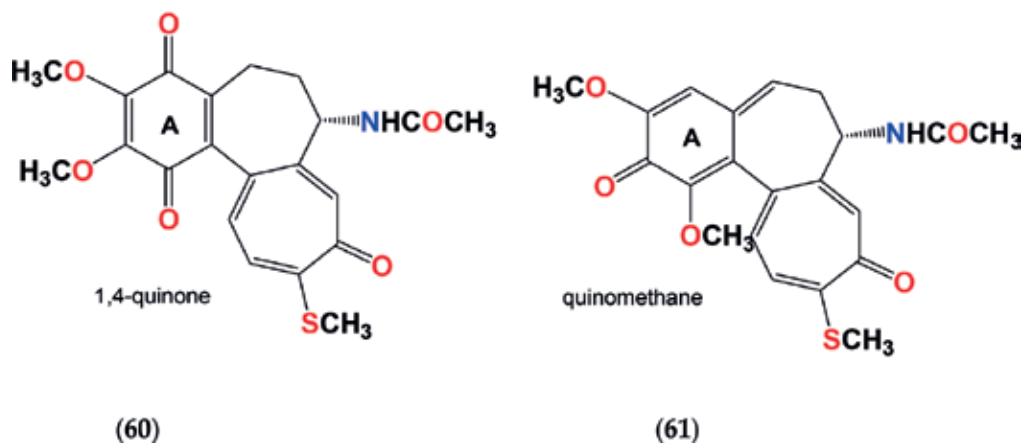


Figure 6. Thiocolchicines with modified ring A: **60** 1,4-quinone and **61** quinomethane.

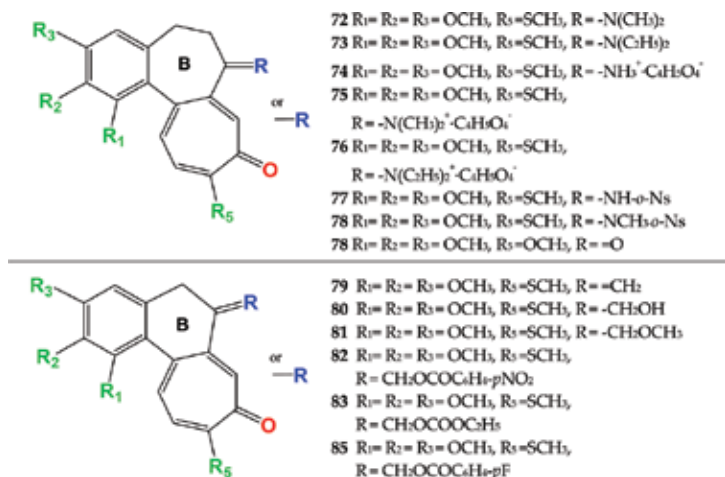


Figure 7. Thiocolchicines modified on ring B.

From compound **79** acetamido $-\text{NHCOCH}_3$ substituent from C-7 has been removed and replaced by $=\text{CH}_2$ group [56]. Hybrids of vindoline, anhydrovinblastine, and vinorelbine with thiocolchicine **31** podophyllotoxin and baccatinIII have been tested in arresting cell cycle and cytotoxic activity [57]. Series of thiocolchicine-podophyllotoxin conjugates have been obtained and their tubulin activity has been tested [58].

Compounds **80**, **81**, **82**, **83**, **84**, and **85** have been synthesized by four synthesis steps from colchicine **1** to thiocolchicine **31** then to 7-deacetylthiocolchicine **36** which has been converted into **80** and then to **81**, **82**, **83**, **84**, **85** and eight others which possess six-membered ring B [59].

5. Bioactivity of colchicine and its derivatives

Colchicine **1** has been known and used from ancient times, despite its toxicity to cure acute gout attacks because of its anti-inflammatory properties. After administration of colchicine **1**, it is mainly metabolized in liver *via* demethylation by cytochrome P450 system (isoform CYP 3A4) to 2-demethylcolchicine **2** and 3-demethylcolchicine **3** [11]. Colchicine **12** was described as a metabolite in rats produced by cytochrome P450 3A4 isoform [60], but it does not occur in humans *in vivo* [61]. Colchicine's most common toxicity is gastrointestinal (nausea, vomiting, diarrhea, abdominal pain) which occurs during first 24 hours after overdose. Toxic effect of colchicine appears after oral administration of 7–60 mg of colchicine and is fatal, symptoms occur in about 4 h and death in about 4 days. Severe colchicine overdose may be treated with a colchicine-specific antigen-binding immunoglobulin [11].

Beside colchicine **1** has many naturally occurring derivatives many attempts have been made to discover more effective and less toxic analogs by modifying the substituents of its basic structure.

Colchicine blocks mitosis metaphase due to different anti-mitotic effects: disruption of mitotic spindle formation and second disruption of the sol-gel formation. Colchicine can also interact with lipid membranes. The interaction between colchicine and membrane results with significant alternations of both the properties of the lipid membrane and alkaloid [39]. Tubulin is an α and β heterodimer initially identified as the cellular colchicine-tubulin protein [10, 62]. Colchicine can interact with human serum albumin, which has been studied by spectroscopic method [63, 64]. Study of colchicine-tubulin complex showed that colchicine binds at the location where it prevents curved tubulin from adopting a straight structure, which inhibits assembly. Microtubules are cytoskeletal polymers of tubulin involved in many cellular functions [65]. Their dynamic instability is controlled by many proteins and compounds such as colchicine.

Colchicine and its biologically active derivatives, especially thiocolchicine and its derivatives, have been extensively tested on cancer cell lines for *in vitro* cytotoxicity, in mice, evaluated for inhibition of tubulin polymerization [66], on axonal cytoskeleton of rat peroneus nerve [67]. Thiocolchicine has been studied as a potent compound to treat Peyronie's disease [68]. Derivatives of thiocolchicine have been tested *ex vivo* to human T-lymphoblastoid (CEM) cells [69].

6. Cytotoxic activity of colchicine and its derivatives

Cytotoxic activity of colchicine has been known for many decades. In 1968, it was known that colchicine can efficiently bind to tubulin. Its antitumor activity derives from its tubulin binding activity [39]. Nowadays, it is known that colchicine can act with α and β tubulin in microtubules and disrupt the formation of microtubules. In past decades, many attempts have been made to design and synthesize new colchicine derivatives which could be less toxic and more effective compounds than colchicine as cytotoxic agents. On the basis of years of screening colchicine derivatives, their activity against human cancer cell lines structure: activity relationship has been established. It was found out that derivatives with alkylthio substituents at C-10 position and modified at C-7 usually are more active and less toxic than colchicine. One of the most known active semi-synthetic colchicine derivatives is thiocolchicine (10-methylthiocolchicine) **31**. Some of the obtained derivatives seem to be effective and promising agents against selected human cancer cell lines and possibly in the future could be used as anticancer drugs. Cytotoxic activity of colchicine derivatives has been tested in *in vitro* experiments on mice (KLN205, A2C12, yB8, yD12, β D10, yA7, yA3, B3, β D5, A2B1, yD1) [70] or hamster (CHO-K1) [45] cancer cell lines and human cancer cell lines such as: MFC-7 human breast adenocarcinoma [40, 45, 47, 54, 71, 72] and MDA-MB-231 [47, 72] human Caucasian breast adenocarcinoma, SK-Br-3 human breast cancer cell line [46], DLD-1 [47] and LOVO [47] human colon adenocarcinoma, HCT-5 colon cancer, HCT-15 colon carcinoma [44, 45], A549 human lung adenocarcinoma [44, 52–55, 57, 58, 70], DMS-114 small lung cell cancer [44], SKOV-3 ovarian cancer [46], OVCAR-3 ovarian carcinoma [44], A2780 human ovarian carcinoma cell line [73], 1A9 human ovarian carcinoma [53], KB human epidermoid carcinoma [46, 53, 57], PC-3 prostate cancer [40], H460 human large cell lung carcinoma [71], SF268 human astrocytoma [71], HTC-8 human ileocecal carcinoma cell [46, 57], DU-145 human prostate carcinoma [46], SKMEL-2 human skin malignant melanoma [46, 54], SKMEL-5 human skin malignant melanoma [44], RXF-631 renal carcinoma [44], SNB-19 CNS carcinoma [44], RPMI-7951 malignant melanoma [56], TE671 human medulloblastoma [56], HepG2 human hepatocyte carcinoma [70], CaCo-2 human colon carcinoma [70], and CAKI-1 kidney carcinoma [54]. As a positive control in cytotoxic tests were used: colchicine, doxorubicin or camptothecin and MTT tests [39, 57] or SRB tests MTS assay [70]. Values of IC_{50} for compounds **1**, **4**, **7**, **8**, **31**, **32**, **33**, **34**, and **35** are given in **Table 1**. Naturally occurring colchicine and other colchicine-like alkaloids were tested against human cancer cell lines and usually showed much better activity than parent compound.

Thiocolchicine **31** showed good activity against A2780 human ovarian carcinoma cell line with value of IC_{50} 1.6 nM [73]. The water-soluble compound **69** (salt of succinic acid of *N,N*-dimethyl-*N*-deacetylthiocolchicine) showed selective activity against HTC-8 0.022 μ g/mL and SK-BR-3 0.012 0.022 μ g/mL cancer cells [46]. The second salt of succinic acid of *N*-deacetylthiocolchicine **72** showed activity against five of tested cancer cell lines 0.001–0.005 μ g/mL (HTC-8, SK-BR-3, A549, DU145, KB) [46].

Thiocolchicine derivative **83** modified at C-7 position showed good cytotoxic activity against A549, RPMI-7951, and TE671 cancer cell lines 0.001 nM/mL [56]. Derivatives **66**, **67**, and **68** showed good cytotoxic activity against A549, SKOV-3, SKMEL-2, HCT-15, and MCF-7 cancer cell lines with IC_{50} values 5.2–29.8 nM [52]. **69** and **70** showed significant activity against

Cell line compound	DLD-1	LoVo	MCF-7	MDA MB-231	H460	SF268
1	43.0 [47]	118.8 [47]	41.3 [47]	25.3 [47]	32 [71]	25 [71]
4	—	—	52 [71]	—	44 [71]	39 [71]
7	—	—	151 [71]	—	165 [71]	354 [71]
8	—	—	2440 [71]	—	3200 [71]	981 [71]
31	4.2 [47]	13.6 [47]	55.5 [47]	81.2 [47]	—	—
32	51.2 [47]	19.5 [47]	56.1 [47]	148.3 [47]	—	—
33	71.8 [47]	56.1 [47]	764.4 [47]	704.2 [47]	—	—
34	177.3 [47]	149.6 [47]	564.2 [47]	1103.8 [47]	—	—
35	316.7 [47]	438.0 [47]	873.6 [47]	1773.3 [47]	—	—
Doxorubicin	510.6 [47]	520.2 [47]	1210.1 [47]	935.5 [47]	—	—
Camptothecin	—	—	0.309 [71]	—	0.024 [71]	0.043 [71]

Table 1. The IC_{50} values (nM) of compounds tested against cancer cell lines: MCF-7 [47], MDA-MB-231 [47], DLD-1 [47], LoVo [47], H460 [71] and SF268 [71]. Data were obtained from triplicate experiments. Doxorubicin was used as positive control (MTT test) [47].

tumor cell lines: A549, 1A9, and KB with values of IC_{50} 0.02–0.06 $\mu\text{g}/\text{mL}$ [53]. Hybrids of vindoline, anhydrovinblastine, and vinorelbine with thiocolchicine have been tested in arresting cell cycle and against A549 cell lines [57].

Many of tested colchicine derivatives and thiocolchicine derivatives obtained by partial synthesis were assayed measuring mitotic arrest in L1210 murine leukemia cell cultures [70], their binding to tubulin *in vitro*, their antitumor activity against the P388 lymphocytic leukemia screen in mice, and their inhibition of swelling produced in rat paws by injection with uric acid. To measure inhibition in binding different colchicine derivatives to tubulin, many tests have been used *in vitro* and *in vivo*: CD spectra [74], radiolabeled compounds, and cancer cell lines.

The effect on tubulin can be assessed *in vitro* by measuring inhibition of tubulin polymerization [53, 66, 70] and binding of radiolabeled colchicine to tubulin [75]. Significant inhibition in binding to tubulin greater than colchicine **1** was observed with 3-demethylcolchicine (**3**), 10-methylthiocolchicine **31**, and 3-demethyl-10-methylthiocolchicine **48** [76]. Significant inhibition of binding radiolabeled colchicine to purified tubulin was observed with thiocolchicine and 3-demethylthiocolchicine (**Table 2**).

Colchicine showed to be too much toxic to be used as a drug candidate for cancer diseases. Colchicine is much more less toxic than colchicine [77]. Through past decades many derivatives were tested against cancer cell lines to checked their cytotoxic activity and activity *in vitro* to disrupt microtubule network and spindle formation. Binding of colchicine analogs to tubulin measured by competition for labeled colchicine is for **1** 5×10^{-6} , **31** 4×10^{-6} , and **41** $2\text{--}3 \times 10^{-5}$ [76]. Inhibition of tubulin assembly by thiocolchicine derivatives **69** and **70** is IC_{50} 8.7 μM and IC_{50} 3.8 μM , respectively [53]. The compounds **72**, **76**, and **77** showed potent inhi-

Inhibitor added	Inhibitor:radiolabeled colchicine (%)	
	1:1	10:1
Non-radiolabeled 1	25	83
2	14	60
3	25	77
31	55	94
48	41	89

Table 2. Inhibition [%] of binding radiolabeled colchicine to purified tubulin [76].

bition of tubulin assembly $IC_{50} = 0.8\text{--}1.1 \mu\text{M}$, for comparison for **1** is $1.5 \mu\text{M}$ [54]. Compound **83** showed good inhibition of tubulin polymerization and inhibition of colchicine binding (%), IC_{50} $3.4 \mu\text{M}$ and 60% and **79** IC_{50} $2.4 \mu\text{M}$ and 91%; **82** IC_{50} $6.6 \mu\text{M}$ and 78% [56]. Hybrid thicolchicine-vindoline causes cell cycle arrest in the G2/M phase [57]. Inhibition of tubulin polymerization has been studied with thicolchicine-podophyllotoxin conjugates, where **31** was modified at C-7 substituent [63].

In vivo P388 mouse leukemia test data P388 for colchicine **1** is 0.5, **31** is 0.18, and **48** is 5 [mg/kg] [76].

7. Pharmacological use of colchinoids

7.1. Colchicine prodrugs

Some of colchicines have been tested as prodrugs. Zyn-linked™ colchicines which are conjugates of colchicine derivatives with proprietary lipophylic molecules (ZYN-160 4-formyl-thicolchicine, PKH139, PKH153, PKH147) via acid cleavable linkages (PKH155, PKH159, ZYN-217) produced prodrugs (PKH140, PKH154, PKH156, PKH158, ZYN-162) with enhanced antitumor activity (A2780 human ovarian carcinoma cell line) [73]. Conjugates have blocked cell in the G2/M phase of the cell cycle and were up to 100-fold less active *in vitro* than unlinked drug [73]. Ring B-modified colchicine derivative CT20126 showed immunosuppressive and cytotoxic activity [78]. *N*-acetylcolchinol phosphate is a prodrug (ZD6126) derived from colchicine [79]. Thicolchicine dimers IDN5404 and IDN5676 have been tested as prodrugs active as inhibitor of Topo-I and without loss of the spindle poison properties [80]. Colchitaxel is another active compound with cytotoxic activity which combines colchicine and paclitaxel [81].

7.2. Drugs with colchicine

Besides antitumor activity, colchicine has anti-inflammatory properties. Colchicine reduces the formation of uric acid crystals in the affected joint and thereby reduces the amount of acute inflammation and pain. It also decreases the levels of uric acid in the blood or the amount that is excreted in the urine. More recently colchicine has been proposed as a potential drug in treatment for various conditions (except gout), what can open new way of its possible future application. Nowadays, colchicine is the useful drug in illnesses: familial Mediterranean fever (FMF),

liver cirrhosis, disk problems, Behçet syndrome, prevention of post-pericardial syndrome, primary biliary cirrhosis, hepatic cirrhosis, dermatitis herpetiformis, Paget's disease of bone, pseudogout, and idiopathic pulmonary fibrosis.

Colchicine can be used to treat familial Mediterranean fever in children 4 years of age and older.

Colchicine is available as a tablet, capsule, and a gel. In tablet form, it is available in a generic 0.6 mg tablet and as Colcrys 0.6 mg tablet. It is available as a capsule in a generic form of 0.6 mg and as Mitigare 0.6 mg capsule. There is a topical gel form of *Colchicum autumnale*, available as ColciGel. Colchicine is commonly administered orally, and use of the topical gel is rare. Due to toxicity of colchicine from 2009, the injectable form is not available. Dosing is dependent on age of patient and kind of illness.

Usually, colchicine is a major component of tablets or capsules in which in a single tablet or capsule its amount is in range of 0.5 or 0.6 mg, sometimes is used as an injection (disk problems). Usually a man/woman of 60 kg takes a dose of 0.5–4.8 mg/day [82, 83]. Since 2008, only oral use of colchicine for patients is possible because of 50 cases of serious adverse events [84]. The known medicines with colchicine are: Colchicum Dispert[®], Colcrys, Mitigare, and Colchimax. Col-Benemid or Proben-C is a drug where next to colchicine probenecid is added as uricosuric agent.

7.3. Drugs with colchicine derivatives

One of the known colchicine derivatives that has been used for the treatment of Hodgkin's lymphoma and chronic granulocytic leukemia is *N*-deacetyl-*N*-methylcolchicine, brand name is Colcemid [72]. Moreover, its efficacy against melanoma and prostatic cancer has been established.

Thiocolchicoside (=glucopyranosyl derivative of the semi-synthetic 3-*O*-demethylthiocolchicine 41), is well-known as a muscle relaxing agent and as an anti-inflammatory drug substance [85]. This compound is registered in different countries under the trade names of Colcamyl, Coltramyl, Coltrax, Miorel, and Musco-Ril. Muscle spasm is one of the main factors responsible for chronic pain, and because this particular drug reduces muscle tone, it is used in therapy for the treatment of contractures and inflammatory conditions that affect the muscular system [48].

8. Docking studies

A new tool for searching new potent anticancer agents is docking studies. Some years ago it became possible to study new compounds of possible biological activity by new technical methods like molecular modeling and docking studies [37, 86–90].

9. Conclusion

The way to search new colchicine derivatives especially thiocolchicine derivatives seems to be worth trying because of its promising cytotoxicity. Many new derivatives have been obtained, have been tested for many different cancer cell lines, and many of them seem to be promising anticancer agents in the future.

Scientists still keep designing and synthesizing more and more colchicine derivatives for searching almost ideal anticancer agent. New methods, such as molecular modeling and docking studies, seem to be useful tool in searching for new colchicine derivatives as effective cytotoxic agents.

Conflict of interest

The author declares no conflict of interest.

Author details

Joanna Kurek

Address all correspondence to: joankur@amu.edu.pl

Chemistry Department, Adam Mickiewicz University, Poznań, Poland

References

- [1] Roubille F, Kritikou E, Busseuil D, Barrère-Lemaire S, Tardif J-C. Colchicine: An old wine in a new bottle? *Anti-Inflammatory and Anti-Allergy Agents in Medicinal Chemistry*. 2013;**12**:1-23. DOI: 10.2174/187152313804998623
- [2] Cook JW, Loudon JD. In: Manske RH. editor. *The Alkaloids*. Vol. 2. New York: Academic Press; 1952. p. 261
- [3] Wildman WC, Pursey BA. In: Manske RH. editor. *The Alkaloids*. Vol. 11. New York: Academic Press; 1962. pp. 41-413
- [4] Papageorgiou N, Briasoulis A, Lazaros G, Imazio M, Tousoulis D. Colchicine for prevention and treatment of cardiac diseases: A meta-analysis. *Cardiovascular Therapeutics*. 2013;**35**(1):10-18. DOI: 10.1111/1755-5922.12226
- [5] Indraratna PL, Virk S, Gurram D, Day RO. Use of colchicine in pregnancy: A systematic review and meta-analysis. *Rheumatology (Oxford, England)*. 2017;**23**. DOI: 10.10093/rheumatology/kex353
- [6] Wang MX, Deng XL, Mu BY, Cheng YJ, Chen YJ, Wang Q, Huang J, Zhou RW, Huang CB. Effect of colchicine in prevention of pericardial effusion and atrial fibrillation: A meta-analysis. *Internal and Emergency Medicine*. 2016;**11**(6):867-876. DOI: 10.1007/s11739-016-1496-5
- [7] Hemkens LG, Ewald H, Gloy VL, Arpagaus A, Olu KK, Nidorf M, Glinz D, Nordmann AJ, Briel M. Cardiovascular effects and safety of long-term colchicine treatment: Cochrane review and meta-analysis. *Heart*. 2016;**102**(8):590-596. DOI: 10.1136/heartjnl-2015-308542

- [8] Agarwal SK, Vallurupalli S, Uretsky BF, Hakeem A. Effectiveness of colchicine for the prevention of recurrent pericarditis and post-pericardiotomy syndrome: An updated meta-analysis of randomized clinical data. *European Heart Journal—Cardiovascular Pharmacotherapy*. 2015;**1**(2):117-125. DOI: 10.1093/ehjcvp/pvv001
- [9] Imazio M, Brucato A, Forno D, Ferro S, Belli R, Trincherò R, Adler Y. Efficacy and safety of colchicine for pericarditis prevention. Systematic review and meta-analysis. *Heart*. 2012;**98**(14):1078-1082. DOI: 10.1136/heartjnl-2011-301306
- [10] Terkeltaub RA. Colchicine update: 2008. *Seminars in Arthritis and Rheumatism*. 2008; **38**:411-419. DOI: 10.1016/j.semarthrit.2008.08.006
- [11] Bhat A, Naguwa SM, Cheema GS, Gershwin ME. Colchicine revisited. *Annals of the New York Academy of Sciences*. 2009;**1173**:766-773. DOI: 10.1111/j.1749-6632.2009.04674.x
- [12] Smilde BJ, Woudstra L, Fong Hing G, Wouters D, Zeerleder S, Murk JL, van Ham M, Heymans S, Juffermans LJ, van Rossum AC, Niessen HWM, Krijnem PAJ, Emmens RW. Colchicine aggravates coxsackievirus B3 infection in mice. *International Journal of Cardiology*. 2016;**216**:58-65. DOI: 10.1016/j.ijcard.2016.04.144
- [13] Lennerz C, Barman M, Tantawy M, Sopher M, Whittaker P. Colchicine for primary prevention of atrial fibrillation after open-heart surgery: Systematic review and meta-analysis. *International Journal of Cardiology*. 2017;**S0167-5273**(17):32407-32415. DOI: 10.1016/j.ijcard.2017.08.039
- [14] Salih M, Smer A, Charnigo R, Ayan M, Darrat YH, Traina M, Morales GX, DiBiase L, Natale A, Elayi CS. Colchicine for prevention of post-cardiac procedure atrial fibrillation: Meta-analysis of randomized controlled trials. *International Journal of Cardiology*. 2017;**15**(243):258-262. DOI: 10.1016/j.ijcard.2017.04.022
- [15] Dasgeb B, Kornreich D, McGuinn K, Okon L, Brownell I, Sackett DL. Colchicine: An ancient drug with novel applications. *The British Journal of Dermatology*. 2017. DOI: 10.1111/bjd.15896
- [16] Puzas IÁ, Álvarez ML, Menendez FÁ, Yuste Romero S, Gómez Prieto O. Wells' syndrome successfully treated with colchicine. *Case Reports in Dermatology*. 2017;**9**:65-69. DOI: 10.1159/000477756
- [17] Cutler SJ, Cutler HG, editors. *Biologically Active Natural Products, Pharmaceuticals*. 2000. p. 84
- [18] Budavari S. *The Merck Index: An Encyclopedia of Chemicals, Drug and Biologicals*. Rahway, New York: Merck&Co.; 1989
- [19] Saxton JE. *The Alkaloids, A Specialist Periodical Report*. vol. 2. London W1V0BN: The Chemical Society Burlington House; 1972. p. 144
- [20] Herbert RB. The biosynthesis of plant alkaloids and nitrogenous microbial metabolites. 2.2. Colchicine. *Natural Product Reports*. 1999;**16**:199-208; Bentley KW. β -Phenylethylamines and the isoquinoline alkaloids. 17. Colchicine and related alkaloids. *Natural Product Reports*. 2002;**19**:332-356; Herbert RB. β -Phenylethylamines and the isoquinoline alkaloids. 3.2. Colchicine. *Natural Product Reports*. 2001;**18**:148-170; Bentley KW.

- β -Phenylethylamines and the isoquinoline alkaloids. 21. Colchicine. Natural Product Reports. 1991;7:358-366; Herbert RB. The biosynthesis of plant alkaloids and nitrogenous microbial metabolites. 2.2. Colchicine. Natural Product Reports. 1992;9:507-519; Bentley KW. The biosynthesis of plant alkaloids and nitrogenous microbial metabolites. 21. Colchicine and its analogues. Natural Product Reports. 1992;9:365-396; Bentley KW. The biosynthesis of plant alkaloids and nitrogenous microbial metabolites. 21. Colchicine and related alkaloids. Natural Product Reports. 1994;11:555-576; Bentley KW. The biosynthesis of plant alkaloids and nitrogenous microbial metabolites. 18. Colchicine and related alkaloids. Natural Product Reports. 1995;12:419-441
- [21] Saxton JE. The Alkaloids, A Specialist Periodical Report. Vol. 3. London W1V0BN: The Chemical Society Burlington House; 1973. p. 300
- [22] Suri OP, Gupta BD, Suri KA, Sharma AK, Satti NK. A new glycoside, 3-O-demethylcolchicine-3-O- α -D-glucopyranoside, from *Gloriosa Superba* seeds. Natural Product Letters. 2001;15(4):217-219. DOI: 10.1080/10575630108041284
- [23] Korner A, Kohn S. Development and optimization of a stability indicating method on a monolithic reversed-phase column for colchicum dry extract. Journal of Chromatography A. 2005;1089(1-2):148-157. DOI: 10.1016/j.chroma.2005.06.084
- [24] Chaudhuri PK, Thakur RS. 1,2-Didemethylcolchicine: A new alkaloid from *Gloriosa superba*. Journal of Natural Products. 1993;56(7):1174-1176. DOI: 10.1021/np50097a025
- [25] Saxton JE. editor. The alkaloids, A Specialist Periodical Report. Vol. 1. London, W1V0BN : The Chemical Society Burlington House; 1971. p. 457
- [26] Pelletier PJ, Caventou JB. Examen chimique de plusieurs végétaux de la famille des colchicènes, et du principe actif qu'ils renferment. Annales de Chimie Physique. 1820;14:69-81
- [27] Dewar MJS. Structure of colchicine. Nature. 1945;155:141. DOI: 10.1038/155141d0
- [28] Kashiwara YM, Sun L, Tatematsu H, Bastow KF, Lee KH. Structures of tetra-O-demethylcolchicine, -isocolchicine, and 10-O-demethylcolchicine derivatives. Heterocycles. 1993;36:2531-2540. DOI: 10.3987/COM-93-6478
- [29] Bastow KF, Tatematsu H, Sun L, Fukushima Y, Lee KH. Synthesis and biological evaluation of tetrademethyl isocolchicine derivatives as inhibitors of DNA topoisomerase action *in vitro*. Bioorganic & Medicinal Chemistry Letters. 1993;(3):227-234. DOI: 10.1016/S0968-0896(00)82125-2
- [30] Bastow KF, Tatematsu H, Bori ID, Fukushima Y, Lee K-H. Induction of reversible protein-linked DNA breaks in human osteogenic sarcoma cells by novel cytotoxic colchicine derivatives which inhibit DNA topoisomerase II *in vitro*: Absence of cross-resistance in a colchicine-resistant sub-clone. Bioorganic & Medicinal Chemistry Letters. 1993;3:1045-1050. DOI: 10.1016/S0960-894X(00)80284-X
- [31] Akyama K. Jpn. Kokai Tokyo. JP 05 38999 (Chem. Abstr., 1994, 120, 245578.). 1993
- [32] Boye O, Hamel E, Brossi A. Medicinal Chemistry Research. 1991;1:149-159

- [33] Muzaffar A, Hamel E, Brossi A. Reaction of Colchiceinamide with phosgene and with thiophosgene: Structures and antitubulin activity of tetracyclic oxazolones, oxazothiones and thiazolones of the colchicine series. *Heterocycles*. 1990;**31**(11):2037. DOI: 10.3987/COM-90-5558
- [34] Muzaffar A, Brossi A. Thiocolchicinethiones: Acid hydrolysis of natural and iso-isomers. *Synthetic Communications*. 1990;**6**:713. DOI: 10.1080/00397919008052314
- [35] Muzaffar A, Brossi A, Hamel E. Partial synthesis and antitubulin activity of minor colchicum alkaloids: *N*-acetoacetyl-deacetylcolchicine and 2-demethylspeciosine (Speciocolchine). *Journal of Natural Products*. 1990;**53**(1):1021-1024. DOI: 10.1021/np50070a044
- [36] Cazzava M, Pietra F. A general entry to 10-halocolchicides and 9-haloisocolchicides. *Synthetic Communications*. 1997;**27**(19):3405. DOI: 10.1080/00397919708005641
- [37] Ravelli RBG, Gigant B, Curmi PA, Jourdain I, Lachkar S, Sobel A, Knossow M. Insight into tubulin regulation from a complex with colchicine and stathmine-like domain. *Nature*. 2004;**428**:198-202. DOI: 10.1038/nature02393
- [38] Lagnoux D, Darbre T, Lienhard Schmitz M, Reymond J-L. Inhibition of mitosis by glycopeptide dendrimer conjugates of colchicine. *Chemistry—A European Journal*. 2005;**11**(13):3941-3950. DOI: 10.1002/chem.200401294
- [39] Mons S, Veretout F, Carlier M-F, Erk I, Lepault J, Trudel E, Salesse C, Ducray P, Mioskowski C, Lebeau L. The interaction between lipid derivatives of colchicine and tubulin: Consequence of the interaction of the alkaloid with lipid membrane. *Biochemical Biophysica Acta*. 2000;**1468**:381-396. DOI: 10.1016/S0005-2736(00)00279-0
- [40] Yang B, Zhu ZC, Goodson HV, Miller MJ. Synthesis and biological evaluation of ring-C modified colchicine analogs. *Bioorganic & Medicinal Chemistry Letters*. 2010;**20**:3831-3833. DOI: 10.1016/j.bmcl.1010.03.065
- [41] Poulev A, Bombardelli E, Ponzzone C, Zenk M. Regioselective bioconversion of colchicine and thiocolchicine into their corresponding 3-demethyl derivatives. *Journal of Fermentation and Bioengineering*. 1995;**79**(1):33-38. DOI: 10.1016/0922-338X(95)92740-4
- [42] Dubey KK, Ray AR, Behera BK. Production of demethylated colchicine through microlab transformation and scale-up process development. *Process Biochemistry*. 2008;**43**:252-257. DOI: 10.1016/j.procbio.2007.12.002
- [43] Wolach B, Gotfried M, Jedeikin A. Colchicine analogues: Effect on amyloidogenesis in a murine model in vitro, on polymorphonuclear leukocytes. *European Journal of Clinical Investigation*. 1992;**22**(9):630-634. DOI: 10.1111/j.1365-2362.1992.tb01516.x
- [44] Sun L, Hamel E, Lin CM, Hastie SB, Pyluck A, Lee K-H. Antitumor agent. 141. Synthesis and biological evaluation of novel thiocolchicine analogs: *N*-acyl-, *N*-aroyl- and *N*-(substituted benzyl) deacetylthiocolchicines as a potent cytotoxic and antimetabolic compounds. *Journal of Medicinal Chemistry*. 1993;**36**(10):1474-1479. DOI: 10.1021/jm00062a021
- [45] De Vincenzo R, Scambia G, Ferlini C. Antiproliferative activity of colchicine analogues on MDR-positive and MDR negative human cancer cell lines. *Anti-Cancer Drug Design*. 1998;**13**(1):19-33

- [46] De Vincezo R, Ferlini C, Distefano M. Biological evaluation on different human cancer cell lines of novel colchicine analogues. *Oncology Research*. 1999;**11**(3):145-152
- [47] Kurek J, Boczoń W, Murias M, Myszkowski K, Borowiak T, Wolska I. Synthesis of sulfur containing colchicine derivatives and their biological evaluation as cytotoxic agents. *Letters in Drug Design & Discovery*. 2014;**11**(3):279-289. DOI: 10.2174/15701808113106660086
- [48] Gelmi ML, Pocar D, Pontremoli G, Pellegrino S, Bombardelli E, Fontana G, Riva A, Balduini W, Carloni S, Cimino M, Johnson F. Demethoxy-3-glycosylaminothiocolchicines: Synthesis of a new class of putative muscle, relaxant compounds. *Journal of Medicinal Chemistry*. 2006;**49**(18):5571-5577. DOI: 10.1021/jm060585t
- [49] Kerekes P, Brossi A. Esters of 1-O-demethylthiocolchicine s: Formation of isomers in chloroform solution. *Helvetica Chimica Acta*. 1985;**68**(3):571-579. DOI: 10.1002/hlca.19850680306
- [50] Guan J, Brossi A, Zhu XK, Wang HK, Lee KH. Oxidation products of phenolic thiocolchicines: Ring a quinones and dienones. *Synthetic Communications*. 1998;**28**:1585-1590. DOI: 10.1080/00397919808006862
- [51] Bombardelli E. *Eur. Pat. Appl.*, EP870761/98 (Chem. Abstr. 1998, 129, 290269)
- [52] Lee SH, Park S-K, Kim J-M, Kim M-H, Kim KH, Chum KW, Cho KH, Youn J-Y, Namgoong SK. New synthetic thiocolchicine derivatives as low-toxic anticancer agents. *Archiv der Pharmazie—Chemistry in Life Sciences*. 2005;**388**:582-589. DOI: 10.1002/ardp.200500148
- [53] Nakagawa-Gotto K, Chen C, Hamel E, Wu C-C, Bastow KF, Brossi A, Lee KH. Antitumor agents. Part 236: Synthesis of water-soluble colchicine derivatives. *Bioorganic & Medicinal Chemistry Letters*. 2005;**15**:235-238. DOI: 10.1016/j.bmcl.2004.07.098
- [54] Guan J, Zhu X-K, Tachibana Y, Bastow KF, Brossi A, Hamel E, Lee KH. Antitumor agents. 185. Synthesis and biological evaluation of tridemetoxythiocolchicine analogues as novel topoisomerase II inhibitors. *Journal of Medicinal Chemistry*. 1998;**41**:1956-1961. DOI: 10.1021/jm980007f
- [55] Kozaka T, Nakagawa-Goto K, Shi Q, Lai CY, Hamel E, Bastow KF, Brossi A, Lee K-H. Antitumor agents 273. Design and synthesis of *N*-alkyl-thiocolchicinoids as potential antitumor agent. *Bioorganic & Medicinal Chemistry Letters*. 2010;**20**:4091-4094. DOI: 10.1016/j.bmcl.2010.05.081
- [56] Banwell M, Peters SC, Greenwood RJ, Mackay MF, Hamel E, Lin CM. Semisyntheses, X-ray crystal structures and tubulin-binding properties of 7-oxodeacetamidocolchicine and 7-oxodeacetamidoisocolchicine. *Australian Journal of Chemistry*. 1992;**45**(10):1577-1588. DOI: 10.1071/CH9921577
- [57] Passarella D, Giardini A, Peretto B, Fontana G, Sacchetti A, Silvani A, Ronchi C, Cappelletti G, Cartelli D, Borlak J, Danielli B. Inhibitors of tubulin polymerization: Synthesis and biological evaluation of hybrids of vindofine, anhydrovinblastine and vinorelbine with thiocolchicine, podophylotoxin and baccatin III. *Bioorganic & Medicinal Chemistry*. 2008;**16**:6269-6285. DOI: 10.1016/j.bmc.2008.04.025

- [58] Capelletti G, Cartelli D, Peretto B, Ventura M, Riccioli M, Colombo F, Snaith JS, Borrelli S, Passarella D. Tubulin-guided dynamic combinatorial library of thiocolchicine-podophyllotoxin conjugates. *Tetrahedron*. 2011;**67**:7354-7357. DOI: 10.1016/j.tet.2011.07.038
- [59] Sun L, McPhail AT, Hamel E, Lin CM, Hastie S, Chang JJ, Lee K-H. Antitumor agents. 139. Synthesis and biological evaluation of thiocolchicine analogues 5,6-dihydro-6-(S)-(acyloxy)- and 5,6-dihydro-6-(S)[(aroyloxy)methyl]-1,2,3-trimethoxy-9-(methylthio)8H-cyclohepta[a]naphthalen-8-ones as novel cytotoxic and antimitotic agents. *Journal of Medicinal Chemistry*. 1993;**36**:544-551. DOI: 10.1021/jm00057a004
- [60] Schonharting M, Mende G, Siebert G. Hoppe-Seyler's. *Zeitschrift für Physiologische Chemie*. 1974;**355**:1991
- [61] Tateishi T, Soucek P, Caraco Y, Guengerich FP, Wood AJJ. Colchicine biotransformation by human liver microsomes: Identification of cyp3a4 as the major isoform responsible for colchicine demethylation. *Biochemical Pharmacology*. 1997;**53**(1):111-116. DOI: 10.1016/S0006-2952(96)00693-4
- [62] Pal D, Mahapatra P, Manna T, Chakrabati P, Bhattacharyya B, Banerje A, Basu G, Roy S. Conformational properties of α -tubulin tail peptide: Implication for tail-body interaction. *Biochemistry*. 2001;**40**:15512-15519. DOI: 10.1021/bi015677t
- [63] Sułowska A, Maciążek-Jurczyk M, Bojko B, Równicka J, Zubik-Skupień I, Temba E, Pentak D, Sułkowski WW. Competitive binding of phenylbutazone and colchicine to serum albumin in multidrug therapy: A spectroscopic study. *Journal of Molecular Structure*. 2008;**881**:97-106. DOI: 10.1016/j.molstruc.2007.09.001
- [64] Hu YJ, Liu Y, Zhao RM, Qu SS. Interaction of colchicine with human serum albumin investigated by spectroscopic methods. *International Journal of Biological Macromolecules*. 2005;**37**:122-126. DOI: 10.1016/j.ijbiomac.2005.09.007
- [65] Sharma S, Poliks B, Chiauzzi C, Ravindra R, Blanden AR, Bane S. Characterization of the colchicine binding site on avian tubulin isotype β VI. *Biochemistry*. 2010;**49**:2932-2942. DOI: 10.1021/bi100159p
- [66] Shi Q, Verdier-Pinard P, Brossi A, Hamel E, Lee KH. Antitumor agents-CLXXV. Antitubulin action of (+)-thiocolchicine prepared by partial synthesis. *Bioorganic & Medicinal Chemistry*. 1997;**5**(12):2277-2282. DOI: 10.1016/S0968-0896(97)00171-5
- [67] Ferri P, Bruno C, Cecchini T, Ciaroni S, Ambrogini P, Guidi L, Cuppini R, Bombardelli E, Morazzoni P, Riva A, Del Grande P. Effects of thiocolchicine on axonal cytoskeleton of rat peroneus nerve. *Experimental and Toxicologic Pathology*. 2002;**54**:211-216. DOI: 10.1078/0940-2993-00249
- [68] Toscano IL, Rezende MV, Mello LF, Pires L, Paulillo D, Glina S. A prospective, randomized, single-blind study comparing intraplaque injection of thiocolchicine and verapamil in Peyronie's disease: A pilot study. *International Brazilian Journal of Urology*. 2016;**42**(5):1005-1009. DOI: 10.1590/S1677-5538.IBJU.2015.0598

- [69] Batrusik D, Tomanek B, Lattová E, Perreault H, Tuszyński J, Fallone G. Derivatives of thiocolchicine and its applications to CEM cells treatment using 19F magnetic resonance *ex vivo*. *Bioorganic Chemistry*. 2010;**38**:1-6. DOI: 10.1016/j.bioorg.2009.10.002
- [70] Passarella D, Peretto B, Blasco y Yepes R, Cappelletti G, Cartelli D, Ronchi C, Snaith J, Fontana G, Danieli B, Borlak J. Synthesis and biological evaluation of novel thiocolchicine–podophyllotoxin conjugates. *European Journal of Medicinal Chemistry*. 2010;**45**:219-226. DOI: 10.1016/j.ejmech.2009.09.047
- [71] Alali FQ, Gharaibeh AA, Ghawanmeh A, Tawaha K, Qandil A, Burgess JP, Sy A, Nakanishi Y, Kroll DJ, Oberlies NH. Colchicinoids from *Colchicum crocifolium* Boiss. (*Colchicaceae*). *Natural Product Research*. 2010;**24**(2):152-159. DOI: 10.1080/14786410.902941097
- [72] Gelmi ML, Motadelli S, Pocar D, Riva A, Bombardelli E, de Vincenzo R, Scambia G. *N*-deacetyl-*N*-aminoacetylthiocolchicine derivatives: Synthesis and biological evaluation on MDR-positive and MDR-negative human cancer cell lines. *Journal of Medicinal Chemistry*. 1999;**42**:5272-5276. DOI: 10.1021/jm981134e
- [73] Baker MA, Gray BD, Ohlsson-Wilhelm BM, Varpenter DC, Muirhead KA. Zyn-linked colchicines: controlled-release lipophilic prodrugs with enhanced antitumor activity. *Journal of Controlled Release*. 1996;**40**(1-2):89-100. DOI: 10.1016/0168-3659(95)00177-8
- [74] Chabin RM, Feliciano F, Hastie SB. Effects of tubulin binding and self-association on the near-ultraviolet circular dichroic spectra of colchicine and analogues. *Biochemistry*. 1990;**29**(7):1869-1875. DOI: 10.1021/bi00459a029
- [75] Brossi A. Bioactive alkaloids. 4. Results of recent investigation with colchicine and physostigmine. *Journal of Medicinal Chemistry*. 1990;**33**:2311-2319. DOI: 10.1021/jm00171a001
- [76] Brossi A, Herman JC, Chrzanowska M, Wolff J, Hamel E, Lin CM, Quin F, Suffness M, Silverton J. Colchicine and its analogues: Recent findings. *Medicinal Research Reviews*. 1988;**8**(1):77-94. DOI: 10.1002/med.2610080105
- [77] Gohar MA, Makkawi M. The antibacterial action of colchicine and colchicine. *The Journal of Pharmacy and Pharmacology*. 1951;**3**(1):415-419. DOI: 10.1111/j.2042-7158.1951.tb13083.x
- [78] Kim SK, Cho SM, Kim H, Seok H, Kim SO, Kwon TK, Chang JS. The colchicine derivative CT20126 shows a novel microtubule-modulating activity with apoptosis. *Experimental & Molecular Medicine*. 2013;**45**:e19. DOI: 10.1038/emm.2013.38
- [79] Davis PD, Dougherty GJ, Blakey DC, Galbraith SM, Tozer GM, Holder AL, Naylor MA, Nolan J, Stratford MRL, Chaplin DJ, Hill SA. ZD6126: A novel vascular-targeting agent that causes selective destruction of tumor vasculature. *Cancer Research*. 2002;**62**(15):7247-7253
- [80] Raspaglio G, Ferlini C, Mozzetti S, Prislei S, Gallo D, Das N, Scambia G. Thiocolchicine dimers: A novel class of topoisomerase-I inhibitors. *Biochemical Pharmacology*. 2005;**69**: 113-121. DOI: 10.1016/j.bcp.2004.09.004

- [81] Bombuwala K, Kinstle T, Popik V, Uppal S, Olesen JB, Viña J, Heckman CA. Colchitaxel, a coupled compound made from microtubule inhibitors colchicine and paclitaxel. *Beilstein Journal of Organic Chemistry*. 2006;**2**:13-21. DOI: 10.1186/1860-5397-2-13
- [82] Imazio M, Brucato A, Cemin R. A randomized trial for acute pericarditis. *New England Journal of Medicine*. 2013;**369**:1522-1528. DOI: 10.1056/NEJMoa1208536
- [83] Terkeltaub RA, Furst DE, Bennet K, Cook KA, Crockett RS, Davis MW. High versus low dosing of oral colchicine for early acute gout flare: Twenty-four-hour outcome of the first multicenter, randomized, double-blind, placebo-controlled parallel-group, dose-comparison colchicine study. *Arthritis and Rheumatism*. 2010;**62**:1060-1068. DOI: 10.1002/art.27327
- [84] Cocco G, Chu DCC, Pandolfi S. Colchicine in clinical medicine. A guide for internists. *European Journal of Internal Medicine*. 2010;**21**:503-508. DOI: 10.1016/j.ejim.2010.09.010
- [85] Gervasi M, Sisti D, Benelli P, Fernández-Peña E, Calcabini C, Rocchi MBL, Lanata L, Bagnasco M, Tonti A, Viberto S, Sestili P. The effect of topical thiocolchicoside in preventing and reducing the increase of muscle tone, stiffness and soreness. *Medicine*. 2017;**96**(30):1-8. DOI: 10.1097/MD.00000000000007659
- [86] Abolhasani H, Zarghi A, Hamzeh-Mivehroud M, Alizadeh AA, Shahbazi J, Mojjarrad SD. *In-silico* investigation of tubulin binding modes of a series of novel antiproliferative spiroisoxazoline compounds using docking studies. *Iranian Journal of Pharmaceutical Research*. 2015;**14**(1):141-147
- [87] Hu MJ, Zhang B, Yang HK, Liu Y, Chen YR, Ma TZ, Lu L, You WW, Zhao PL. Design, synthesis and molecular docking studies of novel indole-pyrimidine hybrids as tubulin polymerization inhibitors. *Chemical Biology & Drug Design*. 2015;**86**(6):1491-1500. DOI: 10.1111/cbdd.12616
- [88] Kumbhar BV, Borogaon A, Panda D, Kunwar A. Exploring the origin of differential binding affinities of human tubulin isotypes $\alpha\beta$ II, $\alpha\beta$ III and $\alpha\beta$ IV for DAMA-colchicine using homology modelling, molecular docking and molecular dynamics simulations. *PLoS One*. 2016;**11**(5):e0156048. DOI: 10.1371/journal.pone.0156048
- [89] Li H, Liu T, Xuan H, Fang S, Zhao C. A combination of pharmacophore modeling, virtual screening, and molecular docking studies for a diverse set of colchicine site inhibitors. *Medicinal Chemistry Research*. 2014;**23**(11):4713-4723. DOI: 10.1007/s00044-014-1028-7
- [90] Nguyen TL, McGrath C, Hermone AR, Burnett JC, Zaharevitz DW, Day BW, Wipf P, Hamel E, Gussio R. A common pharmacophore for a diverse set of colchicine site inhibitors using a structure-based approach. *Journal of Medicinal Chemistry*. 2005;**48**(19):6107-6116. DOI: 10.1021/jm050502t

Natural Products as Cytotoxic Agents in Chemotherapy against Cancer

Abdelmajid Ziad, Inass Leouifoudi, Mounir Tilaoui,
Hassan Ait Mouse, Mouna Khouchani and
Abdeslam Jaafari

Additional information is available at the end of the chapter

<http://dx.doi.org/10.5772/intechopen.72744>

Abstract

Nature continues to produce a great wealth of natural molecules endowed with cytotoxic activity toward a large panel of tumor cells. Some of these molecules are used in chemotherapy, and others have shown great anti-tumor and anti-metastatic potential in preclinical trials. This review discusses some examples of these molecules that have been studied in our laboratory and others. We report a differential cytotoxic activity of some monoterpenes (carvacrol, tymol, carveol, carvone, and isopulegol) against a panel of tumor cell lines. The carvacrol was the most cytotoxic molecule both *in vitro* and *in vivo* as demonstrated by preclinical studies using the DBA2/P815 mice model. On the other hand, polyphenols were also studied with respect to their cytotoxic effects. Interestingly, these compounds showed a prominent cytotoxic activity toward a panel of cancer cells with differential molecular mechanisms. In addition, we report a very strong antitumor efficacy of artemisinin, a sesquiterpen lactone from *Artemisia annua*, together with an antimetastatic potential as demonstrated by preclinical experiments. Furthermore, some of the molecular mechanisms involved in these effects are described.

Keywords: natural products, monoterpenes, polyphenols, artemisinin, cytotoxicity

1. Introduction

Natural drugs have formed the basis of traditional medicine systems that have been used for centuries by different cultures [1]. An immense number of these natural sources and their isolated components have demonstrated beneficial therapeutic effects, such as anticancer, antioxidant, immunomodulatory, antimicrobial, and anti-inflammatory properties [2, 3].

Studies reported that plant-derived drugs represent about 25% of the American prescription drug market [4]. Also, natural products play an important role in the health care of 20% of the world's people who mainly reside in developed countries and 119 chemicals compounds, derived from 90 plant species, can be considered as important drugs in many countries [5]. Based on a recent review, from 79 Food and Drug Administration anticancer and antiviral approved drugs from 1983 to 2002, 9 of them were isolated directly from plants and 21 among them were natural-products-based drug. Furthermore, between 39 conventional anti-cancer molecules, 13 of them were derived on a pharmacophore obtained from natural drugs [5, 6]. Actually, nature continues to be an attractive source of new molecules discovery due to important chemical diversity of the thousands of plant, animal, marine organisms, and micro-organism species. Today, about 60% of drugs are of natural origin [7] (**Tables 1–3**).

Several molecules used as conventional chemotherapy are of natural origin. Some of these molecules and their use are described in **Tables 2** and **3**.

Drug	Utilization	Mechanism of action	Source
Aspirine	Analgesic, anti-inflammatory, anti-pyrtic	Inhibition of cyclo-oxygenase	Plant
Atropine	Pupil dilatator	Anti-cholinergic on muscarinic receptors	Plant
Cafeine	Stimulating	Antagonist of adenosine receptors	Plant
Codeine	Analgesic, anti-tussive	Antagonist of opoide receptors	Plant
Digoxine	Cardiotonic	Inhibition of membrane pump N ⁺ /K ⁺ ATPase	Plant
Eugenol	Touth pain	Reduction of sensorial nerve excitability	Plant
Morphine	Analgesic	Antagonist of opoide receptors	Plant
Pilocarpine	Glaucoma	Antagonist of muscarinic receptors	Plant
Quinine	Prophylaxis of malaria	Inhibition of protein synthesis	Plant
Taxol	Anticancer	Antimitotic	Plant
Penicilline	Antibiotic	Inhibition of cell membrane	Micro-organism
Tetracycline	Antibiotic	Inhibition of protein synthesis	Micro-organism
Cyclosporine A	Immunosuppressor	Inhibition of lymphocytes T proliferation	Micro-organism
Aurantiosides	Antifungal	Inhibition of tubulin polymerization	Marine organism
Spongistatine 1	Antifungal	Inhibition of tubulin polymerization	Marine organism
Manoalide	Analgesic, anti-inflammatory	Inhibition of phospholipase A2	Marine organism

Table 1. Some natural drugs derived from plants, micro-organisms, or marine organisms [8].

Drug	Utilization
Actinomycine	Germinale cells tumor, sarcoma
Bléomycine	Cervix cancer, Germinale cells tumor, and neck
Daunomycine	Leukemia
Doxorubicine	Lymphoma, breast, lung and ovarian cancer, sarcoma
Epirubicine	Breast cancer
Idarubicine	Leukemia and breast cancer
Mitomycine C	Colorectal, gastric, anal, and lung cancer
Streptozonecine	Gastric and endocrine tumors

Table 2. Some anticancer drugs derived from micro-organisms [8].

Drug	Utilization	Mechanism of action
Citarabine	Leukemia, lymphoma	Inhibition of DNA synthesis
Bryostatine 1	Experimental phase	Activation of protein kinase C
Dolastatine 10	Experimental phase	Inhibition of microtubules and pro-apoptotic effect
Ecteinascidine 743	Experimental phase	Alkylation of DNA
Aplidine	Experimental phase	Inhibition cell cycle progression
Halicondrine B	Experimental phase	Interaction with tubuline
Discodermolide	Experimental phase	Stabilization of tubuline
Cryptophycine	Experimental phase	Hyperphosphorylation of Bcl-2

Table 3. Some anticancer drugs derived from marine organisms [8].

2. Phytotherapy and cancer

2.1. Generalities

There is a numerous plants involved in the prevention and/or treatment of cancer. As for other diseases, many anticancer drugs are derived from plants (**Table 4**). Studies reported that more than 200 drugs are of herbal origin. The vinca-alcaloids and the taxans are the main groups, which occupy an important place in anticancer chemotherapy.

2.2. Examples of natural products with important cytotoxic activity

2.2.1. Cytotoxic activity of some natural monoterpenes

The chemical composition of plant-extracts is known for being very rich and diversified. Thus, a single extract may contain more than hundreds of interactive biomolecules [9]. Therefore, finding and discovering those responsible for the biological Activity become essential. Many monoterpenes, such as eugenol, have been described in the literature to have

Drugs	Utilization
Vincristine	Leukemia, lymphoma, breast cancer, and lung cancer
Vinblastine	Lymphoma, kidney cancer, germinal cells cancer, and breast cancer
Paclitaxel	Breast cancer, ovarian, lung, and d'ovaire, de poumon, bladder, and neck cancer
Docetaxel	Breast and lung cancer
Topotecan	Ovarian and lung cancer
Irinotecan	Colorectal and lung cancer

Table 4. Anticancer drugs derived from plants [8].

a wide range of important biological activities [10]; it possesses *in vitro* and *in vivo* antiviral activity against human herpesvirus [11]. Carvone promoted protection of 75–87.5% against convulsions at 300–400 mg/kg [12]. Isopulegol and carvone showed significant bactericidal and fungicidal activities [13]. Also, the combination of these molecules between them or with conventional molecules could have a synergistic effect [14, 15]. Furthermore, carvacrol, extract of thyme essential oil, is one of natural products with important biological activities. It has been reported to have an important antitumor effect [9, 16]. Here, we present a summary of our findings [17] on the cytotoxic activity as well as their molecular mechanisms of six natural monoterpenes compounds (carvacrol, thymol, carveol, carvone, eugenol, and isopulegol).

2.2.1.1. *In vitro* cytotoxic effect of the products against a panel of target cells

The antitumor activity of the products was evaluated against the following five tumor cell lines: P-815, K-562, CEM, MCF-7, and MCF-7 resistant to gemcetabine (MCF-7-gem). The results are summarized in **Figure 1**, which shows that the cytotoxic effect depends on the nature of the products as well as on the target cell lines. In general, the effect of the products is dose-dependent. Moreover, the cytotoxic activity of carvacrol, thymol, carveol, carvone, eugenol, and isopulegol is more important against P-815 and CEM tumor cell lines compared to the other tested cell lines. The carvacrol is the most cytotoxic compared to other compounds. Against P-815, K-562 and CEM cancer cell lines, eugenol, carveol, and carvone exhibit also a strong cytotoxic activity. The IC_{50} values are ranging from 0.09 to 0.24 μ M (**Table 5**). Nevertheless, those compounds showed a less effect toward MCF-7 and very lowest one against MCF-7-gem cancer cell lines as demonstrated by the IC_{50} values ranging from 0.26 to 0.87 μ M. Comparing the activity of thymol and isopulegol on the tumor cell lines studied, it shows that P-815 is the most sensitive with an IC_{50} = 0.15 and 0.09 μ M, respectively. Importantly, acquired resistance to gemcetabine by MCF-7 cell line was linked with a development of resistance to thymol, carveol, carvone, and eugenol but not to isopulegol or carvacrol (**Table 5**).

2.2.1.2. Synergy

Our results demonstrate that the combination of natural monoterpene with MTX or Cis showed a synergistic effect at used concentrations (IC_{20}) of each tested molecules (monoterpenes, cisplatin, and methotrexate). The interactions between these molecules exhibit a cell lysis ranging between 53 and 62%. Furthermore, a slight cytotoxicity was shown after the combinations between monoterpene-cisplatin and monoterpene-methotrexate (**Table 6**).

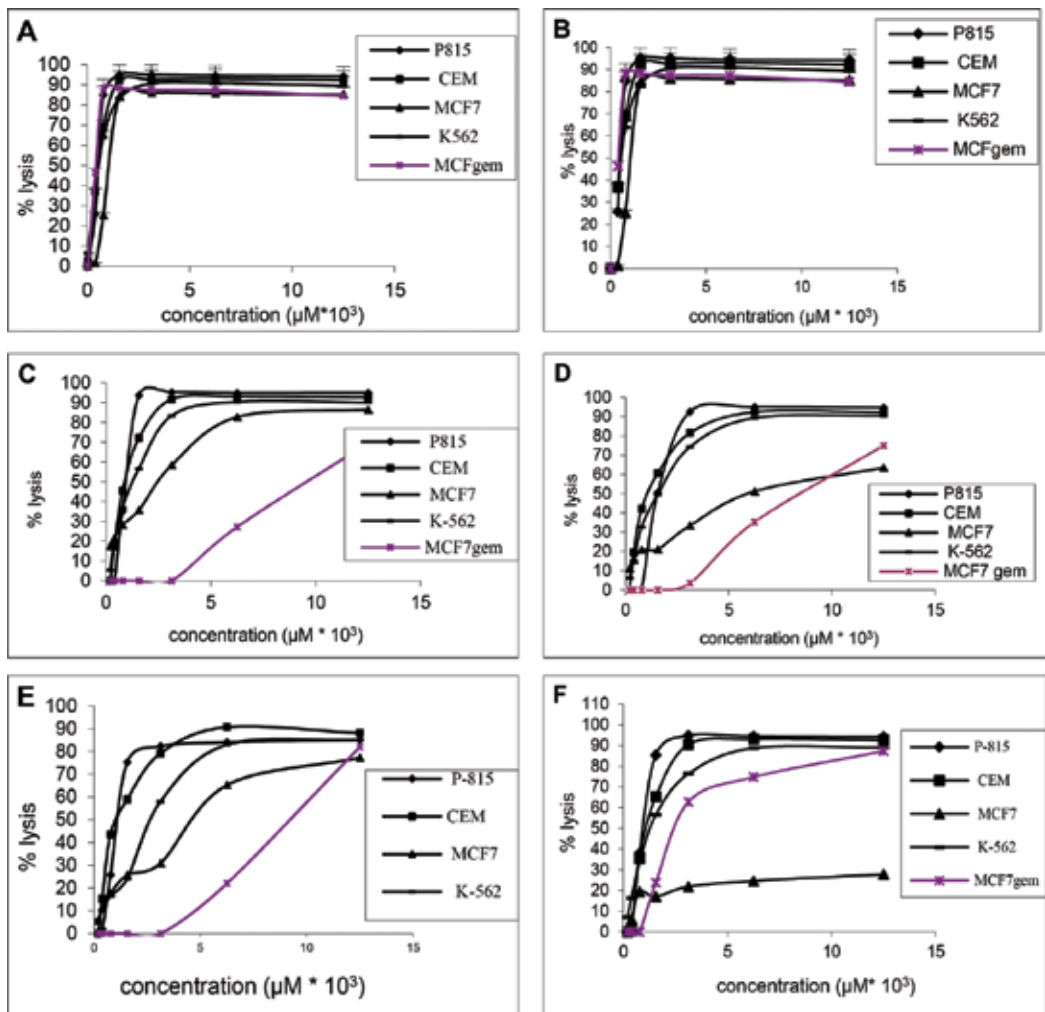


Figure 1. Cytotoxic effect of carvacrol (A), thymol (B), carveol (C), carvone (D), eugenol (E) and isopulegol (F) against different tumor cell lines: P815 (◆), CEM (■), K562 (□), MCF-7 (▲) and MCF-7 gem (*).

Product	P815	CEM	K-562	MCF-7	MCF-7/gem
Carvacrol	0.067	0.042	0.067	0.125	0.067
Thymol	0.15	0.31	0.44	0.48	—
Carveol	0.11	0.11	0.13	0.26	0.45
Carvone	0.16	0.11	0.17	0.63	0.91
Eugenol	0.10	0.09	0.24	0.41	0.87
Isopulegol	0.09	0.11	0.13	—	0.25

Table 5. IC₅₀ (μM) of the tested monoterpenes against different target cell lines.

Combination	Fa	CI
C-MTX	54.9	0.17
C-Cis	56.6	0.01
T-MTX	61	0.14
T-Cis	57.6	0.01
Cl-MTX	53.3	0.17
Cl-Cis	57.9	0.01
Cn-MTX	51.2	0.17
Cn-Cis	58.5	0.01
E-MTX	58.6	0.15
E-Cis	55.9	0.01
I-MTX	58.5	0.15
I-Cis	62.3	0.01

Table 6. Affected fraction (Fa) and combination index (CI) of molecule combinations.

2.2.1.3. Effect of carvacrol, thymol, carveol, carvone, eugenol, and isopulego on the cell cycle progression

At the molecular level, carveol- and carvacrol treatment-induced cell cycle arrest in S phase. Nevertheless, thymol and isopulegol stopped it in G0/G1 phase. Regarding the eugenol and carvone, they have no effect cell cycle progression (**Figure 2**).

2.2.1.4. In vivo antitumor effect of carvacrol

Our experimental model was based on the use of the P-815 tumor-bearing DBA-2 mice to investigate the cell-killing induced by carvacrol. Experiments were carried out by oral administration (gavage) of carvacrol dissolved in vegetal oil to 6- to 8-week-old DbA-2/6 mice (6 mice for each group) (Orleans, France) weighting 18–22 g for 7 days. The tumor volume was measured for up to 30 days. The tumor volume at day n , (T_{vn}) was calculated using the formula: $Tv = (l \times W^2)/2$, where l equals the length of the tumor and W the width, as described by Yoshikawa [18]. Interestingly, during the first 18 days, there was no statistical difference ($p < 0.94$) in the volumes of the tumors in all the groups of mice, including the control group ($0.4\text{--}0.5 \pm 0.1 \text{ cm}^3$). Nevertheless, after 18 days, the tumor volume was reduced for the treated groups; this decrease occurred more rapidly in the group “C” who received 100 mg/kg/day than the group “B” treated with 50 mg/kg/day ($p < 0.05$ at day 21th). Compared to untreated group, the tumor volume increased quickly reaching 1.5 cm^3 at 23rd day. Furthermore and importantly, the tumor volume reduction was accompanied by a notable increase of mice survival (**Figure 3**). The antitumor activity of carvacrol has not been has not been

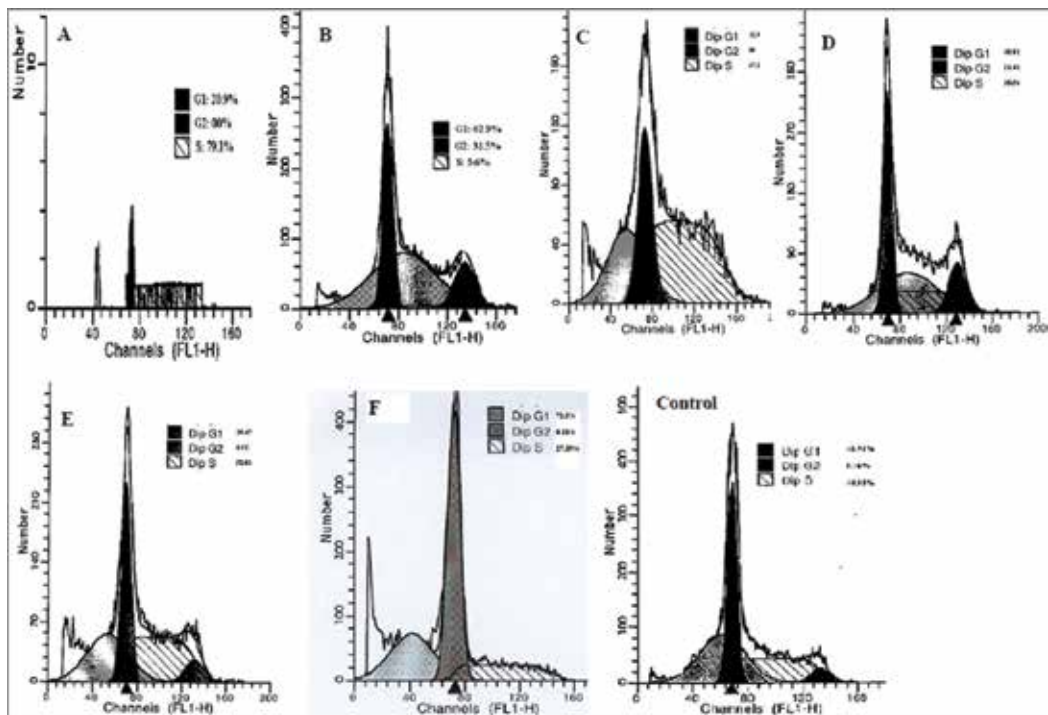


Figure 2. Effect of the tested products on cell cycle progression. The samples were analyzed using a FACStar plus flow cytometer and the WinMDI software. Results are the mean \pm SEM of three tests. (A) Carvacrol, (B) thymol, (C) carveol, (D) carvone, (E) eugenol, and (F) isopulegol.

widely discussed in the literature. At the best of our knowledge, this is the first study that reported the oral administration of carvacrol for successive 7 days significant decrease tumor volume, body weight loss, and delayed mortality (data not shown). These results corroborate those published by Karkabounas who demonstrated that carvacrol exhibited 30% reduction of 3,4-benzopyrene carcinogenic activity *in vivo* [19].

Studies were carried out by gavage of carvacrol dissolved in vegetable oil to mice (6–8 week-old) for 7 days. Group “A” (untreated) treated with 100 μ l/day of vegetal oil only. Groups “B” and “C” received 50 and 100 mg/kg/day of carvacrol dissolved in 100 μ l of vegetal oil, respectively. Mice were weighted and the tumor volume was calculated by measurement of the width (*W*) and the length (*l*) for three times a week up to day 30. The tumor volume at day *n* (*TVn*) was measured using the following formula: $TV = (l \times W^2)/2$. The experiments are the mean \pm SEM of two tests.

2.2.1.5. Discussion

Monoterpenes (carvacrol, thymol, carveol, carvone, eugenol, and isopulegol) have been found to exert antitumor effect. In fact, eugenol was described to exhibit cell death by apoptosis in

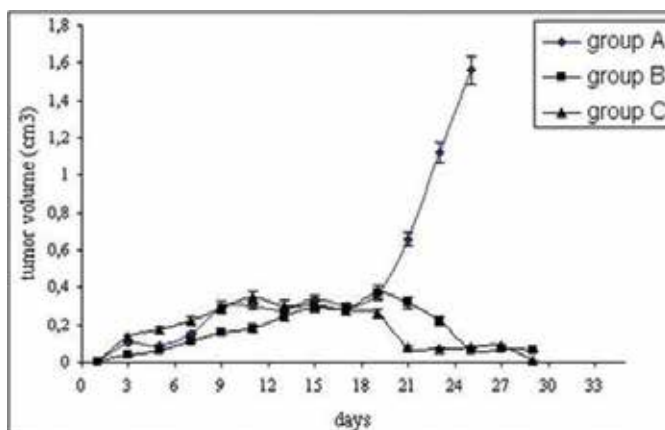


Figure 3. *In vivo* antitumor effect of carvacrol.

mastocyte [20] and melanoma cells [21]. Also, it has been demonstrated not to be mutagenic neither carcinogenic [22]. Carveol has chemopreventive activity against mammary cancer when fed during the initiation phase [23]. Carvone prevents chemically induced lung and for stomach carcinoma development [24]. Carvacrol and thymol significantly reduced the level of DNA damage induced in K-562 cells by the strong oxidant H_2O_2 [25]. Furthermore, carvacrol has an important *in vitro* antitumor effect against tumor cell lines like Hep-2 [26] and A-549 [16, 27]. As shown in **Table 5**, the monoterpenes studied induced a differential cytotoxic activity against a panel of tumor cell lines. P-815 and CEM cell lines are the most sensitive targets to all tested molecules. Although the effects of these products are dose-dependent, the carvacrol is the most cytotoxic molecule as revealed by the IC_{50} values (**Table 5**). Importantly, unlike isopulegol and carvacrol, the acquired resistance to gemcitabine by MCF-7 tumor cell line was associated with a resistance to thymol, carveol, and carvone. Taken together, these results suggest that these compounds could have a similar pathway. The differential sensitivity of the studied monoterpenes toward MCF-7 and MCF-7-gem could be linked to the expression level of ribonucleotide reductase subunit R1 [28]. Furthermore, the cell cycle analysis showed that carveol- and carvacrol treatment-induced cell cycle arrest in S phase when thymol and isopulegol stopped it in G0/G1 phase. Nevertheless, the eugenol and carvone have no effect cell cycle progression. These results suggest that the molecular mechanistic pathway of the cytotoxicity exhibited by those molecules is more complicated and is not related only with the cell cycle. It was reported that monoterpenes decreased expression of cyclin-dependent kinase cdk4, cyclin D1, and cdk2 and increased expression of cyclin E and cdk inhibitor p21 [29]. Furthermore, geraniol, farnesol, and isoprenoids perillyl alcohol exhibited a G0/G1 cell cycle arrest by increasing in the expression level of p27 (Kip1) and the cyclin kinase inhibitor proteins p21 (Cip1) and a decreasing in cyclin B1, cyclin A, and cyclin-dependent kinase (Cdk2) expression [14]. Interestingly, our results demonstrate that the interaction of tested monoterpenes at lowest concentration (IC_{20}) with the conventional anticancer molecules (cisplatin and methotrexate) exhibited a synergistic activity (**Table 6**). Thus, this combination may reduce the toxicity of the conventional chemotherapy drugs by reducing their doses.

These results are supported by previous findings reporting that when combined to isoprenoids perillyl alcohol, farnesol, and geraniol showed an additive antiproliferative activity against the human pancreatic cancer cell line MIA PaCa-2 [14]. Also, Chander et al. reported that in chemotherapy of breast tumors, the combination of limonene, natural monoterpene, and 4-hydroxyandrostenedione, inhibitor of aromatase, was more effective than each drug used alone [30]. Interestingly, in our study, we reported a synergistic effect and not an additive one suggesting that only low doses of each monoterpene combined with tolerable low doses of methotrexate or cisplatin (IC_{20}) showed an important effect (60% lysis).

2.2.2. Polyphenols: a potent cytotoxic molecules

Natural polyphenols have received increasing interest in the human health due to their benefit effects against several diseases attributed particularly to their antioxidant activity [31]. Beside their well-known and effective antioxidant activity [32, 33], several polyphenols shown a high cytotoxic effect against cancer cell lines through targeting cellular and molecular processes involved in cancer progression and metastasis. The antitumor potential of these active ingredients is due to their effect as modulators of oxidative stress [34], apoptosis inducers [35] cell proliferation inhibitor [36], tumor cell cycle blockers [37], and angiogenesis/metastasis suppressors [38]. These bioactive compounds have shown promising antitumor properties in both *in vitro* and *in vivo* interventions [39, 40]. These structural variations may be responsible for their various health benefits, including antioxidant [41], and anti-proliferative mechanisms, as well as regulation of key signaling protein and enzyme functions [42], and as promising immunostimulating effect on normal immune cells [43]. The relationship among natural polyphenols, antitumor activity, and cancer was identified by various studies on the ability of these compounds to act as cancer chemopreventive and/or chemotherapeutic agents [44]. In this purpose, a variety of natural polyphenols have been identified to interfere with carcinogenesis particularly through apoptosis induction and the modulation of oxidative stress [45, 46].

2.2.2.1. Polyphenols and apoptosis induction

Large number of studies has focused on the ability to introduce apoptosis on cancer therapy under cellular control conditions [47, 48]. The intrinsic and extrinsic molecular pathways involved in the regulation of the apoptotic process have recently been evaluated and give promising results. Several proapoptotic receptors have been selectively developed activating the intrinsic pathway, particularly including the antiapoptotic proteins, the Bcl-2 family proteins, and the p53 signaling pathways [49–51]. In this purpose, polyphenols could inhibit tumor cell proliferation via the programmed cell death (apoptosis) using both intrinsic and extrinsic cell pathways. As reported, polyphenols such as EGCG: (–)-epigallocatechin-3-gallate, resveratrol, naringenin, quercetin, hydroxytyrosol, and curcumin, through different intrinsic signaling pathways from mitochondrial intermembrane space, may inhibit NF- κ B-dependent signal related to proliferation and survival [52], cause cell cycle arrest through upregulation of p53 [53], stabilize and activate the tumor suppressor gene p53 [54], and downregulate the expression of Bcl-2, and Bcl-XL anti-death proteins, favoring apoptosis induction via the activation of multiple caspases activity and cytochrome-c (cyt-c) [55, 56]. These polyphenols have

been shown to promote apoptosis in different cancers particularly breast, lung, prostate, leukemia, colon, cervical, or melanoma [57, 58]. In breast cancer cells, naringenin demonstrated anti-estrogenic activity in estrogen-rich status and estrogenic activity in estrogen-deficient status [59]. Additionally, few early studies suggested that gavage of polyphenols in green tea (EGCG), even at low doses, prevented colon carcinogenesis by inhibiting metastasis and angiogenesis through apoptosis induction [60]. Few years ago, our research group has published an article [61] on natural polyphenols extracted from olive mill waste (OMW) and their implication in anticancer activity, where the *in vitro* cytotoxic and apoptotic assays involving several phenolic compounds found in those specific phenolic extracts (particularly including, quercetin, naringenin, apigenin, hydroxytyrosol, oleuropein, and its derivatives) have been discussed. The *in vitro* cytotoxic effect of olive mill waste extracts was evaluated using the MTT assay (methyl tetrazolium test). The IC_{50} values ranged from 4.8 to 7.6 $\mu\text{g/ml}$ (Table 7), which demonstrate an effective cytotoxicity of these phenolic compounds at low doses. We have demonstrated that the cytotoxic potential of these phenolic extracts was exhibited via apoptosis induction by DNA fragmentation test using agarose gel electrophoresis (Figure 4A). DNA isolated from MCF7 tumor cells was treated with OMW extracts at concentrations corresponding to the IC_{50} values and incubated for 24 h. To confirm the cell-death mechanism of these natural extracts, the apoptosis analysis was performed using the Annexin V biotin-streptavidin FITC test. We reported that phenolic extracts induced significantly apoptosis (Figure 4B) compared to untreated cells (Figure 4C). Interestingly, those polyphenols have not shown any cytotoxic effect against human normal cells (PBMC) (Figure 5). Hence, it triggered apoptosis in a dose-dependent manner on a breast cancer cell line (MCF-7) without any effects on normal cells by enhancing the viability with 12–16% in 48 h, compared to methotrexate (conventional cytotoxic drug), which suppressed 20% viability of these cells.

Taken together, these data showed the differential and selective cytotoxic effect of natural polyphenols. In this sense, Miccadei et al. [43] have shown that polyphenolic extracts from the edible part of artichoke (*Cynara scolymus* L) may selectively inhibit the growth of human hepatoma cells with little or no toxicity against normal hepatocytes cells based on their differential redox status. Interestingly, the authors have shown that Artichoke extracts exhibit a pro-oxidant activity in breast cancer cells and an antioxidant effect on normal hepatocytes. Moreover, some flavanols may have a significant effect on cytokine release from both unstimulated and lipopolysaccharides-stimulated PBMCs [62]. Oral administration of naringenin suppressed breast cancer metastases after surgery by modulating the host immunity [63].

2.2.2.2. Role of polyphenols in therapy-induced senescence

Cellular senescence is a physiological process of irreversible cell-cycle arrest that contributes to various physiological and pathological processes of aging. It is an alternative and a novel

Samples	S1	S2	S3	S4	S5
IC_{50} ($\mu\text{g/ml}$)	6.95 ± 0.15	5.3 ± 0.1	4.75 ± 0.05	7.75 ± 0.15	5.3 ± 0.2

Table 7. IC_{50} values of the cytotoxicity of OMW polyphenolic extracts against MCF-7 breast cancer cell line.

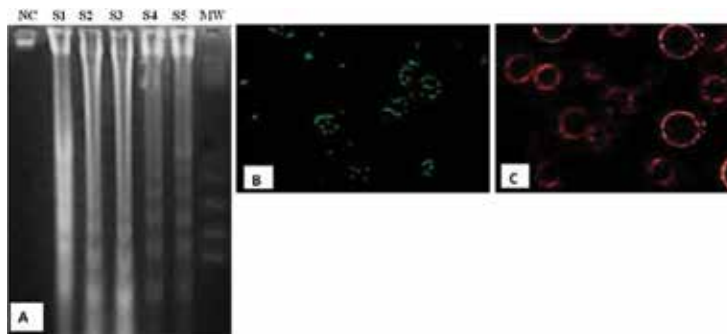


Figure 4. Apoptosis-induction analysis in MCF-7 cell line. (A) Phenolic extracts induced DNA fragmentation was detected by agarose gel electrophoresis of DNA isolated from MCF-7 tumor cells. Cells were incubated for 24 h with OCE (corresponding to IC_{50} concentrations). S1 to S5: Olive mill waste extracts samples. Positive control (WM): DNA weight marker. DNA of untreated cells was used as negative control (NC). (B) Annexin V biotin-streptavidin FITC test. MCF-7 tumor cells (2×10^6 cells) were treated with $25 \mu\text{g/ml}$ of OCE and incubated for 24 h. The assay is based on the ability of Annexin V (green fluorescence) to bind to the phosphatidylserine exposed on the surface of cells undergoing apoptosis. Cells cultured in a medium without serum were used as a positive control (C).

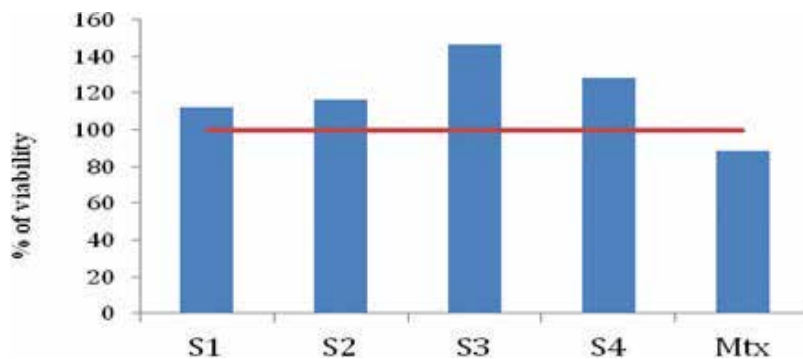


Figure 5. Cytotoxic effect of OMW polyphenolic extracts on normal human peripheral blood mono mononuclear cells (PBMC) from normal donors.

therapeutic strategy to the cytotoxic treatment which leading to cytostasis approach target for aging and aging-related diseases [64]. Although senescence cells have irreversibly lost their capacity for cell division, they are still viable and remain metabolically active [65]. Prosenescence is usually associated with telomere erosion after repeated cell divisions and occurs in response to abnormal oncogenic signaling, oxidative stress, and DNA damage [66]. To this purpose, natural compounds targeting the epigenetic control of senescence are under investigations to develop additional prosenescence cancer therapeutic strategies [67]. Several anticancer polyphenolic compounds from fruit and vegetables have been shown to be potential chemopreventive and anticancer bioactive compounds [68] to induce cellular growth arrest through the induction of a ROS-dependent premature senescence. Among them, 20(S)-ginsenoside Rg3, a compound extracted from ginseng, and bisdemethoxycurcumin, a natural derivative of curcumin, caused senescence-like growth arrest and increased ROS production, respectively, in human glioma

cells [69] (and human breast cancer cell [70]. Therefore, high doses of polyphenolic extracts from artichoke may induce apoptosis and decrease cell proliferation of the human breast cancer cell line, MDA-MB231 via the induction of premature senescence through epigenetic and ROS-mediated mechanisms [71]. Importantly, the authors have shown that Artichoke extracts have a pro-oxidant activity in breast cancer cells [72] and an antioxidant effect on normal hepatocytes [43]. Therefore, it has been hypothesized that Polyphenolic artichoke extracts could selectively inhibit the tumor cells growth with no cytotoxicity on healthy cells related on their differential cellular redox status. Furthermore, treatment with a low dose of resveratrol exhibits its chemopreventive and anticancer activities by induction of premature senescence in lung cancer cells. This event is associated with an increase in ROS generation and DNA double strands break through the up-regulation of NADPH oxidase-5 expression [73]. The inhibitory effect of resveratrol was verified *in vitro* and *in vivo*, respectively, on gastric cells cancer and nude mice xenograft model. Low doses of resveratrol treatment arrested gastric cancer cells in the G1 phase and led to senescence instead of apoptosis and exerted inhibitory effect on gastric development and significantly decreased the fraction of Ki67-positive cells in the nude mice tumor specimens [74]. Interestingly, Resveratrol and quercetin administers in subapoptotic doses can induce senescence-like growth arrest in glioma tumors treatment [75]. The concept of prosenescence therapy has emerged over the past few years as a novel therapeutic approach to treat cancers, which may be viewed either as an independent anticancer approach or as a combined strategy with conventional chemo/radiotherapy [76]. In a neoadjuvant setting, prosenescence therapy could be also used with traditional treatments in order to reduce tumor mass before surgery; whereas in adjuvant therapy, the engagement of prosenescence could be helpful in reducing the statistical risk of cancer relapse [77]. Although the effective potential of polyphenol in anticancer therapy as well as their other various beneficial effects on human health, the poor bioavailability of these active ingredients still a pending issue which limits their potential effects and their incorporation on western medicine. Further aimed challenging studies are needed to improve the absorption, distribution, and metabolism in order to develop the *in vivo* use and in clinical interventions.

2.2.3. Artemisinin: a cytotoxic molecule with medical interests

Artemisinin, the active component of Qinghao (Chinese name of *Artemisia annua* L.) was discovered in 1972 by Professor Tu's team [78], a discovery that was recognized by her receipt of the Nobel Prize in medicine in 2015. Artemisinin belongs to the family of sesquiterpene lactone with an endoperoxide bridge found to be important for its activity. The yield of artemisinin that can be extracted from *Artemisia annua* ranges from 0.01 and 0.8% of the dry weight [79]. This amount of extraction represents a serious limitation on the drug commercialization. Consequently, genetic engineering techniques have been used with the aim to improve the production of artemisinin in cell plant cultures and in transgenic plants as well.

2.2.3.1. *In vitro* cytotoxic properties of artemisinin

A significant cytotoxicity of artemisinin against tumors has been recently documented. It suggests that artemisinin, commonly used against malaria, can be used to prevent and treat cancer [80–83]. It is a relatively safe drug, with known pharmacokinetics and pharmacodynamics studies. In fact, *in vitro* work on the effects of artemisinin, at different concentrations, shows

that artemisinin significantly inhibited growth and colony formation of human hepatocellular carcinoma cells through inducing apoptosis pathway [84]. Artemisinin at 20 $\mu\text{mol/l}$ for 24 or 48 h of exposure inhibits growth and cell viability of human ovarian carcinoma cell lines (OVCAR-432 and SK-OV-3) [85]. Moreover, a recent study from our laboratory demonstrated that artemisinin has a differential effect on cancer cells. In fact, artemisinin induced lysis on the murin mastocytoma cancer cell line (P815) with $\text{IC}_{50} = 12 \mu\text{M}$ and on kidney adeno-carcinoma cell line of hamster with $\text{IC}_{50} = 52 \mu\text{M}$ [86]. Furthermore, artemisinin was described to possess an anticancer effect on breast, lung, prostate, colon, leukemia, and other cancer cell types. Despite its efficacy, artemisinin has pharmacokinetic limitations such as poor bioavailability and low solubility in water or oil [87]. Thus, it was developed with semi-synthetic derivatives drugs to overcome some of these problems. So far, semi-synthetic derivative of artemisinin such as artesunate and dihydroartemisinin have been demonstrated to exert an important *in vitro* anti-cancer activity against different cancer cell lines. In breast cancer cells (MCF-7), artemisinin is less active, and the activity in these cells can be estrogen receptors-mediated ($\text{ER}\beta$ and $\text{ER}\alpha$) which are implicated in cell proliferation [88]. In metastatic nasopharyngeal carcinoma cell lines (CNE-2 and CNE-1), the less sensitivity to artemisinin seems to be related to the over expression of polycomb complex protein BMI-1 [89]. Previously, Efferth et al. described a profound cytotoxic activity of artesunate, a semi-synthetic derivative of artemisinin, against 55 cancer cell lines of the U.S. National Cancer Institute with IC_{50} ranged from 246 nM to 100 μM , by activating the expression of CDC25A and EGFR genes in cancer cells [83]. Another study by Efferth et al. showed that artesunate cytotoxicity on isogenic *Saccharomyces cerevisiae* with defined genetic defects, involved the implication of two putative target genes, BUB3 and CLN2 [82]. Furthermore, it was described that the anticancer activity of artesunate, arteether, and artemether (semi-synthetic derivative of artemisinin) is associated with the basal mRNA expression of 464 genes linked to proliferation of cells [90]. Generally, artemisinin molecules have been described to be more cytotoxic against cancer than normal healthy cells [86, 91], since normal cells contain significantly less free iron than cancer cells. In general, cancer cells, express more cell surface transferrin receptors and uptake significantly more iron than do normal cells [91].

Several studies have tried to explain, at molecular level, the mechanism of its anti-cancer action. A study on HL-60 cancer cell line demonstrated that rapid production of reactive oxygen species is associated with cell death by apoptosis after artemisinin treated cells [92]. Other factors such as endoplasmic reticulum stress and calcium metabolism can also be associated with the anticancer activity of artemisinins [93, 94]. Endoplasmic reticulum seems to be a possible site for artemisinin action, in HepG2 cancer cell line a derivative fluorescence accumulates preferentially in the endoplasmic reticulum as described by Crespo et al. [95].

Artemisinin has been described to induce apoptosis effect [86, 96, 97], as well as cell cycle arrest, especially at G0/G1 cell cycle transition phase [89, 98]. Multiple lines of evidence suggest that the apoptotic pathway could be due to intra and/or extra-mitochondrial mode of action, and the involvements of iron/heme as well [81, 99]. Two mechanistic pathways have been frequently described to explain the apoptotic effect of artemisinin, vascular endothelial growth factor decrease [100–102], and nuclear factor-kappa B inhibition [103, 104]. Recently, other processes have also been illustrated in different cancer cell types, by the involvement of NOXA [105], mitogen-activated protein kinase (MAPK) [106], Wnt/ β -catenin

[107], surviving [108], COX [109], c-MYC oncoprotein [93, 110], and epidermal growth factor [111]. Furthermore, it was also reported that the sensitivity to artemisinin action was related to the expression level of proapoptotic (Bax) and antiapoptotic (Bcl2) genes [112]. Also, artemisinin role in the inhibition of cancer is postulated to be associated with direct DNA damage [113] or indirectly in tumor cells involving a cascade of signaling pathways in many hallmarks of cancer [114]. Taken together, these results could explain the apoptotic pathway induction by artemisinin on tested cancer cells [101, 102, 115, 116]. However, we have also reported the possibility of the involvement of another cell death process of artemisinin; probably necrosis [86]. Artemisinin-induced necrosis remains not well documented and may be linked with the increasing level of ATP, defective apoptotic pathways, reactive oxygen species-independent mechanism of programmed cell death and cancer cell line type [86]. Furthermore, we have described that artemisinin interacted synergistically and additively with vincristin to reduce cancer cell proliferation [86], suggesting a possible use of artemisinin as an adjuvant to treat cancer.

2.2.3.2. *In vivo anti-tumor and antimetastatic effects*

Artemisinin treatment in oral route at 80 mg/kg considerably reduced the tumor volume growth of P815/DBA2 mice as described by our team [86]. In HepG2 and Hep3B human hepatoma mouse xenograft, artemisinin administered at 50 or 100 mg/kg/day delayed tumor onset, respectively, by 30 and 39.4% [117]. Also, in another study, artemisinin reduced tumor growth at 50% on day 20, when injected intraperitoneally at a concentration of 2.8 mg/kg/day on mammary gland ductal carcinoma in mice [118]. Inhibition of tumor growth and anti-angiogenic effect in MCF-7 mouse xenograft after subcutaneous treatment with artemisinin at dose 100 mg/kg/day for 2 weeks was reported [98]. Interestingly, artemisinin exhibited an anti-metastatic effect [116]. In fact, these authors showed that after orally artemisinin treatment with 50 mg/kg, a reduction of 63.5% of lung metastasis and lymph node metastases decrease in cervical and mediastinal lymph nodes, as well as an inhibition of lymphangiogenesis by 63% of mice. Artemisinin also exhibited inhibitory effects in lung tumor metastasis by 51.8 and 79.6% for 50 and 100 mg/kg/day, respectively. Furthermore, it was described that artesunate given in the drinking water at 167 mg/kg/day suppressed growth of Kaposi's sarcoma-IMM xenograft tumors in nude mice [119]. The antimetastatic effect of artemisinin seems to be associated with the expression of metalloproteinase genes and their effect on $\alpha\beta3$ integrins [120]. Moreover, the decrease of MMP2 with an increase of TIMP-2 in HepG2 and SMMC772 cancer cell lines after artemisinin treatment were reported [121]. Interestingly, the antimetastatic effect of artemisinin could be triggered by enhancing Cdc42 and E-cadherin activation [121]. However, in highly metastatic cancer such as nasopharyngeal cancer (CNE-1, CNE-2 cancer cell lines), artemisinin seems to have a low response due to the overexpression of BMI-1 gene that makes these cancer cells more sensitive to artemisinin drug [122]. In highly metastatic MDA-MB-231 breast tumor cells, artesunate induced resistance as described by Beatrice Bachmeier et al. (2011). This resistance was induced by the activation of transcription factors NF- κ B and AP-1 [123]. Another study showed suppression of invasive and metastatic non-small cell lung cancer after artesunate treatment by the inhibition of urokinase-type plasminogen activator (u-PA), and matrix metalloproteinases (especially MMP-2 and MMP-7) transcription [10].

3. Conclusion

Nature continues to produce a great wealth of natural molecules endowed with cytotoxic activity towards a large panel of tumor cells. More than 60% of these molecules such as vincristine, vincristine, etoposide, teniposide, taxol, navelbine, and camptothecin are used in chemotherapy and others have shown great anti-tumor and anti-metastatic potential in pre-clinical trials [124, 125]. Other natural product (i.e., Romidepsin 14, *Omacetaxine mepesuccinate*) [126] and natural product-derived drugs (i.e., metformin, metformin Polyphenon E, retinoids, soy isoflavones) [127] are in clinical trials. This chapter discusses some examples of these molecules (carvacrol, thymol, carveol, carvone, eugenol, isopulegol, and artemisinin) as well as polyphenols extract that have been studied in our laboratory. Other natural compounds are also under studies and remain promising. It is clear that if we understand the molecular mechanisms of the various interactions between these cytotoxic molecules on the one hand and the tumor cells in their tumoral environments on the other hand, we can develop new therapeutic modalities to overcome the side effects of these molecules and to fight cancer.

Acknowledgements

This work was supported by the Lalla Salma Foundation: Prevention and treatment of cancer-Rabat-Morocco (Research Project N° 09/AP 2013).

Author details

Abdelmajid Zyad^{1*}, Inass Leouifoudi¹, Mounir Tilaoui¹, Hassan Ait Mouse¹,
Mouna Khouchani² and Abdeslam Jaafari¹

*Address all correspondence to: ab.zyad2@gmail.com

1 Laboratory of Biological Engineering, Team of Natural Substances and Cellular & Molecular Immuno-pharmacology, Immuno-biology of Cancer Cells, Sultan Moulay Slimane University, Faculty of Science and Technology, Beni-Mellal, Morocco

2 Department of Oncology-Radiotherapy, University Hospital Mohamed VI, Faculty of medicine, Marrakech, Morocco

References

- [1] Cragg GM, Newman DJ. Natural products: A continuing source of novel drug leads. *Biochimica et Biophysica Acta (BBA): General Subjects*. 2013;**1830**(6):3670-3695
- [2] Tilaoui M, Mouse HA, Jaafari A, Zyad A. Comparative phytochemical analysis of essential oils from different biological parts of *Artemisia herba alba* and their cytotoxic effect on cancer cells. *PLoS One*. 2015;**10**(7):e0131799

- [3] Oliveira AH, de Oliveira GG, Carnevale Neto F, Portuondo DF, Batista-Duarte A, Carlos IZ. Anti-inflammatory activity of *Vismia guianensis* (Aubl.) Pers. extracts and antifungal activity against *Sporothrix schenckii*. *Journal of Ethnopharmacology* 2017;**195**:266-274
- [4] Grifo F, Newman D, Fairfield AS, Bhattacharya B, Grupenhoff JT. The origins of prescription drugs. In: *Biodiversity and Human Health*. 1997. pp. 131-163
- [5] Arvigo R, Balick MJ. *Rainforest Remedies: One Hundred Healing Herbs of Belize*. Wisconsin: Lotus Press; 1993
- [6] Cooper GM. *The Cancer Book: A Guide to Understanding the Causes, Prevention, and Treatment of Cancer*. MA, USA: Jones & Bartlett Learning; 1993
- [7] Cragg GM, Newman DJ. Discovery and development of antineoplastic agents from natural sources. *Cancer Investigation*. 1999;**17**(2):153-163
- [8] Da Rocha AB, Lopes RM, Schwartzmann G. Natural products in anticancer therapy. *Current Opinion in Pharmacology*. 2001;**1**(4):364-369
- [9] Jaafari A, Mouse HA, Rakib EM, Tilaoui M, Benbakhta C, Boulli A, Abbad A, Zyad A. Chemical composition and antitumor activity of different wild varieties of Moroccan thyme. *Revista Brasileira de Farmacognosia*. 2007;**17**(4):477-491
- [10] Rasheed SAK, Efferth T, Asangani IA, Allgayer H. First evidence that the antimalarial drug artesunate inhibits invasion and *in vivo* metastasis in lung cancer by targeting essential extracellular proteases. *International Journal of Cancer*. 2010;**127**(6):1475-1485
- [11] Benencia F, Courreges MC. *In vitro* and *in vivo* activity of eugenol on human herpesvirus. *Phytotherapy Research*. 2000;**14**(7):495-500
- [12] Zheng G-Q, Kenney PM, Lam LK. Sesquiterpenes from clove (*Eugenia caryophyllata*) as potential anticarcinogenic agents. *Journal of Natural Products*. 1992;**55**(7):999-1003
- [13] Naigre R, Kalck P, Roques C, Roux I, Michel G. Comparison of antimicrobial properties of monoterpenes and their carbonylated products. *Planta Medica*. 1996;**62**(03):275-277
- [14] Wiseman DA, Werner SR, Crowell PL. Cell cycle arrest by the isoprenoids perillyl alcohol, geraniol, and farnesol is mediated by p21Cip1 and p27Kip1 in human pancreatic adenocarcinoma cells. *The Journal of Pharmacology and Experimental Therapeutics*. 2007;**320**(3):1163-1170
- [15] Sobral MV, Xavier AL, Lima TC, de Sousa DP. Antitumor activity of monoterpenes found in essential oils. *The Scientific World Journal*. 2014;**2014**:953451
- [16] Zeytinoglu H, Incesu Z, Baser KHC. Inhibition of DNA synthesis by carvacrol in mouse myoblast cells bearing a human N-RAS oncogene. *Phytomedicine*. 2003;**10**(4):292-299
- [17] Jaafari A, Tilaoui M, Mouse HA, M'bark LA, Aboufatima R, Chait A, Lepoivre M, Zyad A. Comparative study of the antitumor effect of natural monoterpenes: Relationship to cell cycle analysis. *Revista Brasileira de Farmacognosia*. 2012;**22**(3):534-540
- [18] Yoshikawa T, Kokura S, Tainaka K, Naito Y, Kondo M. A novel cancer therapy based on oxygen radicals. *Cancer Research*. 1995;**55**(8):1617-1620

- [19] Karkabounas S, Kostoula OK, Daskalou T, Veltsistas P, Karamouzis M, Zelovitis I, Metsios A, Lekkas P, Evangelou AM, Kotsis N. Anticarcinogenic and antiplatelet effects of carvacrol. *Experimental Oncology*. 2006;**28**(2):121-125
- [20] Park BS, Song YS, Yee S-B, Lee BG, Seo SY, Park YC, Kim J-M, Kim HM, Yoo YH. Phosphoser 15-p53 translocates into mitochondria and interacts with Bcl-2 and Bcl-xL in eugenol-induced apoptosis. *Apoptosis*. 2005;**10**(1):193-200
- [21] Ghosh R, Nadiminty N, Fitzpatrick JE, Alworth WL, Slaga TJ, Kumar AP. Eugenol causes melanoma growth suppression through inhibition of E2F1 transcriptional activity. *The Journal of Biological Chemistry*. 2005;**280**(7):5812-5819
- [22] Miller JA, Swanson AB, Miller EC. The metabolic activation of safrole and related naturally occurring alkenylbenzenes in relation to carcinogenesis by these agents. In: *Proceedings International Symposium Princess Takamatsu Cancer Research Fund*; 1979. pp. 111-125
- [23] Crowell PL. Monoterpenes in breast cancer chemoprevention. *Breast Cancer Research and Treatment*. 1997;**46**(2):191-197
- [24] Wattenberg LW, Sparnins VL, Barany G. Inhibition of N-nitrosodiethylamine carcinogenesis in mice by naturally occurring organosulfur compounds and monoterpenes. *Cancer Research*. 1989;**49**(10):2689-2692
- [25] Horvathova E, Turcaniova V, Slamenova D. Comparative study of DNA-damaging and DNA-protective effects of selected components of essential plant oils in human leukemic cells K562. *Neoplasma*. 2007;**54**(6):478-483
- [26] Stamatii A, Bonsi P, Zucco F, Moezelaar R, Alakomi H-L, Von Wright A. Toxicity of selected plant volatiles in microbial and mammalian short-term assays. *Food and Chemical Toxicology*. 1999;**37**(8):813-823
- [27] Koparal AT, Zeytinoglu M. Effects of carvacrol on a human non-small cell lung cancer (NSCLC) cell line, A549. In: *Animal Cell Technology: Basic & Applied Aspects*. Dordrecht: Springer; 2003. pp. 207-211
- [28] Jordheim LP, Guittet O, Lepoivre M, Galmarini CM, Dumontet C. Increased expression of the large subunit of ribonucleotide reductase is involved in resistance to gemcitabine in human mammary adenocarcinoma cells. *Molecular Cancer Therapeutics*. 2005;**4**(8):1268-1276
- [29] Bardon S, Foussard V, Fournel S, Loubat A. Monoterpenes inhibit proliferation of human colon cancer cells by modulating cell cycle-related protein expression. *Cancer Letters*. 2002;**181**(2):187-194
- [30] Chander SK, Lansdown AGB, Luqmani YA, Gomm JJ, Coope RC, Gould N, Coombes RC. Effectiveness of combined limonene and 4-hydroxyandrostenedione in the treatment of NMU-induced rat mammary tumours. *British Journal of Cancer*. 1994;**69**(5):879-882
- [31] Obrenovich ME, Nair NG, Beyaz A, Aliev G, Reddy VP. The role of polyphenolic antioxidants in health, disease, and aging. *Rejuvenation Research*. 2010;**13**(6):631-643

- [32] Leouifoudi I, Harnafi H, Zyad A. Olive mill waste extracts: Polyphenols content, antioxidant, and antimicrobial activities. *Advances in Pharmacological Sciences*. 2015;**2015**: 714138
- [33] Obied HK, Prenzler PD, Konczak I, Rehman A, Robards K. Chemistry and bioactivity of olive biophenols in some antioxidant and antiproliferative *in vitro* bioassays. *Chemical Research in Toxicology*. 2008;**22**(1):227-234
- [34] Mileo AM, Miccadei S. Polyphenols as modulator of oxidative stress in cancer disease: New therapeutic strategies. *Oxidative Medicine and Cellular Longevity*. 2015;**2016**
- [35] Singh M, Bhui K, Singh R, Shukla Y. Tea polyphenols enhance cisplatin chemosensitivity in cervical cancer cells via induction of apoptosis. *Life Sciences*. 2013;**93**(1):7-16
- [36] Thawonsuwan J, Kiron V, Satoh S, Panigrahi A, Verlhac V. Epigallocatechin-3-gallate (EGCG) affects the antioxidant and immune defense of the rainbow trout, *Oncorhynchus mykiss*. *Fish Physiology and Biochemistry*. 2010;**36**(3):687-697
- [37] Ahmad N, Gupta S, Mukhtar H. Green tea polyphenol epigallocatechin-3-gallate differentially modulates nuclear factor κ B in cancer cells versus normal cells. *Archives of Biochemistry and Biophysics*. 2000;**376**(2):338-346
- [38] Oak M-H, El Bedoui J, Schini-Kerth VB. Antiangiogenic properties of natural polyphenols from red wine and green tea. *The Journal of Nutritional Biochemistry*. 2005;**16**(1):1-8
- [39] Alexandre J, Batteux F, Nicco C, Chéreau C, Laurent A, Guillevin L, Weill B, Goldwasser F. Accumulation of hydrogen peroxide is an early and crucial step for paclitaxel-induced cancer cell death both *in vitro* and *in vivo*. *International Journal of Cancer*. 2006;**119**(1):41-48
- [40] Borin TF, Arbab AS, Gelaleti GB, Ferreira LC, Moschetta MG, Jardim-Perassi BV, Iskander ASM, Varma NRS, Shankar A, Coimbra VB. Melatonin decreases breast cancer metastasis by modulating rho-associated kinase protein-1 expression. *Journal of Pineal Research*. 2016;**60**(1):3-15
- [41] Danesi F, Kroon PA, Saha S, de Biase D, D'Antuono LF, Bordoni A. Mixed pro-and anti-oxidative effects of pomegranate polyphenols in cultured cells. *International Journal of Molecular Sciences*. 2014;**15**(11):19458-19471
- [42] Symonds EL, Konczak I, Fenech M. The Australian fruit Illawarra plum (*Podocarpus elatus* Endl., Podocarpaceae) inhibits telomerase, increases histone deacetylase activity and decreases proliferation of colon cancer cells. *The British Journal of Nutrition*. 2013;**109**(12):2117-2125
- [43] Miccadei S, Di Venere D, Cardinali A, Romano F, Durazzo A, Foddai MS, Fraioli R, Mobarhan S, Maiani G. Antioxidative and apoptotic properties of polyphenolic extracts from edible part of artichoke (*Cynara scolymus* L.) on cultured rat hepatocytes and on human hepatoma cells. *Nutrition and Cancer*. 2008;**60**(2):276-283
- [44] Katiyar SK, Matsui MS, Elmets CA, Mukhtar H. Polyphenolic antioxidant (-)-epigallocatechin-3-gallate from green tea reduces UVB-induced inflammatory responses and infiltration of leukocytes in human skin. *Photochemistry and Photobiology*. 1999;**69**(2): 148-153

- [45] Giovannini C, Masella R. Role of polyphenols in cell death control. *Nutritional Neuroscience*. 2012;**15**(3):134-149
- [46] Kang NJ, Shin SH, Lee HJ, Lee KW. Polyphenols as small molecular inhibitors of signaling cascades in carcinogenesis. *Pharmacology & Therapeutics*. 2011;**130**(3):310-324
- [47] Rodríguez ML, Estrela JM, Ortega Á. Natural polyphenols and apoptosis induction in cancer therapy. *Journal of Carcinogenesis & Mutagenesis*. 2013;**6**:1-10
- [48] Nooshinfar E, Bashash D, Safaroghli-Azar A, Bayati S, Rezaei-Tavirani M, Ghaffari SH, Akbari ME. Melatonin promotes ATO-induced apoptosis in MCF-7 cells: Proposing novel therapeutic potential for breast cancer. *Biomedicine & Pharmacotherapy*. 2016;**83**: 456-465
- [49] Andersen MH, Svane IM, Kvistborg P, Nielsen OJ, Balslev E, Reker S, Becker JC, Straten P. Immunogenicity of Bcl-2 in patients with cancer. *Blood*. 2005;**105**(2):728-734
- [50] George J, Singh M, Srivastava AK, Bhui K, Roy P, Chaturvedi PK, Shukla Y. Resveratrol and black tea polyphenol combination synergistically suppress mouse skin tumors growth by inhibition of activated MAPKs and p53. *PLoS One*. 2011;**6**(8):e23395
- [51] Schneider G, Krämer OH. NF κ B/p53 crosstalk—A promising new therapeutic target. *Biochimica et Biophysica Acta (BBA): Reviews on Cancer*. 2011;**1815**(1):90-103
- [52] Obregon DF, Rezai-Zadeh K, Bai Y, Sun N, Hou H, Ehrhart J, Zeng J, Mori T, Arendash GW, Shytle D. ADAM10 activation is required for green tea (-)-epigallocatechin-3-gallate-induced α -secretase cleavage of amyloid precursor protein. *The Journal of Biological Chemistry*. 2006;**281**(24):16419-16427
- [53] Arul D, Subramanian P. Naringenin (*citrus flavonone*) induces growth inhibition, cell cycle arrest and apoptosis in human hepatocellular carcinoma cells. *Pathology Oncology Research*. 2013;**19**(4):763-770
- [54] Singh N, Nigam M, Ranjan V, Sharma R, Balapure AK, Rath SK. Caspase mediated enhanced apoptotic action of cyclophosphamide-and resveratrol-treated MCF-7 cells. *Journal of Pharmacological Sciences*. 2009;**109**(4):473-485
- [55] Mukhtar H, Ahmad N. Tea polyphenols: Prevention of cancer and optimizing health. *The American Journal of Clinical Nutrition*. 2000;**71**(6):1698s-1702s
- [56] Fujiki H, Suganuma M, Okabe S, Sueoka E, Sueoka N, Fujimoto N, Goto Y, Matsuyama S, Imai K, Nakachi K. Cancer prevention with green tea and monitoring by a new biomarker, hnRNP B1. *Mutation Research. Fundamental and Molecular Mechanisms of Mutagenesis*. 2001;**480**:299-304
- [57] Roy P, Kalra N, Nigam N, George J, Ray RS, Hans RK, Prasad S, Shukla Y. Resveratrol enhances ultraviolet B-induced cell death through nuclear factor- κ B pathway in human epidermoid carcinoma A431 cells. *Biochemical and Biophysical Research Communications*. 2009;**384**(2):215-220
- [58] Bernini R, Crisante F, Merendino N, Molinari R, Soldatelli MC, Velotti F. Synthesis of a novel ester of hydroxytyrosol and α -lipoic acid exhibiting an antiproliferative

- effect on human colon cancer HT-29 cells. *European Journal of Medicinal Chemistry*. 2011;**46**(1):439-446
- [59] Kim S, Park TI. Naringenin: A partial agonist on estrogen receptor in T47D-KBluc breast cancer cells. *International Journal of Clinical and Experimental Medicine*. 2013;**6**(10):890
- [60] Murakami A. Dose-dependent functionality and toxicity of green tea polyphenols in experimental rodents. *Archives of Biochemistry and Biophysics*. 2014;**557**:3-10
- [61] Leouifoudi I, Mbarki M, Tilaoui M, Amechrouq A, Rakib EM, Mouse HA, Ziad A. Study of the *in vitro* anticancer activity of Moroccan phenolic olive cake extracts. *Journal of Pharmacognosy and Phytochemistry*. 2014;**2**(6):154-165
- [62] Schepetkin IA, Ramstead AG, Kirpotina LN, Voyich JM, Jutila MA, Quinn MT. Therapeutic potential of polyphenols from *Epilobium angustifolium* (fireweed). *Phytotherapy Research*. 2016;**30**(8):1287-1297
- [63] Qin L, Jin L, Lu L, Lu X, Zhang C, Zhang F, Liang W. Naringenin reduces lung metastasis in a breast cancer resection model. *Protein & Cell*. 2011;**2**(6):507-516
- [64] Naylor RM, Baker DJ, Deursen J van. Senescent cells: A novel therapeutic target for aging and age-related diseases. *Clinical Pharmacology and Therapeutics* 2013;**93**(1):105-116
- [65] Jose Marin J, Vergel M, Carnero A. Targeting cancer by inducing senescence. *The Open Enzyme Inhibition Journal*. 2010 [cité 19 Nov. 2017];**3**(1):46-52
- [66] Lee M, Lee J-S. Exploiting tumor cell senescence in anticancer therapy. *BMB Reports*. 2014;**47**(2):51-59
- [67] Banerjee K, Mandal M. Oxidative stress triggered by naturally occurring flavone apigenin results in senescence and chemotherapeutic effect in human colorectal cancer cells. *Redox Biology*. 2015;**5**:153-162
- [68] Khan HY, Zubair H, Ullah MF, Ahmad A, Hadi SM. A prooxidant mechanism for the anticancer and chemopreventive properties of plant polyphenols. *Current Drug Targets*. 2012;**13**(14):1738-1749
- [69] Sin S, Kim SY, Kim SS. Chronic treatment with ginsenoside Rg3 induces Akt-dependent senescence in human glioma cells. *International Journal of Oncology*. 2012;**41**(5):1669-1674
- [70] Li Y-B, Gao J-L, Zhong Z-F, Hoi P-M, Lee SM-Y, Wang Y-T. Bisdemethoxycurcumin suppresses MCF-7 cells proliferation by inducing ROS accumulation and modulating senescence-related pathways. *Pharmacological Reports*. 2013;**65**(3):700-709
- [71] Mileo AM, Di Venere D, Linsalata V, Fraioli R, Miccadei S. Artichoke polyphenols induce apoptosis and decrease the invasive potential of the human breast cancer cell line MDA-MB231. *Journal of Cellular Physiology*. 2012;**227**(9):3301-3309
- [72] Mileo AM, Di Venere D, Abbruzzese C, Miccadei S. Long term exposure to polyphenols of artichoke (*Cynara scolymus* L.) exerts induction of senescence driven growth arrest in the MDA-MB231 human breast cancer cell line. *Oxidative Medicine and Cellular Longevity*. 2015;**2015**:1-11

- [73] Luo H, Yang A, Schulte BA, Wargovich MJ, Wang GY. Resveratrol induces premature senescence in lung cancer cells via ROS-mediated DNA damage. *PLoS One*. 2013;**8**(3): e60065
- [74] Yang Q, Wang B, Zang W, Wang X, Liu Z, Li W, Jia J. Resveratrol inhibits the growth of gastric cancer by inducing G1 phase arrest and senescence in a Sirt1-dependent manner. *PLoS One*. 2013;**8**(11):e70627
- [75] Zamin LL, Filippi-Chiela EC, Dillenburg-Pilla P, Horn F, Salbego C, Lenz G. Resveratrol and quercetin cooperate to induce senescence-like growth arrest in C6 rat glioma cells. *Cancer Science*. 2009;**100**(9):1655-1662
- [76] Cairney CJ, Bilsland AE, Evans TJ, Roffey J, Bennett DC, Narita M, Torrance CJ, Keith WN. Cancer cell senescence: A new frontier in drug development. *Drug Discovery Today*. 2012;**17**(5):269-276
- [77] Acosta JC, Gil J. Senescence: A new weapon for cancer therapy. *Trends in Cell Biology*. 2012;**22**(4):211-219
- [78] Tu Y. The discovery of artemisinin (qinghaosu) and gifts from Chinese medicine. *Nature Medicine* 2011;**17**(10):1217-20
- [79] Van Agtmael MA, Eggelte TA, van Boxtel CJ. Artemisinin drugs in the treatment of malaria: From medicinal herb to registered medication. *Trends in Pharmacological Sciences*. 1999;**20**(5):199-205
- [80] Woerdenbag HJ, Moskal TA, Pras N, Malingré TM, FS e-F, Kampinga HH, Konings AW. Cytotoxicity of artemisinin-related endoperoxides to Ehrlich ascites tumor cells. *Journal of Natural Products*. 1993;**56**(6):849-856
- [81] Lai H, Singh NP. Selective cancer cell cytotoxicity from exposure to dihydroartemisinin and holotransferrin. *Cancer Letters*. 1995;**91**(1):41-46
- [82] Efferth T, Dunstan H, Sauerbrey A, Miyachi H, Chitambar CR. The anti-malarial artesunate is also active against cancer. *International Journal of Oncology*. 2001;**18**(4):767-773
- [83] Efferth T, Sauerbrey A, Olbrich A, Gebhart E, Rauch P, Weber HO, Hengstler JG, Halatsch M-E, Volm M, Tew KD, et al. Molecular modes of action of artesunate in tumor cell lines. *Molecular Pharmacology*. 2003;**64**(2):382-394
- [84] Deng X, Liu Z, Liu F, Pan L, Yu H, Jiang J, Zhang J, Liu L, Yu J. Holotransferrin enhances selective anticancer activity of artemisinin against human hepatocellular carcinoma cells. *Journal of Huazhong University of Science and Technology. Medical Sciences = Hua zhong ke ji da xue xue bao. Yi xue Ying De wen ban = Huazhong keji daxue xuebao. Yixue Yingdewen ban*. 2013;**33**(6):862-865
- [85] Jiao Y, Ge C, Meng Q, Cao J, Tong J, Fan S. Dihydroartemisinin is an inhibitor of ovarian cancer cell growth. *Acta Pharmacologica Sinica*. 2007;**28**(7):1045
- [86] Tilaoui M, Mouse HA, Jaafari A, Ziad A. Differential effect of artemisinin against cancer cell lines. *Natural Products and Bioprospecting*. 2014;**4**(3):189-196

- [87] Li Q, Weina PJ, Milhous WK. Pharmacokinetic and pharmacodynamic profiles of rapid-acting artemisinins in the antimalarial therapy. *Current Drug Therapy*. 2007;**2**(3):210-223
- [88] Firestone GL, Sundar SN. Anticancer activities of artemisinin and its bioactive derivatives. *Expert Reviews in Molecular Medicine*. 2009;**11**:e32
- [89] Wu J, Hu D, Yang G, Zhou J, Yang C, Gao Y, Zhu Z. Down-regulation of BMI-1 cooperates with artemisinin on growth inhibition of nasopharyngeal carcinoma cells. *Journal of Cellular Biochemistry*. 2011;**112**(7):1938-1948
- [90] Efferth T, Davey M, Olbrich A, Rücker G, Gebhart E, Davey R. Activity of drugs from traditional Chinese medicine toward sensitive and MDR1- or MRP1-overexpressing multi-drug-resistant human CCRF-CEM leukemia cells. *Blood Cells, Molecules & Diseases*. 2002;**28**(2):160-168
- [91] Lai H, Sasaki T, Singh NP, Messay A. Effects of artemisinin-tagged holotransferrin on cancer cells. *Life Sciences*. 2005;**76**(11):1267-1279
- [92] Zhou C, Pan W, Wang XP, Chen TS. Artesunate induces apoptosis via a Bak-mediated caspase-independent intrinsic pathway in human lung adenocarcinoma cells. *Journal of Cellular Physiology*. 2012;**227**(12):3778-3786
- [93] Lu J-J, Meng L-H, Shankavaram UT, Zhu C-H, Tong L-J, Chen G, Lin L-P, Weinstein JN, Ding J. Dihydroartemisinin accelerates c-MYC oncoprotein degradation and induces apoptosis in c-MYC-overexpressing tumor cells. *Biochemical Pharmacology*. 2010;**80**(1):22-30
- [94] Lu J-J, Chen S-M, Zhang X-W, Ding J, Meng L-H. The anti-cancer activity of dihydroartemisinin is associated with induction of iron-dependent endoplasmic reticulum stress in colorectal carcinoma HCT116 cells. *Investigational New Drugs*. 2011;**29**(6):1276-1283
- [95] Crespo-Ortiz MP, Wei MQ. Antitumor activity of artemisinin and its derivatives: From a well-known antimalarial agent to a potential anticancer drug. *BioMed Research International*. 2011;**2012**:e247597
- [96] Efferth T. Willmar Schwabe award 2006: Antiplasmodial and antitumor activity of artemisinin—From bench to bedside. *Planta Medica*. 2007;**73**(4):299-309
- [97] Hamacher-Brady A, Stein HA, Turschner S, Toegel I, Mora R, Jennewein N, Efferth T, Eils R, Brady NR. Artesunate activates mitochondrial apoptosis in breast cancer cells via iron-catalyzed lysosomal reactive oxygen species production. *The Journal of Biological Chemistry*. 2011;**286**(8):6587-6601
- [98] Tin AS, Sundar SN, Tran KQ, Park AH, Poindexter KM, Firestone GL. Antiproliferative effects of artemisinin on human breast cancer cells requires the downregulated expression of the E2F1 transcription factor and loss of E2F1-target cell cycle genes. *Anti-Cancer Drugs*. 2012;**23**(4):370-379
- [99] Zhang S, Chen H, Gerhard GS. Heme synthesis increases artemisinin-induced radical formation and cytotoxicity that can be suppressed by superoxide scavengers. *Chemico-Biological Interactions*. 2010;**186**(1):30-35

- [100] Anfosso L, Efferth T, Albini A, Pfeffer U. Microarray expression profiles of angiogenesis-related genes predict tumor cell response to artemisinins. *The Pharmacogenomics Journal*. 2006;**6**(4):269-278
- [101] Chen H-H, Zhou H-J, Wu G-D, Lou X-E. Inhibitory effects of artesunate on angiogenesis and on expressions of vascular endothelial growth factor and VEGF receptor KDR/flk-1. *Pharmacology*. 2004;**71**(1):1-9
- [102] Lee J, Zhou H-J, Wu X-H. Dihydroartemisinin downregulates vascular endothelial growth factor expression and induces apoptosis in chronic myeloid leukemia K562 cells. *Cancer Chemotherapy and Pharmacology*. 2006;**57**(2):213-220
- [103] Thanaketpaisarn O, Waiwut P, Sakurai H, Saiki I. Artesunate enhances TRAIL-induced apoptosis in human cervical carcinoma cells through inhibition of the NF- κ B and PI3K/Akt signaling pathways. *International Journal of Oncology*. 2011;**39**(1):279-285
- [104] Wang Y, Huang Z, Wang L, Meng S, Fan Y, Chen T, Cao J, Jiang R, Wang C. The anti-malarial artemisinin inhibits pro-inflammatory cytokines via the NF- κ B canonical signaling pathway in PMA-induced THP-1 monocytes. *International Journal of Molecular Medicine*. 2011;**27**(2):233-241
- [105] Cabello CM, Lamore SD, Bair WB III, Qiao S, Azimian S, Lesson JL, Wondrak GT. The redox antimalarial dihydroartemisinin targets human metastatic melanoma cells but not primary melanocytes with induction of NOXA-dependent apoptosis. *Investigational New Drugs*. 2012;**30**(4):1289-1301
- [106] Hwang YP, Yun HJ, Kim HG, Han EH, Lee GW, Jeong HG. Suppression of PMA-induced tumor cell invasion by dihydroartemisinin via inhibition of PKC α /Raf/MAPKs and NF- κ B/AP-1-dependent mechanisms. *Biochemical Pharmacology*. 2010;**79**(12):1714-1726
- [107] Li L-N, Zhang H-D, Yuan S-J, Tian Z-Y, Wang L, Sun Z-X. Artesunate attenuates the growth of human colorectal carcinoma and inhibits hyperactive Wnt/ β -catenin pathway. *International Journal of Cancer*. 2007;**121**(6):1360-1365
- [108] Mu D, Chen W, Yu B, Zhang C, Zhang Y, Qi H. Calcium and survivin are involved in the induction of apoptosis by dihydroartemisinin in human lung cancer SPC-A-1 cells. *Methods and Findings in Experimental and Clinical Pharmacology*. 2007;**29**(1):33-38
- [109] Wang J, Hou L, Yang Y, Tang W, Li Y, Zuo J. SM905, an artemisinin derivative, inhibited NO and pro-inflammatory cytokine production by suppressing MAPK and NF- κ B pathways in RAW 264.7 macrophages. *Acta Pharmacologica Sinica*. 2009;**30**(10):1428-1435
- [110] Sertel S, Eichhorn T, Simon CH, Plinkert PK, Johnson SW, Efferth T. Pharmacogenomic identification of c-Myc/max-regulated genes associated with cytotoxicity of artesunate towards human colon, ovarian and lung cancer cell lines. *Molecules*. 2010;**15**(4):2886-2910
- [111] Konkimalla VB, McCubrey JA, Efferth T. The role of downstream signaling pathways of the epidermal growth factor receptor for Artesunate's activity in cancer cells. *Current Cancer Drug Targets*. 2009;**9**(1):72-80
- [112] Karnak D, Xu L. Chemosensitization of prostate cancer by modulating Bcl-2 family proteins. *Current Drug Targets*. 2010;**11**(6):699-707

- [113] Li Y, Wu YL. How Chinese scientists discovered qinghaosu (artemisinin) and developed its derivatives? What are the future perspectives? *Médecine Trop Rev Corps Santé Colon*. 1998;**58**(3 Suppl):9-12
- [114] O'neill PM, Barton VE, Ward SA. The molecular mechanism of action of artemisinin—The debate continues. *Molecules*. 2010;**15**(3):1705-1721
- [115] Wartenberg M, Wolf S, Budde P, Grünheck F, Acker H, Hescheler J, Wartenberg G, Sauer H. The antimalaria agent artemisinin exerts antiangiogenic effects in mouse embryonic stem cell-derived embryoid bodies. *Laboratory Investigation*. 2003;**83**(11):1647-1655
- [116] Wang J, Zhang B, Guo Y, Li G, Xie Q, Zhu B, Gao J, Chen Z. Artemisinin inhibits tumor lymphangiogenesis by suppression of vascular endothelial growth factor C. *Pharmacology*. 2008;**82**(2):148-155
- [117] Hou J, Wang D, Zhang R, Wang H. Experimental therapy of hepatoma with artemisinin and its derivatives: *In vitro* and *in vivo* activity, chemosensitization, and mechanisms of action. *Clinical Cancer Research*. 2008;**14**(17):5519-5530
- [118] Langroudi L, Hassan ZM, Ebtekar M, Mahdavi M, Pakravan N, Noori S. A comparison of low-dose cyclophosphamide treatment with artemisinin treatment in reducing the number of regulatory T cells in murine breast cancer model. *International Immunopharmacology*. 2010;**10**(9):1055-1061
- [119] Dell'Eva R, Pfeffer U, Vené R, Anfosso L, Forlani A, Albini A, Efferth T. Inhibition of angiogenesis *in vivo* and growth of Kaposi's sarcoma xenograft tumors by the anti-malarial artesunate. *Biochemical Pharmacology*. 2004;**68**(12):2359-2366
- [120] Zhao F, Wang H, Kunda P, Chen X, Liu Q-L, Liu T. Artesunate exerts specific cytotoxicity in retinoblastoma cells via CD71. *Oncology Reports*. 2013;**30**(3):1473-1482
- [121] Cavallo F, De Giovanni C, Nanni P, Forni G, Lollini P-L. The immune hallmarks of cancer. *Cancer Immunology, Immunotherapy*. 2011;**60**(3):319-326
- [122] Ho WE, Peh HY, Chan TK, Wong WF. Artemisinins: Pharmacological actions beyond anti-malarial. *Pharmacology & Therapeutics*. 2014;**142**(1):126-139
- [123] Bachmeier B, Fichtner I, Killian PH, Kronski E, Pfeffer U, Efferth T. Development of resistance towards artesunate in MDA-MB-231 human breast cancer cells. *PLoS One*. 2011;**6**(5):e20550
- [124] Demain AL, Vaishnav P. Natural products for cancer chemotherapy. *Microbial Biotechnology*. 2011;**4**(6):687-699
- [125] Newman DJ, Cragg GM. Natural products as sources of new drugs over the last 25 years. *Journal of Natural Products*. 2007;**70**(3):461-477
- [126] Butler MS, Robertson AA, Cooper MA. Natural product and natural product derived drugs in clinical trials. *Natural Product Reports*. 2014;**31**(11):1612-1661
- [127] Cragg GM, Pezzuto JM. Natural products as a vital source for the discovery of cancer chemotherapeutic and chemopreventive agents. *Medical Principles and Practice*. 2016;**25**(Suppl. 2):41-59

Cytotoxicity and Apoptosis Induction by Coumarins in CLL

Omid Gholami

Additional information is available at the end of the chapter

<http://dx.doi.org/10.5772/intechopen.72446>

Abstract

Chronic lymphocytic leukemia (CLL) is one of the leukemia types. Leukemia is cancer of the body's blood-forming cells. Cancer is a disease that is often characterized by too little apoptosis and uncontrolled duplicate of body cells. Apoptosis, or programmed cell death, is a normal component of the development and health of multicellular organisms. Cells die in response to a variety of stimuli during apoptosis. During cancer, pathophysiology apoptosis of the cancerous cells is disrupted, so one of the strategies for cancer chemotherapy is inducing apoptosis in cancerous cells. Myeloid cell leukemia type 1 (Mcl-1) is one of the antiapoptotic Bcl-2 family proteins. It has been shown that the expression of Mcl-1 in CLL is significantly associated with a failure to achieve complete remission following cytotoxic therapy, so regulation of Mcl-1 expression by coumarins could be one of the mechanisms of CLL chemotherapy. Coumarins consist of a large class of phenolic substances found in plants. Different pharmacologic effects of coumarins were reported. One of these effects is cytotoxicity and apoptosis induction in cancerous cells by coumarins. In this chapter, the cytotoxic activity of coumarins and their role in Mcl-1 regulation are discussed.

Keywords: coumarins, apoptosis induction, Mcl-1 expression

1. Chronic lymphocytic leukemia

One of the most prevalent types of leukemia is chronic lymphocytic leukemia (CLL). Leukemia is a type of cancer. Cancer means too little apoptosis of body cells. In the case of cancer, cells have mutations that prevent them from undergoing apoptosis. It is a general belief that CLL is an indolent disease associated with a prolonged (i.e., 10–20 years) clinical course, and unrelated causes to CLL lead to death. But it is true only for less than 30% of cases [1]. By convention, the history of chronic lymphocytic leukemia begins in 1845, but it could be said to have started when the first white cells, “the globuli albicanates,” were noted by Joseph Lieutaud in

1749. During the intervening years, many events have aided in our understanding of the etiology and treatment of CLL. In his discussion of the history of CLL, Rai [2] found it informative to define three eras: (1) the recognition of CLL as a clinical entity, 1845–1924; (2) initial clinical investigations, 1924–1973; and (3) the modern era, 1973–2002.

Overexpression of Bcl-2¹ and Fas-inhibitory molecules such as TOSO is the principle mechanism of apoptosis resistance in CLL cells. CLL lymphocytes are clonal B-cells arrested in the B-cell differentiation pathway at some intermediate stage between the pre-B-cell and mature B-cell, perhaps in the “activated, antigen-experienced” B-cell subset. Phenotypic features of B-cell CLL (B-CLL) lymphocytes are [3–5] (1) extremely low levels of surface membrane immunoglobulin (often abbreviated as SmIg or sIg), (2) expression of one or more B-cell-associated antigens (like CD19, CD20, CD21, CD23, and CD24) [6, 7], and (3) expression of CD5, a T-cell-associated antigen.

Until the early 1980s, it was not possible to study chromosomal abnormalities in CLL because of the inadequate number of metaphases induced by available techniques. Certain genetic abnormalities have been associated with patient outcomes. Patients with complex genomic changes appear to have more aggressive disease [8]. The most frequently observed abnormalities were trisomy 12 and 14q+. The cytogenetic abnormalities appear to be restricted to B-cells in B-CLL [9]. In two studies of patients with CLL using fluorescence in situ hybridization (FISH) techniques, chromosomal abnormalities were noted in 69–82% of the patients, with abnormalities of chromosomes 11, 12, and 13 being most commonly seen.

1.1. Pathophysiology

Chronic lymphocytic leukemia is a monoclonal disease of mature-appearing lymphocytes that accumulate in blood, lymph nodes, spleen, liver, and bone marrow. Most cases (>95%) are characterized by monoclonal lymphocytes expressing normal B-cell surface proteins including immunoglobulin (Ig), CD19, and CD20 and aberrantly expressing CD5, a protein normally found on T-cells. A small minority (<5%) of cases are of T-cell origin, expressing T-cell surface markers such as CD3 and CD4 or CD8. These T-cell leukemias are not uncommon in individuals with ataxia telangiectasia. The molecular biology of T-cell lymphocytic leukemia is distinct from that of B-cell CLL [10].

Molecular and cellular mechanisms of CLL can be divided into two parts.

1.1.1. B-cell receptor-signaling pathways

B-cell receptor (BCR)-signaling pathways are triggered with or without antigen ligation in CLL. After antigenic BCR triggering downstream signaling of the BCR is dominated by the kinases lyn and syk, which transduce survival and antiapoptotic signals [11]. In CLL, the elevated expression of antiapoptotic Mcl-1, which leads to increased survival of malignant cells, occurred by prolonged activation of the MEK/ERK² and Pi3K/AKT³ pathways and with AKT after BCR signaling (**Figure 1**) [12].

¹B-cell CLL Lymphoma 2.

²Mitogen-activated protein kinase/extracellular signal-regulated kinase.

³Phosphatidylinositol-3-kinase and protein kinase B.

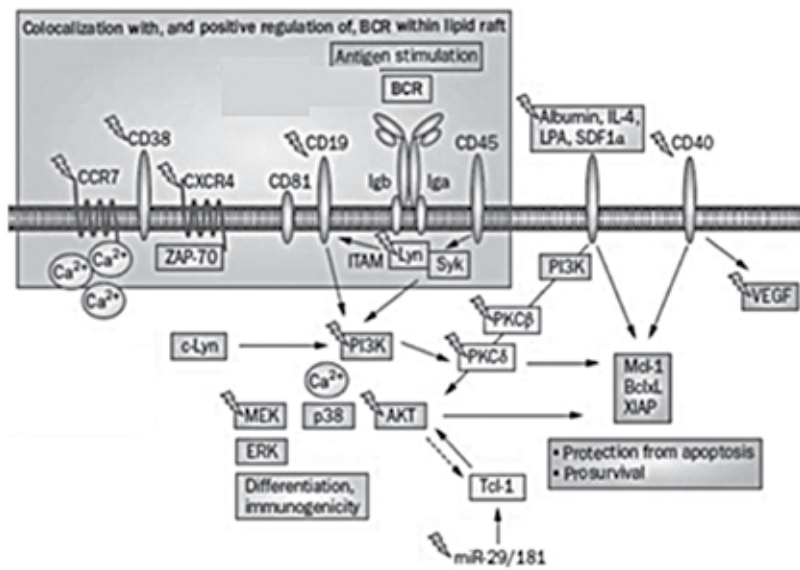


Figure 1. The role of BCR signaling in the biology of CLL [15].

For establishment of BCR-signaling pathways independent of antigen ligation, CD19 is an important surface marker. It has an important role in regulation and amplification of signal transduction via lyn [13]. Zap-70 is another tyrosine kinase that has important role in BCR signaling. When syk is not expressed, it can partially restore BCR signaling [14].

1.1.2. Aberrant apoptotic signaling pathway

Apoptosis is a kind of cell death. Extrinsic pathway of apoptosis triggers by death receptors. In CLL, they are CD95/Fas and trail (tumor-necrosis factor-related apoptosis-inducing ligand). After ligation by ligands (like CD40L), these receptors directly feed into a caspase cascade and lead to cell death [16]. The intrinsic pathway, or mitochondrial pathway, is regulated by the balance between antiapoptotic and proapoptotic members of the Bcl-2 family [15]. "BH3-only" proteins (e.g., Bim, Bid, Bmf, Puma, Bad, and noxa) are another class of Bcl-2 family proteins which can modify this balance (**Figure 2**).

Non-death-transmitted signals drive from developmental cues or sensor platforms. Developmental cues like Bim-dependent B-cell killing upon BCR cross-linking [17] and sensor platforms like the DNA damage sensor network involving the ATM (ataxia telangiectasia mutated) and p53 tumor suppressors, which prominently determine survival and treatment outcomes in CLL [15].

Currently, one of the therapeutic strategies that kill CLL cells is the DNA damage response via p53 that leads to a dominant cell-death signal via Puma [18, 19]. A major problem encountered with this strategy is that a number of patients with CLL harbor defects in the DNA damage machinery that leads to deactivation of the pathway. The challenge thus seems to be to bypass such resistance and produce p53-independent cell death [15].

Another therapeutic strategy is the exploitation of CD95 signaling. But it seems to be restricted, as systemic CD95 triggering leads to fulminant liver toxicity [20]. The role of trail receptor

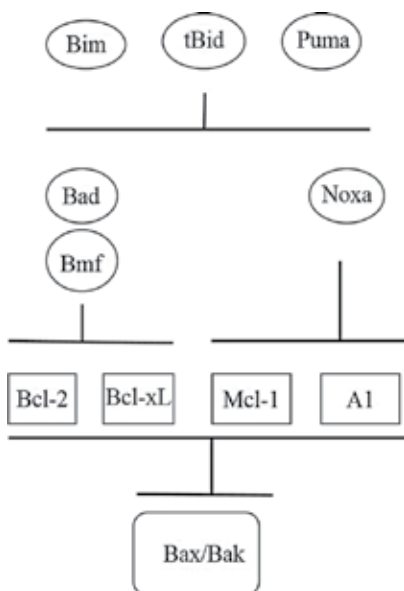


Figure 2. The interaction between Bcl-2 family member proteins [15].

targeting is currently under development. CD40 signaling may also have a positive effect on conventional therapy. It has been shown that CD154 (CD40L) application was able to induce the p53-related transcription factor p73, leading to a sensitization of p53-deficient CLL cells to conventional therapeutics such as fludarabine [21].

A number of approaches have been taken to directly modulate the core components of the Bcl-2 cell-death machinery. The Bcl-2 antisense molecule oblimersen is the most advanced agent in clinical testing. “BH3-mimetics” and “pan-Bcl-2 family antagonists” can mimic the BH3 domain of BH3-only death-inducing proteins and are thought to liberate BH3-only proteins from the inhibition by antiapoptotic Bcl-2 proteins, thus making them effective killers.

2. Apoptosis

Apoptosis means cell suicide. It is a normal component of the development and health of multicellular organisms. Cells perform in a controlled, regulated fashion by apoptosis. Apoptosis is different from another form of cell death called necrosis [22]. Cancer is often characterized by too little apoptosis. In the case of cancer, damaged cells, which should undergo apoptosis, have mutations that prevent them from undergoing apoptosis [22]. Apoptotic cells can be recognized by stereotypical morphological changes (**Figure 3**).

2.1. Pathways of apoptosis

Apoptosis consists of two major pathways: extrinsic pathway and intrinsic (mitochondrial) pathway.

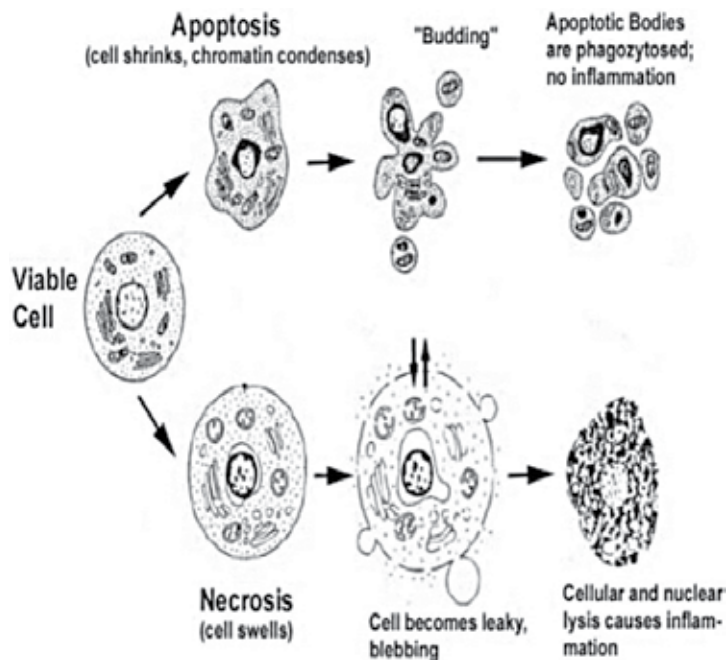


Figure 3. Hallmarks of the apoptotic and necrotic cell-death process. Modified from [23].

2.1.1. Extrinsic pathway

“Death receptors” transmit apoptotic signals after ligation with specific ligands in extrinsic pathway. Death receptors belong to a superfamily, including TNFR-1, Fas/CD95, and the TRAIL receptors DR-4 and DR-5 [24]. Caspase-8 is the hallmark of this pathway. It is activated by a complex named death-inducing-signaling complex (DISC). Activated death receptor recruited adapter molecules like FADD (Fas-associated protein with death domain) or TRADD (tumor necrosis factor receptor type 1-associated DEATH domain). These adapter molecules form the DISC (**Figure 4**). Caspase-8 then cleave and activate other caspases resulting in cell death. These types of cells, which have the capacity to induce such direct and mainly caspase-dependent apoptosis pathways, were classified to type I cells [25].

2.1.2. Intrinsic pathway

In this pathway, the signal does not come from death receptors. In this case, the signal amplified via mitochondria-dependent apoptotic pathways. Bcl-2 family member, Bid, is cleaved by caspase-8 (tBid) and translocates to the mitochondria. tBid in concert with the proapoptotic Bcl-2 family members Bax (Bcl-2-associated x) and Bak (Bcl-2 homologous antagonist/killer) induces the release of cytochrome C and other mitochondrial proapoptotic factors into the cytosol [27].

Cytosolic cytochrome C binds to monomeric Apaf-1 (apoptotic protease-activating factor 1) which then oligomerizes to assemble the apoptosome that triggers the activation of the

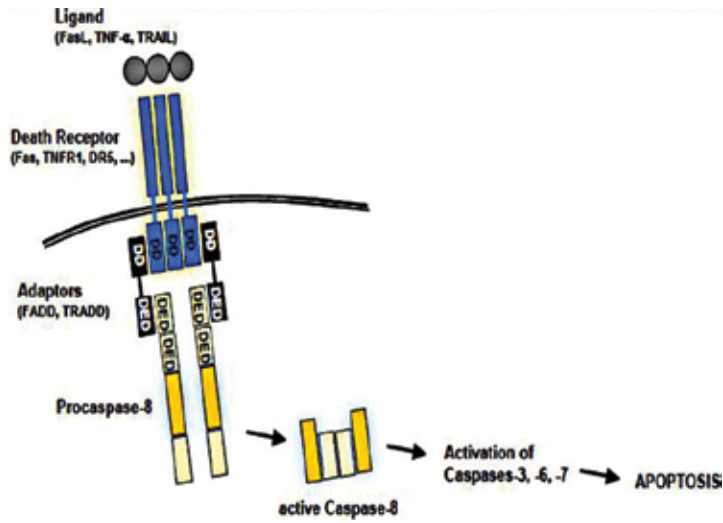
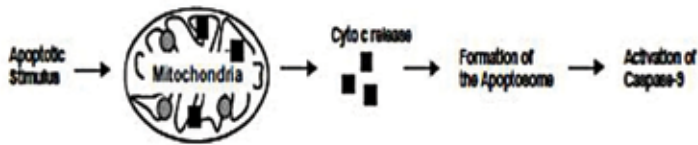


Figure 4. Receptor-mediated caspase activation at the DISC [26].

A. Mitochondrial pathway of caspase activation



B. Apoptosome formation and activation

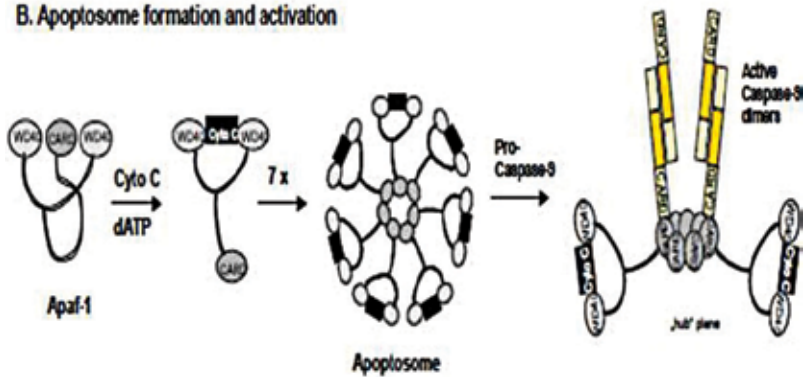


Figure 5. Intrinsic pathway of apoptosis [28].

initiator procaspase-9 [28]. Caspase-9 is the hallmark of intrinsic pathway. Activated caspase-9 ultimately results in cell death by subsequently initiating a caspase cascade involving downstream effector caspases such as caspase-3, caspase-7, and caspase-6 (Figure 5) [29].

2.2. Apoptotic pathway proteins

2.2.1. Caspases are central initiators and executioners of apoptosis

The term caspase is derived from cysteine-dependent aspartate-specific proteases. So far, seven different caspases have been identified in *Drosophila*, and 14 different members of the caspase-family have been described in mammals, with caspase-11 and caspase-12 only identified in the mouse [30, 31]. According to a unified nomenclature, the caspases are referred to in the order of their publication: caspase-1 is ICE (interleukin-1 β -converting enzyme), the first mammalian caspase [32, 33]. There are many documents about the importance of caspases in apoptosis phenomenon. For example, it has been shown that caspase-1, -4, -5, -11, and -12 are involved in the maturation of pro-inflammatory cytokines such as pro-IL-1 β and pro-IL-18 [31] or studies show that caspase-3 and -9 have a role in brain development [34, 35].

Caspases are synthesized as inactive zymogens, the so-called procaspases. Upon maturation, the procaspases are proteolytically processed. The proapoptotic caspases can be divided into the group of initiator caspases including procaspases-2, -8, -9, and -10, and into the group of executioner caspases including procaspases-3, -6, and -7 [26]. As mentioned earlier, in extrinsic apoptosis pathways procaspase-8 is the hallmark of this pathway. In return of caspase-8, caspase-9 is the hallmark of intrinsic pathway. Once the initiator caspases have been activated, they can proteolytically activate the effector procaspases-3, -6, and -7. Effector caspases subsequently cleave a specific set of protein substrates, resulting in the mediation and amplification of the death signal and eventually in the execution of cell death [36].

2.2.2. The Bcl-2 superfamily

Bcl-2 is an oncogene which was the first example of an oncogene that inhibits cell death rather than promoting proliferation. Bcl-2 family of proteins can be defined by the presence of conserved sequence motifs known as Bcl-2 homology domains (BH1 to BH4). Bcl-2 proteins divided to a group of prosurvival members and others to a group of proapoptotic members [37]. Prosurvival proteins include Bcl-2 itself, Bcl-XL, Bcl-w, A1, and Mcl-1, all of which possess the domains BH1, BH2, BH3, and BH4. The proapoptotic group of Bcl-2 members can be divided into two subgroups: the Bax-subfamily consists of Bax, Bak, and Bok, all of which possess the domains BH1, BH2, and BH3. There is another group of proteins named the BH3-only proteins (Bid, Bim, Bik, Bad, Bmf, Hrk, Noxa, Puma, Blk, BNIP3, and Spike) that have only the short BH3 motif, an interaction domain that is both necessary and sufficient for their killing action [38, 39].

Despite the existence of two hypotheses regarding how the Bcl-2 family controls apoptosis, it seems that the central function of mammalian Bcl-2 family members is to guard mitochondrial integrity and control the release of mitochondrial proteins into the cytoplasm [39]. Another hypothesis is that Bcl-2 members might directly control caspase activation [40]. The question is how mitochondrial integrity is affected by proapoptotic Bcl-2 family members? Central to this question are Bax and Bak. The double knockout of Bax and Bak resulted in dramatic impairment of apoptosis during development in many tissues with superfluous cells accumulating in the hematopoietic system and in the brain [26].

BH3-only members function upstream of Bax and Bak. It is shown that members of the BH3-only subfamily are required for the activation of proapoptotic Bax/Bak function. But it should be noted that prosurvival members Bcl-2 and Bcl-XL have a role in this way [41].

In summary, as it is shown in **Figure 6**, in a viable cell antiapoptotic proteins like Bcl-2 antagonize Bax/Bak. In response to an apoptotic stimulus, BH3-only proteins are activated. Activated BH3-only proteins prevent antiapoptotic Bcl-2 members from inhibiting proapoptotic members. Therefore, Bax/Bak are activated and form pores in the mitochondrial membrane. In consequence, cytochrome C and other proapoptotic factors are released from the inner mitochondrial membrane into the cytosol. They cause the formation of the apoptosome and the subsequent activation of the caspase cascade [26].

2.3. Mcl-1 and CLL

Mcl-1 is one of the Bcl-2-related survival proteins but is somewhat structurally distinct and probably lacks a “classical” BH4 domain. It was first discovered in differentiating myeloid cells where Mcl-1 is thought to play a transient role in promoting cell survival, but it has been expressed in various malignant cells, like CLL. Overexpression of Mcl-1 in CLL cells associated with a failure to achieve complete remission following cytotoxic therapy [42].

Mcl-1 protein has a rapid turnover, and it has a short half-life (a few hours). Mcl-1 has a critical role in regulating apoptosis in response to rapidly changing environmental cues. During apoptosis, Mcl-1 is a very efficient substrate for caspases [43–46]. While Mcl-1 is an antiapoptotic protein, its cleavage by caspases converts it into a cell-death-promoting molecule [43]. Therefore, Mcl-1

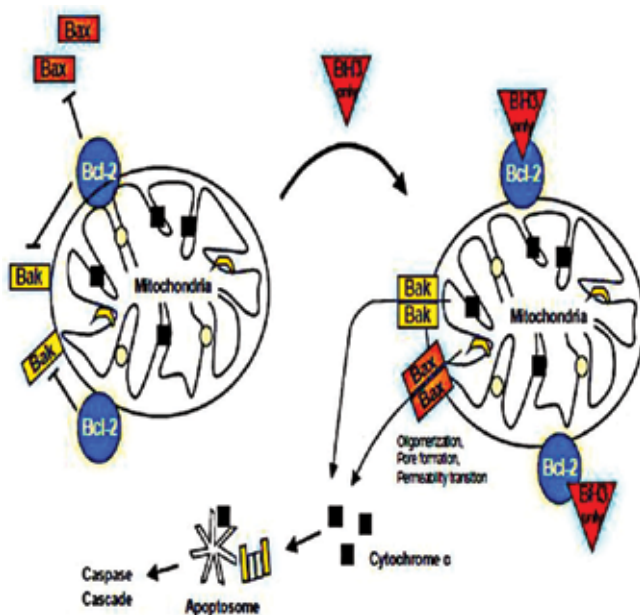


Figure 6. Regulation of apoptosis by the Bcl-2 family [26].

can act as a molecular bodyguard or assassin during apoptosis [47]. Saxena et al. showed that Mcl-1 can play an important role in CLL, by insertion of small sequences in its promoter [47]. They showed the presence of specific insertions in 29% patients with CLL and while in none of the controls. They found that these insertions were correlated with rapid disease progression, with a poor response to chemotherapy and shorter disease-specific survival. By founding of insertions in CD38-negative patients, they suggest that a poor prognostic marker [47] can be present.

Finally, since specific genetic targets are not defined in CLL, Mcl-1 seems to be an appropriate biomolecule to therapeutically manipulate. Mcl-1 protein production and maintenance are dependent on several pathways. At the apical level, the microenvironment provides factors that dramatically increase this protein in CLL cells [48]. Hence, a strategy that interferes with the interaction of microenvironment and CLL cells is a logical approach. Production of Mcl-1 through these signals is carried via increased transcription of the Mcl-1 gene. Transcription and polyadenylation inhibition, albeit not selective, is an approach that works because of AU-rich elements in the transcript of Mcl-1, which leads to its rapid turnover [49]. The N-terminal region of Mcl-1 protein contains 2PEST domains that are rich in proline, glutamic acid, serine, and threonine residues, resulting in a short half-life of the protein [49] and making translation inhibition and rapid degradation of endogenous Mcl-1 via proteasome pathway a viable option to reduce the protein level [50]. Mcl-1 is also essential during early lymphoid development [51] and is abundantly expressed in the germinal center B-cell compartment. Pim kinase and Akt-PI3-kinase pathways and downstream of BLYS have been identified to maintain the Mcl-1 levels in B-cells [52]. The roles of these pathways and consequence of their perturbations need to be investigated in malignant lymphocytes. Similarly, work is needed on posttranslational modification leading to increased or decreased half-life of Mcl-1 protein. Finally, and probably most intriguingly, small molecule antagonists of Mcl-1 protein that bind to the BH3 domain releasing proapoptotic proteins provide a new avenue of research and therapeutics.

3. Coumarins

Coumarins (2H-1-benzopyran-2-one) consist of a large class of phenolic substances found in plants and all of which consist of a benzene ring joined to a pyrone ring. More than 1300 coumarins have been identified as secondary metabolites from plants, bacteria, and fungi. The prototypical compound is known as 1,2 benzopyrone or, less commonly, as *o*-hydroxycinnamic acid and lactone. Coumarins were initially extracted in *tonka* bean (*Dipteryx odorata* Wild) and are reported in about 150 different species distributed over nearly 30 different families, of which a few important ones are *Rutaceae*, *Umbelliferae* (*Apiaceae*), *Clusiaceae*, *Guttiferae*, *Caprifoliaceae*, *Oleaceae*, and *Nyctaginaceae* [53]. They are found at high levels in some essential oils, particularly in *cinnamon* bark oil, *cassia* leaf oil, and *lavender* oil. Coumarin is also found in fruits (e.g., bilberry and cloudberry), green tea, and other foods such as chicory. The richest sources of most coumarins among the higher plants are *Rutaceae* and *Umbelliferone*. The coumarins occur at the highest levels in the fruits, followed by the roots, stems, and leaves although they are distributed throughout all parts of the plant. Environmental conditions and seasonal changes can influence the occurrence in diverse parts of the plant [54].

3.1. Classification

Based on the chemical structure of their compounds, natural coumarins are classified into six groups (Table 1).

Coumarin and its derivatives are principal oral anticoagulants. Coumarin is water insoluble; however, 4-hydroxy substitution confers weakly acidic properties to the molecule that makes it water soluble under slightly alkaline conditions (Figure 7) [54].

The structure of coumarin nucleus (Figure 8) mimics A and B rings of the steroid hormone and binds to the aromatase-binding site with a superior affinity. Upon tactically extending the structure to the tricyclic system, it mimics the steroid hormones that act as SERM/SERD (selective estrogen receptor modulator/selective estrogen receptor downregulator) and thus enhancing the receptor interaction, leading to a development of a potent pharmacophore. 17b-HSD3 (17b-hydroxysteroid dehydrogenase type3), cell division cycle protein, and NF-kB inhibitory activity are potentiated by structural extension with sulfur linked at the C-4 position [55]. It has also been shown that the anticancer activity of coumarins is potentiated by the substitution of imidazole, 1,2,3-triazol, piperidine purine, benzothiazole, substituted phenyl

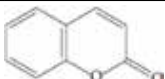
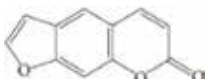
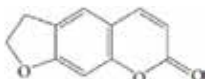
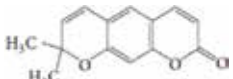
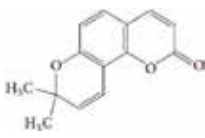

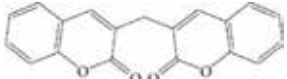
Type of coumarin	General chemical structure
Simple coumarins	
Furano coumarins	
Dihydrofurano coumarins	
Pyrano coumarins (linear types)	
Pyrano coumarins (angular types)	
Phenyl coumarins	
Bicoumarins	

Table 1. Classification of natural coumarins based on their chemical structure.

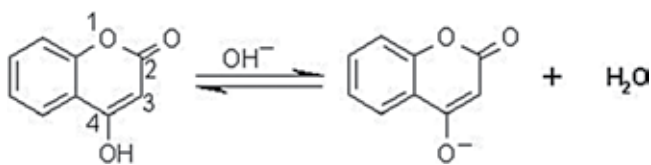


Figure 7. 4-hydroxy substitution of coumarin makes it water soluble in alkaline conditions.

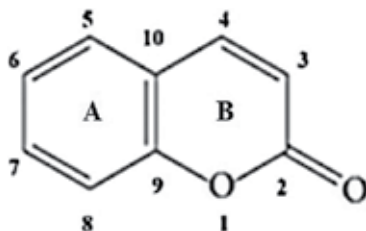


Figure 8. Structure of simple coumarin.

ring, aryl acrylic acid, and chalcone at the fourth position of coumarin nucleus by a linker such as methylene and oxygen [55].

3.2. Coumarins and leukemia

Induction of apoptosis in leukemic cell lines by coumarins and their derivatives is demonstrated in different *in vitro* studies. Coumarin compounds have antiproliferative and/or cytotoxic activity on cancer cells, depending on their substitution pattern [56–58]. It is shown that while long alkyl substitution at C7 position increased the cytotoxic activity against the leukemia cancer cell lines [59], the presence of two hydroxyl groups at C7 and C8 positions seems to improve the potency of methylcoumarins as cytotoxic agents. It is also shown that among 7,8-DHMC (dihydroxy-4-methylcoumarin) derivatives, the longer the C3 alkyl chain, the higher was the activity. This effect of the alkyl group on the cytotoxicity is presumably due to the enhanced lipophilicity of the longer alkyl chains that consequently enhances cell membrane penetration ability of the test compounds. Bromo groups substituted at C4 and C6 positions for DHMCs increased the cytotoxic activity in all the cell lines (**Figure 9A**) [60]. In another study, it was shown that 7-hydroxycoumarin analog containing carboxymethyl ester group on cinnamoyl moiety (**Figure 9B**) showed good antiproliferative activity against leukemic cell lines [61]. It is worth noting that the cinnamoyl moiety at C3 is more effective than alkyl chain moiety for increased cytotoxic effect against leukemic cell line K562 ($IC_{50} = 4.4 \mu\text{M}$ vs. $40.8 \mu\text{M}$).

Moreover, studies showed that molecular hybridization of coumarins increased their cytotoxicity against leukemic cell lines. For example, the hybrids with ortho-dihydroxy groups or ortho-hydroxy-methoxy group on the aromatic A ring exhibit superior antiproliferative activity in comparison with those with such groups on the aromatic B ring. Specially, a new hybrid, 6-methoxy-7-hydroxy-3-(4'-hydroxyphenyl)coumarin, emerged as an important lead compound with excellent antiproliferative, apoptosis-inducing, and cell cycle arrest activities against HL-60 cell line ($IC_{50} = 5.2 \pm 0.6 \mu\text{M}$) (**Figure 10**) [62].

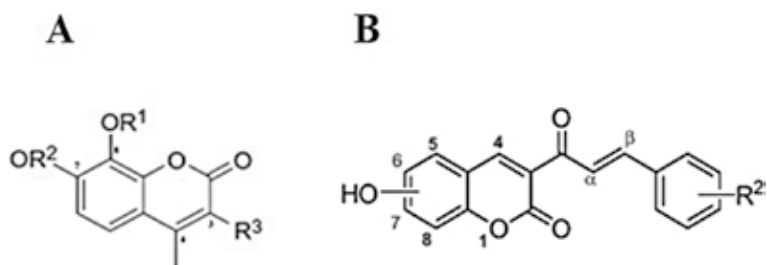


Figure 9. R2 is 4-(COOMe).

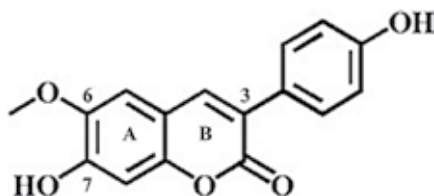


Figure 10. 6-methoxy-7-hydroxy-3-(4' hydroxyphenyl)coumarin) as a new hybrid.

Paul et al. showed that the synthesis of new conjugated coumarin-benzimidazole hybrids displayed appreciable antileukemic activities *in vitro*. They showed that the introduction of ethanolamine at position 7 of coumarin-benzimidazole hybrid (**Figure 11**) shows higher selectivity against leukemia cancer cells (CCRF-CEM, HL-60(TB), K-562, and RPMI-8226) [63].

Other studies showed that hydrazide-hydrazone ($-\text{CO}-\text{NH}-\text{N}=\text{CH}-$) moiety and acrylohydrazone hybrid at position 3 could increase the cytotoxicity against leukemic cell lines (**Figure 12**) [64, 65].

In other studies, it has been shown that the copper complexes with coumarin derivatives could increase the antileukemic effect of coumarin *in vitro* (**Figure 13**).

Specifically, in some studies, the significant inhibitory activity of certain coumarins on the proliferation of leukemic cell lines [58, 66–68] has been reported. In addition, it has been described that such inhibitory effects could be related to either differentiating [58, 66] or proapoptotic activities [67, 68] of the compounds, depending on the distribution of their substituents in the coumarin ring.

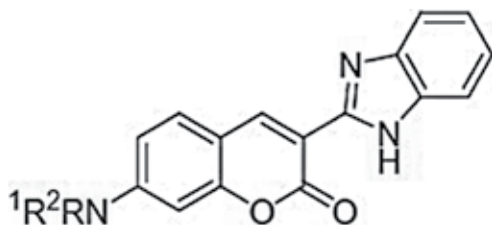


Figure 11. NR²R² is ethanolamine.

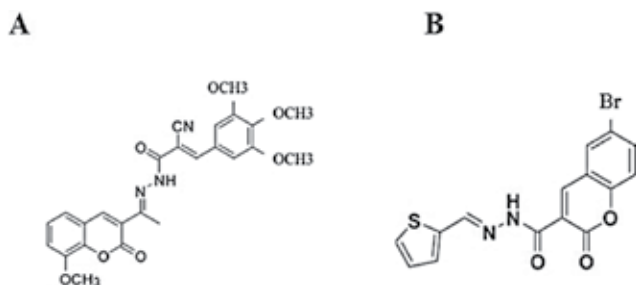


Figure 12. Hydrazide-hydrazone moiety and acrylohydrazone hybrid of coumarin.

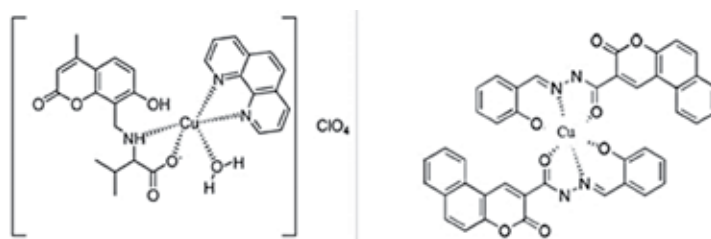


Figure 13. Copper complexes with coumarin.

Kim and colleagues studied the antileukemic effects of decursin (a pyranocoumarin from *Angelica gigas*) and its derivatives (Figure 14) on K562 and U937 cell lines. They studied the ability of these compounds as a tumor-suppressing PKC activator and as an antagonist to phorbol 12-myristate 13-acetate (PMA), a tumor-promoting PKC activator. Based on their results, the structure-activity relationship of decursin and its derivatives is as follows: (i) the coumarin structure is required for antileukemic activity and (ii) the side chain is a determinant of PKC activation and the cytotoxic mechanism in leukemia cells [69].

In another study, Ahn et al. showed the apoptosis induction by decursin in leukemic KBM-5 cells. They showed that decursin activates caspases 9 and 3 and PARP in KBM-5 cells. They also reported that decursin induced apoptosis via downregulation of COX-2-dependent survivin pathway in KBM-5 myeloid leukemia. In KBM-5 cells, it was reported that targeting survivin could overcome the resistance against imatinib [70].

Esculetin (Figure 15) is a simple coumarin found in some traditional medicines. Induction of apoptosis in various leukemic cell lines was shown in different studies. Chu and their colleagues are one of the first teams that reported the antileukemic effects of esculetin. They showed that esculetin inhibits the survival of human promyelocytic leukemia HL-60 cells in a concentration-dependent and time-dependent manner. Esculetin induced the release of cytochrome C from mitochondria into cytosol, reduced Bcl-2 protein expression, and increased caspase activation [71].

Esculetin is a cell cycle-specific antineoplastic agent. It can inhibit the growth of HL-60 and U937 leukemic cells by G1 cell cycle arrest [72, 73]. It also leads to the release of cytochrome C, activation of caspases 3, 8, and 9, downregulation of Bcl-2 protein, and increased the phosphorylation of MEK/ERK and JNK [74–77].

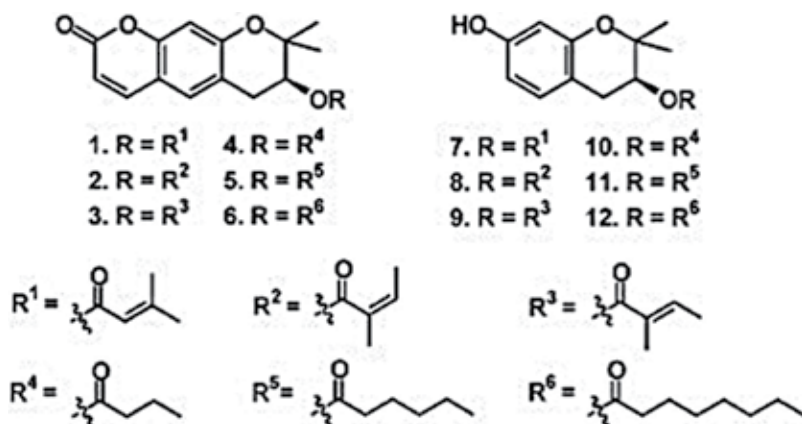


Figure 14. Structures of decursin (1) and its derivatives 2–12.

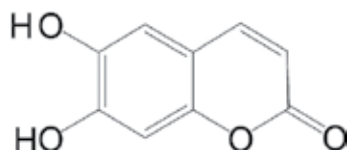


Figure 15. Structure of esculetin.

Tung et al. fractionated and chemically investigated the methanol extract of *Mammea siamensis* flower, an evergreen tree belonging to the family of Calophyllaceae, and distributed throughout Thailand, Myanmar, Laos, Cambodia, and Vietnam. They isolated and identified eight compounds. Among the isolated compounds, three structurally related coumarins kayeassamin A (Figure 16), surangin C, and theraphin B showed significant antiproliferative activity against human leukemia HL-60 cells. Activation of caspases 3 and 8 and sub-G1 arrest by kayeassamin A have been shown in this study and another one [78, 79].

Osthole (Figure 17) is another coumarin where its antileukemic effect has been investigated. It has been shown that osthole has the strongest cytotoxic activity among the coumarins extracted from *Cnidii monnieri Fructus* on HL-60 cell line. The structure-activity relationship established from the results indicated that the prenyl group has an important role in the cytotoxic effects and apoptosis induction [80].

In another study, osthole could increase intracellular drug accumulation, decreased the expression of multidrug resistance gene 1 (MDR1), and could suppress P-gp expression by inhibiting the PI3K/Akt-signaling pathway in myelogenous leukemia K562/ADM cells [81].

Imperatorin, a biologically active furanocoumarin, is another coumarin that is extracted from *Cnidii monnieri Fructus* also showed cytotoxic effect against leukemic cell lines [82–85].

Toddaculin (Figure 18) is another important coumarin where its antileukemic effect is revealed. Vazquez et al. found that toddaculin was the most potent cytotoxic agent among the series of six prenylated coumarins isolated from the stem bark of *Toddalia asiatica* (Rutaceae). They found that while toddaculin at 250 μM ($\text{IC}_{50} = 51.38 \pm 4.39$) was able to induce apoptosis

in U-937 cells, involving decreased phosphorylation levels of ERK and Akt, 50 μ M toddaculin exerted differentiating effects [86].

Umbelliprenin (**Figure 19**) is a prenylated coumarin found in *Ferula* species. Its antileukemic effect was first reported by Gholami and his colleagues. They found that umbelliprenin has cytotoxic and proapoptotic effects on Jurkat and Raji cell lines. They showed that umbelliprenin activates intrinsic and extrinsic pathways of apoptosis by the activation of caspase-8 and -9, respectively. Inhibition of Bcl-2 was also shown [87, 88].

Auraptene (**Figure 20**) is another coumarin that has a structure close to that of umbelliprenin. The difference between the chemical structures of these compounds is that the length of the 7-prenyloxy chain of umbelliprenin is longer and contains 15 instead of 10 carbons. Apoptogenic activity of auraptene on Jurkat cells was shown in detail. Apoptotic effect of auraptene on Jurkat T-cells was exerted by the ER stress-mediated activation of caspase-8 and the subsequent induction of mitochondria-dependent or -independent activation of caspase cascade, which could be suppressed by Bcl-xL [89].

3.3. Mcl-1 and coumarins

Coumarins can regulate the expression of Mcl-1. Their regulation is time- and dose-dependent. The regulation of Mcl-1 expression by auraptene, umbelliprenin, imperatorin, galbanic acid, and gut-70 was studied.

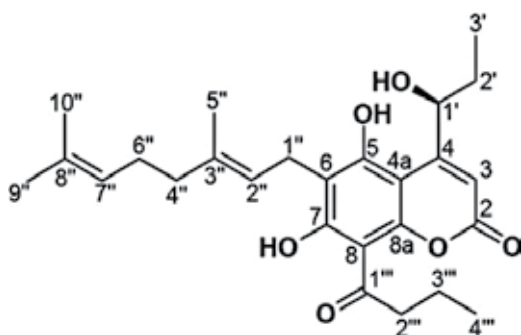


Figure 16. Structure of kayeassamin A.

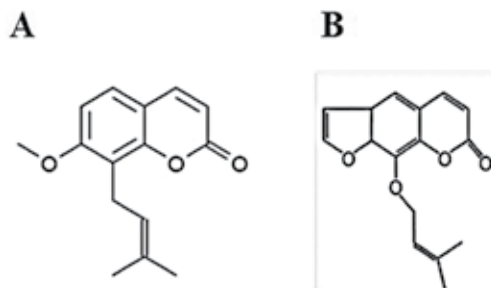


Figure 17. Structure of osthole (A) and imperatorin (B).

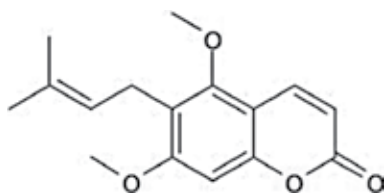


Figure 18. Structure of toddaculin.

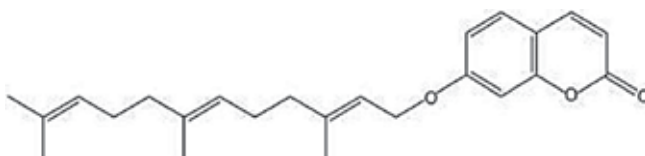


Figure 19. Structure of umbelliprenin.

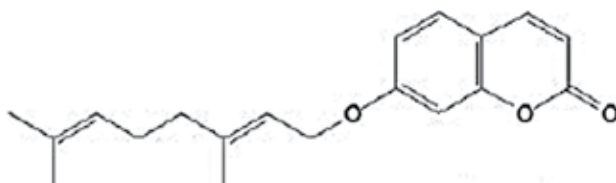


Figure 20. Structure of auraptene.

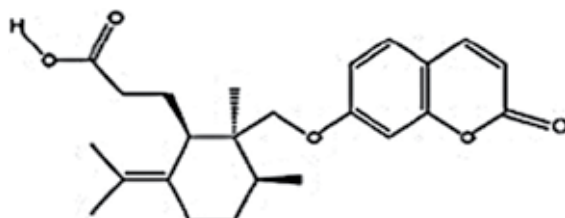


Figure 21. Galbanic acid.

Gholami et al. studied and compared the expression of Mcl-1 gene after the Jurkat cells were incubated by umbelliprenin and auraptene. They showed that umbelliprenin increased the expression of Mcl-1 mRNA from 1 to 3 h of incubation, but this increase has a scale-down pattern. Auraptene decreased the expression of Mcl-1 mRNA for the same incubation times [90, 91]. This pattern is similar for Mcl-1 protein expression [91, 92].

Another natural coumarin where its effect on Mcl-1 expression was studied is galbanic acid (Figure 21). Galbanic acid downregulates the Mcl-1 protein expression dose dependently [93]. Imperatorin (Figure 17B), another natural coumarin like galbanic acid, decreased Mcl-1 protein level in a dose-dependent manner [94].

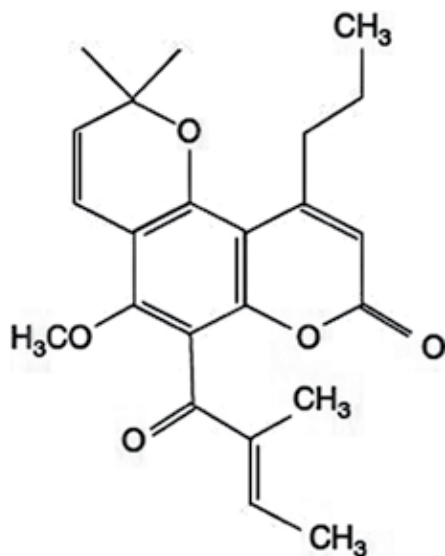


Figure 22. GUT-70.

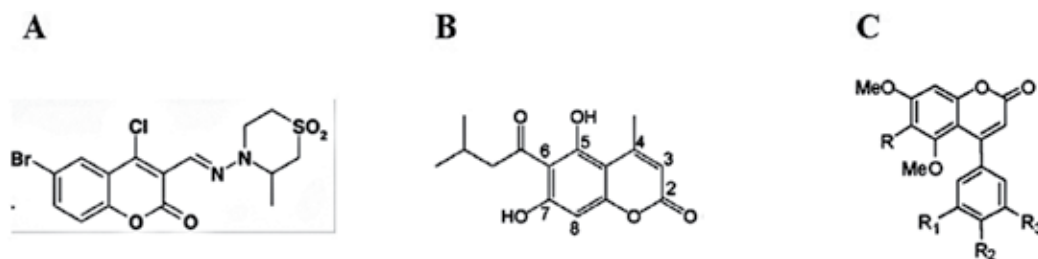


Figure 23. (A) RKS262, (B) DMAC, and (C) 4-aryl coumarin analogs of combretastatin.

GUT-70 (Figure 22), a tricyclic coumarin derived from *Calophyllum brasiliense*, causes Mcl-1 protein upregulation in mantle cell lymphoma (MCL) cell lines [95].

The effect of synthetic coumarins (RKS262, 5,7-dihydroxy-4-methyl-6-(3-methylbutanoyl)-coumarin (DMAC), and 4-aryl coumarin analogs of combretastatin (Figure 23)) on Mcl-1 protein expression was studied. All of these compounds downregulate Mcl-1 protein dose- and time- dependently [96–98].

4. Conclusion

In conclusion, coumarins are one of the important cytotoxic agents. They could induce apoptosis and regulate Mcl-1 expression in CLL cell lines. We hope that they be one of the candidates for chemotherapy of CLL in the future.

Author details

Omid Gholami

Address all correspondence to: omidghphd@gmail.com

Department of Physiology and Pharmacology, Faculty of Medicine, Cellular and Molecular Research Center, Sabzevar University of Medical Sciences, Sabzevar, Iran

References

- [1] Rai R, Stilgenbauer, S. Overview of the Treatment of Chronic Lymphocytic Leukemia. 2017. Available from: <https://www.uptodate.com/contents/overview-of-the-treatment-of-chronic-lymphocytic-leukemia>
- [2] Rai KR. Progress in chronic lymphocytic leukaemia: A historical perspective. *Bailliere's Clinical Haematology*. 1993 Dec;**6**(4):757-765. PubMed PMID: 8038488
- [3] Hallek M, Cheson BD, Catovsky D, Caligaris-Cappio F, Dighiero G, Dohner H, et al. Guidelines for the diagnosis and treatment of chronic lymphocytic leukemia: a report from the International Workshop on Chronic Lymphocytic Leukemia updating the National Cancer Institute-Working Group 1996 guidelines. *Blood*. 2008 Jun 15;**111**(12):5446-5456. PubMed PMID: 18216293. Pubmed Central PMCID: 2972576
- [4] Stevenson FK, Caligaris-Cappio F. Chronic lymphocytic leukemia: revelations from the B-cell receptor. *Blood*. 2004 Jun 15;**103**(12):4389-4395. PubMed PMID: 14962897
- [5] Cheson BD, Bennett JM, Grever M, Kay N, Keating MJ, O'Brien S, et al. National Cancer Institute-sponsored Working Group guidelines for chronic lymphocytic leukemia: Revised guidelines for diagnosis and treatment. *Blood*. 1996 Jun 15;**87**(12):4990-4997. PubMed PMID: 8652811
- [6] Fournier S, Delespesse G, Rubio M, Biron G, Sarfati M. CD23 antigen regulation and signaling in chronic lymphocytic leukemia. *The Journal of Clinical Investigation*. 1992 Apr;**89**(4):1312-1321. PubMed PMID: 1532590. Pubmed Central PMCID: 442993
- [7] Geisler CH, Larsen JK, Hansen NE, Hansen MM, Christensen BE, Lund B, et al. Prognostic importance of flow cytometric immunophenotyping of 540 consecutive patients with B-cell chronic lymphocytic leukemia. *Blood*. 1991 Oct 01;**78**(7):1795-1802. PubMed PMID: 1717071
- [8] Grubor V, Krasnitz A, Troge JE, Meth JL, Lakshmi B, Kendall JT, et al. Novel genomic alterations and clonal evolution in chronic lymphocytic leukemia revealed by representational oligonucleotide microarray analysis (ROMA). *Blood*. 2009 Feb 05;**113**(6):1294-1303. PubMed PMID: 18922857
- [9] Quesada V, Conde L, Villamor N, Ordonez GR, Jares P, Bassaganyas L, et al. Exome sequencing identifies recurrent mutations of the splicing factor SF3B1 gene in chronic lymphocytic leukemia. *Nature Genetics*. 2011 Dec 11;**44**(1):47-52. PubMed PMID: 22158541

- [10] Faguet GB. Chronic Lymphocytic Leukemia: Molecular Genetics, Biology, Diagnosis, and Management. New Jersey: Humana Press; 2004
- [11] Contri A, Brunati AM, Trentin L, Cabrelle A, Miorin M, Cesaro L, et al. Chronic lymphocytic leukemia B-cells contain anomalous Lyn tyrosine kinase, a putative contribution to defective apoptosis. *The Journal of Clinical Investigation*. 2005 Feb;**115**(2):369-378. PubMed PMID: 15650771. Pubmed Central PMCID: 544036
- [12] Longo PG, Laurenti L, Gobessi S, Sica S, Leone G, Efremov DG. The Akt/Mcl-1 pathway plays a prominent role in mediating antiapoptotic signals downstream of the B-cell receptor in chronic lymphocytic leukemia B cells. *Blood*. 2008 Jan 15;**111**(2):846-855. PubMed PMID: 17928528
- [13] Fujimoto M, Poe JC, Jansen PJ, Sato S, Tedder TF. CD19 amplifies B lymphocyte signal transduction by regulating Src-family protein tyrosine kinase activation. *Journal of Immunology*. 1999 Jun 15;**162**(12):7088-7094. PubMed PMID: 10358152
- [14] Gobessi S, Laurenti L, Longo PG, Sica S, Leone G, Efremov DG. ZAP-70 enhances B-cell-receptor signaling despite absent or inefficient tyrosine kinase activation in chronic lymphocytic leukemia and lymphoma B cells. *Blood*. 2007 Mar 01;**109**(5):2032-2039. PubMed PMID: 17038529
- [15] Pleyer L, Egle A, Hartmann TN, Greil R. Molecular and cellular mechanisms of CLL: Novel therapeutic approaches. *Nature Reviews. Clinical Oncology*. 2009 Jul;**6**(7):405-418. PubMed PMID: 19488076
- [16] Carlo-Stella C, Lavazza C, Locatelli A, Vigano L, Gianni AM, Gianni L. Targeting TRAIL agonistic receptors for cancer therapy. *Clinical Cancer Research: An Official Journal of the American Association for Cancer Research*. 2007 Apr 15;**13**(8):2313-2317. PubMed PMID: 17438088
- [17] Adams JM, Cory S. Bcl-2-regulated apoptosis: mechanism and therapeutic potential. *Current Opinion in Immunology*. 2007 Oct;**19**(5):488-496. PubMed PMID: 17629468. Pubmed Central PMCID: 2754308
- [18] Mackus WJ, Kater AP, Grummels A, Evers LM, Hooijbrink B, Kramer MH, et al. Chronic lymphocytic leukemia cells display p53-dependent drug-induced Puma upregulation. *Leukemia*. 2005 Mar;**19**(3):427-434. PubMed PMID: 15674362
- [19] Villunger A, Michalak EM, Coultas L, Mullauer F, Bock G, Ausserlechner MJ, et al. p53- and drug-induced apoptotic responses mediated by BH3-only proteins puma and noxa. *Science*. 2003 Nov 07;**302**(5647):1036-1038. PubMed PMID: 14500851
- [20] Yin XM, Wang K, Gross A, Zhao Y, Zinkel S, Klocke B, et al. Bid-deficient mice are resistant to Fas-induced hepatocellular apoptosis. *Nature*. 1999 Aug 26;**400**(6747):886-891. PubMed PMID: 10476969
- [21] Dicker F, Kater AP, Prada CE, Fukuda T, Castro JE, Sun G, et al. CD154 induces p73 to overcome the resistance to apoptosis of chronic lymphocytic leukemia cells lacking functional p53. *Blood*. 2006 Nov 15;**108**(10):3450-3457. PubMed PMID: 16741250. Pubmed Central PMCID: 1895435

- [22] Dash P. Apoptosis 2001. pp. 1-6. Available from: www.sgul.ac.uk/dept/immunology/~dash
- [23] Van Cruchten S, Van Den Broek W. Morphological and biochemical aspects of apoptosis, oncosis and necrosis. *Anat Histol Embryol.* 2002;**31**(4):214-223
- [24] Ashkenazi A. Targeting death and decoy receptors of the tumour-necrosis factor superfamily. *Nature Reviews Cancer.* 2002 Jun;**2**(6):420-430. PubMed PMID: 12189384
- [25] Scaffidi C, Fulda S, Srinivasan A, Friesen C, Li F, Tomaselli KJ, et al. Two CD95 (APO-1/Fas) signaling pathways. *The EMBO Journal.* 1998 Mar 16;**17**(6):1675-1687. PubMed PMID: 9501089. Pubmed Central PMCID: 1170515
- [26] Gewies A. Introduction to Apoptosis 2003. pp. 1-26. Available from: <http://www.cell-death.de/encyclo/aporev/aporev.htm>
- [27] Luo X, Budihardjo I, Zou H, Slaughter C, Wang X. Bid, a Bcl2 interacting protein, mediates cytochrome c release from mitochondria in response to activation of cell surface death receptors. *Cell.* 1998 Aug 21;**94**(4):481-490. PubMed PMID: 9727491
- [28] Acehan D, Jiang X, Morgan DG, Heuser JE, Wang X, Akey CW. Three-dimensional structure of the apoptosome: Implications for assembly, procaspase-9 binding, and activation. *Molecular Cell.* 2002 Feb;**9**(2):423-432. PubMed PMID: 11864614
- [29] Slee EA, Harte MT, Kluck RM, Wolf BB, Casiano CA, Newmeyer DD, et al. Ordering the cytochrome c-initiated caspase cascade: hierarchical activation of caspases-2, -3, -6, -7, -8, and -10 in a caspase-9-dependent manner. *The Journal of Cell Biology.* 1999 Jan 25;**144**(2):281-292. PubMed PMID: 9922454. Pubmed Central PMCID: 2132895
- [30] Richardson H, Kumar S. Death to flies: *Drosophila* as a model system to study programmed cell death. *Journal of Immunological Methods.* 2002 Jul 01;**265**(1-2):21-38. PubMed PMID: 12072176
- [31] Denault JB, Salvesen GS. Caspases: Keys in the ignition of cell death. *Chemical Reviews.* 2002 Dec;**102**(12):4489-4500. PubMed PMID: 12475198
- [32] Creagh EM, Martin SJ. Caspases: cellular demolition experts. *Biochemical Society Transactions.* 2001 Nov;**29**(Pt 6):696-702. PubMed PMID: 11709057
- [33] Miura M, Zhu H, Rotello R, Hartwig EA, Yuan J. Induction of apoptosis in fibroblasts by IL-1 beta-converting enzyme, a mammalian homolog of the *C. elegans* cell death gene *ced-3*. *Cell.* 1993 Nov 19;**75**(4):653-660. PubMed PMID: 8242741
- [34] Kuida K, Haydar TF, Kuan CY, Gu Y, Taya C, Karasuyama H, et al. Reduced apoptosis and cytochrome c-mediated caspase activation in mice lacking caspase 9. *Cell.* 1998 Aug 07;**94**(3):325-337. PubMed PMID: 9708735
- [35] Kuida K, Zheng TS, Na S, Kuan C, Yang D, Karasuyama H, et al. Decreased apoptosis in the brain and premature lethality in CPP32-deficient mice. *Nature.* 1996 Nov 28;**384**(6607):368-372. PubMed PMID: 8934524
- [36] Earnshaw WC, Martins LM, Kaufmann SH. Mammalian caspases: structure, activation, substrates, and functions during apoptosis. *Annual Review of Biochemistry.* 1999;**68**:383-424. PubMed PMID: 10872455

- [37] Borner C. The Bcl-2 protein family: sensors and checkpoints for life-or-death decisions. *Molecular Immunology*. 2003 Jan;**39**(11):615-647. PubMed PMID: 12493639
- [38] Mund T, Gewies A, Schoenfeld N, Bauer MK, Grimm S. Spike, a novel BH3-only protein, regulates apoptosis at the endoplasmic reticulum. *FASEB Journal: Official Publication of the Federation of American Societies for Experimental Biology*. 2003 Apr;**17**(6):696-698. PubMed PMID: 12594175
- [39] Cory S, Adams JM. The Bcl2 family: Regulators of the cellular life-or-death switch. *Nature Reviews Cancer*. 2002 Sep;**2**(9):647-656. PubMed PMID: 12209154
- [40] Strasser A, O'Connor L, Dixit VM. Apoptosis signaling. *Annual Review of Biochemistry*. 2000;**69**:217-245. PubMed PMID: 10966458
- [41] Bouillet P, Strasser A. BH3-only proteins—Evolutionarily conserved proapoptotic Bcl-2 family members essential for initiating programmed cell death. *Journal of Cell Science*. 2002 Apr 15;**115**(Pt 8):1567-1574. PubMed PMID: 11950875
- [42] Saxena A, Viswanathan S, Moshynska O, Tandon P, Sankaran K, Sheridan DP. Mcl-1 and Bcl-2/Bax ratio are associated with treatment response but not with Rai stage in B-cell chronic lymphocytic leukemia. *American Journal of Hematology*. 2004 Jan;**75**(1):22-33. PubMed PMID: 14695629
- [43] Michels J, Johnson PW, Packham G. Mcl-1. *The International Journal of Biochemistry & Cell Biology*. 2005 Feb;**37**(2):267-271. PubMed PMID: 15474972
- [44] Clohessy JG, Zhuang J, Brady HJ. Characterisation of Mcl-1 cleavage during apoptosis of haematopoietic cells. *British Journal of Haematology*. 2004 Jun;**125**(5):655-665. PubMed PMID:15147382
- [45] Snowden RT, Sun XM, Dyer MJ, Cohen GM. Bisindolylmaleimide IX is a potent inducer of apoptosis in chronic lymphocytic leukaemic cells and activates cleavage of Mcl-1. *Leukemia*. 2003 Oct;**17**(10):1981-1989. PubMed PMID: 14513048
- [46] Herrant M, Luciano F, Loubat A, Auburger P. The protective effect of phorbol esters on Fas-mediated apoptosis in T cells. Transcriptional and posttranscriptional regulation. *Oncogene*. 2002 Jul 25;**21**(32):4957-4968. PubMed PMID: 12118374
- [47] Packham G, Stevenson FK. Bodyguards and assassins: Bcl-2 family proteins and apoptosis control in chronic lymphocytic leukaemia. *Immunology*. 2005 Apr;**114**(4):441-449. PubMed PMID: 15804279. Pubmed Central PMCID: 1782118
- [48] Burger JA, Kipps TJ. CXCR4: A key receptor in the crosstalk between tumor cells and their microenvironment. *Blood*. 2006 Mar 01;**107**(5):1761-1767. PubMed PMID:16269611
- [49] Chen R, Keating MJ, Gandhi V, Plunkett W. Transcription inhibition by flavopiridol: Mechanism of chronic lymphocytic leukemia cell death. *Blood*. 2005 Oct 01;**106**(7):2513-2519. PubMed PMID: 15972445. Pubmed Central PMCID: 1895272
- [50] Maurer U, Charvet C, Wagman AS, Dejardin E, Green DR. Glycogen synthase kinase-3 regulates mitochondrial outer membrane permeabilization and apoptosis by destabilization of MCL-1. *Molecular Cell*. 2006 Mar 17;**21**(6):749-760. PubMed PMID: 16543145

- [51] Opferman JT, Letai A, Beard C, Sorcinelli MD, Ong CC, Korsmeyer SJ. Development and maintenance of B and T lymphocytes requires antiapoptotic MCL-1. *Nature*. 2003 Dec 11; **426**(6967):671-676. PubMed PMID: 14668867
- [52] Woodland RT, Fox CJ, Schmidt MR, Hammerman PS, Opferman JT, Korsmeyer SJ, et al. Multiple signaling pathways promote B lymphocyte stimulator dependent B-cell growth and survival. *Blood*. 2008 Jan 15; **111**(2):750-760. PubMed PMID: 17942753. Pubmed Central PMCID: 2200845
- [53] Venugopala KN, Rashmi V, Odhav B. Review on natural coumarin lead compounds for their pharmacological activity. *BioMed Research International*. 2013; **2013**:963248. PubMed PMID: 23586066. Pubmed Central PMCID: 3622347
- [54] Jain PK, Joshi H. Coumarin: Chemical and pharmacological profile. *Journal of Applied Pharmaceutical Science*. 2012; **02**(06):236-240
- [55] Dandriyal J, Singla R, Kumar M, Jaitak V. Recent developments of C-4 substituted coumarin derivatives as anticancer agents. *European Journal of Medicinal Chemistry*. 2016 Aug 25; **119**:141-168. PubMed PMID: 27155469
- [56] Riveiro ME, De Kimpe N, Moglioni A, Vazquez R, Monczor F, Shayo C, et al. Coumarins: Old compounds with novel promising therapeutic perspectives. *Current Medicinal Chemistry*. 2010; **17**(13):1325-1338. PubMed PMID: 20166938
- [57] Murata T, Itoigawa M, Ito C, Nakao K, Tsuboi M, Kaneda N, et al. Induction of apoptosis in human leukaemia HL-60 cells by furanone-coumarins from *Murraya siamensis*. *The Journal of Pharmacy and Pharmacology*. 2008 Mar; **60**(3):385-389. PubMed PMID: 18284820
- [58] Riveiro ME, Shayo C, Monczor F, Fernandez N, Baldi A, De Kimpe N, et al. Induction of cell differentiation in human leukemia U-937 cells by 5-oxygenated-6,7-methylenedioxy-coumarins from *Pterocaulon polystachyum*. *Cancer Letters*. 2004 Jul 16; **210**(2):179-188. PubMed PMID: 15183533
- [59] You CX, Yang K, Wang CF, Zhang WJ, Wang Y, Han J, et al. Cytotoxic compounds isolated from *Murraya tetramera* Huang. *Molecules*. 2014 Aug 27; **19**(9):13225-13234. PubMed PMID: 25165861
- [60] Miri R, Nejati M, Saso L, Khakdan F, Parshad B, Mathur D, et al. Structure-activity relationship studies of 4-methylcoumarin derivatives as anticancer agents. *Pharmaceutical Biology*. 2016; **54**(1):105-110. PubMed PMID: 26017566
- [61] Molaverdi F, Khoobi M, Emami S, Alipour M, Firuzi O, Foroumadi A, et al. Polyoxygenated cinnamoylcoumarins as conformationally constrained analogs of cytotoxic diarylpentanooids: Synthesis and biological activity. *European Journal of Medicinal Chemistry*. 2013 Oct; **68**:103-110. PubMed PMID: 23973822
- [62] Yang J, Liu GY, Dai F, Cao XY, Kang YF, Hu LM, et al. Synthesis and biological evaluation of hydroxylated 3-phenylcoumarins as antioxidants and antiproliferative agents. *Bioorganic & Medicinal Chemistry Letters*. 2011 Nov 01; **21**(21):6420-6425. PubMed PMID: 21920747

- [63] Paul K, Bindal S, Luxami V. Synthesis of new conjugated coumarin-benzimidazole hybrids and their anticancer activity. *Bioorganic & Medicinal Chemistry Letters*. 2013 Jun 15;**23**(12):3667-3672. PubMed PMID: 23642480
- [64] Elshemy HA, Zaki MA. Design and synthesis of new coumarin hybrids and insight into their mode of antiproliferative action. *Bioorganic & Medicinal Chemistry*. 2017 Feb 01;**25**(3):1066-1075. PubMed PMID: 28038941
- [65] Nasr T, Bondock S, Youns M. Anticancer activity of new coumarin substituted hydrazide-hydrazone derivatives. *European Journal of Medicinal Chemistry*. 2014 Apr 09;**76**:539-548. PubMed PMID: 24607878
- [66] Riveiro ME, Maes D, Vazquez R, Vermeulen M, Mangelinckx S, Jacobs J, et al. Toward establishing structure-activity relationships for oxygenated coumarins as differentiation inducers of promonocytic leukemic cells. *Bioorganic & Medicinal Chemistry*. 2009 Sep 15;**17**(18):6547-6559. PubMed PMID: 19716307
- [67] Riveiro ME, Vazquez R, Moglioni A, Gomez N, Baldi A, Davio C, et al. Biochemical mechanisms underlying the pro-apoptotic activity of 7,8-dihydroxy-4-methylcoumarin in human leukemic cells. *Biochemical Pharmacology*. 2008 Feb 01;**75**(3):725-736. PubMed PMID: 17996847
- [68] Riveiro ME, Moglioni A, Vazquez R, Gomez N, Facorro G, Piehl L, et al. Structural insights into hydroxycoumarin-induced apoptosis in U-937 cells. *Bioorganic & Medicinal Chemistry*. 2008 Mar 01;**16**(5):2665-2675. PubMed PMID: 18060791
- [69] Kim HH, Sik Bang S, Seok Choi J, Han H, Kim IH. Involvement of PKC and ROS in the cytotoxic mechanism of anti-leukemic decursin and its derivatives and their structure-activity relationship in human K562 erythroleukemia and U937 myeloleukemia cells. *Cancer Letters*. 2005 Jun 08;**223**(2):191-201. PubMed PMID: 15896453
- [70] Ahn Q, Jeong SJ, Lee HJ, Kwon HY, Han I, Kim HS, et al. Inhibition of cyclooxygenase-2-dependent survivin mediates decursin-induced apoptosis in human KBM-5 myeloid leukemia cells. *Cancer Letters*. 2010 Dec 08;**298**(2):212-221. PubMed PMID: 20673699. Pubmed Central PMCID: 3689030
- [71] Chu CY, Tsai YY, Wang CJ, Lin WL, Tseng TH. Induction of apoptosis by esculetin in human leukemia cells. *European Journal of Pharmacology*. 2001 Mar 23;**416**(1-2):25-32. PubMed PMID: 11282109
- [72] Lee SH, Park C, Jin CY, Kim GY, Moon SK, Hyun JW, et al. Involvement of extracellular signal-related kinase signaling in esculetin induced G1 arrest of human leukemia U937 cells. *Biomedicine & Pharmacotherapy = Biomedecine & Pharmacotherapie*. 2008 Dec;**62**(10):723-729. PubMed PMID: 18222060.
- [73] Wang CJ, Hsieh YJ, Chu CY, Lin YL, Tseng TH. Inhibition of cell cycle progression in human leukemia HL-60 cells by esculetin. *Cancer Letters*. 2002 Sep 26;**183**(2):163-168. PubMed PMID: 12065091
- [74] Rubio V, Calvino E, Garcia-Perez A, Herraes A, Diez JC. Human acute promyelocytic leukemia NB4 cells are sensitive to esculetin through induction of an apoptotic mechanism. *Chemico-Biological Interactions*. 2014 Sep 05;**220**:129-139. PubMed PMID: 24995577

- [75] Park C, Jin CY, Kwon HJ, Hwang HJ, Kim GY, Choi IW, et al. Induction of apoptosis by esculetin in human leukemia U937 cells: Roles of Bcl-2 and extracellular-regulated kinase signaling. *Toxicology In Vitro*. 2010 Mar;**24**(2):486-494. PubMed PMID: 19786087
- [76] Lin TH, FJ L, Yin YF, Tseng TH. Enhancement of esculetin on arsenic trioxide-provoked apoptosis in human leukemia U937 cells. *Chemico-Biological Interactions*. 2009 Jun 15;**180**(1):61-68. PubMed PMID: 19428345
- [77] Park C, Jin CY, Kim GY, Choi IW, Kwon TK, Choi BT, et al. Induction of apoptosis by esculetin in human leukemia U937 cells through activation of JNK and ERK. *Toxicology and Applied Pharmacology*. 2008 Mar 01;**227**(2):219-228. PubMed PMID: 18031783
- [78] Uto T, Tung NH, Thongjankaew P, Lhieochaiphant S, Shoyama Y. Kayeassamin A isolated from the flower of *Mammea siamensis* triggers apoptosis by activating caspase-3/-8 in HL-60 human leukemia cells. *Pharmacognosy Research*. 2016 Oct-Dec;**8**(4):244-248. PubMed PMID: 27695262. Pubmed Central PMCID: 5004513
- [79] Tung NH, Uto T, Sakamoto A, Hayashida Y, Hidaka Y, Morinaga O, et al. Antiproliferative and apoptotic effects of compounds from the flower of *Mammea siamensis* (Miq.) T. Anders. on human cancer cell lines. *Bioorganic & Medicinal Chemistry Letters*. 2013 Jan 01;**23**(1):158-162. PubMed PMID: 23206866
- [80] Yang LL, Wang MC, Chen LG, Wang CC. Cytotoxic activity of coumarins from the fruits of *Cnidium monnieri* on leukemia cell lines. *Planta Medica*. 2003 Dec;**69**(12):1091-1095. PubMed PMID: 14750023
- [81] Wang H, Jia XH, Chen JR, Wang JY, Li YJ. Osthole shows the potential to overcome P-glycoprotein-mediated multidrug resistance in human myelogenous leukemia K562/ADM cells by inhibiting the PI3K/Akt signaling pathway. *Oncology Reports*. 2016 Jun;**35**(6):3659-3668. PubMed PMID: 27109742
- [82] Bhatti R, Singh J, Saxena AK, Suri N, Ishar MP. Pharmacognostic standardisation and antiproliferative activity of *Aegle marmelos* (L.) *Correa* leaves in various human cancer cell lines. *Indian Journal of Pharmaceutical Sciences*. 2013 Nov;**75**(6):628-634. PubMed PMID: 24591736. Pubmed Central PMCID: 3928725
- [83] Appendino G, Bianchi F, Bader A, Campagnuolo C, Fattorusso E, Tagliatalata-Scafati O, et al. Coumarins from *Opopanax chironium*. New dihydrofuranocoumarins and differential induction of apoptosis by imperatorin and heraclenin. *Journal of Natural Products*. 2004 Apr;**67**(4):532-536. PubMed PMID: 15104479
- [84] Pae HO, Oh H, Yun YG, Oh GS, Jang SI, Hwang KM, et al. Imperatorin, a furanocoumarin from *Angelica dahurica* (Umbelliferae), induces cytochrome c-dependent apoptosis in human promyelocytic leukaemia, HL-60 Cells. *Pharmacology & Toxicology*. 2002 Jul;**91**(1):40-48. PubMed PMID: 12193260
- [85] Kawaii S, Tomono Y, Katase E, Ogawa K, Yano M. Effect of coumarins on HL-60 cell differentiation. *Anticancer Research*. 2000 Jul-Aug;**20**(4):2505-2512. PubMed PMID: 10953319

- [86] Vazquez R, Riveiro ME, Vermeulen M, Mondillo C, Coombes PH, Crouch NR, et al. Toddaculin, a natural coumarin from *Toddalia asiatica*, induces differentiation and apoptosis in U-937 leukemic cells. *Phytomedicine: International Journal of Phytotherapy and Phytopharmacology*. 2012 Jun 15;**19**(8-9):737-746. PubMed PMID: 22537907
- [87] Gholami O, Jeddi-Tehrani M, Iranshahi M, Zarnani AH, Ziai SA. Umbelliprenin from *Ferula szowitsiana* Activates both Intrinsic and Extrinsic Pathways of Apoptosis in Jurkat T-CLL cell line. *Iranian Journal of Pharmaceutical Research : IJPR*. 2013 Summer;**12**(3):371-376. PubMed PMID: 24250644. Pubmed Central PMCID: 3813267
- [88] Ziai SA, Gholami O, Iranshahi M, Zamani AH, Jeddi-Tehrani M. Umbelliprenin induces apoptosis in CLL cell lines. *Iranian Journal of Pharmaceutical Research: IJPR*. 2012 Spring;**11**(2):653-659. PubMed PMID: 24250490. Pubmed Central PMCID: 3832171
- [89] Jun DY, Kim JS, Park HS, Han CR, Fang Z, Woo MH, et al. Apoptogenic activity of auraptene of *Zanthoxylum schinifolium* toward human acute leukemia Jurkat T cells is associated with ER stress-mediated caspase-8 activation that stimulates mitochondria-dependent or -independent caspase cascade. *Carcinogenesis*. 2007 Jun;**28**(6):1303-1313. PubMed PMID: 17301064
- [90] Motlagh FM, Gholami O. Comparison of umbelliprenin and auraptene in cytotoxic effects and myeloid cell leukaemia type-1 (Mcl-1) gene expression. *Indian Journal of Pharmaceutical Sciences*. 2016;**78**(6):827-833
- [91] Gholami O, Jeddi-Tehrani M, Iranshahi M, Zarnani AH, Ziai SA. Mcl-1 is up regulated by prenylated coumarin, umbelliprenin in jurkat cells. *Iranian Journal of Pharmaceutical Research*. 2014 Fall;**13**(4):1387-1392. PubMed PMID: 25587328. Pubmed Central PMCID: 4232805
- [92] Lee JC, Shin EA, Kim B, Kim BI, Chitsazian-Yazdi M, Iranshahi M, et al. Auraptene induces apoptosis via myeloid cell leukemia 1-mediated activation of caspases in PC3 and DU145 prostate cancer cells. *Phytotherapy Research*. 2017 Jun;**31**(6):891-898. PubMed PMID: 28383142
- [93] BS O, Shin EA, Jung JH, Jung DB, Kim B, Shim BS, et al. Apoptotic effect of galbanic acid via activation of caspases and inhibition of Mcl-1 in H460 non-small lung carcinoma cells. *Phytotherapy Research*. 2015 Jun;**29**(6):844-849. PubMed PMID:25753585
- [94] Li X, Zeng X, Sun J, Li H, Wu P, Fung KP, et al. Imperatorin induces Mcl-1 degradation to cooperatively trigger Bax translocation and Bak activation to suppress drug-resistant human hepatoma. *Cancer Letters*. 2014 Jun 28;**348**(1-2):146-155. PubMed PMID: 24680709
- [95] Jin L, Tabe Y, Kimura S, Zhou Y, Kuroda J, Asou H, et al. Antiproliferative and proapoptotic activity of GUT-70 mediated through potent inhibition of Hsp90 in mantle cell lymphoma. *British Journal of Cancer*. 2011 Jan 04;**104**(1):91-100. PubMed PMID: 21139584. Pubmed Central PMCID: 3039813
- [96] Lin MH, Cheng CH, Chen KC, Lee WT, Wang YF, Xiao CQ, et al. Induction of ROS-independent JNK-activation-mediated apoptosis by a novel coumarin-derivative, DMAC, in human colon cancer cells. *Chemico-Biological Interactions*. 2014 Jul 25;**218**:42-49. PubMed PMID: 24812029

- [97] Singh RK, Lange TS, Kim KK, Brard L. A coumarin derivative (RKS262) inhibits cell-cycle progression, causes pro-apoptotic signaling and cytotoxicity in ovarian cancer cells. *Investigational New Drugs*. 2011 Feb;**29**(1):63-72. PubMed PMID: 19865799. Pubmed Central PMCID: 4801487
- [98] Billard C, Menasria F, Quiney C, Faussat AM, Finet JP, Combes S, et al. 4-Arylcoumarin analogues of combretastatins stimulate apoptosis of leukemic cells from chronic lymphocytic leukemia patients. *Experimental Hematology*. 2008 Dec;**36**(12):1625-1633. PubMed PMID:18922614

Cytotoxic Endpoints

Cyto(Geno)Toxic Endpoints Assessed via Cell Cycle Bioassays in Plant Models

Larissa Fonseca Andrade Vieira and
Graciele Lurdes Silveira

Additional information is available at the end of the chapter

<http://dx.doi.org/10.5772/intechopen.72997>

Abstract

Environmental pollution is a matter of great concern. Therefore, researches that aim to access the risk of toxicity of these potential pollutants are welcome in the scientific community. The most common strategy to detect toxic agents is through chemical analysis. However, in the last years, the biological assays are often important for risk assessments. Among the bioassays using living organisms to detect toxicity of a compound, plant models have been highlighted as it is easy to be conducted, has low cost, high sensitivity and presents good correlation with other test systems, including mammals. Besides, it is in accordance with the Toxicology Guidelines for the twenty-first century, which claims for bioassays that could substitute the ones that use animals as models. At cellular level, the cytotoxicity, genotoxicity, and mutagenicity are the parameters determined by the endpoints as mitotic index, DNA fragmentation, induction of cell death, and malfunction of cellular structures leading to chromosome and cell cycle alterations. Each of these endpoints will be presented in details in this chapter.

Keywords: cell cycle analysis, chromosome alterations, DNA fragmentation, TUNEL assay, comet assay

1. Introduction

Concerns of the world society and authorities over the environment are imperative. Hereby the growing environmental pollution and how to slow down or mitigate it are key points of discussion. Various aspects need to be approached as regards understanding the whole process and dynamics of pollutants in the environment. Among the first actions required to

ensure the quality and health of the environment, in both the short and long terms, it is fundamental to obtain information about contaminating agents.

Overall, research in the environmental area is based on analyses and physicochemical characteristics of pollutants. However, it has been recognized that the effects of these compounds on living organisms, as well as their toxicity mechanisms, are excellent tools to complement the obtained physicochemical data [1], being important for decision-making and in the search for preventive, mitigating measures as well as alternatives to this scenario.

In this sense, the biological effects of pollutants can be assessed *in vivo* (in situ and ex situ) and *in vitro* via bioassays using test organisms, allowing to evaluate their toxic potential in a rapid and efficacious manner and at relatively low cost. Overall, the response in relation to toxicity can be given a different organization level, such as behavior, physiology, anatomy, cell, and DNA, among others, with each organism and test representing a certain endpoint. The integrity of the genetic material and its consequence for the proliferation and reproduction of model organisms are the most targeted outcomes and estimate the dimension of the risks of compounds to the environment and living beings in a real and functional manner [2–4].

Among the different bioassays performed in living organisms, those that use higher plants as models to evaluate the biological effects of environmental pollutants stand out. Besides being validated by the US Environmental Protection Agency (US EPA) as efficacious in the determination of toxicological risks in toxicity monitoring programs, they present important characteristics such as high sensitivity, fewer false-negative responses, low cost, not requiring approval from ethics commissions, and being as efficient as assays performed in animal models or even human cells [5–8]. In addition, they are in accordance with the Toxicology Guidelines for the twenty-first century, which calls for models that substitute animal ones to assess toxic risks [9].

Among the assays using higher plants highlighted by the Genetic Toxicology (Gene-Tox) program of the US EPA described by Ma [10], one of the most widespread is the *Allium* test. It was developed and described in 1938 by Levan [11] and consists in the evaluation of alterations in the mitotic phases of root meristem cells of *Allium cepa* [12]. In general terms, the test can be applied to any plant model that presents chromosomes of easy visualization under the microscope. It is employed to evaluate the cell cycle in meristematic root tip cells, observing disturbances in the frequency of cells in division as well as induction of alterations in the mitotic phases or in the interphase nucleus, arising from action of the tested pollutant.

In this chapter, the main characteristics of the assay based on evaluation of the cell cycle will be presented, as well as the endpoints that can be assessed and used for evaluation, determination of cyto(genoto)xicity, and understanding of the mechanisms of action of potential environmental pollutants.

2. Cytogenetic analyses applied to environmental toxicology

Plants constitute a system of great importance as bioindicators of pollution, having long been used for this end. International institutions such as the United Nations Environmental

Programme (UNEP), the World Health Organization (WHO), and the US EPA approve the use of bioassays with plants to investigate toxic effects of chemical agents released into the environment [13].

The use of plants as models to evaluate the toxicity and mutagenicity of substances or pollutants enables the analysis both in the natural environment (in situ) and in the laboratory (ex situ). They are excellent tools to complement the physicochemical analyses of investigated compounds, as they allow a practical confirmation of the theory developed in studies on the physicochemical properties of the potentially dangerous materials [1, 14, 15].

Tests *ex situ* commonly use meristematic root tip cells as biological material for analysis. In the natural environment, the root is the first part of the plant to be exposed to toxic agents dispersed in the soil and water. Therefore, the analysis of root cells represents a rapid method for the monitoring of toxicity. Moreover, the observed damage to the DNA and/or chromosomes of plant cells can be extrapolated to further organisms based on the universality of the DNA structure and genetic code [16]. This way, if a chemical substance causes damage to the DNA of one plant, it should also be considered potentially damaging to the DNA of other organisms [17].

The assay with meristematic root tip cells is based on cytogenetic evaluations involving the movement of chromosomes during the mitotic division, which allows deriving the mechanisms of action of the pollutant. The root of a propagule (bulb, seeds, cutting, etc.) is exposed to the agent that shall be tested. By the end of the exposure interval, the meristem is separated from the root and fixed; a slide is subsequently prepared, generally by squashing technique, and the meristematic cells are stained with acetic orcein and/or Schiff's reagent (for the detailed methodology, see [18]). The slide is observed under light microscope, and various parameters of the cell cycle are evaluated. The cell cycle stages, including interphase and mitotic division (prophase, metaphase, anaphase, and telophase), are observed, and the alterations detected in each phase are recorded. Based on the results, the assessed endpoints are (1) frequency of dividing cells or mitotic index (MI), given by the sum of cells in phase M (mitosis) divided by the total number of observed cells, being expressed in number of dividing cells out of every 100 observed cells; (2) total frequency of chromosome alterations (CA), given by the sum of all observed alterations, independently of type and division phase, divided by the total number of observed cells, expressed as number of altered cells out of 100 observed cells; or (3) nuclear alterations (NA), related to the presence of abnormal interphase nuclei, with unusual form or extremely condensed appearance, also given by the sum of total observed alterations by the total number of counted cells, and expressed as the number of alterations out of 100 cells (for calculations, see [19]).

In summary, the tested agent can be characterized as cytotoxic when it alters the normal MI (increase or reduction) of the used plant model, hence causing malfunctioning of cell structures and possibly leading to cell death, and/or genotoxic if the alterations observed throughout the cycle are related to DNA breakage, including the formation of micronuclei. These bodies are considered a mutagenicity parameter as they represent damage not corrected by the cell repair system and, thus, permanent and transmissible to the subsequent cell generations. An alteration can also be classified as aneugenic, when it is related to malformation or malfunctioning of the mitotic spindle or the attachment of the chromosomes on the spindle and leads to gain or loss of one or more chromosomes, or clastogenic, when associated to

breakages and rearrangements in the DNA or chromosomes [16, 20, 21]. Each of these endpoints and possible alterations that can be observed throughout the mitotic cell cycle, and their consequences, will be detailed next.

3. What can cell cycle analyses reveal?

Evaluation of the cell cycle, which comprises the interphase (G1, S, and G2) and the M phase (mitosis-prophase, metaphase, anaphase, and telophase), allows gaining knowledge about the organizational structure of the chromosomes and how they behave during the cell division. As mentioned previously in this chapter, such assessment can be employed to determine the toxicity of a chemical compound. Alterations in the mitotic index help determine the degree of cytotoxicity of an agent, whereas chromosome alterations observed in the cell cycle define the genotoxicity of the agents and their capacity of causing damage to the DNA, which may or may not be repaired by the cellular repair mechanisms. Together, the cell cycle alterations express the cyto(genoto)xicity of chemical compounds and environmental pollutants and are used to investigate their toxic potential.

Several endpoints can be monitored in the division of meristematic cells, such as the chromosomal and nuclear aberrations previously described, besides the formation of micronuclei.

To better understand the alterations observed in the cell cycle, it is necessary to remember that the movement of chromosomes for segregation of the DNA into the daughter cells relies on the mitotic spindle, formed by microtubules. The whole dynamics of the mitotic process thus depend on the binding of the microtubules to the chromosome centromeres, besides microtubule polymerization and depolymerization mechanisms. In this sense, alterations in these dynamics affect the segregation of chromosomes to the daughter cells and may be considered the first origin of alterations observed in the cell cycle. Hence, as consequences of alterations in the spindle and correct attachment of the chromosomes, we can cite the interruption of the cell cycle in metaphase, originating c-metaphases (**Figure 1A**) and formation of polyploid cells (**Figure 1B**), as consequence, and multipolar anaphase (**Figure 1C**), non-oriented chromosomes at the equatorial plan (**Figure 1D**) or delayed segregation of the chromosomes/chromatids in anaphase/telophase (**Figure 1E and F**) [21–24].

When interference in the polymerization and depolymerization of the microtubules occurs, the cell cycle may be paralyzed in metaphase, and the chromosomes are visualized as well condensed, with well-defined centromere and spread inside the cell [22]. In the laboratory, this situation is caused with substances' denominated blockers, such as colchicine, which gives this alteration its name: colchicine metaphase or c-metaphase (**Figure 1A**). These extremely condensed and separated chromosomes are used in karyotype studies of the species, as they allow observing the morphology of each chromosome individually.

Polyploidy emerges as a consequence of the prolonged effect of a substance or toxic compound in the cells. In the absence of the spindle, the cell with duplicated DNA, represented by the chromosome with two chromatids, returns to interphase, initiating a new cell cycle. In the G1

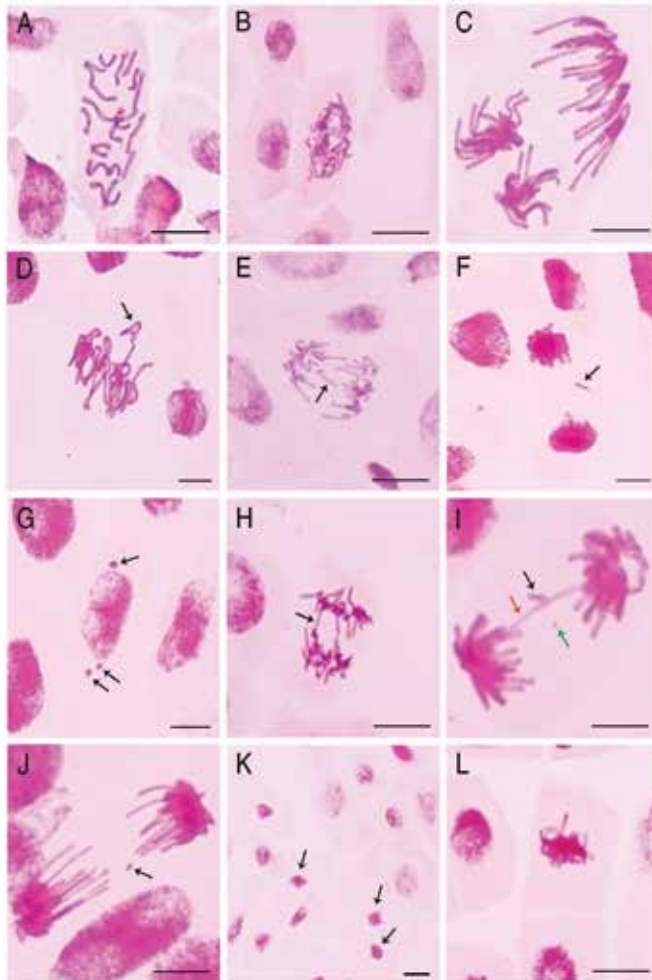


Figure 1. Example of cell cycle alterations observed in meristematic cells of *Allium cepa* (onion) and *Lactuca sativa* (lettuce) root tips. (A) C-metaphasis in lettuce exposure to methyl methanesulfonate (MMS); (B) polyploidy metaphasis in lettuce exposure to cadmium; (C) multipolar anaphases in onion exposure to atrazine herbicide; (D) non-oriented chromosome (black arrow) in onion metaphasis exposure to cadmium; (E) not normal/laggard segregation (black arrow) in lettuce anaphase exposure to cadmium; (F) not normal/laggard segregation (black arrow) in onion telophase exposure to MMS; (G) micronuclei in onion exposure to MMS; (H) anaphase bridge (black arrow) in lettuce exposure to spent Potliner (SPL); (I) anaphase bridge (red arrow) in onion exposure to MMS with a fragment (black arrow) and a micronucleus (green arrow); (J) chromosome fragments (black arrow) in onion exposure to MMS; (K) condensed nuclei (black arrow) in lettuce exposure to atrazine herbicide; and (L) stickiness chromosome in lettuce exposure to SPL. Images obtained in a light microscope at oil objective (100 \times). Bars 10 μ m.

nucleus, each chromatid of the chromosome starts representing one DNA molecule of the cell that will be replicated in the S phase. Upon initiating a new mitotic cycle, after G₂, the proteins of the chromosome's protein scaffold keep the sister chromatids united, and the cell starts mitosis with a duplicated number of chromosomes, characterizing polyploidy. Under light microscope, a cell is characterized as polyploid when an excess number of chromosomes and/or cell volume larger than usual can be observed at the end of prophase or beginning of metaphase (**Figure 1B**).

Multipolar anaphase and abnormal segregation of chromatids in anaphase/telophase also arise from the action of chemical substances on the organization of the microtubules. These alterations are observed as a consequence of incorrect binding of the mitotic spindle to the centromere of the chromosomes [24] or from the shortening and elongation of some microtubules of the mitotic spindle out of synchrony with the other microtubules. Unequal disjunction of the chromosomes may thus occur (non-oriented chromosomes, **Figure 1D**), giving rise to micronuclei (**Figure 1G**) when these chromosomes cannot be reincorporated into the main nucleus along with the other chromosomes [25].

So far, some alterations of the cell cycle have been demonstrated which arise from effect of the toxic agent on the malformation of a cellular structure. Together, these alterations characterize an aneugenic effect and mechanism of the toxic agent, as they can have as consequences the increase or decrease in the number of chromosomes of the species. All these aneugenic alterations represent the cytotoxicity of a given substance, as they relate to a cell structure.

The action of toxic substances can also occur directly on the DNA. In this case, they are observed in the cell cycle as alterations in chromosome structure. Since the effects occur on the genetic material in this case, the mechanism of action of the substance is clastogenic and represents its genotoxicity.

The most evident clastogenic effect when observing the cell cycle under the microscope is the presence of bridges (**Figure 1H and I**) and chromosome fragments (**Figure 1I**) arising from breakages in the DNA molecule. Overall, one of the consequences of the breakage is the loss of telomeres, a region in the terminal extremity of the chromosomes that has the function of ensuring the chromosome protection and stability. With the loss of the chromosome stability, fusion of the terminal portion of two chromosomes may occur. Upon division, chromosomes with two centromeres are observed as bridges in anaphase/telophase (**Figure 1H and I**), where each of the centromeres is linked to the spindle of one of the cell poles.

The chromosome region originated from the breakage that is devoid of centromere is denominated acentric fragment (**Figure 1J**). These chromosome fragments, due to containing parts of the genetic material, are recognized by the cell and involved in membrane during cell division, giving rise to micronuclei, which are easily observed in cells of the F1 generation [7].

Several authors highlight and affirm that micronuclei are the most effective and simple endpoint for the analysis of mutagenic effects caused by chemical compounds, owing to their arising from non- or incorrectly repaired damage in the parental cells. They are easily observed in daughter cells as a structure similar to the main nucleus but with smaller size (**Figure 1G**). Indeed, the micronucleus is easily recognized in the cell visualized under the microscope, particularly if the preparation was accomplished using a DNA-specific dye. In several cytological study models, including human blood cells in culture, the micronuclei assay is applied as a marker of mutagenicity. However, as explained here, it can originate from both acentric fragments and entire chromosomes that were not bound to the spindle. Since each of these causes of micronuclei formation originates from a distinct mechanism of action, assessment of the entire cell cycle, if possible, together with evaluation of micronuclei induction is seen as the cheapest strategy to determine the mechanism of action of the studied substance or compound.

All these reported alterations, if persistent and deleterious, activate the cell death mechanisms. Under light microscope, the evidence for occurrence of cell death is the observation of highly condensed interphase nuclei (**Figure 1K**), with very heterochromatic chromatin, appearing well rounded, darker, and smaller than the normal interphase nuclei [26, 27].

The cell death process due to abiotic stress is cytologically characterized by condensed nuclei and molecularly by DNA fragmentation [26]. This death mechanism is related to destruction and subsequent elimination of damaged cells [28].

Toxic substances can also trigger the formation of sticky chromosomes (**Figure 1L**). Overall, they are characterized by alterations in the physicochemical structure of the DNA, proteins, or both, formed from complexes with phosphate groups of the DNA, inter- and intrachromatid linkages, and DNA condensation [22, 29]. These factors promote loss of the normal characteristics of condensation, causing the formation of agglomerates [22, 30]. Chromosome stickiness is considered a highly toxic alteration [31] that hinders the segregation of the chromatids and the normal continuation of the cell division, which may trigger the cell death process, avoiding that the toxic effect be passed onto the following generation.

Of the observed alterations, chromosome stickiness is considered the most intriguing as regards the classification in aneugenic or clastogenic, in function of the mechanisms involved in their occurrence in the cell cycle. Here, it is considered a complex cyto(genotoxic) effect arising from previous events, for instance, polyploidy or excessive breakages and bridges in the DNA molecule, present at different levels. As regards the consequences of stickiness to the cell, some authors like Andrade et al. [31] cite that the high frequency of stickiness may activate the cell death mechanisms. Thus, the induction of severe stickiness cannot be repaired by the cells, having as consequence the heterochromatinization of the whole nucleus.

4. Investigation of cell death mechanisms and DNA damage applied to environmental toxicology

DNA fragmentation, previously reported as the clastogenic effect of a toxic agent in the cell, is one of the mechanisms related to the cell death process. It can be evaluated through application of techniques available as kits containing a marker for fragmentation.

The Terminal d-UTP Nick End Labeling (TUNEL) assay is one of the tests used for the analysis of DNA fragmentation and investigation of the cell death mechanisms. It is based on incorporation of nucleotides (d-UTP = 2'-deoxyuridine, 5'-triphosphate) marked with a fluorochrome (fluorescein isothiocyanate, FITC) in the free 3'OH region of the breakages in the DNA chain by the enzyme terminal deoxynucleotidyl transferase (TdT) [26, 32]. This reaction relies on the capacity of the enzyme TdT of coupling a deoxy-uracyl-fluorescein (d-UTP) conjugated to the 3'OH end of the broken DNA [32, 33]. The incorporation of fluorescein-12-d-UTP is then amplified by various enzymatic reactions [34]. These nucleotides can be marked with a fluorescent dye and detected by fluorescence microscopy or the laser of a cytometer [35].

Under fluorescence microscope, the cells can be visualized with different fluorescence intensities in function of the marker, fluorescein. They are then classified as (A) not marked (**Figure 2**), thus without fragmentation; (B) weakly marked (**Figure 2**), therefore presenting light damage that can still be recovered, since the cell death process involves several steps and only the final ones represent a “one-way road”; and (C) strongly marked (**Figure 2**), associated to cells with high frequency of fragmented DNA and in advanced stage of cell death [18].

The comet assay or single cell gel electrophoresis (SCGE) is another technique very useful to identify DNA damage. It allows the detection of damage to the genetic material caused by rupture of chains, alkali-labile sites (ALS), incomplete excision repair sites, and reticulations, induced by alkylating or intercalating agents and oxidative damage, even before the cell repair system acts. Further, it allows verifying the damage present after the cell repair process.

In plants, it is broadly used in ecotoxicological studies of environmental pollutants and is characterized by its high sensitivity and specificity, low cost, and rapidness in detecting the genotoxic effects, requiring small sample size, and allowing for simple analysis. The evaluation can be performed at individual cell level or applied to any cell population, without requirement of cell division. In summary, it can be executed in three versions and detect a broad spectrum of damage to the genetic material [36, 37].

The three possible versions of the comet assay differ with regard to the pH of the electrophoresis buffer, which can be neutral, slightly alkaline, and alkaline-alkaline. In the neutral method, ruptures of the DNA double strand are detected. In the moderately alkaline version, simple breakages in the DNA and the double helix are observed. In turn, in the alkaline-alkaline approach, used in the majority of the studies owing to its greater sensitivity, breakages of single and double strands as well as alkali-labile sites and crosslinks are quantified. The choice of the comet assay version depends on the type of damage that shall be observed [38].

The comet assay can be used to complement the cytogenetic data obtained from the cell cycle analyses, as it detects genomic lesions caused to the DNA arising from the action of mutagens. Unlike mutations, the lesions identified by the comet assay are prone to repair. The technique

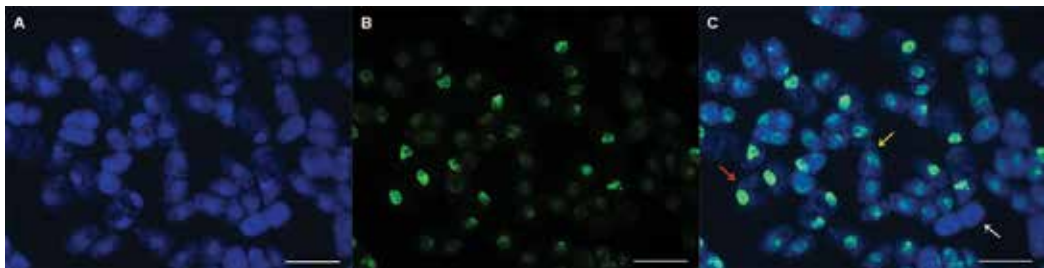


Figure 2. Meristematic cells of *Lactuca sativa* L. (lettuce) treated with MMS submitted to the TUNEL test. (A) Image captured with filter at wavelength of 345–358 nm (for DAPI). (B) Image captured with filter at wavelength of 488–495 nm. (C) Result of overlapping of images A and B made through the AxioVision program, where it is possible to observe unmarked nuclei, without damage (white arrow); weakly marked nuclei, with slight damage (yellow arrow); and strongly marked nuclei, with severe damage (red arrow) to DNA. Images obtained in a microscope of fluorescence (Olympus BX 60) on 40× objective. Bars 50 μm .

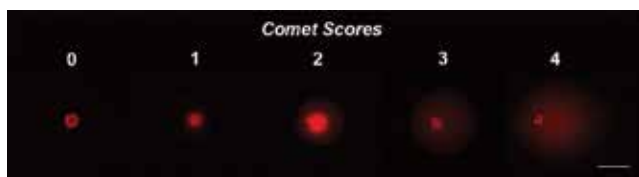


Figure 3. Meristematic cells of *Allium cepa* L. (onion) treated with water (score 0) and spent Potliner (SPL) (scores 1–4) submitted to the comet assay. The scores 0–4 are attributed according to visual analysis of nucleoids. Images obtained in a microscope of fluorescence (Olympux BX 60) on 40× objective. Bars 50 μ m.

consists in the immersion of viable cells in agarose gel, lysis of the cell membrane by detergents and alkaline salts, and subsequent electrophoresis. Under alkaline electrophoresis conditions, cell DNAs that have suffered damage present higher rate of migration toward the anode, owing to breakages of simple or double strands and alkali-labile sites, simulating the appearance of a comet (head and tail) [39]. The level of damage is measured by observing the degree of fragmentation (score) of the genetic material in the electrophoresis, whereby the damaged DNA presents higher rate of migration toward the anode, and the least damaged shows greater migration rate. The four scores most commonly used in the visual identification under the microscope are presented in **Figure 3**.

5. Final considerations

Bioassays with plants usually comprise macroscopic tests, which involve evaluations of germination and initial plantlet development (growth of root and aerial part), as well as microscopic evaluations, including the observation of alterations during the cell cycle in meristematic cells exposed to the tested chemical agent. The results of these bioassays allow determining the phytotoxicity, cytotoxicity, genotoxicity, and mutagenicity of the pollutant or chemical compound in question.

Both in the macroscopic and microscopic evaluations, the root is the plant organ used in the tests. It is particularly useful in these eco(genotoxicological tests, as it is the first part of the plant to be exposed to environmental pollutants. For macroscopic assessment, the observation of root growth is a rapid and sensitive method for environmental monitoring, but does not contribute to the understanding of toxicity mechanisms.

Root tips contain meristematic cells that present intensive cell division, allowing a rapid and adequate evaluation of the cell cycle, constituting the microscopic assessments whose measurable parameters have been described here. Besides providing important information to determine the mode of action of a given agent, the described microscopic evaluations are directly related to the growth parameter assessed in the macroscopic assay. In plants, as sessile organisms, the growth of an organ is closely related to the increase in the number of cells in the tissue composing it. This way, alterations in the endpoint mitotic index, assessed in the microscopic assay, explain what can be seen with the naked eye. In turn, the endpoint associated to the malfunctioning of cell structures like the mitotic spindle explains alterations

in the mitotic index as well as cell death, which is an endpoint characterized by increase in condensed nuclei and which contributes to the reduction of the mitotic index. Nevertheless, the endpoint associated to DNA fragmentation can be assessed not only by direct observation of the cell cycle but also through more specific techniques such as the TUNEL or comet assays. These methods ultimately explain and confirm the induction of cell death, which, as already reported, contributes for a mitodepressive and phytotoxic effect on root growth.

In conclusion, based on the endpoints that can be assessed through cell cycle analyses, cytotoxicity as well as genotoxicity and mutagenicity of environmental pollutants can be determined in a rapid and reliable manner. Such tests are highly useful to monitor and assess the risk of potentially toxic substances that are released into the environment.

Acknowledgements

We would like to thank Coordenação de Aperfeiçoamento de Pessoal de Nível Superior (Capes) for providing postgraduate scholarships to the authors of this work.

Author details

Larissa Fonseca Andrade Vieira* and Graciele Lurdes Silveira

*Address all correspondence to: lfandrade.vieira@gmail.com

Biology Department, Federal University of Lavras, Lavras, MG, Brazil

References

- [1] Baderna D, Maggioni S, Boriani E, Gemma S, Molteni M, Lombardo S, Colombo A, Bordonali S, Rotella G, Lodi M, Benfenati E. A combined approach to investigate the toxicity of an industrial landfill's leachate: Chemical analyses, risk assessment and in vitro assays. *Environmental Research*. 2011;**111**(4):603-613. DOI: 10.1016/j.envres.2011.01.015
- [2] Matejczyk M, Płaza GA, Nałęcz-Jawecki G, Ulfig K, Markowska-Szczupak A. Estimation of the environmental risk posed by landfills using chemical, microbiological and ecotoxicological testing of leachates. *Chemosphere*. 2011;**82**(7):1017-1023. DOI: 10.1016/j.chemosphere.2010.10.066
- [3] Bianchi J, Mantovani MS, Marin-Morales MA. Analysis of the genotoxic potential of low concentrations of Malathion on the *Allium cepa* cells and rat hepatoma tissue culture. *Journal of Environmental Sciences*. 2015;**36**:102-111. DOI: 10.1016/j.jes.2015.03.034
- [4] Bianchi J, Casimiro-Fernandes TC, Marin-Morales MA. Induction of mitotic and chromosomal abnormalities on *Allium cepa* cells by pesticides imidacloprid and

- sulfentrazone and the mixture of them. *Chemosphere*. 2016;**144**:475-483. DOI: 10.1016/j.chemosphere.2015.09.021
- [5] Ennever FK, Andreano G, Rosenkranz HS. The ability of plant genotoxicity assays to predict carcinogenicity. *Mutation Research/Genetic Toxicology*. 1988;**205**(1-4):99-105. DOI: 10.1016/0165-1218(88)90013-4
- [6] Çelik TA, Äslanturk ÖS. Cytotoxic and genotoxic effects of *Lavandula stoechas* aqueous extracts. *Biologia*. 2007;**62**(3):292-296. DOI: 10.2478/s11756-007-0051-2
- [7] Palmieri MJ, Andrade-Vieira LF, Trento MVC, Eleutério MWF, Lubert J, Davide LC, Marcussi S. Cytogenotoxic effects of spent pot liner (SPL) and its main components on human leukocytes and meristematic cells of *Allium cepa*. *Water, Air, & Soil Pollution*. 2016;**227**(5):1-10. DOI: 10.1007/s11270-016-2809-z
- [8] Reis GB, Ishii T, Fuchs J, Houben A, Davide LC. Tissue-specific genome instability in synthetic interspecific hybrids of *Pennisetum purpureum* (Napier grass) and *Pennisetum glaucum* (pearl millet) is caused by micronucleation. *Chromosome Research*. 2016;**24**(3):285-297. DOI: 10.1007/s10577-016-9521-0
- [9] Hartung T. Toxicology for the twenty-first century. *Nature*. 2009;**460**(7252):208-212. DOI: 10.1038/460208a
- [10] Ma T. The international program on plant bioassays and the report of the follow-up study after the hands-on workshop in China. *Mutation Research/fundamental And Molecular Mechanisms of Mutagenesis*. 1999;**426**(2):103-106. DOI: 10.1016/S0027-5107(99)00049-4
- [11] Levan A. The effect of colchicine on root mitoses in *Allium*. *Hereditas*. 1938;**24**(4):471-486. DOI: 10.1111/j.1601-5223.1938.tb03221.x
- [12] Fiskesjö G. The *Allium* test as a standard in environmental monitoring. *Hereditas*. 1985;**102**(1):99-112. DOI: 10.1111/j.1601-5223.1985.tb00471.x
- [13] Grant WF. Higher plant assays for the detection of chromosomal aberrations and gene mutations—A brief historical background on their use for screening and monitoring environmental chemicals. *Mutation Research*. 1999;**426**(2):107-112. DOI: 10.1016/S0027-5107(99)00050-0
- [14] Sandalio LM, Dalurzo HC, Gómez M, Romero-Puertas MC, Del Rio LA. Cadmium-induced changes in the growth and oxidative metabolism of pea plants. *Journal of Experimental Botany*. 2001;**52**(364):2115-2126. DOI: 10.1093/jexbot/52.364.2115
- [15] Palmieri MJ, Lubert J, Andrade-Vieira LF, Davide LC. Cytotoxic and phytotoxic effects of the main chemical components of spent pot-liner: A comparative approach. *Mutation Research*. 2014;**763**:30-35. DOI: 10.1016/j.mrgentox.2013.12.008
- [16] Andrade-Vieira LF. Toxicity of landfills assessed by plant cytogenetic approaches. In: Cabral GBC, Botelho BAE, editors. *Landfills: Waste Management, Regional Practices and Environmental Impact*. 1st ed. New York: Nova Publishers; 2012. pp. 319-330

- [17] Rank J, Nielsen MH. *Allium cepa* anaphase–telophase root tip chromosome aberration assay on N-methyl-N-nitrosourea, maleic hydrazide, sodium azide, and ethyl methanesulfonate. *Mutation Research/Genetic Toxicology and Environmental Mutagenesis*. 1997;**390**(1):121-127. DOI: 10.1016/S0165-1218(97)00008-6
- [18] Silveira GL, Lima MGF, dos Reis GB, Palmieri MJ, Andrade-Vieria LF. Toxic effects of environmental pollutants: Comparative investigation using *Allium cepa* L. and *Lactuca sativa* L. *Chemosphere*. 2017;**178**:359-367. DOI: 10.1016/j.chemosphere.2017.03.048
- [19] Aragão FB, Palmieri MJ, Ferreira A, Costa AV, Queiroz VT, Pinheiro PF, Andrade-Vieira LF. Phytotoxic and cytotoxic effects of *Eucalyptus* essential oil on *Lactuca sativa* L. *Allelopathy Journal*. 2015;**35**(2):259-272
- [20] Campos JMS, Davide LC, Soares GLG, Viccini LF. Mutagenic effects due to allelopathic action of fern (Gleicheniaceae) extracts. *Allelopathy Journal*. 2008;**22**(1):143-152
- [21] Leme DM, Marin-Morales MA. *Allium cepa* test in environmental monitoring: A review on its application. *Mutation Research*. 2009;**682**(1):71-81. DOI: 10.1016/j.mrrev.2009.06.002
- [22] Andrade-Vieira LF, Ferreira MFS, Bernardes PM, Oliveira WBS. Toxicidade de Agrotóxicos: Uma abordagem Citogenética e Molecular. In: Pratisoli D, Junior WCJ, Zago HB, Alves FR, Viana UR, Junior HJGS, Rodrigues C, editors. *Tópicos Especiais em Produção Vegetal III*. 1st ed. Alegre: UFES; 2012. pp. 39-79
- [23] Campos JMS, Viccini LF, Andrade LF, Davide LC, Rodrigues GS. Genetic toxicology and environmental mutagenesis in Allelopathic interactions. In: Narwal SS, Catalán CAN, Sampietro DA, Vattuone MA, Politycka B, editors. *Plant Bioassays*. 1st ed. Houston, Texas: Studium Press; 2008. pp. 81-96
- [24] Freitas AS, Cunha IMF, Andrade-Vieira LF, Techio VH. Effect of SPL (spent pot liner) and its main components on root growth, mitotic activity and phosphorylation of histone H3 in *Lactuca sativa* L. *Ecotoxicology and Environmental Safety*. 2016;**124**:426-434. DOI: 10.1016/j.ecoenv.2015.11.017
- [25] Fernandes TCC, Mazzeo DEC, Marin-Morales MA. Origin of nuclear and chromosomal alterations derived from the action of an aneugenic agent – trifluralin herbicide. *Ecotoxicology and Environmental Safety*. 2009;**72**(6):1680-1686. DOI: 10.1016/j.ecoenv.2009.03.014
- [26] Andrade-Vieira LF, Gedraite LS, Campos JMS, Davide LC. Spent pot liner (SPL) induced DNA damage and nuclear alterations in root tip cells of *Allium cepa* as a consequence of programmed cell death. *Ecotoxicology and Environmental Safety*. 2011;**74**(4):882-888. DOI: 10.1016/j.ecoenv.2010.12.010
- [27] Andrade-Vieira LF, Campos JMS, Davide LC. Effects of spent pot liner on mitotic activity and nuclear DNA content in meristematic cells of *Allium cepa*. *Journal of Environmental Management*. 2012;**107**:140-146. DOI: 10.1016/j.jenvman.2012.04.008
- [28] Danon A, Delorme V, Mailhac N, Gallois PR. Plant programmed cell death: A common way to die. *Plant Physiology and Biochemistry*. 2000;**38**:647-655. DOI: 10.1016/S0981-9428(00)01178-5

- [29] El-Ghamery AA, El-Kholy MA, El-Yousser MAA. Evaluation of cytological effects of Zn^{2+} in relation to germination and root growth of *Nigella sativa* L. and *Triticum aestivum* L. *Mutation Research*. 2003;**537**(1):29-41. DOI: 10.1016/S1383-5718(03)00052-4
- [30] Babich H, Segall MA, Fox KD. The *Allium* test – A simple, eukaryote genotoxicity assay. *The American Biology Teacher*. 1997;**59**(9):580-583. DOI: 10.2307/4450386
- [31] Andrade LF, Campos JMS, Davide LC. Cytogenetic alterations induced by SPL (spent potliners) in meristematic cells of plant bioassays. *Ecotoxicology and Environmental Safety*. 2008;**71**(3):706-710. DOI: 10.1016/j.ecoenv.2008.02.018
- [32] Behboodi BSH, Samadi L. Detection of apoptotic bodies and oligonucleosomal DNA fragments in cadmium-treated root apical cells of *Allium cepa* Linnaeus. *Plant Science*. 2004;**167**(3):411-416. DOI: 10.1016/j.plantsci.2004.04.024
- [33] Gaverieli Y, Sherman Y, Ben-Sasson SA. Identification of programmed cell death in situ via specific labeling of nuclear DNA fragmentation. *The Journal of Cell Biology*. 1992;**119**(3):493-501. DOI: 10.1083/jcb.119.3.493
- [34] Martins, CF, Dode, MN, Bao, SN, Rumpf, R. Metodo de TUNEL: Uma ferramenta alternativa para avaliar a integridade do DNA de espermatozoides bovinos. *Embrapa Cerrados-Documents (INFOTECA-E)*. 2007;1-26
- [35] Vermes I, Haanen C, Reutelingsperger C. Flow cytometry of apoptotic cell death. *Journal of Immunological Methods*. 2000;**243**(1):167-190. DOI: 10.1016/S0022-1759(00)00233-7
- [36] Yildiz M, Ciğerci İH, Konuk M, Fidan AF, Terzi H. Determination of genotoxic effects of copper sulphate and cobalt chloride in *Allium cepa* root cells by chromosome aberration and comet assays. *Chemosphere*. 2009;**75**:934-938. DOI: 10.1016/j.chemosphere.2009.01.023
- [37] Azqueta KB, Gutzkow KB, Brunborg G, Collins AR. Towards a more reliable comet assay: Optimizing agarose concentration, unwinding time and electrophoresis conditions. *Mutation Research*. 2011;**724**(1):41-45. DOI: 10.1016/j.mrgentox.2011.05.010
- [38] Lanier C, Manier N, Cuny D, Deram A. The comet assay in higher terrestrial plant model: Review and evolutionary trends. *Environmental Pollution*. 2015;**207**:6-20. DOI: 10.1016/j.envpol.2015.08.020
- [39] Pavao PRG, Gontijo AMDMC, Ribeiro DA, Salvadori DMF. Ausencia de efeito genotoxico induzido por esteroides anabolizantes em indivduos fisiculturistas. *Revista Brasileira de Educao Fsica e Esporte*. 2007;**21**(1):5-10. DOI: 10.1590/S1807-55092007000100001

Role of Cytotoxicity Experiments in Pharmaceutical Development

Ildikó Bácskay, Dániel Nemes, Ferenc Fenyvesi,
Judit Váradi, Gábor Vasvári, Pálma Fehér,
Miklós Vecsernyés and Zoltán Ujhelyi

Additional information is available at the end of the chapter

<http://dx.doi.org/10.5772/intechopen.72539>

Abstract

Through the twentieth century, the road from synthesizing a new drug molecule to become an actual product got longer than ever before. Cytotoxicity assays are a quick way to assess a certain chemical compound's effects on a given human cell line. The most well-known techniques are the MTT- and the LDH-assays. These tests are cheap, easy to execute, but not very precise and dependent on various environmental factors and also, they show no detail about the time-dependency of the toxic effect. Cytotoxicity experiments are a crucial part of a modern pharmaceutical development process. They are a cheap and safe way to get vital information about a new molecule's biological attributes focusing on its basic tolerability. These studies not only save human lives and test animals, but they save the time and resources to be spared on a test molecule which is a complete failure having no *in vitro* safety.

Keywords: cytotoxicity, pharmaceutical development, preformulation, cell cultures, *in vitro* toxicity

1. Role of cytotoxicity tests in the pharmaceutical development

Pharmaceutical safety is essential factor in the development of every medicament [1]. The early stage of the formulation development must include wide toxicity screening of the applied components; not exclusively the API, but all the incorporated excipients as well. When a formulation of a new chemical with interesting biological properties enters this process, it will undergo extensive testing designed to address and solve many complex issues [2]. However, the pharmaceutical effectiveness is essential, but might seem as an insufficient factor of a

successful medication [3]. The formulated delivery system must support the administration of the API to improve patient compliance [4]. Moreover excipients are able to enhance the API's effectiveness in many cases [5]. Besides their role in solubility or stability issues many excipients are used as penetration enhancers, since their effect on biological membranes [6]. It has been concluded that this advantageous property of excipients must be considered before the formulation but toxicity aspect shows great impact as well [7]. To optimize the procedure cost of this part of preclinical phase, simple but reliable methods must be performed [8]. Traditional drug toxicity tests are great possibilities for the pharmaceutical developers, not only because of the associated loss of human life or health, but also because of immense financial loss of investment [9]. Early application of appropriate cell-based assays in drug development offers the single-most impactful solution to the challenge of human toxicity [10]. *In vitro* cell line models for evaluating toxicity should predict human specific toxicity. This may be due in part to the success that *in vitro* screening for certain absorption, distribution, metabolism, and elimination (ADME) endpoints has seen over the past 10 years. *In vitro* systems designed to evaluate permeability, interaction with membrane transporter systems, and metabolic stability in cell models with human relevance reduced this failure rate to less than 10% [11]. To ensure success in toxicology evaluation methods, comprehensive and tiered screening methods must be employed. To avoid adverse results or conclusions, potential liabilities and limitations of the experiments must be investigated [12]. It is unlikely that a single *in vitro* viability test or cell line model would be sufficient as a final decision point for toxicity [13]. In a well-built toxicity screening procedure, different test types on different cell cultures must be performed.

In tiered approach, *in vitro* toxicity screening models are based on the cell viability alteration of different human cell lines. These determinations must be well characterized and predictive of *in vivo* effects with a low incidence of false positive or negative results. The methods must have the capacity to evaluate various molecules in a short period of time with a minimum amount of compound. The results should provide information on potential mechanisms of toxicity, and subcellular targets as well. These results might ensure useful data for the inventors to modify structures of API or alter the amount or types of excipients that are applied in the delivery system development. The modified compositions can be re-screened for toxicity without large cost. The first decisive step is the cell line selection. According to the desired administration route, developers are able to select the most appropriate cell cultures for the *in vitro* assessments [7]. Nowadays, a wide range of different immortalized or primary cell and tissue models are available from safe sources for *in vitro* toxicity evaluation. However a well selected cell type ensures valuable information about the developed dosage form, the investigators often faced difficulties; since the main strengths and weakness of the models must be considered wisely. Routine toxicity screening procedures require a robust cell culture model that can be maintained easily in flasks and 96-well culture plates or inserts. The cells must be genetically stable and provide reproducible results in each assessment. The cells should be well characterized in terms of their doubling time, optimal growth conditions, and biochemistry. Various human cell lines are used routinely to evaluate toxicity. For example, Caco-2, HaCaT, CaLu, HeLa, 3 T3, HEK293, and many more. During the cell line selection process, it is important to totally characterize the morphology and understand the relevant biochemistry of the cells. These data are required to understand the background of potential mechanisms of toxicity [14]. *In vitro* cytotoxicity assays offer special and early identification of potential

cytotoxicity of compounds, the property that might lead to irritancy during the application. *In vitro* toxicity tests are found to be advantageous in preclinical studies because of their eligibility, cost effectiveness, and reproducibility. Cell viability assays are developed to measure activities attributable to cellular maintenance and survival. Beside metabolic biomarkers, such as mitochondrial reductase, ATP reductase etc., homeostatic enzyme activities can be monitored as well [15]. During these measurements, various compounds can be routinely investigated with a relatively short incubation. In case of cytotoxicity assays, the test focuses on to detect loss of membrane integrity associated with cell death [16].

Lactate dehydrogenase (LDH) is one of the most preferred marker for cell death. LDH assay is a robust and most cost-effective method for cell cytotoxicity measurements. Real time cell condition monitoring is a relatively new possibility in toxicity screening. During these evaluation methods, a special instrument measures impedance-based signals in both cellular and cell invasion assays without any exogenous label use [17]. These systems are able to detect cell responses continuously and non-invasively without disrupting the natural cell environment. Moreover, not exclusively cell-mediated cytotoxicity and cell adhesion assays, but even receptor-mediated signaling and virus-mediated cytopathogenicity tests can be performed [18]. These experiments allow more flexibility, quick results, and illustrious precision although relatively high expenses must be considered during the experimental design. High variety of assays provide an excellent possibility in ranking compounds for consideration in drug discovery. As it was shown, the highest expenses of pharmaceutical development occur in the preclinical and clinical studies. By the application of these *in vitro* tests, the inventors are able to reduce risk significantly. Assays, performed on cell culture models, are able to unequivocally support the process of drug development by perfecting efficiency and improving the probability of success.

2. Use of cytotoxicity tests

2.1. Application of cytotoxicity tests

Nowadays the development of a new drug molecule costs around 1 billion dollars and out of 10,000–30,000 possible candidates, only 1 will find its way to the drug market [19]. This means that the number of companies, which have actual financial background for such a research, is decreasing and the whole process of drug development is slowing down. This is the consequence of ICH's GCP protocol, which in one hand, not only created a worldwide secure standard for clinical trials of new drug molecules, but also radically increased the expenses. On the other hand, non-drug related medical researches, such as medical devices (insulin pumps, implants, etc.), also appeared on the market and the requirements of GCP was too complicated and usually unnecessary.

Such circumstances lead to the increased popularity and development of cell culture model systems. Cell lines are a cheap way to investigate the effect of any questioned molecule or device on a given cell type. They can primarily be purchased from cell banks such as European Collection of Authenticated Cell Cultures (ECACC) and the American Type Culture Collection (ATCC). Cell lines can either be primary as they are directly isolated from a tissue or organ. Their structure, protein expression patterns, metabolism, and genetical code are identical with

the *in vivo* cells. Also, they are very sensitive to any effect during cultivation and they have a determined lifespan, meaning that they can only endure a limited number of passages. Secondary cell lines are immortalized by some method, which means that they have a hypothetically infinite lifespan. However, we can say from our own experience that for example Caco-2 cells are best suited for transport experiments (where they have to create a monolayer on an insert) between the 20th and the 30th passages. After 50 passages, the cells are hardly able to reproduce their own number, thus, they are no longer sufficient for cell viability tests.

Also, it is crucial to choose the right cell line for the given experiment. If the question is the biocompatibility of a chemical compound, which is about to be used on humans, then a human cell line must be chosen for the given experiment and even, an appropriate organ should be selected. A good summarizing table was created by Amelian et al. [20] (**Table 1**).

As it can be seen, there are multiple available cell lines with the same origin. The selection and the test system must be based on the later application of the device/compound, as each cell line has a different medium requirement and cultivation method as they can act differently in cell viability tests.

Also, because anti-proliferative drugs main attribute is their cytotoxicity, the following methods are ideal for testing these substances on cell lines. Because the secondary, immortalized cells can be seen as cancer cells (because their apoptotic or growth stop signals are suppressed by mutations), they are capable to react to certain promising anti-cancer molecules like their *in vivo* counterparts.

2.2. Advantages of cytotoxicity tests

As scientific and medical studies are getting more expensive over the recent decades, most of the universities, research institutes are underfinanced, the importance of a certain method's price is greater than ever before. Animal experiments are expensive and the administrative burden is overwhelming, so they are only used when no other test is suitable. Also, every year new plants and their respective metabolites are described and through the various methods of

Cell line	Origin	Application
HeLa, A431	Epithelial cervical cancer	Very rapid growth, cells commonly used in cancer research
Caco-2, HT29, HCT-116	Colon adenocarcinoma	Studies of absorption <i>via</i> intestinal epithelium, toxicity tests
U2OS	Osteosarcoma cells	Studies of transport and absorption of drugs
SkBr3, MCF-7, MDA-MB231, ZR-75-1	Breast cancer	Studies of transport and absorption of drugs, screening anticancer compounds
Calu-3	Serous cells of submucosal gland	Studies of absorption <i>via</i> bronchial epithelium, metabolic and transport model to study drug delivery to the respiratory epithelium
HaCaT	Adult human skin	Penetration of drug through the skin
16HBE140	Bronchial epithelium	Studies of absorption and excretion through the bronchial epithelium

Table 1. Most common cell lines used in cytotoxicity studies [20].

chemistry, new molecules are synthesized, and even an older compound might be re-evaluated for a new indication. Secondary cell lines are ideal for the screening of the enormous amount of test subjects. If the right cell line is chosen, not just the cytotoxicity, but the biological activity of the chosen material can be measured. In short time, multiple experiments can be carried out, with high reproducibility in the same test system. If we use more than one method, with different signaling mechanisms and different cell lines, we will have a more complex view on the *in vitro* toxicity data. This means more information when planning the *in vivo* experiments. Generally, it can be said, that if a compound proves to be non-toxic, then *in vivo* it will be tolerable. If it is moderately toxic, there is a chance that the 3D structure and the different cell types of an organ or the human body can effectively recover from the cytotoxic damage or the damage will only be minimal.

2.3. Disadvantages of cytotoxicity tests

The results of the cytotoxicity tests require additional consideration. They—even if the right cell lines were used—are not an automatic green light for *in vivo* application. If a given chemical proves to be non-toxic, it only means that we do not necessarily have to start our next experiment in an animal with the smallest dosage, but from a medium or a high concentration, to determine the maximum single dose, maximum daily dose and the LD50 value. Also, if we do not use the appropriate cell line—like testing an ointment preservative on enterocytes—then the scientific value of our study will be questioned. The cytotoxicity tests usually end up in a specific IC50 value. These values usually cannot be compared, because these tests are highly dependent on the parameters of the test system. Such parameters can be: cell line, passage number of the cells, number of cells/well, volume of medium/well, growth time of a plate, concentration/volume of reagent, manufacturer of the reagent, length of incubation, reaction time, solubilization solution (if needed) even the performance of the spectrophotometer. We suggest that instead of using static IC50 values, trends, comparisons should be seen. Stating that compound A has an IC50 value of 0.5 mg/ml and B has 0.25 mg/ml should be changed that A is about twice as tolerable, than B. This fact does not decrease the significance of the cytotoxicity tests, but prevents to deny of a scientifically accurate study, because the written IC50 value cannot be reproduced. Another issue is that a specific compound can interact with the reagents or the mechanism of the method, thus a false positive or negative result can be detected. Such interaction can only be found if we use more than one method or in the scientific literature. If we only use one type of cytotoxicity test, the scientific value will be low and the chance of detecting false results will be high. This is not necessarily caused by a specific interaction, but because of the given test system, the whole method will over- or underestimate cytotoxicity. Thus, it is advisable to use different types of tests, so link MTT with LDH or RT-CES, but not with XTT, because they are both tetrazolium based assays and have the same limitations.

3. Description of different cytotoxicity tests

The cellular damage caused by different chemical compounds can be various and thus, the methods to measure this effect are numerous. To select the proper test, we must know: number

of treated cells, number of treatments, what kind of treatment the cells got, do we need these cells later, or the chosen method can terminate them? Also, do we want to know the kinetics of the post-treatment population's changes or simply what happens with the cells after a short incubation with the selected chemical? The price, the reliability, the user-friendliness of the kit is an important question too. The mechanism of cytotoxicity can be various so a single method only gives a simple view on a chosen material. Multiple tests and methods must be used before anyone can make a solid point about the biocompatibility of a chemical compound. Also, it must be noted, that a compound can interfere with the detection mechanism of a certain assay, resulting in a false positive or negative result; thus, multiple methods are needed to avoid such cases.

3.1. Assays

Cell viability assays are usually cheap, easy-to-perform methods, where after a given incubation with the selected chemical compound, the number of the surviving cells is measured by some method. They use no antibodies or radioactive chemicals. Usually, these assays are carried out on 96- or 384-well plates, making them ideal for screening experiments. It must be noted, that in some special cases, multiple measurements can be made, but these methods are not suited for long-term, kinetical or time-dependent killing studies. We must be aware of the fact, that most methods use some kind of "signal molecule" which—in normal cases—is directly proportional with the number of cells. If there is an uncontrolled factor that increases or decreases the strength of the signal, we can get false positive or false negative results. Such factor is usually increased uptake into the cell or increased activity of the specific enzyme, responsible for the creation of the signaling molecule. Usually not a single enzyme, but multiple proteins catalyze the reaction, so the overall metabolic state of the cell must be considered. It can be said that additional filters for background measuring can greatly increase the sensitivity. Nearly all eukaryotic cells can perform these biochemical reactions, but previous research can avoid incompatibility with certain cell lines. In the following table, the most well-known cell viability assays are listed. Prices are approximating, and they mean the price of 1000 tests of the kit, according to the manufacturer (**Table 2**).

Name	Mechanism	How to detect	Price (€)
XTT	Enzymatic activity	Spectrophotometer	235
MTT	Enzymatic activity	Spectrophotometer	129
WST-1	Enzymatic activity	Spectrophotometer	235
WST-8	Enzymatic activity	Spectrophotometer	420
MTS	Enzymatic activity	Spectrophotometer	172
LDH	Enzymatic activity	Spectrophotometer	315
Resazurin	Enzymatic activity	Spectrofluorometer	110
Neutral Red	Lysosomal uptake	Spectrophotometer	339

Table 2. Most common cytotoxicity assay methods.

MTT assay is a cheap, popular way, to measure cell death [21]. The reduction of the tetrazolium structure in the MTT dye 3-(4,5-dimethylthiazol-2-yl)-2,5-diphenyltetrazolium bromide leads to a colored formazan product—this is the basic chemical reaction in every tetrazolium based assay. The MTT dye has a positive charge, thus it is taken up by the cells and intracellular oxidoreductases catalyze the mentioned reaction. The oxidative state of the cell and the mitochondrial respiratory chain are essential in the conversion. Basically, the concentration of NADH limits the process and any chemical compound that modifies the oxidative potential of the cell can possibly decrease or increase the signal of the assay [22]. If this effect is not linked with direct cytotoxic activity, then, it may lead to a false positive or negative result. Various reports have already indicated that certain test compounds have radically different results in tetrazolium assay, than in other methods because of the possible antioxidant capabilities [23]. The reaction starts immediately, but 1–4 h should pass before measuring the absorbance of the test system—the exact time must be setup according to the parameters of the current test system. A too short amount of time might result in low signal strength; a too long may mask the difference between different treatments/concentrations. Various organic solvents might be used to dissolve final product, the insoluble, purple formazan crystals, but we suppose an isopropanol:hydrochloride acid (25:1) solution, because it is safe and cheap to use. The acidification of the system is required, to reduce the amount of the original yellow dye, thus, give us a stronger main signal. The absorbance must be measured at 570 nm (Figures 1 and 2).

XTT, MTS, WST-1, and WST-8 assays are the improved versions of the old MTT. The final product of the reaction is soluble in water/cell culture medium; yet, the solubility of the original dye is greatly reduced, they must be used at 1–2 mg/ml concentrations instead of the 0.2–0.5 mg/ml of the original MTT dye [24]. The XTT and the WST-1/8 compounds have a negative charge, so they cannot penetrate the cell membrane; their reduction takes place in the extracellular space [22]. To enhance the effectiveness of transmembrane oxidoreductases, an

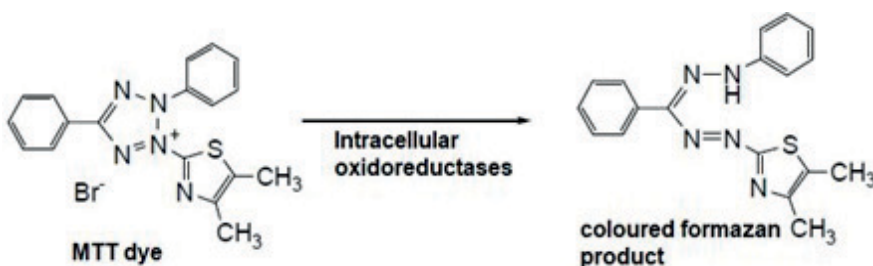


Figure 1. MTT dye reaction, the tetrazolium ring opens as a result of the reduction.

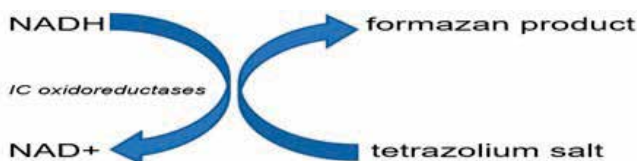


Figure 2. Simplified mechanisms of MTT and MTS assays.

intermediate electron acceptor (IEA in figure) is required, which gets reduced by NADH and intensifies the final signal of the assay. The specific IEA (such as phenazine ethyl sulfate) is usually part of the assay kits and its concentration must be determined according to the given test system. The MTS is at least partially reduced in the intracellular compartment, thus an IEA is not essentially needed [22]. Because, the final formazan product is soluble in water, the solubilization step is unnecessary; these assays are more flexible to combine with additional methods and easier to carry out (Figures 3 and 4).

Resazurin assay (or Alamar Blue) is based on the enzymatic conversion of the cell permeable blue resazurin to the pink resorufin [25]. Both chemicals are soluble in water and the assay provides higher sensitivity than the previous methods, because the detection is based on fluorescence, not spectrophotometry. Also, it must be noted that the reagent is toxic, so the appropriate reaction time must be based on the sensitivity of the given cell line so the toxicity of the reagent can be distinguished from the tested chemical. The fluorescence should be measured with 560 nm excitation/590 nm emission filters. Also, it can be combined with other techniques such as caspase activity assay because of the different detection method and the non-interference of the respective mechanisms [26] (Figure 5).

LDH assay is based on the activity of a cytoplasmic enzyme, the lactate dehydrogenase which reduces the NAD to NADH. NADH then reduces a tetrazolium dye (or other reagent) whose concentration can be measured spectrophotometrically [27]. The assay is mainly used for the detection of membrane leakage which correlates with the cell damage. The most common reagent is the 2-p-iodophenyl-3-p-nitrophenyl tetrazolium chloride (INT) which forms a red formazan product. The LDH is quite stable for the duration of the assay in the extracellular space and its amount is dependent on the cell size and oxidative activity, but similar among the cells of the same cell line. It is excellent when compared with other tetrazolium based methods because it can measure the damaged cells as well, not just the dead ones. Also in special cases, it can be used to detect the intracellular LDH concentration. A limitation of this method is that serum has a high LDH activity on its own, so serum-supplemented mediums are not ideal for

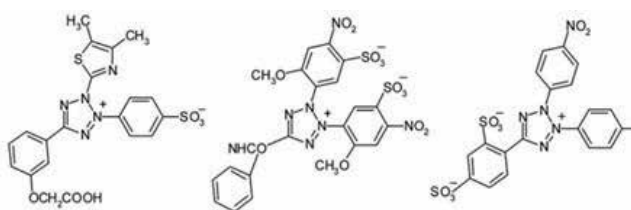


Figure 3. Chemical formulae of the new generation tetrazolium assays from left to right: MTS, XTT, and WST-1/8.

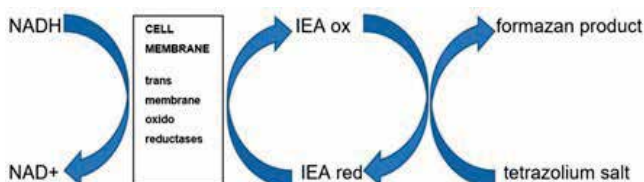


Figure 4. Simplified mechanism of the XTT and WST-1/8 assay.

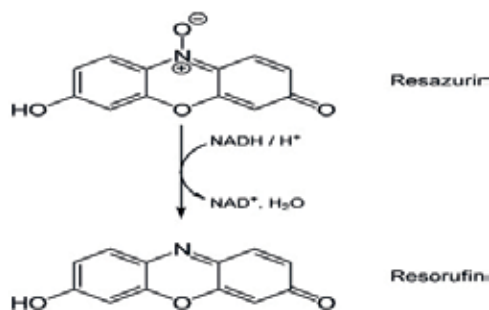


Figure 5. Mechanism of the Resazurin assay.

the LDH assay or multiple wash steps are needed before applying the assay reagent on the cells. Another problem is that if the cells are dead (or growth is inhibited), but the specific cytotoxic chemical does not distort the cell membrane, then the actual number of dead cells is underestimated. A solution of it can be the usage of control compounds which have a similar way-of-killing, than the tested chemical [28] (**Figure 6**).

Neutral red assay is not based on a directly enzymatic biochemical reaction, but the dye is taken up by the cells and it stains the lysosomes of the cells [29]. A weak cationic compound, the neutral red is taken up by micropinocytosis or by non-ionic diffusion and is accumulated into the lysosomes [30]. After the cytotoxic treatment with the possibly cytotoxic chemical, the cells should be washed, then the staining solution must should be added to the test system. After an appropriate time of incubation, the dye must be removed and the cells are washed again. The incubation with a solubilization solution forces the cells to excrete the neutral red dye and thus, the concentration of it can be measured at 540 nm. As damaged cells can only take up and store neutral red at a decreased rate and dead cells are not stained at all, it is a sensitive assay, but, the cells are washed, disturbed multiple times which—if not carried out smoothly enough—can decrease the cell number, destroy the monolayer or other kind of collateral damage can happen to the cells (**Figure 7**).

3.2. RT-CES

The simple cytotoxicity assays are limited in case of kinetical or time-dependent killing experiments. Simply, multiple measurements cannot be executed, because the test system is disturbed, some xenobiotics (tetrazolium dyes, other cofactors, etc.) are added to the cells or in case of some methods, the cells are solubilized. The reagents used in the assays can be directly

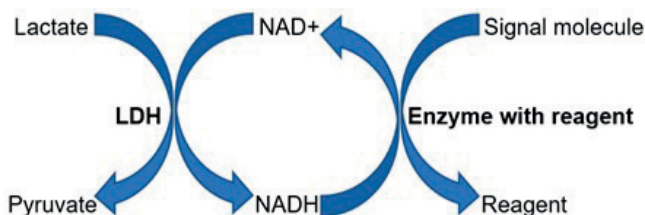


Figure 6. Mechanism of LDH membrane leakage assay.

cytotoxic or at least they modify the cells biochemical equilibrium and activity in a way that the results are no longer relevant for the latter *in vivo* experiments. This means that after a certain treatment with the probably cytotoxic compound, we can only make an end-point measurement because the test system is irreversibly changed after the addition of the given signaling molecule(s). Also, if the tested chemical can absorb light or is capable of fluorescence, it can interfere with the detection system. Because of these limitations the need for a non-invasive, yet precise method resulted in the invention of real-time cell electronic sensor.

This technique is based on the impedance changes of the cell populations [31]. The cells are seeded into special E-plates, which are available in multiple size (4-, 8-, 16-, 96-wells, etc.). These special devices have a positive and a negative electrode in every well, and a low voltage alternate current flows through the well. As the cells grow, they have a higher impedance (resistance in AC circuits); and as they die, the impedance value lowers. This effect has literally no impact on the cells, so it is a non-invasive technique. The length of the experiment is theoretically unlimited, as there is no end-point of AC current flow. For this reason, the cell growth can be measured during multiple treatments of the cells, and not just the cytotoxic or non-toxic effects, but the possible recovery of the cells can be studied as well. It is important, that first, a part of the cell medium and the solution of the screened chemical must be placed into the wells of the E-plate, thus the connected software can detect it as a background, with zero impedance, so chemicals with ionic charges do not interfere with the measured signal. The cells should be added to the wells after the background detection in a high-density suspension. Also, the whole experiment can be stopped at any point, to remove the test solution or to add a new compound to test system (**Figure 8**).

However, this system is ideal for cell viability studies, it has some disadvantages as well. The devices and the E-plates have a high price and a limited number of slots to use. The E-plates can be used multiple times after a specific cleaning protocol, but the sensitive, microelectronic sensing arrays are easily damaged by washing and organic solvents. This means, that it is not suited for high performance screening experiments, because multiple assays can be done during the same amount of time.

3.3. Other methods

Sulforhodamin B is a dye which stains the total protein amount of the cells [33]. The reagent is an aminoxanthene dye which binds stoichiometrically with the amino-acids under acidic pH. First, the cells must be fixed with trichloroacetic acid, then washed and dried and the wells respective optical density measured for background detection. The sulforhodamin B must be added after this, and it should stain the cells for 20–30 min. After a wash step, the stained cells must be solubilized and the absorbance measured at 565 nm. The protocol is quite long and

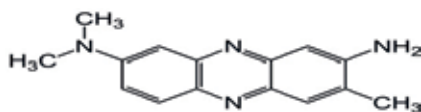


Figure 7. Neutral red dye.

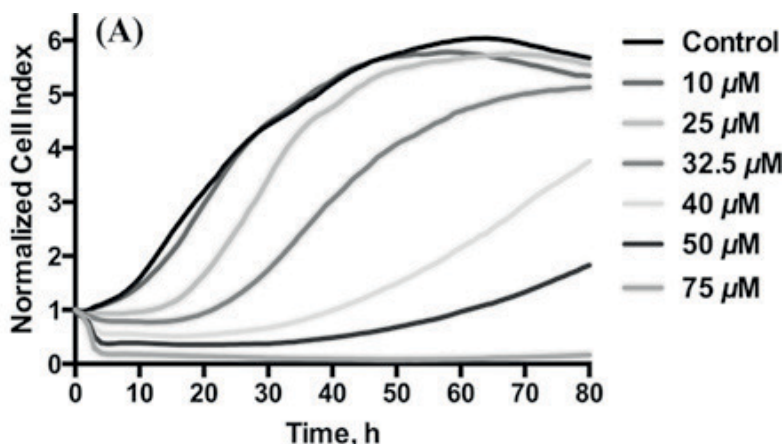


Figure 8. A typical RT-CES diagram showing a time and dose dependent cytotoxicity of 2,6-dichloro-(1,4)-benzoquinone [32].

requires an experienced crew to execute perfectly. Also, the total protein only works, if the cells grew in the presence of the cytotoxic chemical, otherwise, the dead cells cannot be distinguished from the viable ones. However, there are several studies indicating that the sulforhodamin B results correlate well with the MTT results [34]. A slight advantage of this method is that because of the multiple wash steps, the tested chemicals can hardly interact with the dye, unlike other enzyme-based methods. The optimization with the specific cell line is also much easier because the lack of dependence on metabolic activity (**Figure 9**).

Calcein-AM/Hoechst 33342 and propidium iodide are dyes that stain viable and dead cells [35]. In appropriate concentration, Calcein-AM, a lipophilic derivative of calcein is capable pass through cell membranes and stains the cell, as intracellular enzymes cleave the lipophilic carbon chain from the dye [36]. Hoechst 33342 binds the A-T rich regions of the DNA. Propidium iodide stains the nucleus of the cell, but cannot penetrate the cell membrane, thus it only binds to the dead cells. As the two reagents can be detected at different wavelengths, multiple emission and excitation filters are needed. Also, every cell line has a different binding rate and the ideal concentration must be found through testing, as the cytosol of the cells can be stained by each dye and instead of spectrophotometric detection, manual counting is needed with a microscope with the specific filters/lamps (**Figure 10**).

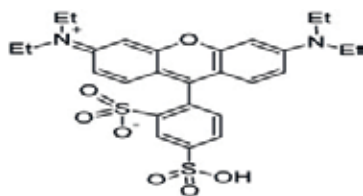


Figure 9. Sulforhodamin B.

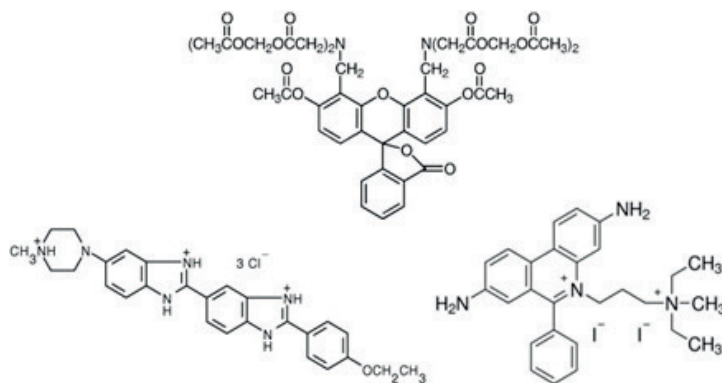


Figure 10. Chemical formula of the Calcein-AM (upper image), Hoechst 33342 (left image) and the propidium iodide (right image).

3.4. Comparison between *in vitro* cytotoxicity data and *in vivo* data

As the whole, medical science and industry is based on the modification, repair of damaged or badly functioning cells and tissues in human or animal body, the correlation between *in vitro* and *in vivo* data is crucial. Do these artificial test systems, cell lines truly replicate how a real tissue would react to a certain treatment or compound? The answer is based on the application of multiple *in vitro* methods and the careful planning of the *in vivo* experiments. A good example of the practice is the study of Yu et al. [37]. *Xanthii fructus* is a traditional Chinese herbal drug and clinical reports indicated its renal toxicity. The study was based on MTT and LDH assays of the main components of the herbal drug on a renal cell line, as well as acute and chronic toxicity experiments in rats. While the main component of the drug, the atractyloside potassium salt showed no cytotoxicity on the cell lines, the water extract of the fruit had an inhibitory effect in case of high concentrations on the MTT assay, but no membrane damage on the LDH assay. These results indicate that the secondary components of the water extract have cytotoxic capabilities and the exact mechanism of killing might involve the suppressed metabolic activity of the cells, but not the damage of the cell membrane. The acute *in vivo* toxicity showed that only high concentrations could terminate the rats and cause abnormalities in the organs and the chronic toxicity showed only minor changes in the highest concentration group. Overall, this complex study created a much more accurate, scientific point of view about the toxicity of *Xanthii fructus*, what chemicals are responsible for its toxicity, what are the exact dosages, and what are the side effects that are caused by the herbal drug. It could only be made by the co-application of various *in vivo* and *in vitro* methods.

4. Conclusion

The importance of cytotoxicity assays in early drug development is unquestionable although it must be concluded that no assay technology for detecting cytotoxicity *in vitro* is perfect. Strong arguments can be made for and against using cell viability or cytotoxicity assays as a reliable model of human medication. Depending upon the objectives of the investigation, either

viability or cytotoxicity assays can be performed. Cytotoxicity assays based on membrane integrity changes are positive-readout assay which are most typically indicated for shorter-term exposure models (48 h or less). These assays may not properly determine the absolute degree of early or late stage cytotoxicity since the kinetics of biomarker emergence or degradation. Viability assays measure the level of biomarker activity inversely correlated with cytotoxicity, and therefore may be used at any endpoint during a compound/cell incubation period. Each biomarker of viability and cytotoxicity has advantages and disadvantages. Moreover in early drug discovery, *in vitro* evaluations of new drug candidates is often met with skepticism since their reliability and *in vivo* correlatability. It can be concluded that however there is some validity to this argument, it is important to put *in vitro* toxicity data into consideration during pharmaceutical development.

Author details

Ildikó Bácskay*, Dániel Nemes, Ferenc Fenyvesi, Judit Váradi, Gábor Vasvári, Pálma Fehér, Miklós Vecsernyés and Zoltán Ujhelyi

*Address all correspondence to: bacsokay.ildiko@pharm.unideb.hu

Department of Pharmaceutical Technology, Faculty of Pharmacy, University of Debrecen, Debrecen, Hungary

References

- [1] Horvath S. Cytotoxicity of drugs and diverse chemical agents to cell cultures. *Toxicology*. 1980;**16**:59-66
- [2] Diaz D, O'Brien PJ. Defining the sequence of events in cerivastatin toxicity using a high content multi-parametric cytotoxicity assay. *European Pharmaceutical Review*. 2006;**11**:38-45
- [3] Bolt M, Card J, Racz W, et al. Disruption of mitochondrial function and cellular ATP levels by amiodarone and N-desethylamiodarone in initiation of amiodarone-induced pulmonary cytotoxicity. *The Journal of Pharmacology and Experimental Therapeutics*. 2001;**298**:1280-1289
- [4] Buxser S, Vroegop S. Calculating the probability of detection for inhibitors in enzymatic or binding reactions in high throughput screening. *Analytical Biochemistry*. 2005;**340**:1-13. DOI: 10.1016/j.ab.2005.01.034
- [5] Ujhelyi J, Ujhelyi Z, Szalai A, Laszlo JF, Cayasso M, Vecsernyes M, Porszasz R. Analgesic and anti-inflammatory effectiveness of sitagliptin and vildagliptin in mice. *Regulatory Peptides*. 2014;**194-195**:23-29. DOI: 10.1016/j.regpep.2014.09.006
- [6] Xia M, Huang R, Witt K, et al. Compound cytotoxicity profiling using quantitative high-throughput screening. *Environmental Health Perspectives*. 2008;**116**:284-291. DOI: 10.1289/ehp.10727

- [7] Van Outryve S, Schrijvers D, van den Brande J, Wilmes P, Bogers J, van Marck E, Vermorken JB. Methotrexate associated liver toxicity in a patient with breast cancer: Case report and literature review. *The Netherlands Journal of Medicine*. 2002;**60**:216-222
- [8] Pohjala L, Tammela P, Samanta SK, Yli-Kauhaluoma J, Vuorela P. Assessing the data quality in predictive toxicology using a panel of cell lines and cytotoxicity assays. *Analytical Biochemistry*. 2007;**362**:221-228. DOI: 10.1016/j.ab.2006.12.038
- [9] Segall MD, Barber C. Addressing toxicity risk when designing and selecting compounds in early drug discovery. *Drug Discovery Today*. 2014;**19**:688-693. DOI: 10.1016/j.drudis.2014.01.006
- [10] O'Brien PJ, Irwin W, Diaz D, Howard-Cofield E, Krejsa CM, Slaughter MR, et al. High concordance of drug-induced human hepatotoxicity with *in vitro* cytotoxicity measured in a novel cell based model using high content screening. *Archives of Toxicology*. 2006;**80**:580-604. DOI: 10.1007/s00204-006-0091-3
- [11] Olson H, Betton G, Robinson D, Thomas K, Monro A, Kolaja G, et al. Concordance of the toxicity of pharmaceuticals in humans and in animals. *Regulatory Toxicology and Pharmacology*. 2000;**32**:56-67. DOI: 10.1006/rtph.2000.1399
- [12] Ujhelyi Z, Fenyvesi F, Váradi J, Fehér P, Kiss T, Veszelka S, Deli MA, Vecsernyés M, Bácskay: Evaluation of cytotoxicity of surfactants used in self-micro emulsifying drug delivery systems and their effects on paracellular transport in Caco-2 cell monolayer. *European Journal of Pharmaceutical Sciences*. 2012;**47**:564-573. DOI: 10.1016/j.ejps.2012.07.005
- [13] Róka E, Ujhelyi Z, Deli M, Bocsik A, Fenyvesi É, Sente L, Fenyvesi F, Vecsernyés M, Váradi J, Fehér P, Gesztelyi R, Félix C, Perret F, Bácskay IK. Evaluation of the cytotoxicity of α -cyclodextrin derivatives on Caco-2 cell line and human erythrocytes. *Molecules*. 2015;**20**:20269-20285. DOI: 10.3390/molecules201119694
- [14] Wienkers LC, Heath TG. Predicting *in vivo* drug interactions from *in vitro* drug discovery data. *Nature Reviews. Drug Discovery*. 2005;**4**:825-833. DOI: 10.1038/nrd1851
- [15] Dykens JA, Will Y. The significance of mitochondrial toxicity testing in drug development. *Drug Discovery Today*. 2007;**12**:777-785. DOI: 10.1016/j.drudis.2007.07.013
- [16] Gonzalez R, Tarloff J. Evaluation of hepatic subcellular fractions for Alamar blue and MTT reductase activity. *Toxicology In Vitro*. 2001;**15**:257-259. DOI: 10.1016/S0887-2333(01)00014-5
- [17] Ito K, Hallifax D, Obach RS, Houston JB. Impact of parallel pathways of drug elimination and multiple cytochrome P450 involvement on drug-drug interactions: CYP2D6 paradigm. *Drug Metabolism and Disposition*. 2005;**33**:837-844. DOI: 10.1124/dmd.105.003715
- [18] Machala M, Blaha L, Lehmler HJ, Pliskova M, Májková Z, Kapplová P, Sovadinová I, Vondráček J, Malmberg T, Robertson LW. Toxicity of hydroxylated and quinoid PCB metabolites: Inhibition of gap junctional intercellular communication and activation of aryl hydrocarbon and estrogen receptors in hepatic and mammary cells. *Chemical Research in Toxicology*. 2004;**17**:340-347. DOI: 10.1021/tx030034v

- [19] Veljkovic V, Veljkovic N, Este JA, Huther A, Dietrich U. Application of the EIIP/ISM bioinformatics concept in development of new drugs. *Current Medicinal Chemistry*. 2007;**14**:441-453. DOI: 10.2174/092986707779941014
- [20] Amelian A, Wasilewska K, Megias D, Winnicka K. Application of standard cell cultures and 3D *in vitro* tissue models as an effective tool in drug design and development. *Pharmacological Reports*. 2017;**69**:861-870. DOI: 10.1016/j.pharep.2017.03.014
- [21] Mosmann T. Rapid colorimetric assay for cellular growth and survival: Application to proliferation and cytotoxic assays. *Journal of Immunological Methods*. 1983;**65**:55-63
- [22] Berridge MV, Herst PM, An ST. Tetrazolium dyes as tools in cell biology: New insights into their cellular reduction. *Biotechnology Annual Review*. 2005;**11**:127-152. DOI: 10.1016/S1387-2656(05)11004-7
- [23] Wang P, Henning SM, Heber D. Limitations of MTT and MTS-based assays for measurement of antiproliferative activity of green tea polyphenols. *PLoS One*. 2010;**5**:e10202. DOI: 10.1371/journal.pone.0010202
- [24] Scudiero DA, Shoemaker RH, Paull KD, Monks A, Tierney S, Nofziger TH, Currens MJ, Seniff D, Boyd MR. Evaluation of a soluble tetrazolium/formazan assay for cell growth and drug sensitivity in culture using human and other tumor cell lines. *Cancer Research*. 1988;**48**:4827-4833
- [25] Ahmed SA, Gogal RM Jr, Walsh JE. A new rapid and simple non-radioactive assay to monitor and determine the proliferation of lymphocytes: An alternative to [3H]thymidine incorporation assay. *Journal of Immunological Methods*. 1994;**170**:211-224. DOI: 10.1016/0022-1759(94)90396-4
- [26] Wesierska-Gadek J, Gueorguieva M, Ranftler C, Zerza-Schnitzhofer G. A new multiplex assay allowing simultaneous detection of the inhibition of cell proliferation and induction of cell death. *Journal of Cellular Biochemistry*. 2005;**96**:1-7. DOI: 10.1002/jcb.20531
- [27] Allen M, Millett P, Dawes E, Rushton N. Lactate dehydrogenase activity as a rapid and sensitive test for the quantification of cell numbers *in vitro*. *Clinical Materials*. 1994;**16**:189-194. DOI: 10.1016/0267-6605(94)90116-3
- [28] Smith SM, Wunder MB, Norris DA, Shellman YG. A simple protocol for using a LDH-based cytotoxicity assay to assess the effects of death and growth inhibition at the same time. *PLoS One*. 2011;**6**:e26908. DOI: 10.1371/journal.pone.0026908
- [29] Cavanaugh PF Jr, Moskwa PS, Donish WH, Pera PJ, Richardson D, Andrese AP. A semi-automated neutral red based chemosensitivity assay for drug screening. *Investigational New Drugs*. 1990;**8**:347-354. DOI: 10.1007/BF00198590
- [30] Zhang SZ, Lipsky MM, Trump BF, Hsu IC. Neutral red (NR) assay for cell viability and xenobiotic-induced cytotoxicity in primary cultures of human and rat hepatocytes. *Cell Biology and Toxicology*. 1990;**6**:219-234. DOI: 10.1007/BF00249595

- [31] Solly K, Wang X, Xu X, Strulovici B, Zheng W. Application of real-time cell electronic sensing (RT-CES) technology to cell-based assays. *Assay and Drug Development Technologies*. 2004;**2**:363-372. DOI: 10.1089/adt.2004.2.363
- [32] Wang W, Qian Y, Li J, Moe B, Huang R, Zhang H, Hrudey SE, Li XF. Analytical and toxicity characterization of halo-hydroxyl-benzoquinones as stable halobenzoquinone disinfection byproducts in treated water. *Analytical Chemistry*. 2014;**86**:4982-4988. DOI: 10.1021/ac5007238
- [33] Vichai V, Kirtikara K. Sulforhodamine B colorimetric assay for cytotoxicity screening. *Nature Protocols*. 2006;**1**:1112-1116. DOI: 10.1038/nprot.2006.179
- [34] Haselsberger K, Peterson DC, Thomas DG, Darling JL. Assay of anticancer drugs in tissue culture: Comparison of a tetrazolium-based assay and a protein binding dye assay in short-term cultures derived from human malignant glioma. *Anti-Cancer Drugs*. 1996;**7**:331-338
- [35] Ciancio G, Pollack A, Taupier MA, Block NL, Irvin GL 3rd. Measurement of cell-cycle phase-specific cell death using Hoechst 33342 and propidium iodide: Preservation by ethanol fixation. *The Journal of Histochemistry and Cytochemistry*. 1988;**36**:1147-1152. DOI: 10.1177/36.9.2457047
- [36] Tenopoulou M, Kurz T, Doulias PT, Galaris D, Brunk UT. Does the calcein-AM method assay the total cellular 'labile iron pool' or only a fraction of it? *The Biochemical Journal*. 2007;**403**:261-266. DOI: 10.1042/BJ20061840
- [37] Yu J, Song MZ, Wang J, Li YF, Lin P, Que L, Bao Z. *In vitro* cytotoxicity and *in vivo* acute and chronic toxicity of *Xanthii fructus* and its processed product. *BioMed Research International*. 2013;**2013**:403491. DOI: 10.1155/2013/403491

Nanomaterials and Nanoparticles and Nanocrystals

Biocompatibility of Doped Semiconductors Nanocrystals and Nanocomposites

Anielle Christine Almeida Silva,
Mariana Alves Pereira Zóia,
Lucas Ian Veloso Correia,
Fernanda Van Petten Vasconcelos Azevedo,
Aline Teodoro de Paula, Larissa Prado Maia,
Layara Santana de Carvalho, Loyna Nobile Carvalho,
Maria Paula Camargo Costa,
Layssa Carrilho Giarretta, Renata Santos Rodrigues,
Veridiana de Melo Ávila, Luiz Ricardo Goulart and
Noelio Oliveira Dantas

Additional information is available at the end of the chapter

<http://dx.doi.org/10.5772/intechopen.77197>

Abstract

Exposure of humans and environment to nanocrystals are inevitable, and nanotoxicological analyses are a requirement. The wide variety of nanocrystals with different applications is increasing, and characterization of their effects after exposure includes their potential toxicity and uses. This review summarizes the characterization of doped nanocrystals and nanocomposites, Ca-doped ZnO, Ag- and Eu-doped ZnO and Ni-doped ZnONCs, their biocompatibility and applications. This review uncovers how these nanocrystals present desirable biocompatible properties, which can be useful as antitumoral and antimicrobial inducing agents, which differ markedly from toxic properties observed in other general nanocrystals.

Keywords: nanocrystals, nanocomposites, biocompatibility, doping, composites

1. Introduction

Cancer is one of the most common and serious diseases currently, considered a public health problem [1–3]. The prostate cancer, according to INCA, is the most accessible in men in Brazil and difficult diagnoses for slow development and absence of signaling in the early stages of the disease, and can progress to more advanced stages with metastasis. The success in treatment depend on the extent of cancer at the time of diagnosis and, thus, nanotechnology can be a tool to improve diagnostic technique and for improve the quality of treatments [4–10].

Breast cancer is considered as a heterogeneous disease in its pathological characteristics. The follow-up of the disease is quite complex, mainly due to the existence of the various tumor subtypes, which have different expression profile, therapeutic response and clinical behavior [4, 11–15]. The molecular classification divides breast cancers into many groups, based on molecular expression profile. Triple negative breast cancer (TNBC), characterized by lack of expression of estrogen receptor (ER), progesterone receptor (PR) and human epidermal growth factor receptor type 2 (HER2), comprises the highest invasive potential and worst clinical outcome [16, 17]. In addition, this breast cancer presents survival rates significantly lower and recurrence rates significantly higher compared to other breast cancer subtypes [17–19]. Moreover, the identification of specific targeted therapy and improved diagnosis for TNBC is fundamental.

In the last decades, cancer has been presenting itself as a health problem public interest, raising the urgent interest in research for the development of drugs with antitumor activity. Nanotechnology has been a tool for development of new nanoparticles with antineoplastic properties [5, 20–23].

In recent years, with the emergence of certain biomedical problems, such as increased infections of pathogenic strains resistant to antimicrobials and the development of new cancers, the development of new effective tools has been extremely important. Therefore, the use of nanotechnology is important, since depending on the size and shape of nanocrystals it is possible to control their physical and chemical properties [24, 25].

The concern about pathogens and multi-drug microorganisms in food, veterinary and medical industry are boosting the demand for new antimicrobial substances. Since a large number of microorganisms have showed resistance against different antibiotics, the potential antimicrobial substance should be able to destroy or inhibit these microorganisms in different matrices and do not promote resistance [26–29]. Moreover, this compound should be cheap, easy to use, bacteria specific and non-toxicity to the human or animals.

Pathogenic microbial contamination and eradication of organic pollutants have been a major threat to mankind and the environment. Therefore, the development of new, more efficient materials with improved photocatalytic and antimicrobial activity is of great importance.

The increase in bacterial resistance towards conventional antibiotics generally occurs because some bacteria form slime which facilitates adhesion and formation of biofilms on any surface or implantable devices [30, 31]. Thus, the formation of biofilms increases bacterial resistance,

preventing the action of antibiotics [32–36]. In order to reduce microbial adhesion, several researchers have been studying nanocrystals with antimicrobial properties as a promising tool to control microbial adhesion, since nanocrystals with catalytic properties have the potential to reduce biofilm formation [32, 35, 37–40].

Therefore, in the book chapter we investigated the cytotoxicity of Ag or Ca doped ZnO NCs in normal and tumor cells, as well as, the viability of ZnO doped with Ag, Eu, Ni and your nanocomposites against microorganisms.

2. Doped semiconductors nanocrystals and nanocomposites

The development of nanoparticles for medical purposes has been widely investigated, since when the size is greatly reduced at the nanometric scale, the reason surface/volume increase generating new and interesting properties, such as a greater ability to absorb drugs, probes and proteins [41]. In addition to size and shape, a crystalline nanoparticle (NPs) alters as both physical and biological properties. For example, Spanó et al. have shown that amorphous nanoparticles are more genotoxic than crystalline (nanocrystals) [42]. In addition, a crystal phase in which nanocrystals (NCs) themselves also enables physical and biological properties [43].

The use of nanoparticles and nanocrystals as novel therapeutic antimicrobial agents have been described some of the metallic compounds possess antimicrobial property especially inorganic metal oxides [44]. Moreover, the alliance of nanotechnology and biology has brought to fore metals in the form of nanoparticles as potential antimicrobial agents.

Several types of nanocrystals have been synthesized in order to obtain an efficient nanomaterial. However, it is important to emphasize that nanocrystals must be biocompatible and specific [45]. Based on this and knowing that zinc oxide nanocrystals (ZnO) are biocompatible materials, according to the US Food and Drug Administration (FDA), in this chapter we investigated this nanocrystal.

Nanocrystals of zinc oxide (ZnO) exhibit many important characteristics, such as high catalytic activity, chemical and physical stability, as well as ultraviolet (UV) absorption [46, 47]. The technique most used to produce defects aiming to increase the catalytic activity in ZnO nanocrystals is based on the choice of synthesis methods [34], use of nanocomposite photocatalysts [48], and doping with impurities [49].

ZnO nanocrystals have the unique ability to induce oxidative stress in cancer cells and bacteria, being one of the main mechanisms of cytotoxicity and bactericidal action [32, 50, 51]. This property is due to the semiconductor nature of ZnO, which induces the generation of reactive oxygen species (ROS), leading to oxidative stress and cell death or bacteria [52–54]. Another type of nanocrystalline that enters the category of biocompatible is nickel because it is a basic element that is part of metalloproteins, being vital for living beings. Nickel (Ni), silver (Ag) and calcium (Ca) nanocrystals and oxide have several advantages as antimicrobial and antitumor agents [55–57].

Figure 1 shows the three-dimensional structures of the zinc, calcium, silver and nickel oxides, subsequently exemplifying the doping process and nanocomposites. The doping process consists of the substitution of ions in the crystalline structure of the nanocrystal. For example, in silver-doped ZnO nanocrystals, silver ions substitute the ions of Zn in the crystalline structure of ZnO.

The formation of nanocomposites is the mixing of two types of nanocrystals in order to potentiate a certain physical property, or the presence of two interesting physical properties.

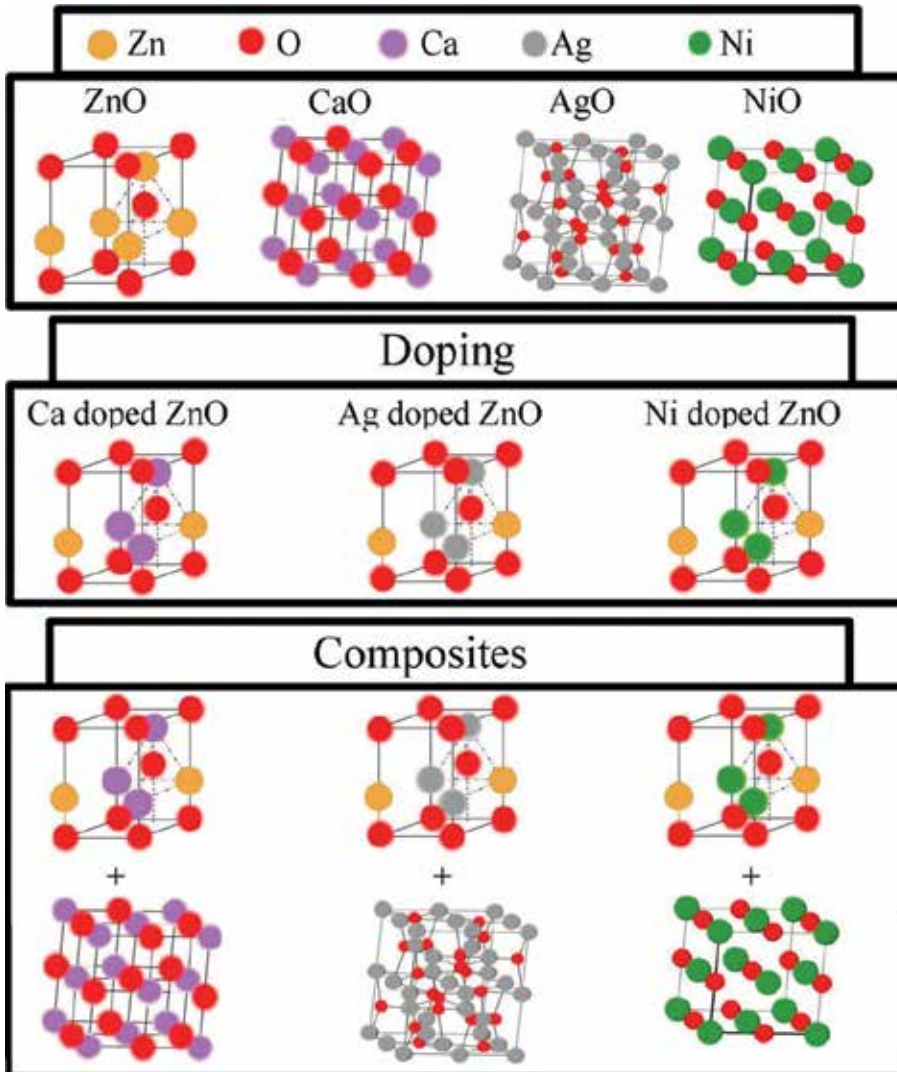


Figure 1. Three-dimensional structures of the zinc oxide, calcium oxide, silver oxide and nickel oxide, subsequently exemplifying the doping process and nanocomposites.

Chu et al. demonstrated that the mixture of titanium dioxide nanocrystals with silver oxide enhanced the photocatalytic performance [58]. Thus, as the photocatalytic performance of nanocrystals is directly related to antineoplastic effect and bactericidal action the study of the mixture of nanocrystals (nanocomposites) is extremely important.

2.1. Cytotoxicity of doped nanocrystals and nanocomposites in cells

Normal epithelial cell line (RWPE-1), prostate cancer cells (PC3) and human breast adenocarcinoma (MDA-MB-231), were cultured in RPMI medium supplemented with 10% fetal bovine serum (FBS) and 0.1% gentamycin. For the RWPE-1 strain, the medium was further enriched with epidermal growth factor (10 ng/mL) and bovine pituitary extract. Cells were maintained at 37°C, 5% CO₂. The cells were grown in 25 cm² bottles and transferred before reaching the confluence level (80%). Cell viability was determined by the 3-(4,5-dimethylthiazol-2-yl)-2,5-diphenyltetrazolium bromide (MTT) assay. Cells (1 × 10⁵/well) were seeded in 96-well plates and incubated overnight for adherence. The culture medium was removed and replaced with medium containing the nanocrystals in different concentrations diluted in PBS and evaluated at 24 hours. After the indicated period, MTT (5 mg/mL) was added and the plates were incubated for 4 hours. Then, 50 μL of sodium dodecyl sulfate (SDS) (20%) was added in each well to dissolve the formazan crystal. The absorbance was measured at 570 nm. Next, the cell viability calculation was performed.

Figure 2 show the viability of nanocrystals in function of concentration for the (a) normal epithelial cell line (RWPE-1) and (b) prostate cancer cells (PC3) at 24 hours. In the RWPE-1 cells

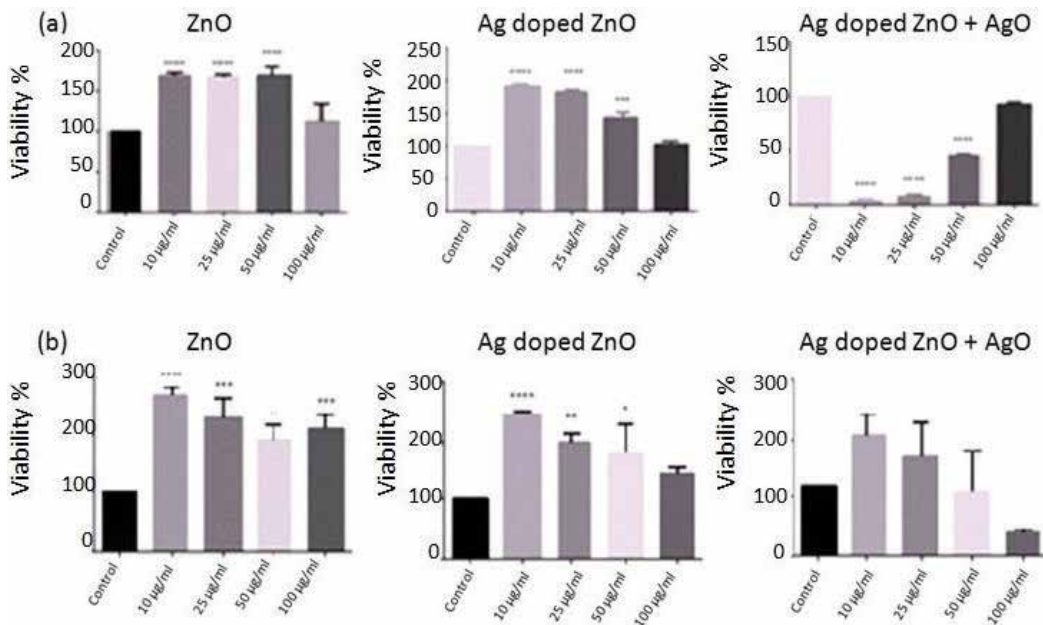


Figure 2. Viability of (a) RWPE and (b) PC3 after treatment with ZnO, Ag doped ZnO and nanocomposite (Ag doped ZnO and 68% of AgO NCs) with different concentration after 24 hours.

the ZnO NCs and Ag doped ZnO was not observed cytotoxic effect. However, in the composite formed by Ag doped ZnO and 68% of AgO NCs occurs the reduction in cell viability. For PC3 cells the ZnO and Ag doped ZnO NCs had no cytotoxic effect at all concentrations, but the composite had a significant inhibitory effect on cell viability, however, there was an increase in cell viability for PC3 cells at concentrations of 10 and 25 µg/mL in 24 hours time.

Figure 3 show the viability of Ca doped ZnO, ZnO and CaO nanocrystals in function of concentration for the human breast adenocarcinoma (MDA-MB-231) cells at 24 hours. The cytotoxic potential of CaO nanocrystals was extremely lower against cells and ZnO was performed significantly damage in cells. Interestingly, the Ca doped ZnO NCs displayed high cytotoxicity against the cells. The Ca doped ZnO NCs reduced the viability in a not dose-dependent manner, damaging about 40–93% of cells at concentrations of 12.5–100 µg/mL.

2.2. Cytotoxicity of doped nanocrystals and nanocomposites in bacteria

The ZnO doped with silver and europium has been tested in preliminary study against Gram-negative *Escherichia coli* and Gram-positive *Staphylococcus aureus* and *Enterococcus faecalis* using different methods. The agar well diffusion test was made according to Clinical and Laboratory Standards Institute and the resazurin microtiter assay plate testing was also performed.

The inhibition zone produced by ZnO doped with silver increase in Ag dopant concentration. The antimicrobial action proposed for nanocrystal against microorganisms can be related with: (a) the adherence of the nanomaterials on the surface of the bacteria, which can lead to physical blockage of transport channels of the cells; (b) the oxidation of membranes lipids by reactive oxygen species (ROS) like H_2O_2 , singlet oxygen and hydroxyl radicals [44].

The viability assay against *S. aureus* and *E. coli* showed that the Ag and europium (Eu) doped ZnO NCs inhibited these microorganisms. However, the increase of Eu doping and Eu_2O_3 NCs promoted the growth of the microorganisms (**Figure 4**). Concentrations greater than 1% Eu occurs the formation of a nanocomposite that constitutes of Eu and Ag doped ZnO and EuO . The use of nanocrystals as antimicrobial substance should be promisor in different

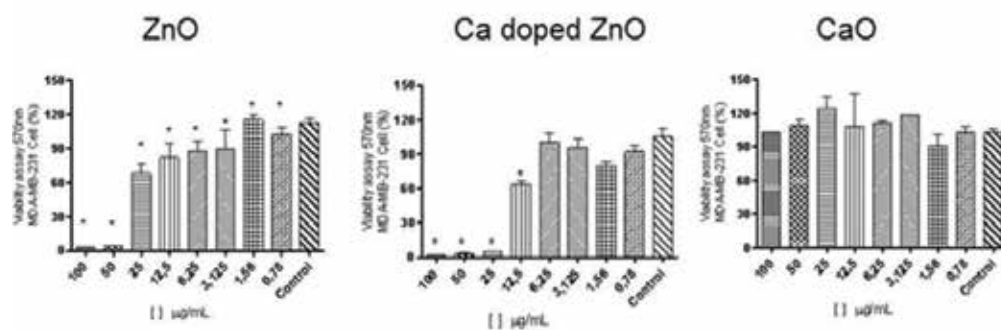


Figure 3. Viability after treatment with ZnO, Ca doped ZnO and CaO nanocrystals in function of concentration for the MDA-MB-231 cells at 24 hours.

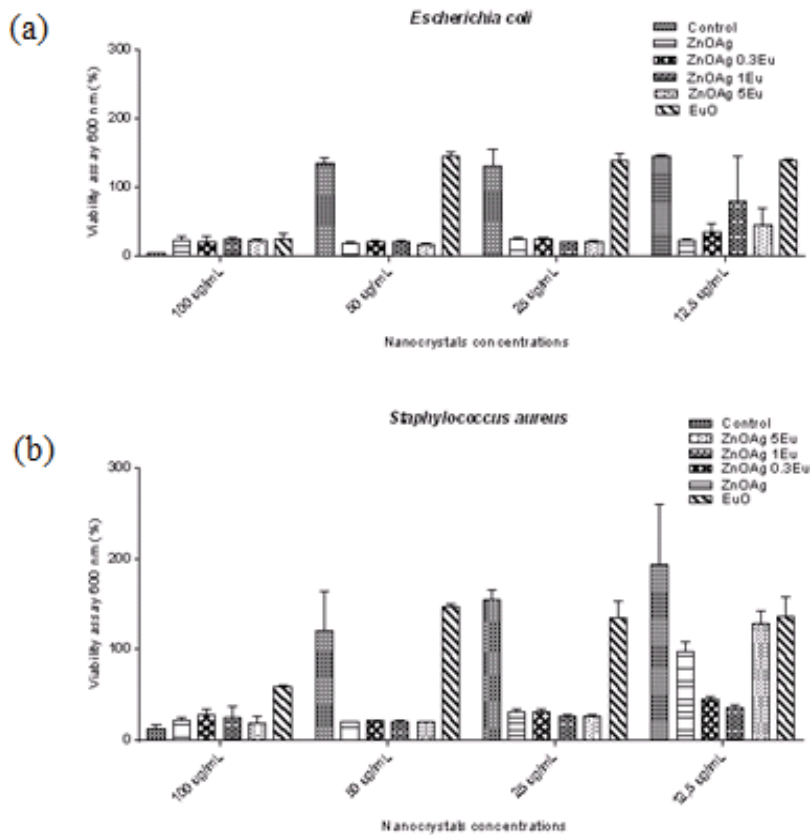


Figure 4. Viability assay against *S. aureus* and *E. coli* of Ag and Eu doped ZnO, and ZnO and EuO NCs.

areas. These NCs could be a potential antimicrobial, which can be apply in food, veterinary and medical industry. However, complementary studies should be done to better understand the effects of this compound on biological molecules.

The potential antimicrobial activity of nanocrystals against potential pathogens have been studied. On the other hand, large number of microorganisms have showed resistance against antibiotics [59, 60]. Zinc (Zn) and nickel (Ni) are transition metals that generate free electrons, so when these ions are incorporated into nanocrystals may amplify the bactericidal effect [61–64].

The viability assay against *Proteus vulgaris* and *Klebsiella pneumonia* with different concentration of the nanocomposite hybrid (Ni doped ZnO + NiO NCs), ZnO and NiO NCs (**Figure 5**). Observed that NiO NCs showed antimicrobial activity against all microorganisms tested. *P. vulgaris* was the most sensitive in presence of NiO NCs, whereas *K. pneumonia* was more resistant. The antimicrobial effect may be due to production of electron–hole pairs. After a cascade of reactions, hydrogen peroxide is produced and penetrate into the cell, destroy the membrane, denatures proteins and damages DNA causing cell death [31, 38, 51]. Therefore, due to its simple preparation, low cost and antibacterial activity, these NCs have potential to be used as antibacterial agents against a wide range of microorganisms.

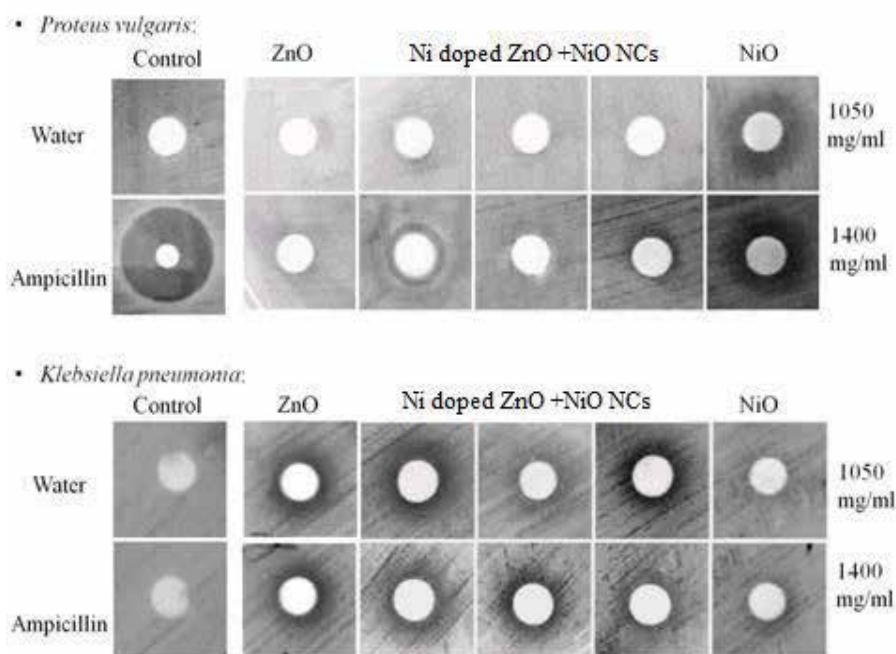


Figure 5. Viability assay against *Proteus vulgaris* and *Klebsiella pneumoniae* with different concentration of the nanocomposite hybrid with ZnO, Ni doped ZnO + NiO and NiO NCs.

3. Conclusion

The cytotoxicity analysis of Ag or Ca doped ZnO NCs in normal, tumor prostate and breast cells was possible to identify the antitumor effect potentialization when these ions (Ag and Ca) were incorporated into ZnO NCs. In this way, these doped NCs can become a target in the treatment of cancer. The viability assay against microorganisms showed that the increase of Eu doping in ZnO NCs promoted the growth of the microorganisms and Ni doped ZnO with NiO NCs are more efficient than NiO NCs to *K. pneumoniae*.

Acknowledgements

The authors gratefully acknowledge financial support from the following agencies: CAPES, FAPEMIG, MCT/CNPq.

Conflict of interest

The authors have no conflicts of interest.

Author details

Anielle Christine Almeida Silva^{1*}, Mariana Alves Pereira Zóia³, Lucas Ian Veloso Correia², Fernanda Van Petten Vasconcelos Azevedo², Aline Teodoro de Paula³, Larissa Prado Maia³, Layara Santana de Carvalho^{1,3}, Loyna Nobile Carvalho^{1,3}, Maria Paula Camargo Costa^{1,3}, Layssa Carrilho Giaretta^{1,3}, Renata Santos Rodrigues², Veridiana de Melo Ávila², Luiz Ricardo Goulart³ and Noelio Oliveira Dantas¹

*Address all correspondence to: aniellechristineas@gmail.com

1 Laboratory of New Insulation and Semiconductor Materials, Institute of Physics, Federal University of Uberlândia, Uberlândia, Brazil

2 Laboratory of Biochemistry and Animal Toxins, Institute of Genetics and Biochemistry, Federal University of Uberlandia, Uberlândia, Brazil

3 Laboratory of Nanobiotechnology, Institute of Genetics and Biochemistry, Federal University of Uberlândia, Uberlândia, Brazil

References

- [1] Jemal A, Siegel R, Ward E, Hao Y, Xu J, Murray T, Thun MJ. Cancer statistics, 2008. *CA: a Cancer Journal for Clinicians*. 2008;**58**(2):71-96
- [2] Siegel RL, Miller KD, Jemal A. Cancer statistics, 2017. *CA: a Cancer Journal for Clinicians*. 2017;**67**(1):7-30
- [3] American Cancer Society. *Cancer Facts & Figures 2017*. 2017;**21**(20):2525-2538
- [4] Ferlay J, Soerjomataram I, Dikshit R, Eser S, Mathers C, Rebelo M, Parkin DM, Forman D, Bray F. Cancer incidence and mortality worldwide: Sources, methods and major patterns in GLOBOCAN 2012. *International Journal of Cancer*. 2015;**136**(5):E359-E386
- [5] Sanna V, Sechi M. Nanoparticle therapeutics for prostate cancer treatment. *Maturitas*. 2012:27-32
- [6] Villanueva T. Prostate cancer: Prostate quartet. *Nature Reviews. Cancer*. 2011;**11**(3):159
- [7] Bashir MN. Epidemiology of prostate cancer. *Asian Pacific Journal of Cancer Prevention*. 2015;**16**(13):5137-5141
- [8] Stewart RW, Lizama S, Peairs K, Sateia HF, Choi Y. Screening for prostate cancer. *Seminars in Oncology*. 2017;**44**(1):47-56
- [9] Emberton M. Is a negative prostate biopsy a risk factor for a prostate cancer related death? *The Lancet Oncology*. 2017;**18**(2):162-163
- [10] Litwin MS, Tan H-J. The diagnosis and treatment of prostate cancer. *JAMA*. 2017;**317**(24):2532

- [11] Tao Z, Shi A, Lu C, Song T, Zhang Z, Zhao J. Breast cancer: Epidemiology and etiology. *Cell Biochemistry and Biophysics*. 2015;**72**(2):333-338
- [12] Tomao F, Papa A, Zaccarelli E, Rossi L, Caruso D, Minozzi M, Vici P, Frati L, Tomao S. Triple-negative breast cancer: New perspectives for targeted therapies. *OncoTargets and Therapy*. 2015;**8**:177-193
- [13] Schneider KA. All About Breast Cancer. *Couns. About Cancer*; 2011. pp. 151-185
- [14] Scully OJ, Bay B-H, Yip G, Yu Y. Breast cancer metastasis. *Cancer Genomics Proteomics*. 2012;**9**(5):311-320
- [15] BCSC. Types of breast cancer. In: *Breast Cancer Soc. Canada*. 2014. p. 1
- [16] Foulkes WD, Smith IE, Reis-Filho JS. Triple-negative breast cancer. *The New England Journal of Medicine*. 2010;**363**(20):1938-1948
- [17] Harbeck N, Gnant M. Breast cancer. *Lancet*. 2017;**389**(10074):1134-1150
- [18] Bondarenko O, Juganson K, Ivask A, Kasemets K, Mortimer M, Kahru A. Toxicity of Ag, CuO and ZnO nanoparticles to selected environmentally relevant test organisms and mammalian cells in vitro: A critical review. *Archives of Toxicology*. 2013;**87**(7):1181-1200
- [19] Akram M, Iqbal M, Daniyal M, Khan AU. Awareness and current knowledge of breast cancer. *Biological Research*. 2017;**50**(1):33
- [20] Hu F, Ran Y, Zhou Z, Gao M. Preparation of bioconjugates of CdTe nanocrystals for cancer marker detection. *Nanotechnology*. 2006;**17**(12):2972-2977
- [21] Li YY, Tian YH, Nie GJ. Antineoplastic activities of Gd@C82(OH)₂₂ nanoparticles: Tumor microenvironment regulation. *Science China. Life Sciences*. 2012;**55**(10):884-890
- [22] Jia F, Liu X, Li L, Mallapragada S, Narasimhan B, Wang Q. Multifunctional nanoparticles for targeted delivery of immune activating and cancer therapeutic agents. *Journal of Controlled Release*. 2013;**172**(3):1020-1034
- [23] Liechty WB, Peppas NA. Expert opinion: Responsive polymer nanoparticles in cancer therapy. *European Journal of Pharmaceutics and Biopharmaceutics*. 2012;**80**(2):241-246
- [24] Kolodziejczak-Radzimska A, Jesionowski T. Zinc oxide-from synthesis to application: A review. *Materials (Basel)*. 2014;**7**(4):2833-2881
- [25] Wang ZL. Zinc oxide nanostructures: Growth, properties and applications. *Journal of Physics. Condensed Matter*. 2004;**16**(25):R829-R858
- [26] Appendini P, Hotchkiss JH. Review of antimicrobial food packaging. *Innovative Food Science and Emerging Technologies*. 2002;**3**(2):113-126
- [27] O'Neil J. Review on antimicrobial resistance. In: *Antimicrob. Rsesistance Tackling a Cris. Heal. Wealth Nations*. 2014 (December)
- [28] Verraes C, Van Boxstael S, Van Meervenne E, Van Coillie E, Butaye P, Catry B, de Schaetzen MA, Van Huffel X, Imberechts H, Dierick K, Daube G, Saegerman C, De Block J, Dewulf J,

- Herman L. Antimicrobial resistance in the food chain: A review. *International Journal of Environmental Research and Public Health*. 2013;**10**(7):2643-2669
- [29] Balouiri M, Sadiki M, Ibensouda SK. Methods for in vitro evaluating antimicrobial activity: A review. *Journal of Pharmaceutical Analysis*. 2016;**6**(2):71-79
- [30] Mah TFC, O'Toole GA. Mechanisms of biofilm resistance to antimicrobial agents. *Trends in Microbiology*. 2001;**9**(1):34-39
- [31] Singh S, Singh SK, Chowdhury I, Singh R. Understanding the mechanism of bacterial biofilms resistance to antimicrobial agents. *The Open Microbiology Journal*. 2017;**11**(1):53-62
- [32] Pati R, Mehta RK, Mohanty S, Padhi A, Sengupta M, Vaseeharan B, Goswami C, Sonawane A. Topical application of zinc oxide nanoparticles reduces bacterial skin infection in mice and exhibits antibacterial activity by inducing oxidative stress response and cell membrane disintegration in macrophages. *Nanomedicine: Nanotechnology, Biology, and Medicine*. 2014;**10**(6):1195-1208
- [33] Dizaj SM, Lotfipour F, Barzegar-Jalali M, Zarrintan MH, Adibkia K. Antimicrobial activity of the metals and metal oxide nanoparticles. *Materials Science and Engineering: C*. 2014;**44**:278-284
- [34] Espitia PJP, de Soares NFF, Coimbra JS d R, de Andrade NJ, Cruz RS, Medeiros EAA. Zinc oxide nanoparticles: Synthesis, antimicrobial activity and food packaging applications. *Food and Bioprocess Technology*. 2012;**5**(5):1447-1464
- [35] Ma Z, Garrido-Maestu A, Jeong KC. Application, mode of action, and in vivo activity of chitosan and its micro- and nanoparticles as antimicrobial agents: A review. *Carbohydrate Polymers*. 2017;**176**:257-265
- [36] Lakshmaiah Narayana J, Chen JY. Antimicrobial peptides: Possible anti-infective agents. *Peptides*. 2015;**72**:88-94
- [37] Liu J-J, Chang Q, Bao M-M, Yuan B, Yang K, Ma Y-Q. Silicon quantum dots delivered phthalocyanine for fluorescence guided photodynamic therapy of tumor. *Chinese Physics B*. 2017;**26**(9):98102
- [38] Arakha M, Pal S, Samantarrai D, Panigrahi TK, Mallick BC, Pramanik K, Mallick B, Jha S. Antimicrobial activity of iron oxide nanoparticle upon modulation of nanoparticle-bacteria interface. *Scientific Reports*. 2015;**5**:14813
- [39] Durán N, Nakazato G, Seabra AB. Antimicrobial activity of biogenic silver nanoparticles, and silver chloride nanoparticles: An overview and comments. *Applied Microbiology and Biotechnology*. 2016;**100**(15):6555-6570
- [40] Jian HJ, Wu RS, Lin TY, Li YJ, Lin HJ, Harroun SG, Lai JY, Huang CC. Super-cationic carbon quantum dots synthesized from Spermidine as an eye drop formulation for topical treatment of bacterial keratitis. *ACS Nano*. 2017;**11**(7):6703-6716
- [41] Silva ACA, Dantas NO, Silva MJB, Spanó MA, Goulart LR. Functional nanocrystals: Towards biocompatibility, nontoxicity and biospecificity. In: *Advances in Biochemistry & Applications in Medicine*. 1st ed. Wilmington: Open Access eBooks; 2017. pp. 1-27

- [42] Reis É d M, Rezende AAA d, Santos DV, Oliveria PF d, Nicolella HD, Tavares DC, Silva ACA, Dantas NO, Spanó MA. Assessment of the genotoxic potential of two zinc oxide sources (amorphous and nanoparticles) using the in vitro micronucleus test and the in vivo wing somatic mutation and recombination test. *Food and Chemical Toxicology*. 2015;**84**:55-63
- [43] Reis É d M, de Rezende AAA, de Oliveira PF, Nicolella HD, Tavares DC, Silva ACA, Dantas NO, Spanó MA. Evaluation of titanium dioxide nanocrystal-induced genotoxicity by the cytokinesis-block micronucleus assay and the drosophila wing spot test. *Food and Chemical Toxicology*. 2016;**96**:309-319
- [44] Sawai J. Quantitative evaluation of antibacterial activities of metallic oxide powders (ZnO, MgO and CaO) by conductimetric assay. *Journal of Microbiological Methods*. 2003;**54**(2):177-182
- [45] Sousa CJA, Pereira MC, Almeida RJ, Loyola AM, Silva ACA, Dantas NO. Synthesis and characterization of zinc oxide nanocrystals and histologic evaluation of their biocompatibility by means of intraosseous implants. *International Endodontic Journal*. 2014;**47**(5):416-424
- [46] Tankhiwale R, Bajpai SK. Preparation, characterization and antibacterial applications of ZnO-nanoparticles coated polyethylene films for food packaging. *Colloids and Surfaces B: Biointerfaces*. 2012;**90**(1):16-20
- [47] Warheit DB. How meaningful are the results of nanotoxicity studies in the absence of adequate material characterization? *Toxicological Sciences*. 2008;**101**(2):183-185
- [48] Pawinrat P, Mekasuwandumrong O, Panpranot J. Synthesis of Au-ZnO and Pt-ZnO nanocomposites by one-step flame spray pyrolysis and its application for photocatalytic degradation of dyes. *Catalysis Communications*. 2009;**10**(10):1380-1385
- [49] Li Y, Zhao X, Fan W. Structural, electronic, and optical properties of Ag-doped ZnO nanowires: First principles study. *Journal of Physical Chemistry C*. 2011;**115**(9):3552-3557
- [50] Dryden M. Reactive oxygen therapy: A novel antimicrobial. *International Journal of Antimicrobial Agents*. 2017;**51**(3):299-303
- [51] Premanathan M, Karthikeyan K, Jeyasubramanian K, Manivannan G. Selective toxicity of ZnO nanoparticles toward gram-positive bacteria and cancer cells by apoptosis through lipid peroxidation. *Nanomedicine Nanotechnology, Biology and Medicine*. 2011;**7**(2):184-192
- [52] Salnikow K, Su W, Blagosklonny MV, Costa M. Carcinogenic metals induce hypoxia-inducible factor-stimulated transcription by reactive oxygen species-independent mechanism. *Cancer Research*. 2000;**60**(13):3375-3378
- [53] Sawai J, Yoshikawa T. Quantitative evaluation of antifungal activity of metallic oxide powders (MgO, CaO and ZnO) by an indirect conductimetric assay. *Journal of Applied Microbiology*. 2004;**96**(4):803-809

- [54] Javed Akhtar M, Ahamed M, Kumar S, Majeed Khan M, Ahmad J, Alrokayan SA. Zinc oxide nanoparticles selectively induce apoptosis in human cancer cells through reactive oxygen species. *International Journal of Nanomedicine*. 2012;7:845-857
- [55] Ahamed M, Ali D, Alhadlaq HA, Akhtar MJ. Nickel oxide nanoparticles exert cytotoxicity via oxidative stress and induce apoptotic response in human liver cells (HepG2). *Chemosphere*. 2013;93(10):2514-2522
- [56] Roy A, Gauri SS, Bhattacharya M, Bhattacharya J. Antimicrobial activity of CaO nanoparticles. *Journal of Biomedical Nanotechnology*. 2013;9(9):1570-1578
- [57] Kim JS, Kuk E, Yu KN, Kim JH, Park SJ, Lee HJ, Kim SH, Park YK, Park YH, Hwang CY, Kim YK, Lee YS, Jeong DH, Cho MH. Antimicrobial effects of silver nanoparticles. *Nanomedicine: Nanotechnology, Biology and Medicine*. 2007;3(1):95-101
- [58] Chu H, Liu X, Liu J, Li J, Wu T, Li H, Lei W, Xu Y, Pan L. Synergetic effect of Ag₂O as co-catalyst for enhanced photocatalytic degradation of phenol on N-TiO₂. *Materials Science and Engineering: B Solid-State Materials Advanced Technology*. 2016;211:128-134
- [59] Padmavathy N, Vijayaraghavan R. Enhanced bioactivity of ZnO nanoparticles—An antimicrobial study. *Science and Technology of Advanced Materials*. 2008;9(3):35004
- [60] Pasquet J, Chevalier Y, Pelletier J, Couval E, Bouvier D, Bolzinger MA. The contribution of zinc ions to the antimicrobial activity of zinc oxide. *Colloids and Surfaces A: Physicochemical and Engineering Aspects*. 2014;457(1):263-274
- [61] Minzanova ST, Mironov VF, Mironova LG, Nizameev IR, Kholin KV, Voloshina AD, Kulik NV, Nazarov NG, Milyukov VA. Synthesis, properties, and antimicrobial activity of pectin complexes with cobalt and nickel. *Chemistry of Natural Compounds*. 2016;52(1):26-31
- [62] Denkhaus E, Salnikow K. Nickel essentiality, toxicity, and carcinogenicity. *Critical Reviews in Oncology/Hematology*. 2002;42(1):35-56
- [63] Mandal BK. *Nanobiomaterials in Antimicrobial Therapy*. Elsevier; 2016
- [64] Saito M. Antibacterial, deodorizing, and UV absorbing materials obtained with zinc oxide (ZnO) coated fabrics. *Journal of Industrial Textiles*. 1993;23(2):150-164

Toxicity of Titanate Nanosheets on Human Immune Cells

Yasumitsu Nishimura, Daisuke Yoshioka,
Naoko Kumagai-Takei, Suni Lee,
Hidenori Matsuzaki, Kei Yoshitome and
Takemi Otsuki

Additional information is available at the end of the chapter

<http://dx.doi.org/10.5772/intechopen.72234>

Abstract

Titanium oxide is regarded as a bio-inert material, but studies concerning the toxic effects of titanium dioxide (TiO₂), particularly nano-scaled TiO₂ particles, have been accumulating that indicate nano-scaled TiO₂ particles show more harm and cause greater alteration of immune functions compared with large particles. Inorganic nanosheets have been the focus of increasing interest because of their ultrathin structure, as well as diversity of compounds and structures leading to various functions. Oxide nanosheets are included in the group comprising inorganic nanosheets, and titanate nanosheets (TiNSs) represent a form of oxide nanosheets. We therefore examined the toxicity of nano-scaled 2D materials of TiNSs on human immune cells. Our study revealed that TiNSs have the potential to cause harm through caspase-dependent apoptosis of human peripheral blood mononuclear cells (PBMCs) to the same degree as asbestos. Furthermore, isolated monocytes developed marked vacuoles prior to cell death upon exposure to TiNSs, which were found in the vacuoles and indicated engulfment of TiNSs. A consideration of these findings with the co-localization of vacuoles with endocytosed fluorescence-labeled dextran indicates that TiNSs entered the endosomal pathway, leading to the formation of vacuoles in monocytes and subsequent cell death. TiNSs might therefore affect immune functions through interference of endo-lysosomal functions.

Keywords: titanate nanosheets, apoptosis, vacuole formation, endosome

1. Introduction

Titanium oxide is used broadly in industrial production for ceramics, materials containing composite oxides and photocatalysts, and even as a food additive. In addition, titanium and its

alloy are used for various kinds of biomaterials such as artificial joints and dental implants, where generation of titanium oxide (titania) film is beneficial because of its bio-inertness [1–3]. Titanium oxide was therefore regarded as a harmless material. However, studies detailing the toxic effects of titanium oxide have been accumulating recently as shown in the next section. The International Agency for Research on Cancer (IARC) decided in 2010 to change its categorization of titanium dioxide (TiO_2) from “Group 3: Not classifiable as to carcinogenicity to humans” to “Group 2B: Possibly carcinogenic to humans”. This conclusion resulted from sufficient evidence in experimental animals and inadequate evidence from epidemiological studies. The carcinogenicity of titanium oxide was evaluated by examining the relationship between exposure to titanium oxide and the risk of lung cancer in two previously conducted case-control studies, which showed no detectable excess risk of lung cancer [4]. In contrast, two studies using animal experiments demonstrated elevated lung cancer in rats exposed to fine or ultrafine TiO_2 [5, 6]. Additionally, it is estimated that the total production of nano- TiO_2 would reach approximately 2.5 million metric tons (MT) per year in 2025 from 40,000 MT in 2006 in the US [7], which means we would become more exposed to nano-scaled materials of titanium oxide in the future, thereby motivating us to better clarify the toxicological effects of this material. The various forms of titanium oxide are known and include spheres, rods, needles and fibers, as well as sheets. Titanate nanosheets (TiNSs) are crystalline materials composed of titanium and oxygen with a very thin and flat structure representing 2D materials. TiNSs are expected to be valuable materials in industry for production of UV- or corrosion-resistant films, dielectric thin films and catalysts. Therefore, we recently examined the effects of exposure to TiNSs on human immune cells (manuscript of an original article under preparation). Here, we would like to review the progress of studies regarding the toxicity of titanium oxides, summarize our recent study concerning the toxicity of TiNSs and finally discuss the findings obtained from that study.

2. Toxicity of titanium dioxide materials

The following two studies form the basis for the decision to reappraise the carcinogenicity of TiO_2 . In 1985, Lee et al. conducted *in vivo* experiments with rats and reported the occurrence of bronchioalveolar adenomas carcinomas and squamous cell carcinomas in a portion of both sexes exposed by inhalation to fine TiO_2 , which possesses a micro-scaled diameter [5]. The study by Heinrich et al. demonstrated that exposure to ultrafine TiO_2 nano-scaled particles caused tumors in comprising squamous cell carcinomas, adenocarcinomas and benign squamous cell tumors in female rats [6]. In addition, Schins et al. evaluated data in the literature and reported that tumorigenesis by TiO_2 involves a mechanism of genetic damage caused by reactive oxygen species (ROS) and reactive nitrogen species (RNS) that were produced by a TiO_2 exposure-induced inflammatory response [8]. Naturally occurring TiO_2 is distinguished as rutile and anatase due to the difference in crystal structure. It has been reported that an anatase type of nano- TiO_2 showed higher production of ROS and more toxic characteristics compared with a rutile type of the material in an *in vitro* experiment with human fibroblasts and lung epithelial cells [9]. In addition, it has been demonstrated that TiO_2 nanoparticles caused high production of 8-hydroxyl-2'-deoxyguanosine (8-OHdG), a DNA adduct, which contributed to the development of tumor, whereas the nanoparticles did not cause DNA breakage in human

lung fibroblasts of IMR-90 [10]. Chen et al. demonstrated that single intratracheal instillation with TiO₂ nanoparticles caused altered expression of mouse lung-tissue genes involved in pathways associated with the cell cycle, apoptosis, chemokines and the complement system [11]. TiO₂ nanoparticles increased expression of placenta growth factor (PlGF), CXCL1, CXCL5 and CCL3, and results were similar to those observed in an *in vitro* experiment with human THP-1 cells. Warheit et al. demonstrated the difference in effects resulting from exposure to nano-TiO₂ rods and dots [12]. Moreover, their study compared various kinds of TiO₂ and demonstrated that the pulmonary effects caused by exposure to ultrafine TiO₂ differ based on the crystal structure and composition of TiO₂ [13]. These findings show evidence for the toxicity of titanium oxide, but the toxicity of nano-scaled materials needs to be examined further, particularly the crucial role played by the size, crystal structure and composition of TiO₂ in regard to toxicity.

3. Studies concerning nano-scaled titanium dioxide particles

Before examining TiNSs, previous studies regarding the toxicity of nano-scaled TiO₂ materials should be reviewed. The toxicological effect of TiO₂ nanoparticles on skin and in dermal tissue is of interest to medical science and manufacturers because TiO₂ is used as a physical photoprotective agent in sunscreen and as a whitening agent in cosmetics. It is unlikely that TiO₂ nanoparticles easily reach dermal tissue. Experiments using human skin-transplanted mice show that TiO₂ nanoparticles did not penetrate the barrier of an intact epidermis [14]. Sadrieh et al. [15] and Newman et al. [16] also demonstrated no significant penetration of TiO₂ nanoparticles through the epidermis. However, this does not eliminate concern regarding its toxicity on skin because an *in vitro* experiment using cell lines of keratinocytes, sebocytes, fibroblasts and melanocytes showed decreases in viable cells, an increase in apoptosis and decreases in the differentiation markers of those cells [14]. Moreover, several studies have shown actual penetration of TiO₂ nanoparticles through skin. Bennat and Muller-Goymann demonstrated that TiO₂ nanoparticles are able to pass through skin using an oil-in-water emulsion [17]. Another study demonstrated that TiO₂ nanoparticles reached the deep area of the epidermis in the pig ear after topical skin exposure to the nanoparticles, some of which even reached the brain, whereas there was no penetration in an *in vitro* experiment using isolated porcine skin [18]. Once TiO₂ nanoparticles pass through the epidermis due to the broken or unhealthy status of the epidermal barrier, they produce harmful effects on the tissue. A study utilizing *in vitro* experiments confirmed the phototoxicity of nano-sized TiO₂ in an experiment with human skin keratinocytes of HaCaT under irradiation of UVA, which is mainly dependent on the ROS production level [19]. Furthermore, a study investigating the mechanism of toxicity of TiO₂ nanoparticles upon exposure to UVA found that exposure to TiO₂ caused decreases in the mitochondrial membrane potential and ATP level and an increase in caspase 3 activity [20]. It has also been shown that subcutaneous injection with TiO₂ nanoparticles promoted dermal sensitization induced by dinitrochlorobenzene (DNCB) [21]. Moreover, intradermal administration with TiO₂ nanoparticles resulted in aggravated skin lesions such as those of atopic dermatitis related to mite antigen in NC/Nga mice [22]. These findings indicate that TiO₂ nanoparticles do not penetrate through the epidermis easily as long as the barrier is healthy, but these nanoparticles have the potential to cause toxic

effects on dermal tissue when that barrier is broken. Pulmonary exposure to TiO₂ nanoparticles is expected to result in these toxic effects because a barrier comprising pulmonary tissue is not tough. In addition, alveolar macrophages are always ready to engulf particles in the region, leading to inflammatory responses. Sager et al. used F344 rats to examine the pulmonary response to intratracheal instillation of nano-sized ultrafine TiO₂ in comparison to fine TiO₂ particles. Administration with ultrafine TiO₂ caused higher levels of polymorphonuclear neutrophil (PMN) cell number, lactate dehydrogenase (LDH) activity, albumin and inflammatory cytokines compared with fine TiO₂ [23]. Interestingly, they also examined the amounts of TiO₂ in trachea-bronchial and thymic lymph nodes at days 7 and 42 after administration and then measured alterations in those tissues during that period. Ultrafine TiO₂ showed a faster decline of the remaining amount in trachea-bronchial nodes than fine TiO₂. In addition, although both ultrafine and fine TiO₂ were translocated to lymph nodes, the amount was higher for ultrafine TiO₂ than fine TiO₂. There was also a striking difference in the amounts of lavagable and non-lavagable components between fine and ultrafine TiO₂ in the lungs. Eight-one percent of ultrafine TiO₂ was non-lavagable, suggesting migration to the interstitium, even at day 7 post-exposure, whereas 91% of fine TiO₂ was still lavagable at this stage. Shinohara et al. investigated pulmonary clearance kinetics of TiO₂ nano- and sub-micron particles by intratracheal administration to male F344 rats [24], and results confirmed the translocation of administered TiO₂ to the thoracic lymph nodes that increased in a time- and dose-dependent manner. van Ravenzwaay also observed that inhaled TiO₂ nanoparticles reached the lungs and draining lymph nodes [25]. These findings indicate that it is easier for TiO₂ nanoparticles to migrate from bronchoalveolar to interstitial tissue or be cleared by alveolar macrophages, leading to increased inflammatory responses, and that TiO₂ nanoparticles have a greater potential to influence the function of immune cells. Actually, several studies have reported alteration of immune functions following administration with TiO₂ through the respiratory pathway. Chang et al. demonstrated that intratracheal instillation with TiO₂ nanoparticles caused an increase in GATA-3 and decrease in T-bet mRNA levels, which are master genes for Th2 and Th1 cell development, respectively [26]. Mishra et al. examined the effect of administration with TiO₂ nanoparticles as an adjuvant in an experiment utilizing a murine asthma model. It was found that TiO₂ nanoparticles augmented airway hyper-responsiveness, lung damage and a mixed Th2/Th1 dependent immune response, associated with increases in Stat3, Socs3, NF-κB, IL-6 and TNF-α [27]. The effect of intradermal administration with TiO₂ nanoparticles as mentioned above should also be understood in relation to acquired immunity. NC/Nga mice treated with TiO₂ nanoparticles showed over production of IL-4 in the skin, IgE and histamine levels in serum, as well as aggravation of skin lesions [22]. Studies using intraperitoneal administration of TiO₂ nanoparticles are valuable for an understanding of the immunological influences of these particles. Larsen et al. showed that mice receiving intraperitoneal treatment with TiO₂ nanoparticles and OVA and subsequently challenged with aerosols of OVA responded with high production of IgE and IgG1 antibodies specific for OVA in serum with increases in eosinophils, neutrophils and lymphocytes in bronchoalveolar lavage fluid (BALF), which suggests induction of a Th2-dominant immune response [28]. Moreover, Moon et al. demonstrated that intraperitoneal injection with TiO₂ nanoparticles results in the damaged development and proliferation of B and T cells, a decreased cytokine production by LPS-stimulated peritoneal macrophages and a decreased

percentage of NK cells in splenocytes, leading to an increased tumor growth of implanted B16F10 melanoma cells [29]. Several *in vitro* studies also provide further information regarding the direct effects of TiO₂ nanoparticles on immune cells. Munidasa et al. reported that TiO₂ nanoparticles showed greater influence on the antigen presenting activity of monocytes and alveolar macrophages [30]. In addition, Moon et al. showed a reduction in lymphocyte proliferation induced by lipopolysaccharide (LPS) or concanavalin A (Con A) upon exposure to TiO₂ nanoparticles [29]. The overall results of these *in vivo* or *in vitro* studies indicate that nano-scaled TiO₂ particles have the potential to cause harmful outcomes if they enter the body. In addition, it is also clear that nano-scaled TiO₂ particles cause greater alteration of immune functions compared with large particles. Therefore, we planned to examine the toxicity of nano-scaled 2D materials composed of titanium and oxygen (TiNSs) on human immune cells.

4. The characteristics of titanate nanosheets (TiNSs)

Techniques to synthesize nano-scaled 2D materials have been studied recently. The basis of this field is derived from the development of methods for manipulating graphene, a carbon nanosheet with a thickness of one atom, which triggered the subsequent development of various 2D nanomaterials [31–33]. It is against this background that inorganic nanosheets have acquired greater interest because they have an ultrathin structure as well as a diversity of compounds and structures leading to various functions [34–36]. Oxide nanosheets are included in the group comprising inorganic nanosheets, and titanate nanosheets (TiNSs) represent a form of oxide nanosheets. Although TiNSs are composed of a TiO₆ octahedron as the particles of TiO₂, TiNSs have the unique crystal structure of lepidocrocite, differing from anatase or rutile, which results in a shape having an ultralow thickness and high aspect ratio [34]. In the 1990s, Sasaki et al. first succeeded in delaminating layered titanate into single titanate nanosheets [37, 38], and TiNSs are now incorporated into useful applications such as photocatalysts, semiconductors and dielectric materials [39–42]. However, the following characteristics suggest possible harmful effects of TiNSs. First, it is noteworthy that TiNSs have a very large surface area per gram due to their ultralow thickness, which is generated from the limited height of one and a half of a sideways TiO₆ octahedron together with the repeated linkage of the octahedron horizontally [34]. Such a large surface of TiNSs might enhance the toxic machinery of bulk titanium particles. Second, the large surface of TiNSs is known to be negatively charged due to oxygen atoms existing at the edges of the octahedron, and this suggests the possible influence of TiNSs through a cationic interaction. In addition to TiNSs delaminated from layered titanate, it has been reported that TiNSs with a small diamond shape and crystal structure of lepidocrocite can be synthesized in a bottom-up manner [43, 44], which allows TiNSs to be synthesized at a small scale. Dr. Yoshioka, one of our colleagues, has modified that method to synthesize TiNSs in our group. **Figure 1** shows images of TiNSs taken by transmission electron microscopy (TEM). The TiNSs showed a diamond shape with about 20- and 30-nm diagonals, which is almost the same as that reported in a previous study [43]. Additionally, the TiNSs showed the characteristic peaks of a lepidocrocite structure confirmed by X-ray diffraction analysis. Since it was verified that TiNSs could be synthesized, we therefore started to examine the effect of TiNSs on human immune cells using *in vitro* experiments.

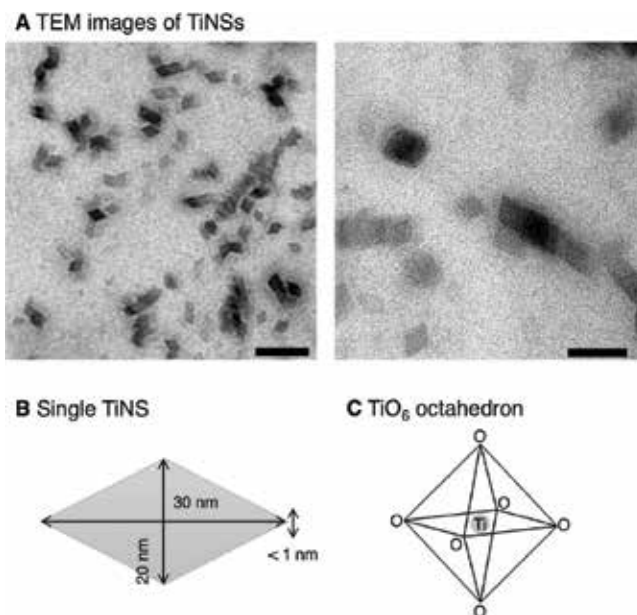


Figure 1. TEM images of TiNSs used in the present study and illustrations of a single TiNS and TiO_6 octahedron. (A) TiNSs were synthesized by Dr. Yoshioka and observed by TEM. These images show the uniform diamond shapes of TiNSs in our present study. Some TiNSs appear to be piled up showing darker diamonds. Scale bars of 100 (left) and 50 nm (right) are shown. (B) Illustration of single TiNSs having a diamond shape with almost 20- and 30-nm diagonals, based on TEM images. (C) Illustration of a TiO_6 octahedron in the orthostatic position, of which TiNSs are composed. TiNSs have the depth of one and a half of a sideways TiO_6 octahedron [34].

5. TiNSs-caused cell death and vacuole formation

Before the culture experiments, the diameters of TiNSs in water and in culture media supplemented with 10% of FBS were measured using a Zetasizer. The results showed that the diameter of about 25 nm in water is consistent with the size estimated by TEM images, while that in the media was about 422 nm, indicating induced agglomeration of TiNSs in the culture media. In addition, TiNSs in water showed a zeta potential of -22.1 mV. To examine the effects of exposure to TiNSs on human immune cells, peripheral blood mononuclear cells (PBMCs) were prepared and cultured with various doses of TiNSs, or with asbestos as a control cytotoxic material, for 7 days. Exposure to asbestos caused an increase in annexin V (Anx)-positive apoptosis of cells when exposed to more than a dose of $1 \mu\text{g}/\text{ml}$ at day 2 after culture, whereas apoptosis was not observed in the culture exposed to TiNSs even at the maximum dose of $10 \mu\text{g}/\text{ml}$. However, exposure to TiNSs caused dose-dependent apoptosis to the same degree as asbestos at day 7 of the culture. The effects of exposure to bulk TiO_2 particles and crystalline silica were compared with TiNSs, but they did not cause apoptosis of PBMCs. The cell death induced by exposure to TiNSs or asbestos, but not to TiO_2 or silica, was also confirmed by measuring the sub-G1 population, apoptotic cells with a low DNA content, using flow cytometry. Interestingly, marked formation of vacuoles was observed in the culture of PBMCs exposed to TiNSs but not the other materials. It was confirmed by staining with fluorescence-labeled antibodies to CD14 that

vacuole formation was present in monocytes but not in lymphocytes. Q-VD-OPh, a pan-caspase inhibitor, suppressed the increase in Anx⁺ cells induced by TiNSs as well as asbestos. The increase in apoptotic cells caused by TiNS exposure was also observed in the culture of isolated CD14⁺ monocytes as well as CD4⁺ lymphocytes. These findings indicate that TiNSs have the potential to cause caspase-dependent apoptosis in immune cells, particularly where monocytes show the formation of large vacuoles prior to apoptosis upon exposure to TiNSs.

6. Identification of intra-vacuolar TiNSs in monocytes

The results obtained from the cell cultures demonstrated the characteristic toxicity of TiNSs for monocytes, comprising apoptosis associated with the striking formation of vacuoles. Therefore, we investigated the presence of intracellular microstructures in monocytes exposed to TiNSs. Monocytes were isolated from human PBMCs, cultured with TiNSs at 10 µg/ml and then harvested at day 1 or 2 after the culture for subsequent TEM observations. The TEM images showed rapid formation of vacuoles in monocytes even at day 1, and the number and size of vacuoles increased at day 2. It is noteworthy that nano-scaled materials with TiNS-like shapes were found within the vacuoles of the monocytes and that most of the material was located near the inner surface of the vacuolar membrane (**Figure 2**). In order to confirm whether these intra-vacuolar nano-scaled materials were TiNSs, we observed the inner surface of the vacuolar membrane in monocytes using scanning electron microscopy (SEM), followed by energy dispersion X-ray (EDX) analysis for titanium. SEM observations showed that there was a rough area in the inner surface of the vacuolar membrane in monocytes harvested at day 1 after the culture with TiNSs. The rough area of the vacuolar membrane was also seen in other monocytes exposed to TiNSs. Analysis of the rough area by EDX confirmed the presence of titanium, in contrast to results for the cytosolic region in TiNS-exposed or control monocytes. These overall findings indicate that TiNSs were actually engulfed by monocytes and included in the vacuoles.

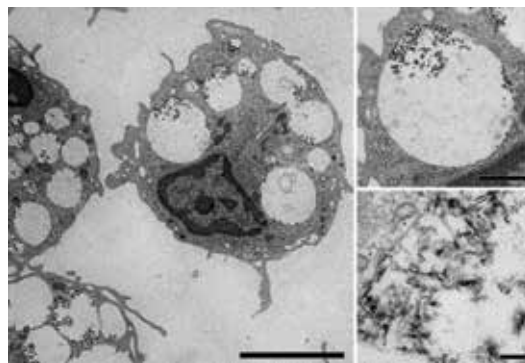


Figure 2. Observation of microstructures in TiNS-exposed monocytes by transmission electron microscope (TEM). The images are taken at day 1 after culture with TiNSs. It can be seen that monocytes have obvious vacuoles even at this early time. Additionally, nano-scaled materials with TiNS-like shapes can be seen inside the vacuoles, and most of the nano-scaled material is located near the vacuolar membrane. Finally, it was confirmed by scanning electron microscopy (SEM) with energy dispersion X-ray (EDX) analysis that these materials included titanium, indicating that the material contained TiNSs. Scale bars of 5 µm (left), 1 µm (upper right) and 100 nm (bottom right) are shown.

7. Relation between TiNSs-caused vacuoles and endosomal pathway

Previous studies have reported formation of vacuoles originating from endocytic organelles, where the vacuolization of late endosomes was induced by the inhibition of kinases for regulation of vesicular transport and sorting [45–47], and several bacterial toxins induced vacuoles having an endosomal/lysosomal origin [48–50]. To examine the relation between TiNS-induced vacuoles and the endosomal pathway, monocyte-derived adherent cells were incubated with fluorescence-dye-labeled dextran to visualize endosome structures. The adherent cells were prepared using a pre-culture of PBMCs. TiNSs were then added to the culture of endosome-visualized adherent cells at 10 $\mu\text{g/ml}$, and observations were then made of vacuoles using the fluorescence derived from dextran. In the control culture without TiNSs, a diffuse fluorescence was observed. However, exposure to TiNSs induced vacuoles in the adherent cells, where most of the vacuoles showed co-localization with the fluorescence derived from endocytosed dextran. These observations indicate that TiNS-induced formation of vacuoles is related with some part of the endosomal pathway.

8. Discussion

Our study revealed the unique toxicity of TiNSs. This 2D nano-scaled material has the harmful potential to cause caspase-dependent apoptosis of immune cells to the same degree as asbestos. In particular, monocytes showed formation of marked vacuoles prior to cell death upon exposure to TiNSs, which were later found in the vacuoles and suggest the actual engulfment of TiNSs by monocytes. A consideration of these findings with the observation regarding co-localization of vacuoles with endosomal dextran indicates that engulfed TiNSs entered the endosomal pathway, leading to the formation of vacuoles in monocytes and subsequent cell death. As mentioned previously, TiNSs have a very large surface area per gram. **Figure 3** represents an illustration showing the large surface area of 2D nano-materials. Nano-scaled spheres with a diameter of 20 nm have a volume of 4189 nm^3 and surface area of 1257 nm^2 . Diamond-shaped nanosheets with diagonals of 20 and 30 nm, a depth of 1 nm and resulting volume of 300 nm^3 have the same density as a nanosphere. The total volume of 14 nanosheets (4200 nm^3) is almost equivalent to the volume of one nanosphere (4189 nm^3), but those nanosheets result in a total surface area of 8400 nm^2 as the sum of both sides, which is 6.68 times as large as the surface area of the nanosphere. Thus, nanosheets have an extremely large surface that probably enhances the chemical activities of titanium oxide, which might contribute to the toxicity of TiNSs. In addition, TiNSs are negatively charged on the surface due to the presence of the oxygen atom, which might cause cationic interference in endo-lysosomes that leads to the formation of vacuoles. Various kinds of stimulation such as oxidative stress disrupt the integrity of the lysosomal membrane and cause lysosomal-membrane permeabilization (LMP), which triggers cell death including caspase-dependent apoptosis [51, 52]. Autophagy is the machinery of the intracellular degradation process, which is also the part of the intracellular membrane system and is linked to the endo-lysosomal pathway [51, 53]. Furthermore, recent studies have been accumulating concerning a new type of cell death associated with large vacuoles, named methuosis, although it is thought

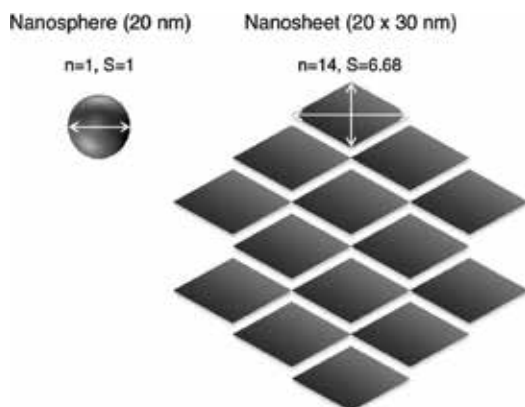


Figure 3. Illustration of a comparison of volume and surface area between nanosphere and nanosheet. A nanosphere with a diameter of 20 nm has a volume of 4189 nm³ and surface area 1257 nm². A diamond-shaped nanosheet with 20- and 30-nm diagonals and depth of 1 nm has the same density as a nanosphere. Fourteen nanosheets have almost the same volume as a nanosphere but possess a total surface area of 8400 nm² as the sum of both sides, which are 6.68 times as large as the surface area of the nanosphere.

that this type of cell death does not require caspases [54, 55]. Some of the machineries mentioned above might be related to the cell death caused by TiNSs. TiNSs in the endosomal pathway might affect immune functions executed by cell surface receptors through interference of endosomal trafficking. Additionally, CD4⁺ lymphocytes were also damaged by exposure to TiNSs, which suggests possible alteration of immune responses in a direct manner caused by TiNSs. Further investigation concerning these issues will contribute to a clarification of the toxic machinery of TiNSs and the immunotoxicological effects of TiNSs.

Acknowledgements

The authors thank Ms. Tamayo Hatayama, Shoko Yamamoto and Miho Ikeda for their technical help. The authors declare that there is no conflict of interests regarding the publication of this chapter.

Author details

Yasumitsu Nishimura^{1*}, Daisuke Yoshioka², Naoko Kumagai-Takei¹, Suni Lee¹, Hidenori Matsuzaki¹, Kei Yoshitome¹ and Takemi Otsuki¹

*Address all correspondence to: yas@med.kawasaki-m.ac.jp

¹ Department of Hygiene, Kawasaki Medical School, Kurashiki, Japan

² Department of Natural Sciences, Kawasaki Medical School, Kurashiki, Japan

References

- [1] Okido M, Nishikawa K, Kuroda K, Ichino R, Zhao ZW, Takai O. Evaluation of the hydroxyapatite film coating on titanium cathode by QCM. *Materials Transactions*. 2002; **43**(12):3010-3014
- [2] Yamamoto D, Iida T, Kuroda K, Ichino R, Okido M, Seki A. Formation of amorphous TiO₂ film on Ti using anodizing in concentrated H₃PO₄ aqueous solution and its osteoconductivity. *Materials Transactions*. 2012; **53**(3):508-512
- [3] Yamamoto D, Kawai I, Kuroda K, Ichino R, Okido M, Seki A. Osteoconductivity of anodized titanium with controlled micron-level surface roughness. *Materials Transactions*. 2011; **52**(8):1650-1654
- [4] Ramanakumar AV, Parent ME, Latreille B, Siemiatycki J. Risk of lung cancer following exposure to carbon black, titanium dioxide and talc: Results from two case-control studies in Montreal. *International Journal of Cancer*. 2008; **122**(1):183-189
- [5] Lee KP, Trochimowicz HJ, Reinhardt CF. Pulmonary response of rats exposed to titanium dioxide (TiO₂) by inhalation for two years. *Toxicology and Applied Pharmacology*. 1985; **79**(2):179-192
- [6] Heinrich U, Fuhst R, Rittinghausen S, Creutzenberg O, Bellmann B, Koch W, et al. Chronic inhalation exposure of wistar rats and 2 different strains of mice to diesel-engine exhaust, carbon-black, and titanium-dioxide. *Inhalation Toxicology*. 1995; **7**(4):533-556
- [7] Robichaud CO, Uyar AE, Darby MR, Zucker LG, Wiesner MR. Estimates of upper bounds and trends in nano-TiO₂ production as a basis for exposure assessment. *Environmental Science & Technology*. 2009; **43**(12):4227-4233
- [8] Schins RP, Knaapen AM. Genotoxicity of poorly soluble particles. *Inhalation Toxicology*. 2007; **19**(Suppl 1):189-198
- [9] Sayes CM, Wahi R, Kurian PA, Liu Y, West JL, Ausman KD, et al. Correlating nanoscale titania structure with toxicity: A cytotoxicity and inflammatory response study with human dermal fibroblasts and human lung epithelial cells. *Toxicological Sciences*. 2006; **92**(1):174-185
- [10] Bhattacharya K, Davoren M, Boertz J, Schins RP, Hoffmann E, Dopp E. Titanium dioxide nanoparticles induce oxidative stress and DNA-adduct formation but not DNA-breakage in human lung cells. *Particle and Fibre Toxicology*. 2009; **6**:17
- [11] Chen HW, SF S, Chien CT, Lin WH, SL Y, Chou CC, et al. Titanium dioxide nanoparticles induce emphysema-like lung injury in mice. *The FASEB Journal*. 2006; **20**(13):2393-2395
- [12] Warheit DB, Webb TR, Sayes CM, Colvin VL, Reed KL. Pulmonary instillation studies with nanoscale TiO₂ rods and dots in rats: Toxicity is not dependent upon particle size and surface area. *Toxicological Sciences*. 2006; **91**(1):227-236
- [13] Warheit DB, Webb TR, Reed KL, Frerichs S, Sayes CM. Pulmonary toxicity study in rats with three forms of ultrafine-TiO₂ particles: Differential responses related to surface properties. *Toxicology*. 2007; **230**(1):90-104

- [14] Kiss B, Biro T, Czifra G, Toth BI, Kertesz Z, Szikszai Z, et al. Investigation of micronized titanium dioxide penetration in human skin xenografts and its effect on cellular functions of human skin-derived cells. *Experimental Dermatology*. 2008;**17**(8):659-667
- [15] Sadrieh N, Wokovich AM, Gopee NV, Zheng J, Haines D, Parmiter D, et al. Lack of significant dermal penetration of titanium dioxide from sunscreen formulations containing nano- and submicron-size TiO₂ particles. *Toxicological Sciences*. 2010;**115**(1):156-166
- [16] Newman MD, Stotland M, Ellis JI. The safety of nanosized particles in titanium dioxide- and zinc oxide-based sunscreens. *Journal of the American Academy of Dermatology*. 2009; **61**(4):685-692
- [17] Bennat C, Muller-Goymann CC. Skin penetration and stabilization of formulations containing microfine titanium dioxide as physical UV filter. *International Journal of Cosmetic Science*. 2000;**22**(4):271-283
- [18] Wu J, Liu W, Xue C, Zhou S, Lan F, Bi L, et al. Toxicity and penetration of TiO₂ nanoparticles in hairless mice and porcine skin after subchronic dermal exposure. *Toxicology Letters*. 2009;**191**(1):1-8
- [19] Yin JJ, Liu J, Ehrenshaft M, Roberts JE, PP F, Mason RP, et al. Phototoxicity of nano titanium dioxides in HaCaT keratinocytes—Generation of reactive oxygen species and cell damage. *Toxicology and Applied Pharmacology*. 2012;**263**(1):81-88
- [20] Xue C, Luo W, Yang XL. A mechanism for nano-titanium dioxide-induced cytotoxicity in HaCaT cells under UVA irradiation. *Bioscience, Biotechnology, and Biochemistry*. 2015; **79**(8):1384-1390
- [21] Hussain S, Smulders S, De Vooght V, Ectors B, Boland S, Marano F, et al. Nano-titanium dioxide modulates the dermal sensitization potency of DNCB. *Particle and Fibre Toxicology*. 2012;**9**:15
- [22] Yanagisawa R, Takano H, Inoue K, Koike E, Kamachi T, Sadakane K, et al. Titanium dioxide nanoparticles aggravate atopic dermatitis-like skin lesions in NC/Nga mice. *Experimental Biology and Medicine (Maywood, N.J.)*. 2009;**234**(3):314-322
- [23] Sager TM, Kommineni C, Castranova V. Pulmonary response to intratracheal instillation of ultrafine versus fine titanium dioxide: Role of particle surface area. *Particle and Fibre Toxicology*. 2008;**5**:17
- [24] Shinohara N, Oshima Y, Kobayashi T, Imatanaka N, Nakai M, Ichinose T, et al. Pulmonary clearance kinetics and extrapulmonary translocation of seven titanium dioxide nano- and submicron materials following intratracheal administration in rats. *Nanotoxicology*. 2015;**9**(8):1050-1058
- [25] van Ravenzwaay B, Landsiedel R, Fabian E, Burkhardt S, Strauss V, Ma-Hock L. Comparing fate and effects of three particles of different surface properties: nano-TiO₂, pigmentary TiO₂ and quartz. *Toxicology Letters*. 2009;**186**(3):152-159
- [26] Chang X, Fu Y, Zhang Y, Tang M, Wang B. Effects of Th1 and Th2 cells balance in pulmonary injury induced by nano titanium dioxide. *Environmental Toxicology and Pharmacology*. 2014;**37**(1):275-283

- [27] Mishra V, Baranwal V, Mishra RK, Sharma S, Paul B, Pandey AC. Titanium dioxide nanoparticles augment allergic airway inflammation and Socs3 expression via NF-kappaB pathway in murine model of asthma. *Biomaterials*. 2016;**92**:90-102
- [28] Larsen ST, Roursgaard M, Jensen KA, Nielsen GD. Nano titanium dioxide particles promote allergic sensitization and lung inflammation in mice. *Basic & Clinical Pharmacology & Toxicology*. 2010;**106**(2):114-117
- [29] Moon EY, Yi GH, Kang JS, Lim JS, Kim HM, Pyo S. An increase in mouse tumor growth by an in vivo immunomodulating effect of titanium dioxide nanoparticles. *Journal of Immunotoxicology*. 2011;**8**(1):56-67
- [30] Munidasa DT, Koike E, Kobayashi T. An in vitro study of the effect of size and timing of administration of titanium dioxide particles on antigen presenting activity of alveolar macrophages and peripheral blood monocytes. *Inhalation Toxicology*. 2009;**21**(10):849-856
- [31] Geim AK. Graphene: Status and prospects. *Science*. 2009;**324**(5934):1530-1534
- [32] Geim AK, Novoselov KS. The rise of graphene. *Nature Materials*. 2007;**6**(3):183-191
- [33] Novoselov KS, Geim AK, Morozov SV, Jiang D, Zhang Y, Dubonos SV, et al. Electric field effect in atomically thin carbon films. *Science*. 2004;**306**(5696):666-669
- [34] Osada M, Sasaki T. Two-dimensional dielectric nanosheets: Novel nanoelectronics from nanocrystal building blocks. *Advanced Materials*. 2012;**24**(2):210-228
- [35] Ma R, Sasaki T. Nanosheets of oxides and hydroxides: Ultimate 2D charge-bearing functional crystallites. *Advanced Materials*. 2010;**22**(45):5082-5104
- [36] Chhowalla M, Shin HS, Eda G, Li LJ, Loh KP, Zhang H. The chemistry of two-dimensional layered transition metal dichalcogenide nanosheets. *Nature Chemistry*. 2013;**5**(4):263-275
- [37] Sasaki T, Watanabe M. Osmotic swelling to exfoliation. Exceptionally high degrees of hydration of a layered titanate. *Journal of the American Chemical Society*. 1998;**120**(19):4682-4689
- [38] Sasaki T, Watanabe M, Hashizume H, Yamada H, Nakazawa H. Macromolecule-like aspects for a colloidal suspension of an exfoliated titanate. Pairwise association of nanosheets and dynamic reassembling process initiated from it. *Journal of the American Chemical Society*. 1996;**118**(35):8329-8335
- [39] Shibata T, Sakai N, Fukuda K, Ebina Y, Sasaki T. Photocatalytic properties of titania nanostructured films fabricated from titania nanosheets. *Physical Chemistry Chemical Physics*. 2007;**9**(19):2413-2420
- [40] Osada M, Ebina Y, Funakubo H, Yokoyama S, Kiguchi T, Takada K, et al. High- κ dielectric nanofilms fabricated from titania nanosheets. *Advanced Materials*. 2006;**18**(8):1023-1027
- [41] Sakai N, Ebina Y, Takada K, Sasaki T. Electronic band structure of titania semiconductor nanosheets revealed by electrochemical and photoelectrochemical studies. *Journal of the American Chemical Society*. 2004;**126**(18):5851-5858

- [42] Sasaki T, Watanabe M. Semiconductor nanosheet crystallites of quasi-TiO₂ and their optical properties. *The Journal of Physical Chemistry B*. 1997;**101**(49):10159-10161
- [43] Tae EL, Lee KE, Jeong JS, Yoon KB. Synthesis of diamond-shape titanate molecular sheets with different sizes and realization of quantum confinement effect during dimensionality reduction from two to zero. *Journal of the American Chemical Society*. 2008;**130**(20):6534-6543
- [44] Ohya T, Nakayama A, Shibata Y, Ban T, Ohya Y, Takahashi Y. Preparation and characterization of titania thin films from aqueous solutions. *Journal of Sol-Gel Science and Technology*. 2003;**26**(1):799-802
- [45] Johnson EE, Overmeyer JH, Gunning WT, Maltese WA. Gene silencing reveals a specific function of hVps34 phosphatidylinositol 3-kinase in late versus early endosomes. *Journal of Cell Science*. 2006;**119**(Pt 7):1219-1232
- [46] Jefferies HB, Cooke FT, Jat P, Boucheron C, Koizumi T, Hayakawa M, et al. A selective PIKfyve inhibitor blocks PtdIns(3,5)P(2) production and disrupts endomembrane transport and retroviral budding. *EMBO Reports*. 2008;**9**(2):164-170
- [47] Cuesta-Geijo MA, Galindo I, Hernaez B, Quetglas JI, Dalmau-Mena I, Alonso C. Endosomal maturation, Rab7 GTPase and phosphoinositides in African swine fever virus entry. *PLoS One*. 2012;**7**(11):e48853
- [48] Papini E, Satin B, Bucci C, de Bernard M, Telford JL, Manetti R, et al. The small GTP binding protein rab7 is essential for cellular vacuolation induced by *Helicobacter pylori* cytotoxin. *The EMBO Journal*. 1997;**16**(1):15-24
- [49] Nagahama M, Itohayashi Y, Hara H, Higashihara M, Fukatani Y, Takagishi T, et al. Cellular vacuolation induced by *Clostridium perfringens* epsilon-toxin. *The FEBS Journal*. 2011;**278**(18):3395-3407
- [50] Johnson C, Kannan TR, Baseman JB. Cellular vacuoles induced by *Mycoplasma pneumoniae* CARDS toxin originate from Rab9-associated compartments. *PLoS One*. 2011;**6**(7):e22877
- [51] Kroemer G, Jaattela M. Lysosomes and autophagy in cell death control. *Nature Reviews Cancer*. 2005;**5**(11):886-897
- [52] Settembre C, Fraldi A, Medina DL, Ballabio A. Signals from the lysosome: A control centre for cellular clearance and energy metabolism. *Nature Reviews. Molecular Cell Biology*. 2013;**14**(5):283-296
- [53] Levine B, Mizushima N, Virgin HW. Autophagy in immunity and inflammation. *Nature*. 2011;**469**(7330):323-335
- [54] Maltese WA, Overmeyer JH. Methuosis: Nonapoptotic cell death associated with vacuolization of macropinosome and endosome compartments. *American Journal of Pathology*. 2014;**184**(6):1630-1642
- [55] Mbah NE, Overmeyer JH, Maltese WA. Disruption of endolysosomal trafficking pathways in glioma cells by methuosis-inducing indole-based chalcones. *Cell Biology and Toxicology*. 2017;**33**(3):263-282

General Cytotoxicity and Its Application in Nanomaterial Analysis

Magdalena Jedrzejczak-Silicka and Ewa Mijowska

Additional information is available at the end of the chapter

<http://dx.doi.org/10.5772/intechopen.72578>

Abstract

The recent increasing interest in the use of different nanoparticles in biological and medical applications encouraged scientists to analyse their potential impact on biological systems. The biocompatibility analyses of novel materials for medical applications are conducted using quantitative and qualitative techniques collected by the International Standards Organization (ISO). The well-known assays, such as tetrazolium-based assays used for mitochondrial function monitoring, LDH for membrane permeability determination and neutral red uptake (NRU) describing lysosome function, need to be optimised due to specific properties of wide range of nanomaterials. Physicochemical properties of nanoparticles (NPs) such as size, composition, concentration, shape and surface (e.g., charge, coating, aspect ratio), as well as the cell type play a crucial role in determining the nanomaterial toxicity (also uptake pathway(s) of NPs). Different nanomaterials exhibit different cytotoxicity from relatively non-toxic hexagonal boron nitride to rutile TiO₂ NPs that induce oxidative DNA damage in the absence of UV light. Finally, the results of the nanomedical analysis can be enriched by holographic microscopy that gives valuable information about the doubling time (DT), cell segmentation, track cell movement and changes in cell morphology. The results can be also completed by phenotype microarrays (PMs) and atomic force microscopy (AFM) techniques that fulfil experimental data.

Keywords: general cytotoxicity, nanomaterials, AFM analysis, holographic analysis, phenotype microarrays

1. Introduction

This chapter is dedicated to selected methods used to analyse the biocompatibility/cytotoxicity of different nanomaterials. The effect of nanomaterials on cellular metabolism and relative viability can differ according to their properties and experimental design. As shown by Frewin et al. [1],

biocompatibility analyses of novel materials for medical applications are conducted using quantitative and qualitative techniques. These techniques have been collected by the International Standards Organization (ISO) 10,993¹ (ISO-10993-1, 2009; ISO-10993-5, 2009; ISO-10993-6, 2007).

Nanotechnology and nanobiotechnology have focused scientists' attention in the last few years on their application in biomedical research, such as detecting and monitoring systems of cells within the body, delivery systems for various drugs, hyperthermia treatment, photodynamic therapy and tissue engineering [2]. The term 'nano' may be considered a different state of aggregation of matter in all its states—solid, liquid, gas and plasma [3].

The phenomenon of nanoparticles is based on their different physical (optical and electromagnetic), chemical (catalytic) and mechanical properties that depend on particle size, as well as surface and quantum effects. The surface effects manifest as scaling of physical properties (increased atomic fraction on particle surface compared to the interior), which includes increased chemical reactivity and reduced melting point of nanoparticles compared to larger particles of bulk material. NPs have a very large surface area in comparison to microparticles and larger materials, making this large surface area available for chemical reactions [4]. In addition, nanoparticles can be classified according to their composition (inorganic and organic, lipid-based and polymeric NPs), dimensionality, morphology, uniformity and agglomeration [Table 1] [3, 5]. Another classification divides nanomaterials into three groups: zero-dimensional materials (quantum dots), varying in shape and diameter; one-dimensional materials (nanorods and nanowires) and two-dimensional materials (nanobelts, nanodisks and nanosheets) [2].

The toxicity and cytotoxicity of nanomaterials are complex and depend on various factors, such as chemical composition, crystalline structure, size (at the nanolevel, the basic physicochemical properties of materials can change with variation in size) or aggregation. Nanomaterial composition determines its chemical interaction with cells, cellular uptake mechanisms and intracellular localisation. Chemical composition may also induce oxidative stress. For example, silver nanoparticle aggregates are more toxic than asbestos; CNTs are highly toxic and evoke much more damaging effect to the lungs than carbon black or silica NPs, but titanium oxide, iron oxide and zirconium oxide NPs are less toxic than asbestos [3, 6].

The crystalline structure effect of NP toxicity causes that some nanomaterials with a specific crystalline structure do not exhibit high toxicity, but other allotropes can strongly affect cell viability and exert an effect on human organism. Sato and co-workers [7] demonstrated that TiO₂ allotropes exhibited different toxicity. Rutile TiO₂ NPs (200 nm) induced oxidative DNA damage in the absence of UV light and also TiO₂ NPs (10–20 nm) stimulated reactive oxygen species (ROS) production under corresponding conditions; in contrast, anatase NPs of the same size did not cause this effect [3, 8, 9].

Another factor that determines nanomaterial toxicity is the size of NPs. In most cases, smaller nanoparticles are able to pass through physiological barriers. Small-size nanoparticles can

¹ISO-10993 ISO-10993-1 (ISO-10993-1 (2009) - Biological evaluation of medical devices — Part 1: Evaluation and testing within a risk management process; ISO-10993-5 (2009) - Biological evaluation of medical devices — Part 5: Tests for in vitro cytotoxicity; ISO-10993-6 (2007) - Biological evaluation of medical devices — Part 6: Tests for local effects after implantation

Classes	Types	Structure	Size	Properties
Carbon-based nanoparticles	Carbon nanotubes (CNTs)	Single-walled CNT (SWCNTs)	Diameter between 0.4 and 100 nm; length between several nanometres up to centimetres	Improved compressive strength, tensile bending strength, flexural strength, durability, piezoelectric response, sensing ability
		Multi-walled CNT (MWCNTs)		
	Graphene (GF) and graphene oxide (GO)	Hydrophobic two-dimensional single monoatomic layers (GF) Oxidised form of GF (GO)	From 0.1 up to 300 μm	Large area; its surface can be easily functionalized with functional groups; ideal for high drug loading via π - π stacking, hydrophobic or electrostatic interactions; exceptional mechanical properties
	Nanodiamonds (ND)	Truncated octahedral structure	Diameter between 2 and 10 nm	Large area, enhanced biocompatibility, good mechanical strength, surface functionality, colloidal stability
Inorganic nanoparticles	Gold nanoparticles (GNPs, AuNPs)	Colloidal gold, nanorods, nanowires	Sizes of 1–100 nm	Absorb and scatter light; catalyst applications; anti-fungal, anti-microbial properties
	Silver nanoparticles (AgNPs)	Colloidal silver, spherical silver nanoparticles, diamond, octagonal, thin sheets	Diameter between 1 and 100 nm in size	Significant anti-microbial properties
	Iron oxide nanoparticles (IONPs)	Magnetite (Fe_3O_4); oxidised form maghemite ($\gamma\text{-Fe}_2\text{O}_3$)	Sizes of 1 and 100 nm	Superparamagnetic properties; the surface area-to-volume ratio is significantly high; higher binding capacity and excellent dispersibility
Mesoporous nanoparticles (MSN, MSNPs)	Nanosilica	Solid material with a porous, hexagonal, cubic and cage type	50–300 nm	Porous structure and large surface area; chemical stability; surface functionality and biocompatibility

Table 1. Types of nanomaterials [3, 5, 7].

enter cells by phagocytosis and other mechanisms (e.g., micropinocytosis, receptor-mediated endocytosis (RME) pathways mediated by caveolae, clathrin and caveolae/clathrin-independent endocytosis) [10, 11]. NP ability to enter the cells determines adhesive interactions, such as van der Waals forces, steric interactions or electrostatic charges [3, 12, 13]. Moreover, NPs smaller than 100 nm are not phagocytized as opposed to larger nanoparticles, but they enter via RME pathways [2, 11]. NP uptake can also occur in the absence of specific cell surface receptors. Nanoparticles smaller than 50 nm can easily enter most cells (with greater cytotoxicity),

while nanoscale devices smaller than 20 nm can cross blood vessels and cumulate in tissues [2]. Particles with larger surface area display tendency to agglomerate in the liquid, interact with molecules, such as proteins and DNA and may cause oxidation and DNA damage [3, 4, 14].

It is known that the shape (aspect ratio) also determines cellular uptake efficiency and may affect cell viability. Additionally, surface chemistry of nanomaterials modulates the response of biological systems and distribution in the organism. Surface functionalisation (with Fe_3O_4 , gold nanoparticles; type of bonding on the surface, e.g., covalent, noncovalent; dispersing agents, e.g., PEG) is a crucial factor that can significantly change the toxicity of NPs and prevent NPs from aggregating; it can also change their fate in biological systems [2, 3, 11]. For example, functionalization of MWCNTs with sodium sulfonic acid salt ($-\text{SO}_3\text{Na}$ or -phenyl- SO_3Na) increased their biocompatibility in comparison with unfunctionalised or carboxylic acid-functionalized ($-\text{COOH}$) MWCNTs [15]. Cellular uptake depends on different factors, such as nanomaterial and cell type, but also on environmental properties and the complexity of culture media. These specific conditions determine the aggregation process, which makes the interpretation of data on nanoparticle biodistribution or uptake difficult [3]. NP agglomerates affect and limit the direct extrapolation of *in vitro* data (providing a basis for understanding the mechanism of NP cytotoxicity and their uptake at the cellular level) to *in vivo* exposure [11, 16].

Intercellular localization of NPs and their interaction with cell components, such as the membrane, mitochondria, lysosomes and/or nucleus, are essential [11]. NPs can affect cell and organelle membranes, induce oxidative stress (ROS), DNA damage and mutagenesis and evoke apoptosis and protein up-/downregulation [11]; they can also modulate immune response [3, 17].

2. Nanoparticle cytotoxicity analyses and their limitations

The cytotoxicity study is an essential and crucial step in testing novel substances/nanomaterials in the context of biological and medical applications. Assays based on tetrazolium salts, like MTT (2-(4,5-dimethyl-2-thiazolyl)-3,5-diphenyl-2H-tetrazolium bromide), nitroblue tetrazolium (NBT) and the second-generation tetrazolium salts, such as XTT (sodium 2,3-bis(2-methoxy-4-nitro-5-sulfophenyl)-5-[(phenylamino)-carbonyl]-2H-tetrazolium inner salt), MTS (5-[3-(carboxymethoxy)phenyl]-3-(4,5-dimethyl-2-thiazolyl)-2-(4-sulfophenyl)-2H-tetrazolium inner salt) and WST-1 (sodium 5-(2,4-disulfophenyl)-2-(4-iodophenyl)-3-(4-nitrophenyl)-2H-tetrazolium inner salt) are basic tools for cytotoxicity determination, but nanomaterial testing is associated with certain challenges. The type of nanomaterials, manufacturing conditions, colloidal dispersion, chemical purity and photocatalytic activity of NPs may determine the usage of most traditional assays. Interactions between nanoparticles and molecules (i.e., reactants) used in well-established assays significantly affect the results and are one of the reasons of result variations [18, 19]. In assays based on colorimetric and fluorescence measurements, it has been found that nanomaterials, such as carbon nanotubes (CNTs), graphene/graphene oxide nanosheets, TiO_2 nanoparticles or boron nitride, interact with chromophore molecules, which may lead to false-positive results [19–21]. In other cases, the total surface area of NPs was sufficient to adsorb the reagent or fluorescent molecules, especially those with aromatic rings, which in turn led to false-negative results [21]. These results suggest

using alternative cytotoxicity assays based on tetrazolium salts, e.g., XTT, WST-1, INT or other assays that complement the analysis, e.g., Alamar Blue (AB), neutral red uptake (NRU) assay, LDH leakage assay, flow cytometry, cell death analysis (using trypan blue or annexin V/propidium iodide), protein concentration measurements using the Bradford assay, measurements of mitochondrial membrane permeability (MMP) or loss of glutathione (e.g., GSH) and the activation of proinflammatory cytokines (e.g., IL-6, IL-8 and/or TNF- α) [15, 19, 21].

A number of studies have been carried out to verify the effect of NPs on assay reagents [22]. Wörle-Knirsch and co-workers [23] indicated that CNT analysed using the MTT assay caused false-positive results due to the strong interaction between CNT and the insoluble formazan crystals [19, 23]. In the aforementioned study, SWCNTs were analysed on A549 (human alveolar epithelial cell line), ECV304 (endothelial cells derived from umbilical cord) and NR8383 (rat alveolar macrophage cell line) cell cultures and the results obtained in the MTT assay were verified by WST-1, LDH, mitochondrial membrane potential (MMP) and annexin V/PI analysis. The MTT assay indicated that SWCNTs affected cell viability, reducing it almost by 60% after a 24-h incubation period. Moreover, the decreased cell viability did not recover after longer incubation or higher concentrations of nanotubes. The results of the MTT assay were verified using WST-1, and no reduction in viability was detected. LDH and MMP assays confirmed WST-1 results, and flow cytometry using annexin V/propidium iodide showed lack of necrosis and/or apoptosis. Wörle-Knirsch et al. [23] concluded that nanotoxicological assays needed standardising with regard to the tested nanomaterial

Lupu and Popescu [24] used the MTT assay to evaluate TiO₂ toxicity. The effect of TiO₂ nanoparticles on living models is crucial due to their utilisation in food, beauty care and pharmacology industries. Additionally, TiO₂ nanoparticles are known to exhibit photocatalytic properties: the ability to catalyse redox reactions of molecules adsorbed on the surface during light exposition ($\lambda < 385$ nm). Photocatalytic reaction may occur by direct charge transfer of electrons (e^-) and holes (h^+) generated by light on the surface of titania nanoparticles. The reaction may be also mediated by reactive oxygen species (ROS), e.g., hydroxyl radicals (OH) or superoxide anions (O_2^-) formed at the interface of TiO₂ and water. Lupu and Popescu [24] clearly demonstrated that TiO₂ nanoparticles induced transformation of noncellular MTT to formazan. Formazan formation was found to be proportional to titania NPs, and this process was enhanced by daylight exposure. Moreover, the results obtained in the experiment without cellular model were validated using three cell lines—V79-4, HeLa and B16. The results demonstrated false viability that increased up to 14% for TiO₂ concentrations higher than 50 μgml^{-1} [24]. In addition, the TiO₂-MTT reaction was analysed in PBS environment. The reaction rate (formazan production rate) was proportional to TiO₂ and UV radiations (at 312 and 365 nm wavelengths) and inversely proportional to initial concentration of MTT. Moreover, reaction efficiency was enhanced by the presence of Na₂HPO₄ (phosphate concentration of 0.005 M for maximum efficiency), which is the basic component of PBS [25].

Casey et al. [26, 27] proved that single-walled carbon nanotubes (HiPco®) interacted with indicator dyes applied in Coomassie Blue, AlamarBlue™, neutral red uptake, MTT and WST-1 assays. In all cases, nanotubes interacted with dyes, which resulted in the reduction of the associated absorption/fluorescent emission. A spectroscopic study demonstrated that SWCNTs interacted with Coomassie and reduced the absorbance for all concentrations tested

(0.003–0.800 mgml⁻¹). As regards the AlamarBlue™ analysis (fluorescent measurements of all single-walled carbon nanotube solutions), quenching was monitored as a function of SWCNT concentration and plotted as an emission ratio at 595 nm by 540 nm excitation for the AB assay (5% solution of AB in culture medium) against SWCNT concentration. Another assay measuring NR uptake also showed SWCNT's ability to quench NR emission and was described as a function of SWCNT concentration. The MTT assay used in the cited study was found to interact with CNT. The reduction in MTT was associated with SWCNT concentration (absorption reduction was higher with increasing SWCNT concentration). For the WST-1 assay, it was concluded that the reduction in WST-1 absorbance was dependent on nanotube concentrations above 0.0125 mgml⁻¹. Casey et al. concluded that Coomassie, AB, NRU, MTT and WST-1 assays were not appropriate for the cytotoxicity analysis of carbon nanotubes [26, 27].

Limitations of MTT in cytotoxicity studies on graphene and graphene-related materials have been demonstrated in numerous publications. CCK-8 (tetrazolium-8-[2-(2-methoxy-4-nitrophenyl)-3-(4-nitrophenyl)-5-(2,4-disulfophenyl)-2H-tetrazolium] monosodium salt) assays are an attractive alternative for the MTT test. Evaluation of graphene adsorption was based on cell-free adsorptive experiments and demonstrated a gradual reduction of MTT to 93% during 2-h incubation, whereas CCK-8 was significantly reduced to 73% after exposure to graphene for 2 h. The intensity of graphene adsorption to MTT and CCK-8 was time-dependent. The quantity of the CCK-8 reagent absorbed by graphene was higher than that of MTT. It was reported that the π - π conjugated system of the CCK-8 molecule was much stronger than that of MTT due to three benzene rings and one five-membered heterocycle. MTT contains only two benzene rings and two five-membered heterocycles. Another reason for that process is that benzene ring groups strongly affect the adsorption. It was also noted that graphene can suppress the fluorescence effect caused by electron transfer from the dye molecule to the graphene surface. Although MTT and CCK-8 reagents are not fluorescent dyes, both of them display a positive electron on the molecules, similar to some known fluorescent dyes. Thus, it is possible that electron transfer occurs during the incubation with graphene and interferes with the dye molecule that contacts the enzymes. Jiao et al. noted that CCK-8 molecules can be more significantly disturbed by graphene than by the MTT reagent. Additionally, optical properties of graphene may also result in the loss of light signals used for detection in assays *in vitro* [28].

Cytotoxicity can also be determined using the lactate dehydrogenase (LDH) assay. The LDH assay is performed to exclude interactions between nanomaterials and fluorophore molecules [19]. The LDH assay, similar to the MTT assay, is a colorimetric method; thus, it can also interact with nanoparticles (e.g., CNT). Formazan crystals can be absorbed on the surface of MWNT (multi-walled nanotubes) through a strong π - π stacking interaction. The analysis of Ali-Boucetta et al. [19] proved that media containing the released LDH showed the same absorbance (at 490 nm) as MWNT:F127 (multi-walled nanotubes dispersed in the presence of Pluronic 127) dispersion in culture media. Ali-Boucetta et al. [19] proposed LDH assay modification that would eliminate the potential risk of interference of assay components with NPs (modified method vs. traditional procedure is presented in **Figure 1**).

In the experiment of Han et al. [29], copper (Cu-40), silver (Ag-35 and Ag-40) and titanium dioxide (TiO₂-25) were used to validate the popular assay. It was found that LDH was inactivated in

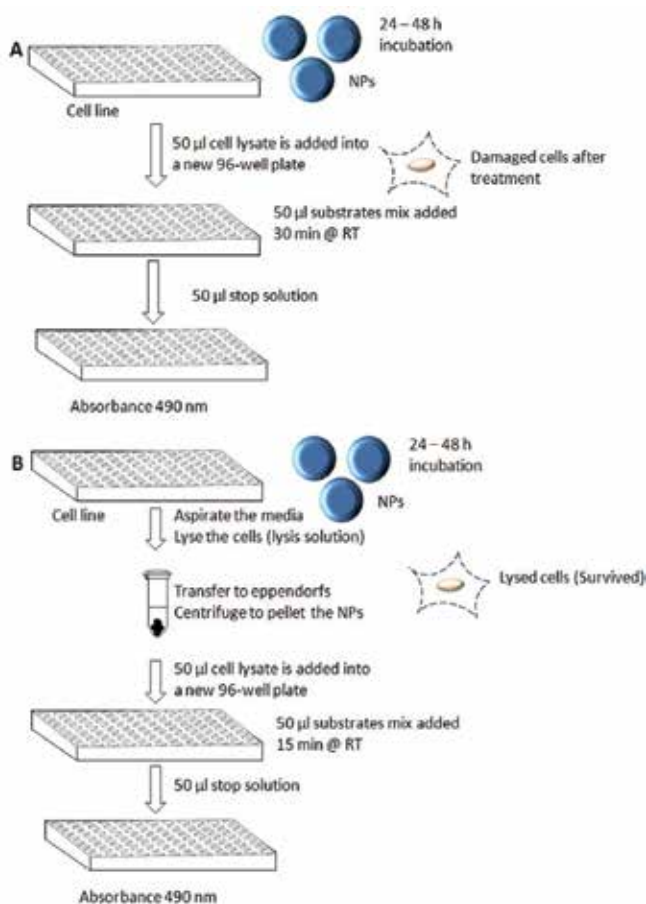


Figure 1. Schematic of the original (A) and modified LDH assay (B) [19].

the presence of Cu-40 and Ag-35 in a dose-dependent manner. The effect of TiO₂-25 and Ag-40 NPs was not significant. In conclusion, these authors underlined the necessity to interpret the results with caution because of metal-catalysed oxidation [29].

Wang et al. [30] proposed modifying the LDH assay that would correct the erroneous results caused by potential interference of nanotubes with reporter chromophore, resulting in its adsorption on nanoparticle surface. The idea of this modification is based on the incubation of LDH derived from a known number of cells (e.g., DH82 macrophage cells) or a purified LDH standard (lactic dehydrogenase enzyme purified from rabbit muscle) with a precise amount (at different concentrations ranging from 5 to 100 µgml⁻¹) of SWCNT or SWCNT-ox (carbon nanohorns). This additional procedure enables the quantification of the effects of NPs on the LDH level. The results obtained by Wang and co-workers clearly demonstrated that LDH concentrations decreased with increasing CNT concentration (at a wavelength of 490 nm). On the other hand, the 580 nm peak was elevated at the increased maximum absorbing wavelength. Based on the observation and regression analyses performed by Wang et al. [30], it was suggested that

LDH assay results should be verified by calibration curves in the presence of different SWCNT concentrations (in the range of 5–100 μgml^{-1}) at two wavelengths, 580 and 490 nm, for each LDH assay. This procedure more accurately determines cellular toxicity values [30].

Smith et al. [31] presented a simple protocol modification of the LDH analysis, which included membered additional conditional-specific controls. This modification enables accurate simultaneous measurement of the effects of death and growth inhibition. The additional step provides quantitative information that can be useful in applications such as drug discoveries [31]. Another approach in LDH assay analysis was proposed in the experiments of Chan et al. [32]. Modification of the LDH protocol allows to detect necrosis, including secondary necrosis [32].

In addition, calcein AM (CAM), Live/Death, neutral red, CellTiter®, Aqueous One (96 AQ), Alamar Blue (AB), CellTiter-Blue® (CTB), CytoToxOne™, and flow cytometry were used to determine their utility in nanoparticle toxicity evaluation. In the cited study, it was found that the results of the assay that depended on direct staining of cells were difficult to interpret, because of dye interactions with NPs. The 96 AQ assay proved optimal for NP analysis. The results were not significantly altered by interactions between the test factor and reagents in the assay [16].

Herzog et al. [33] suggested the clonogenic assay to determine real cytotoxic effect on cell cultures due to the false results (positive or negative) that may occur in NP testing. The clonogenic assay (colony formation assay) is based on the ability of a single cell to form a colony. The latter study was based on the ability of A549, BEAS-2B (normal human bronchial epithelial cells) and HaCaT (normal human keratinocytes) cells to form colonies after 7 (for HaCaT cells) and 10 (for A549 and BEAS-2B) days of incubation with SWCNT (HiPco®). The EC_{50} comparison showed that the A549 cell line was more resistant than the other two lines. On the other hand, the analysis based on colony size showed that A549 was more sensitive than HaCaT cells. Although the clonogenic assay provided more accurate results than colorimetric tests, it did not become popular because it was too time-consuming for rapid toxicity screening [19, 33].

3. Difficulties in nanomaterial cytotoxicity analysis: Aggregates, protein corona and NP degradation

Nanomaterials are intensively studied as promising candidates for biomedical applications (e.g., targeted delivery of therapeutic drugs and medical imaging) with a purpose of eventual human administration [34]. NP design for medical applications should not only meet requirements, such as biocompatibility and biodegradability, but also site-specific delivery, long blood circulation and high cargo loading capacity [35]. Different nanomaterials show unique physical and chemical properties that depend, among others, on the type of materials (e.g., Au or Ag, Fe_3O_4 , graphene and graphene oxide), hydrodynamic size, surface charge and aggregation behaviour and have been found to interact, often immediately (within seconds), after contact with biological systems, such as blood or tissue [34, 36, 37]. Nanoparticle aggregation via electrostatic screening can occur in complex aqueous mixtures of cell culture media that contain electrolytes, proteins, lipids and metabolites (highly ionic environment) [11, 38].

NPs at higher concentrations tend to form aggregates (agglomerates) under artificial conditions of *in vitro* cell cultures [16]. Many experiments found that NPs that form aggregates were not as cytotoxic as the same NPs at lower concentrations. Lower concentrations of NPs resulted in better internalisation and biodistribution in the circulatory system and organs [3]. Aggregation process is caused by magnetic attraction forces (types 1, 2 and 4), hydrophobic-hydrophobic interactions (for type 1) or hydrogen bonding between hydroxyl groups [39]. Different types of nanomaterials exhibit different tendency to form aggregates in PBS and culture media. CNTs have a strong tendency to agglomerate due to van der Waals interactions [40]. Metal oxides display higher tendency to form agglomerates in comparison to MWCNT. Metal oxides differ in size but were of similar size in PBS environment; thus, it was concluded that surface chemistry and/or the environment had a more significant effect on the aggregate formation process [14]. The size of aggregates may be dependent on the concentration and they tend to be slightly larger in culture media than in PBS. Moreover, monovalent and divalent cations may affect aggregate formation. Adsorption of media components, serum proteins and Ca^{2+} on nanoparticle surface determines NP aggregations and size distribution [14]. Agglomeration leads to cytotoxicity reduction, because of lower availability of inorganic NPs in contact with cells. In addition, the size of aggregates prevents their cellular internalisation [39]. Studies based on silica nanoparticles indicated that minimization of NP aggregation could be obtained by introducing an optimum balance of inert (e.g., methyl phosphonate) and active (e.g., hydroxyl and aldehyde) functional groups to the surface [41].

The protein layer of several nanometres on particle surface is called protein corona and it can be divided into a peripheral *soft* corona (SC)—dynamic protein exchanges with the surrounding medium—and a *hard* corona (HC)—a layer of more or less temporal constant composition (**Figure 2, Table 2**) [34, 42, 43]. In blood plasma, the surface of nanoparticles mainly adsorbs proteins, but some minor traces of lipids have also been found in the corona structure. Adsorption of proteins on the nanoparticle surface is the result of protein-nanoparticle binding affinities and protein-protein interactions. *Hard* corona interacts directly with the nanomaterial surface. *Soft* corona proteins interact with the hard corona via weak protein-protein interactions. Interestingly, the corona on the NP surface does not completely mask the nanomaterial surface or its functional groups [43]. The formation of protein corona and its thickness is a parameter that is also dependent on protein concentration, temperature, duration of particle-protein interaction, serum concentration and shear stress [34, 44].

Protein corona formation strongly affects cellular uptake mechanism, cell-nanoparticle interactions, intracellular location as well as cellular response (e.g., biocompatibility) [34, 35, 44]. The protein corona on the NP surface is hypothesised to hinder interactions of nanoparticle ligands and the targets on the cell surface [44, 47].

The study of Mirshafiee et al. [44] found that the protein corona formed on BCN-NPs (NPs functionalized with bicyclononyne) incubated in medium with 10% serum and 100% serum consisted of abundant proteins, such as chain A, a novel allosteric mechanism in haemoglobin, fetuin, haemoglobin foetal subunit beta or apolipoprotein A-II precursor. It was also reported that $\geq 88\%$ of proteins in BCN-NP coronas had a molecular weight below 30 kDa. Even relatively low molecular weight proteins created corona that significantly reduced NP

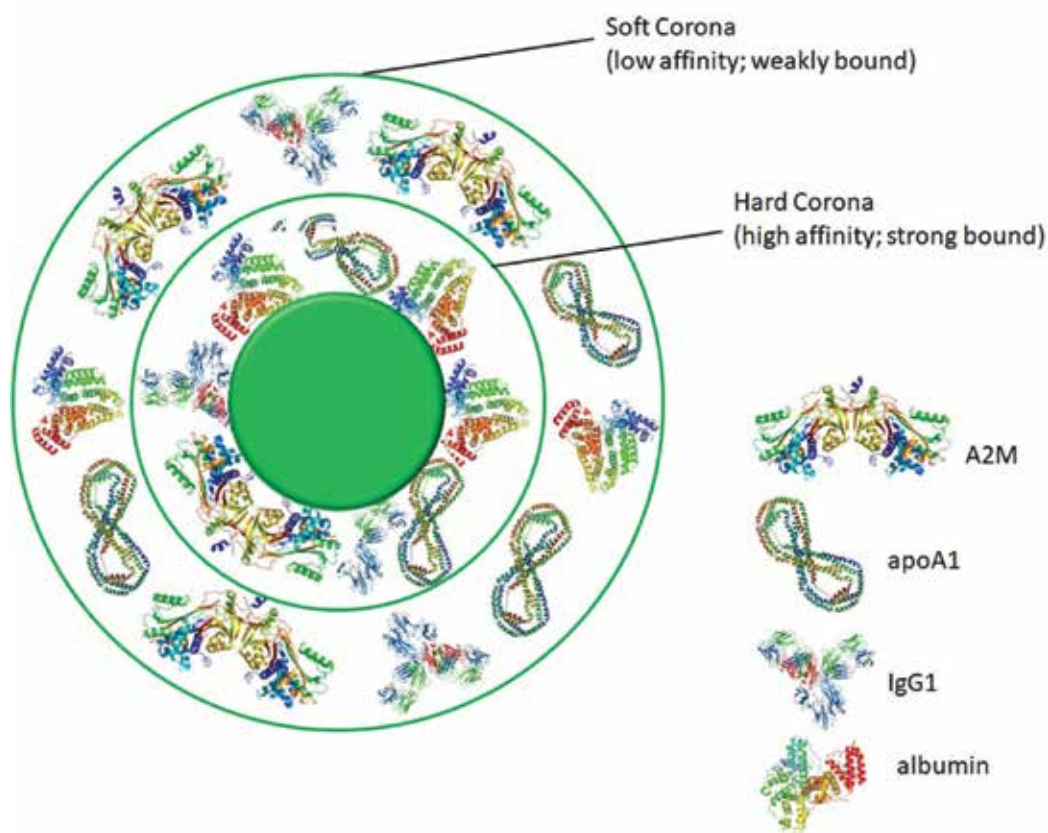


Figure 2. Structure of protein corona [34, 42, 43, 45].

targeting efficiency [44]. Single-walled carbon nanotubes (HiPco®) were also found to interact with cell culture medium and its components. Casey et al. described that SWCNT interacted with the medium via physisorption through van der Waals forces [26, 48].

The process of protein corona formation has a decisive influence on nanoparticle-induced toxicity. For example, silica nanoparticles (AmSil30) precoated with human plasma caused lower cell-death induction in primary human endothelial cells and microvascular endothelial cell line (ISO-HAS1). The resulting effect was dependent on the time of corona formation. The most significant effect was recorded for the early corona, but prolonged incubation with plasma (>30 min) did not counteract membered toxicity [49]. In another example, thrombocytes were used to study the protein corona effect on the biological model. In the latter study, nanoparticles exposed to human plasma for 0.5 min did not activate thrombocytes to form aggregates due to the presence of the plasma protein corona [49]. The impact of protein corona formation on cellular uptake and dispersion state of nanoparticles after exposure to plasma was also investigated. It was found that NPs were monodispersed after short-time exposure (<10 min), whereas aggregates started to form during prolonged exposure (>30 min), but the

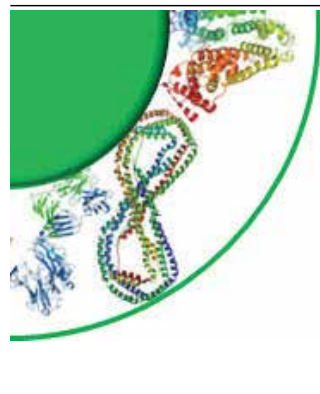
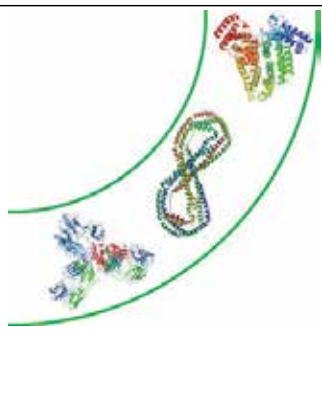
Hard corona	Soft corona
	
<p>Tightly bound proteins</p> <p>Large binding energy adsorption ($\uparrow \Delta G_{ads}$)</p> <p>Lower dissociation rate of proteins with nanoparticles ($\downarrow k_{off}$)</p> <p>Directly interacting with surface of nanoparticles</p> <p>Stable on nanoparticle surface; able to influence the functional response</p>	<p>Loosely bound proteins</p> <p>Low binding energy adsorption ($\downarrow \Delta G_{ads}$)</p> <p>Higher dissociation rate of proteins with nanoparticles ($\uparrow k_{off}$)</p> <p>Protein-protein interaction</p> <p>Fleeting on nanoparticles; irrelevant for the functional response</p>

Table 2. Characteristic features of hard (HC) and soft corona (SC) [46].

tendency to form aggregates was mostly dependent on physicochemical properties of NPs. However, Tenzer et al. [49] did not describe negative effects of AmSil30 precoated with the protein plasma corona. Biological effects of protein-NPs were analysed using two lines: HeLa and U937 [43, 50]. The study conducted by Maiorano et al. [50] demonstrated that AuNPs incubated in two different culture media (DMEM and RPMI) exhibited different protein coronas. RPMI-treated NPs had less prominent protein coronas and, as a consequence, induced stronger toxicity of HeLa and U937 cells [50]. The study of Gräfe et al. [34] reported that the presence of the protein corona reduced the interaction of human brain microvascular endothelial cells (HBMEC) with magnetic nanoparticles coated with PEI (polyethylenimine) during 30 min of incubation [34].

Nanoparticle-induced pathological effects, such as cell death, coagulation, thrombocytosis or cytotoxicity, are also dependent on the type of NPs, but selected cellular model is also crucial in this kind of experiments [49, 51]. For example, polystyrene-based NPs (PS) with different PS-COOH and PS-PO₃ groups coated with the serum protein were effectively taken up by both exposed cell lines (HeLa and hMSCs). NPs with PS-NH₂ and PS-SO₃ groups showed lower uptake by both cell lines [51].

The composition of protein corona was analysed using various methods and it was demonstrated that albumin, immunoglobulin G (IgG), fibrinogen and apolipoproteins were present in

the corona of all the analysed nanoparticles [43]. Corona identification and composition analysis (**Table 3**) provide not only information about its complexity, conditions of PC formation and physicochemical features but also data on toxicity, cellular interactions and uptake, targeting and finally the usefulness in nanomedicine [46].

For example, Urbas et al. [52] demonstrated that three types of nanoparticles, NPs-GO, Fe_3O_4 , and $\text{GO-Fe}_3\text{O}_4$, displayed the ability to deplete various quantities of serum proteins from culture media (**Figure 3**). Graphene oxide and nanocomposite $\text{GO-Fe}_3\text{O}_4$ showed an increase in protein adsorption from culture medium. The results of the bicinchoninic acid (BCA) assay indicated different capacities of NPs to adsorb proteins in cell cultures [52].

Protein corona composition is also known to affect nanoparticle-cell interactions and biological fate of nanomaterials in cells. Gunawan and co-authors characterised the term ‘biological fate’ as describing the subcellular localisation of NPs and the distribution of NPs to specific organs *in vivo* [53]. An interesting study performed by Lesniak et al. [54] showed that silica (SiO_2) nanoparticles (50 nm) exposed to biological fluids (e.g., serum) mediated the interaction of NPs (at $100 \mu\text{g mL}^{-1}$ concentration) with A549 cells. Silica nanoparticles showed different degree and process of internalisation during incubation with the A549 cell line in complete (with 10% foetal bovine serum) and in serum-free medium. NP integration was higher in serum-free medium with accumulation in lysosomes and some of NPs localised free in the cytosol. On the contrary, NPs in complete medium (in the presence of a well-developed corona) were never observed free in the cytoplasmic matrix, but similar to serum-free medium, silica nanoparticles were found to accumulate in lysosomes. Lesniak et al. [54] observed that nanoparticles showed higher tendency to adhere to the cell membrane in serum-free conditions and concluded that the initial stronger adhesion could have partly contributed to higher uptake efficiency. Moreover, the presence of free NPs in the cytosol might be caused by perturbation of the early uptake pathway in cells exposed to serum-free medium (rather than an endogenously regulated cellular process) [53, 54].

Other results described various biological responses of different cell types to NPs with protein corona layers [53]. Single-walled carbon nanotubes preferentially bound IgM relative to IgG

Feature	Techniques for PC analysis
Isolation of NPs-PC	Centrifugation, size exclusion chromatography (SEC), magnetic separation/magnetic flow field fractionation (MgFFF)
PC structure analysis	Dynamic light scattering (DLS), differential centrifugal sedimentation (DCS), transmission electron microscopy (TEM)
Protein quantitation	Bicinchoninic acid (BCA) assay, Bradford assay, thermogravimetric analysis (TGA)
Binding affinity/stoichiometry and protein interaction	Fluorescence correlation spectroscopy (FCS), size exclusion chromatography (SEC), isothermal titration calorimetry (ITC), surface plasmon resonance (SPR), quartz crystal microbalance (QCM), Z-potential measurement, <i>in silico</i> simulation
PC composition	One-dimensional gel electrophoresis (1-DE or SDS-PAGE), two-dimensional gel electrophoresis (2-DE), mass spectrometry (MS)

Table 3. Analytical methods for corona evaluation [46].

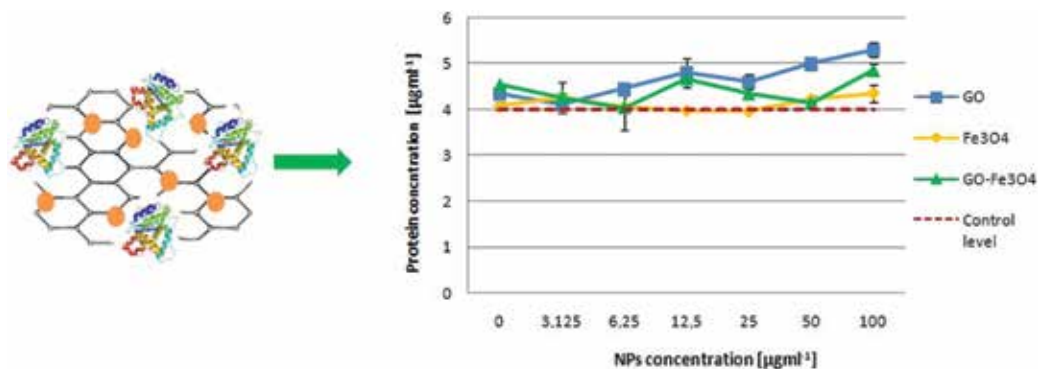


Figure 3. Protein adsorption onto tested NPs after 48-h incubation period in complete cell growth medium [52].

on PEG-SWCNTs due to the surface charge and the conformation of surface functional groups (PEG); this resulted in higher accumulation of the aforementioned NPs in the liver compared to the spleen [55]. Poly(D,L-lactide)-based NPs showed interaction of surface functional group (covalently conjugated with apoB₁₀₀ antibody) with LDL and were highly accumulated by liver macrophages [56]. Solid lipid nanoparticles (SLNs) modified with PEG induced the ABC phenomenon (accelerated blood clearance) upon repeated injections in mice and beagles. Moreover, PEGylated SLNs promoted liver/spleen uptake of NPs [57].

The application of polyethyleneglycol (PEG) for nanoparticle modifications reduces (but not totally suppresses) nonspecific protein corona formation [35, 51]. On the other hand, zwitterionic NPs were described to lack the protein corona [51].

The use of different nanomaterials for biomedical applications is indispensably associated with wide physico-chemical and biocompatibility analyses. The analysis of the effect of nanomaterials on different types of cells in various experimental conditions is an essential step in assessing the response of biological models (*in vitro* and/or *in vivo*) to direct contact with NPs [2]. On the other hand, cells/cell culture conditions as well as living system/biological fluids also affect morphological and physico-chemical properties of nanomaterials. Interesting results were obtained in the degradation process of sandwich-like mesoporous silica flake (mSiO₂) nanomaterial (developed as anticancer drug system) exposed to PSB solution for 24, 48 and 96 h. TEM analysis of mSiO₂ [Figure 4] showed that the porous structure of nanomaterial was degraded already after 24-h incubation in PBS [Figure 4a]. Another deformation found in mSiO₂ flake analysis was visible as large holes [Figure 4b-d]. The intensity of mesoporous silica flake degradation was time-dependent—the degree of deformation was associated with the size of holes formed in the nanoflake structure. The appearance of shapeless silica agglomerates was an additional result of the degradation process. Ninety-six-hour incubation caused deformation holes in silica nanoflakes that reached the point of total destruction of NPs [58].

Evidence of nanostructure biodegradation of the sandwich-like mesoporous silica flakes has also been confirmed in another study. After 48-h incubation, the whole surface of silica nanoflakes was covered with cavities and was entirely destroyed [59]. The mechanism of silica dissolution is based on two simultaneous processes—degradation and re-deposition of silica

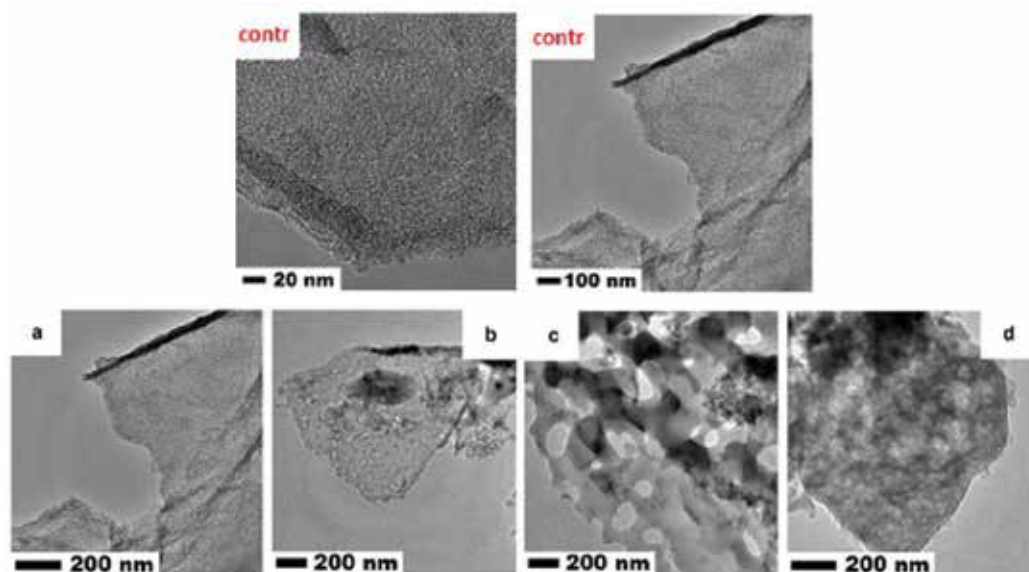


Figure 4. Transmission electron microscopy of $mSiO_2$ ('contr' – control sample) and $mSiO_2$ incubated in PBS, for 24 (a), 48 (b) and 96 h (c, d) [58].

on nanoparticle surface. Moreover, the effect of “self-healing” defects between both Si—O—Si bonds of double-linked Si atoms explains the very low rate of dissolution at the point of zero net proton charge (PZPC) of the surface [60].

A similar effect of PSB incubation on mesoporous silica nanospheres was observed by Yamada and co-workers [61], as these authors found that the $mSiO_2$ porous structure was degradable after 2-day incubation in PBS. After 3-day incubation, $mSiO_2$ displayed size and shape degradation with the final shape deformation and collapse of structures [61]. Another study based on core-shell magnetic mesoporous silica nanoparticles presented comparable results. Silica mesoporous hollow shells immersed in PBS for 2 days displayed structure deformation and additional cavities, whereas 8-day incubation showed complete degradation and coagulation resulting in new structure formation [62]. The erosion of mesoporous silica nanosphere structure modified with titanium dioxide was also observed in contact with *Streptomyces* cells. After 24-h incubation, mesoporous silica shell structure was degraded with simultaneous appearance of agglomerates, which clearly demonstrated that nanomaterial structure and composition could be affected by living cells [63].

4. Novel approaches in cytotoxicity studies

4.1. Phenotype arrays

Phenotype is the effect exerted by molecules (e.g., drugs, nanoparticles, etc.) on a cell, tissue or whole organism; thus, the phenotype screening provides a holistic analysis that usually is more

comprehensive than the sum of its parts. “Phenomix” is a part of complex technologies that also include transcriptomics, proteomics and metabolomics. PMs give a possibility to screen thousands of cellular phenotypes in real time [64].

Phenotype MicroArrays™ (PMs) are a combination of microplate reader (that can measure OD every 1 min over few hours and provide information about kinetics of carbon energy reactions in a selected cell model) and microscopic modules equipped with fluorescence, brightfield, colour brightfield and phase contrast microscopy (for scanning changes in cell morphology during experiments). Phenotypic assays deliver more information and provide better understanding of the metabolic and cytotoxic effect of test substances [65]. Multiplex arrays can generate information on the use of energy pathways (based on the application of different nutrition analyses, PM-M1 to M4), effects of ions (PM-M5), hormones, metabolic effectors (PM-M6 to M8) and anti-cancer agents (PM-M11 to M14) (**Table 4**), cell number, cell health (based on cell health monitoring using phase contrast microscopy and kinetic determination of cellular energy) and apoptotic induction (via cell subpopulation analysis—examination of the increase in circularity due to cell shrinkage and cytoplasm condensation and lower phase signal exhibition) [65]. PMs can be used in genotype/phenotype analyses, cell line characterisation, metabolic reprogramming, cellular phenotype stability, Warburg effect, cell differentiation or bioprocess development [64]. Well-characterised model cell lines (e.g., HepG2, C3A, Colo205, A549, PC-3, IMR90, HL-60 or CEM) with defined metabolic properties can be used with the PM system to determine specific effects of nanomaterials on selected cell lines and to accurately identify the mechanism involved in the NP effect (e.g., mitochondrial toxicology) on the living system [66]. Array wells coated with different substances and combined with the redox assay (MA or MB redox dyes to measure cell energy [NADH] changes) are used for phenotypic determination. Comparison of two cell lines is visualised by bioinformatic software that highlights differences in recorded phenotypes (**Figure 5**) [64, 67].

For example, Phenotype MicroArrays™ (PM-M TOX1 Plate Energetic Substrate Assay, 96-well microplate coated with eight different oxidisable carbon sources—each of the eight nutrition sources coated on one of eight rows on a microplate) give the possibility to screen cell-based energetic phenotype in a target cell model, for example, the MDA-MB-231 RFP breast cancer cell line, using different cellular nutrition sources (e.g., α -D-glucose, inosine, D-galactose, D-glucose-1-phosphate, xylitol, α -ketoglutaric acid, D,L- β -hydroxybutyric acid or pyruvic acid). This kind of multiplex analysis provides information on cell morphology, metabolic activity (metabolic pathway activity), sensitivity in response to particular energetic additives and the final cellular genetic background characterisation. The addition of an apoptotic agent (e.g., oridonin), chemical inhibitor or stimulator provides an opportunity to evaluate the potential mechanism regulating the energy pathway [65, 66]. Another example of PM application was presented by Bochner et al. [68]. Based on four phenotypic assays (PM-M1 to M4, containing 367 substrate nutrients), different human cancer cell lines, including HepG2/C3A, HepG2, Colo 205, A549, PC-3, HL-60 and CCRF-CEM and two murine white and brown adipocyte cell lines were analysed to determine energy-producing pathways. The results showed that human cancer cell lines exhibited distinct metabolic activity profiles. Moreover, white and brown adipocyte cell lines also had different profiles of energetic activity; metabolic fingerprints were established in all cell lines [68]. Similarly, human endothelial cells from the coronary artery

Phenotype MicroArrays™	Feature	Substrates/agents
PM-M TOX1 (Biolog)	Effect of a tested factor on energy production (mitochondrial toxicity)	Eight different carbon source: α -D-glucose, inosine, D-galactose, D-glucose-1-phosphate, xylitol, α -ketoglutaric acid, D,L- β -hydroxybutyric acid, pyruvic acid
PM-M1 (Biolog)	Energetic substrate array	Carbon and energy sources (simple sugars, polysaccharides, carboxylic acids): cyclodextrin, dextrin, glycogen, maltitol, maltotriose, D-maltose, D-trehalose, D-cellobiose, gentiobiose, D-glucose-6-phosphate, D-glucose-1-phosphate, L-glucose, D-glucose, 3-O-methyl-D-glucose, methyl-D-glucoside, D-salicin, D-sorbitol, N-acetyl-D-glucosamine, D-glucosaminic acid, D-glucuronic acid, chondroitin-6-sulphate, mannan, D-mannose, methyl-D-mannoside, D-mannitol, N-acetyl- β -D-mannosamine, D-melezitose, sucrose, palatinose, D-turanose, D-tagatose, L-sorbose, L-rhamnose, L-fucose, D-fucose, D-fructose-6-phosphate, D-fructose, stachyose, D-raffinose, D-lactitol, lactulose, α -D-lactose, melibionnic acid, D-melibiose, D-galactose, α -methyl-D-galactoside, N-acetyl-neuraminic acid, pectin, sedoheptulosan, thymidine, uridine, adenosine, inosine, adonitol, L-arabinose, D-arabinose, β -methyl-D-xylopyranoside, xylitol, myo-inositol, meso-erythritol, propylene glycol, ethanolamine D,L- α -glycerol-phosphate, glycerol, citric acid, tricarballic acid, D,L-lactic acid, methyl D-lactate, methyl pyruvate, pyruvic acid, α -keto-glutaric acid, succinamic acid, succinic acid, mono-methyl succinate, tricarballic acid, L-malic acid, D-malic acid, meso-tartaric acid, acetoacetic acid (a), γ -amino-N-butyric acid, α -keto-butyric acid, α -hydroxy-butyric acid, D,L- β -hydroxy-butyric acid, γ -hydroxy-butyric acid, butyric acid, 2,3-butanediol, 3-hydroxy-2-butanone, propionic acid, acetic acid, hexanoic acid
PM-M2 (Biolog)	Energetic substrate array	Carbon and energy sources/nitrogen sources (protein-derived nutrients, primarily amino acids, dipeptides): Tween 20, Tween 40, Tween 80, gelatin, L-alaninamide, L-alanine, D-alanine, L-arginine, L-asparagine, L-aspartic acid, D-aspartic acid, L-glutamic acid, D-glutamic acid, L-glutamine, glycine, L-histidine, L-homoserine, hydroxy-L-proline, L-isoleucine, L-leucine, L-lysine, L-methionine, L-ornithine, L-phenylalanine, L-proline, L-serine, D-serine, L-threonine, D-threonine, L-tryptophan, L-tyrosine, L-valine, Ala-Ala, Ala-Arg, Ala-Asn, Ala-Asp, Ala-Glu, Ala-Gln, Ala-Gly, Ala-His, Ala-Ile, Ala-Leu, Ala-Lys, Ala-Met, Ala-Phe, Ala-Pro, Ala-Ser, Ala-Thr, Ala-Trp, Ala-Tyr, Ala-Val, Arg-Ala (b), Arg-Arg (b), Arg-Asp, Arg-Gln, Arg-Glu, Arg-Ile (b), Arg-Leu (b), Arg-Lys (b), Arg-Met (b), Arg-Phe (b), Arg-Ser (b), Arg-Trp, Arg-Tyr (b), Arg-Val (b), Asn-Glu, Asn-Val, Asp-Ala, Asp-Asp, Asp-Glu, Asp-Gln, Asp-Gly, Asp-Leu, Asp-Lys, Asp-Phe, Asp-Trp, Asp-Val, Glu-Ala, Glu-Asp, Glu-Glu, Glu-Gly, Glu-Ser, Glu-Trp, Glu-Tyr, Glu-Val, Gln-Glu, Gln-Gln, Gln-Gly, Gly-Ala, Gly-Arg, Gly-Asn, Gly-Asp, α -D-glucose

Phenotype MicroArrays™	Feature	Substrates/agents
PM-M3 (Biolog)	Energetic substrate array	Carbon and energy sources/nitrogen sources (dipeptides): Gly-Gly, Gly-His, Gly-Ile, Gly-Leu, Gly-Lys, Gly-Met, Gly-Phe, Gly-Pro, Gly-Ser, Gly-Thr, Gly-Trp, Gly-Tyr, Gly-Val, His-Ala, His-Asp, His-Glu, His-Gly, His-His (c), His-Leu, His-Lys (d), His-Met, His-Pro, His-Ser, His-Trp, His-Tyr, His-Val, Ile-Ala, Ile-Arg (b), Ile-Asn, Ile-Gln, Ile-Gly, Ile-His, Ile-Ile, Ile-Leu, Ile-Met, Ile-Phe, Ile-Pro, Ile-Ser, Ile-Trp, Ile-Tyr, Ile-Val, Leu-Ala, Leu-Arg (b), Leu-Asn, Leu-Asp, Leu-Glu, Leu-Gly, Leu-His, Leu-Ile, Leu-Leu, Leu-Met, Leu-Phe, Leu-Pro, Leu-Ser, Leu-Trp, Leu-Tyr, Leu-Val, Lys-Ala (d), Lys-Arg (b), Lys-Asp, Lys-Glu, Lys-Gly, Lys-Ile (b), Lys-Leu (b), Lys-Lys, Lys-Met (e), Lys-Phe, Lys-Pro, Lys-Ser, Lys-Thr, Lys-Trp (b), Lys-Tyr (b), Lys-Val (d), Met-Arg (b), Met-Asp, Met-Gln, Met-Glu, Met-Gly, Met-His, Met-Ile, Met-Leu, Met-Lys (e), Met-Met, Met-Phe, Met-Pro, Met-Thr, Met-Trp, Met-Tyr, Met-Val, Phe-Ala, Phe-Asp, Phe-Glu, α -D-glucose
PM-M4 (Biolog)	Energetic substrate array	Carbon and energy sources/nitrogen sources (dipeptides): Phe-Gly, Phe-Ile, Phe-Met, Phe-Phe, Phe-Pro, Phe-Ser, Phe-Trp, Phe-Tyr, Phe-Val, Pro-Ala, Pro-Arg (b), Pro-Asn, Pro-Asp, Pro-Glu, Pro-Gln, Pro-Gly, Pro-Hyp, Pro-Ile, Pro-Leu, Pro-Lys (b), Pro-Phe, Pro-Pro, Pro-Ser, Pro-Trp, Pro-Tyr, Pro-Val, Ser-Ala, Ser-Asn, Ser-Asp, Ser-Glu, Ser-Gln, Ser-Gly, Ser-His (b), Ser-Leu, Ser-Met, Ser-Phe, Ser-Pro, Ser-Ser, Ser-Tyr, Ser-Val, Thr-Ala, Thr-Arg (f), Thr-Asp, Thr-Glu, Thr-Gln, Thr-Gly, Thr-Leu, Thr-Met, Thr-Phe, Thr-Pro, Thr-Ser, Trp-Ala, Trp-Arg, Trp-Asp, Trp-Glu, Trp-Gly, Trp-Leu, Trp-Lys (e), Trp-Phe, Trp-Ser, Trp-Trp, Trp-Tyr, Trp-Val, Tyr-Ala, Tyr-Gln, Tyr-Glu, Tyr-Gly, Tyr-His, Tyr-Ile, Tyr-Leu, Tyr-Lys, Tyr-Phe, Tyr-Trp, Tyr-Tyr, Tyr-Val, Val-Ala, Val-Arg, Val-Asn, Val-Asp, Val-Glu, Val-Gln, Val-Gly, Val-His, Val-Ile, Val-Leu, Val-Lys, Val-Met, Val-Phe, Val-Pro, Val-Ser, Val-Tyr, Val-Val, α -D-glucose
PM-M5 (Biolog)		Ions: NaCl, ammonium chloride, sodium selenite, potassium chloride, calcium chloride, manganese chloride, zinc chloride, copper (II) chloride, cobalt chloride, iodine, sodium phosphate, sodium sulphate, sodium molybdate, sodium tungstate, sodium orthovanadate, potassium chromate, sodium pyrophosphate, sodium nitrate, sodium nitrite, lithium chloride, ferric chloride, magnesium chloride
PM-M6 (Biolog)		Hormone and metabolic effectors: dibutyryl-cAMP, 3-isobutyl-1-methylxanthine, caffeine, epinephrine, norepinephrine, L-leucine, creatine, triiodothyronine, thyroxine, dexamethasone, hydrocortisone, progesterone, β -estradiol, 4,5 α -dihydro-testosterone, aldosterone
PM-M7 (Biolog)		Hormone and metabolic effectors: insulin, resistin, glucagon, ghrelin, leptin, gastrin, exendin-3, hGH (somatotropin), IGF-I, FGF-1 (aFGF), PDGF-AB, IL-1 β , IL-2, IL-6, IL-8

Phenotype MicroArrays™	Feature	Substrates/agents
PM-M8 (Biolog)		Hormone and metabolic effectors: (Arg8) – vasopressin, parathyroid hormone, prolactin, calcitonin, calcitriol (1 α ,25-dihydroxyvitamin D3), luteinizing hormone (LH), luteinizing hormone releasing hormone (LH-RH), chorionic gonadotropin human (HCG), adrenocorticotrophic hormone human (ACTH), thyrotropic hormone (TSH), thyrotropin releasing hormone acetate salt (TRH), IFN- γ , TNF- α , adenosine, Gly-His-Lys acetate salt
PM-M11 (Biolog)		Anti-cancer agents: solasodine, rotenone, aklavine hydrochloride, deguelin(-), celastrol, juglone, sanguinarine sulphate, dactinomycin, methylmethane sulfonate, azathioprine, busulfan, aclarubicin, chloramphenicol, chloroquine diphosphate, cyclophosphamide, diethylcarbamazine citrate, emetine, fluorouracil, hydroxyurea, mechlorethamine, mercaptopurine, quinacrine hydrochloride, streptozosin
PM-M12 (Biolog)		Anti-cancer agents: tamoxifen citrate, thioguanine, acriflavinium hydrochloride, pentamidine isethionate, mycophenolic acid, aminopterin, berberine chloride, emodin, puromycin hydrochloride, neriifolin, 5-fluoro-5'-deoxyuridine, carboplatin, cisplatin, zidovudine (AZT), azacytidine, cycloheximide, azaserine, p-fluoro-phenylalanine, dimethylhydrazine hydrochloride, phenethyl caffeate (CAPE), camptothecin, amygdalin, ellagic acid
PM-M13 (Biolog)		Anti-cancer agents: monocrotaline, altretamine, carmustine, mitoxantrone hydrochloride, urethane, thiotepa, thiodiglycol, pipobroman, etanidazole, semustine, gossypol, formestane, ancitabine hydrochloride, nimustine, aminolevulinic acid hydrochloride, picropodo-phyllotoxin, beta-peltatin, perillyl alcohol, dibenzoylmethane, 6-amino nicotinamide, carmofur, indole-3-carbinol, rifaximin
PM-M14 (Biolog)		Anti-cancer agents: cepharanthine, 4'-demethyl epipodophyllotoxin, miltefosine, elaidyl phosphocholine, podofilox, colchicine, methotrexate, acivicin, floxuridine, lefunomide, rapamycin, 13-cis retinoic acid, all-trans retinoic acid, piceatannol, (+)-catechin, mitomycin C, cytosine-beta-D-arabinofuranoside, daunorubicin hydrochloride, doxorubicin hydrochloride, etoposide, nocodazole, quercetin dihydrate, vinblastine sulphate

Table 4. Array examples [65].

(HCAEC), umbilical vein (HUVEC) and normal lung fibroblasts (NHLFs) were selected for cellular metabolism monitoring also with the use of phenotypic assays (PM-M1 to M4). The results obtained in this study demonstrated that all three cell lines strongly utilised adenosine, inosine, D-mannose and dextrin. HCAEC also metabolised mannan, pectin, gelatine and tri-carballylic acid, while the HUVEC cell line did not exhibit the ability to metabolise any other unique substrates. NHLFs were able to additionally utilise sugars and carboxylic acids [69].

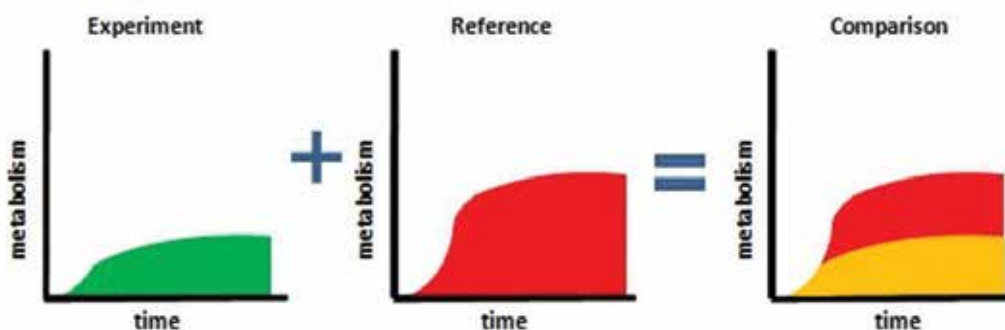


Figure 5. Schematic visualisation that highlights differences in recorded phenotypes [64].

The profiling of human normal and cancer cells was also conducted by Parmar et al. [70]. HEK293, OV90, TOV112D, KLE, MES-SA and SKBR cell lines were selected to determine differences in response to anti-cancer agents using PM (PM-M11 to M14) and the effect of these agents on the mTOR signalling pathway by measuring S6 kinase (S6K) level. From a wide range of anti-cancer drugs, celastrol was found to inhibit the growth of SKBR, MESA-SA and TOV11D and target the mTOR signalling pathway [70]. In another study, Martinez-Reyes et al. [71] reported that mitochondrial metabolism was necessary for histone acetylation, hypoxia-inducible transcription factor (HIF-1) activation and proliferation based on WT-POLG and DN-POLG-HEK293 cell lines [71].

The application of PMs in nanotechnology is only a matter of time, thanks to the efficient and rapid determination of precise sites and modes of action of the tested substances. PMs provide a possibility to compare specificities of the study agents (e.g., drug and nanomaterial-drug conjugates) and the effect of the agent and its side effects. Finally, the PM system can be used for drug interactions or drug-nanomaterial analysis [67, 72].

The limitations of large-scale phenotyping techniques, including PM analysis, are related to the characteristics of all cells. PMs will not reveal the phenotypes of all cells, because cells have many phenotypes that are dependent on their environments. Different cells are constantly adapting in various ways to culture (environment) changes by altering their gene-expression pattern, protein content, membrane and cytoskeleton constitution and surface receptors. Moreover, the PM system will likely not record phenotypes that specifically involve intracellular structures (e.g., cytoskeleton, organelles or surface structures). In addition, the effect of some genes might be cryptic and the function of those genes only occurs under highly specific conditions; thus, it cannot be always determined in conditions provided by PM cultures [73].

Another approach to phenotypic screening is focused on microarray-based three-dimensional (3D) systems. 3D culture models may better mimic the *in vivo* cellular microenvironment and may be critical for cell phenotypes [74]. It should also be mentioned that cell migration, compound-mediated cytotoxicity, cellular adhesion, proliferation and differentiation can also be evaluated using non-invasive, labelled-free xCELLigence system. Electrical impedance monitoring is based on a set of gold microelectrodes fused to the bottom surface of a microtitre plate

well. The magnitude of impedance is dependent on the number of cells, the size and shape of the cells and cell-substrate attachment quality; therefore, it gives the possibility to analyse the effect, for example, of nanomaterials on cell morphology, adhesion and biocompatibility [75].

4.2. Digital holography (DH) microscopy

Holographic (transmission) microscopy is a high-resolution imaging technique that provides label-free and non-invasive, non-phototoxic and non-destructive method for real-time live cell culture analysis [76]. This type of microscopy allows for quantitative and qualitative measurements of living cells (not only cultures of mammalian cells, but also protozoan, bacterial and plant cells) and collecting information about cell surface area, cell viability and morphological changes, such as differentiation, proliferation, motility, cell death, confluence or cell segmentation (calculated from a particular hologram) [77–80]. Traditional brightfield microscopy has some limitations, such as difficulties in visualising individual cells due to their low contrast properties, whereas DH microscopy provides possibility to determine cell number directly in cell culture vessels [81]. The size of the HoloMonitor™ M4 (Phase Holographic Imaging AB, Lund, Sweden) makes it possible to place it in a cell culture incubator, so that cell observations can be conducted over long periods of time without any changes in cell culture conditions [78]. Digital holographic microscopy also enables the formation of three-dimensional (3D) images of the observed objects.

The presented technique is based on the phase shift (φ) of the probing laser light (or other coherent light source) that can be reflected or transmitted through the monitored object. The illuminating light is split into two beams (differing in phase): an object beam and a reference beam [78, 81]. The reference beam remains undisturbed, while the object beam is shifted in phase by the object [79]. Next, the object beam is re-joined and interferes with the reference beam and creates a hologram that is recorded on a digital image sensor (CCD or CMOS) [77, 81]. The total phase shift can be translated into optical thickness (L) and depends on the physical thickness of the examined object, wavelength (λ) and refraction index (n). Optical thickness can be measured at nanometre resolution [78, 81].

Holographic phase imaging is an excellent tool for cell morphometric characterisation and cell migration studies. This technique has recently been applied in clinical diagnostics, e.g., screening for malaria infection of erythrocytes, cancer cell analyses or sperm quality [79]. Interest in the use of DH microscopy in research is constantly increasing. For example, Lajkó et al. [82] analysed the effect of a drug based on GnRH-III (gonadotropin-releasing hormone-III) on melanoma cells. Holographic phase imaging was used to visualise the migratory behaviour of melanoma cells in response to daunorubicin (Dau) coupled with GnRH-III and its derivatives (modified at position 4 with Lys(Ac) (conj1) or Lys(nBu) (conj2)). Cell migration analysis showed increased migration activity when cells were exposed to conj1, whereas conj2 decreased melanoma cell activity and exerted an immobilising effect on tumour cell spreading; thus, it was a better candidate for targeted tumour therapy [82]. Monitoring of HeLa cancer cells and MC3T3-E1 preosteoblast cells via holographic technique was also conducted by Peter et al. [78]. These authors evaluated cell movements and morphological parameters of cells in two experiments. In the first one, the HoloMonitor™ M4 was used to detect the effect of EGCg (green tea—epigallocatechin gallate) on HeLa cell motility. Time-lap images showed that migration, motility and the speed of motility were reduced after EGCg

was added to the culture. The second experiment involved MC3T3 plated on transparent titanate nanotubes (TNT) surface and the impact on adhesion and spreading process of the cells was demonstrated using the HoloMonitor. The authors have concluded that holographic digital microscopy is a useful tool for cellular behaviour analysis, but some limitations have also been found. Peter et al. [78] observed that under certain thicknesses, some parts of the cells (e.g., parts of the thin lamellipodium) slicked into the background surface. It was caused by the limited vertical resolution of the optical system [78].

In our study, the effect of the h-BN-Au nanocomposite on L929 and MCF-7 cell lines was analysed during 12-h incubation using the HoloMonitor™ M4. L929 cells did not show any significant differences in the presence of the nanocomposite and the doubling time (DT) value was similar to DT obtained in the control culture (**Figure 6**). The results obtained for the MCF-7 cell line incubated with h-BN-Au demonstrated a stronger effect on cells. The DT analysis using holographic technique indicated a high reduction of proliferation capacity (the DT value for the MCF-7 control sample was 25.95 h, whereas for experimental cultures, it was 469.9 h) [83].

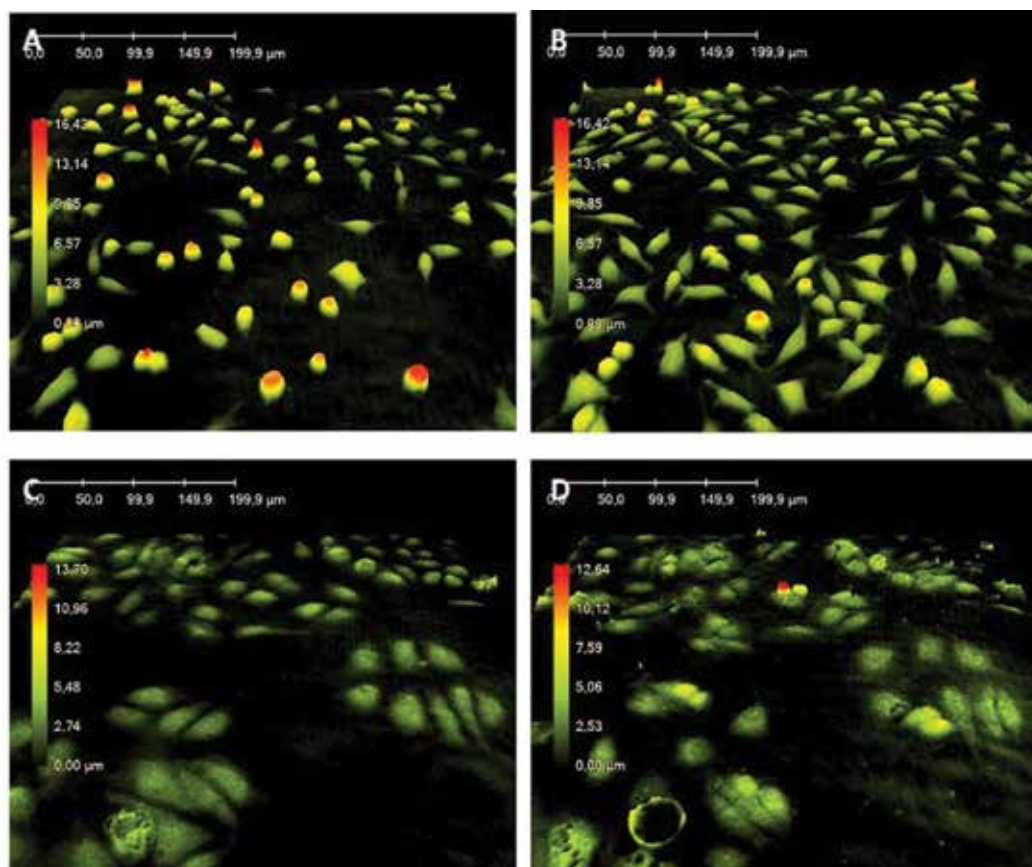


Figure 6. The morphology of the L929 and MCF-7 cell lines incubated with the h-BN-Au nanoparticles. L929 culture time-points at 0 h (A); at 12 h (B); MCF-7 culture time-points at 0 h (C); at 12 h (D) [83].

4.3. Atomic force microscopy (AFM)

Atomic force microscopy (AFM) is based on a laser reflected off a cantilever onto a scanning surface of the examined object and quantitative information about surface morphology and cell spread is collected.

AFM is a crucial technique for determining cell interactions on the surface of the tested material. If material exhibits high biocompatibility, the surface of the material will allow cells to attach (interaction between cell-surface integrin receptors) and adsorb extracellular matrix (ECM) proteins. Surface properties, such as wettability, roughness or surface charge, are important for cellular attachment and lamellipodium/filopodium formation. The AFM measurement provides information on cellular morphology changes and lamellipodium/filopodium permissiveness. The measurement of atomic force microscopy of living cells can be performed in PBS and provides information on cell height, total cell surface area, attachment angle and extension of lamellipodia/filopodia. It is also possible to measure fixed cell (in 4% paraformaldehyde) topography and examine filopodia and lamellipodia. An interesting example is the analysis of H4 and PC12 cell lines plated on different materials—glass, polystyrene (PSt), silicon (Si), nanocrystalline diamond (NCD) and cubic silicon carbide (3C-SiC). In the latter study, AFM analysis demonstrated that the type of the surface determined cell height/area, attachment angle and the reduction of the lamellipodium/filopodium area. Cell-substrate interaction was different for H4 and PC12 cell lines, e.g., for H4 cells; the most negative interaction was recorded for glass, the most positive for 3C-SiC, while PC12 cells had the most negative interaction with glass, but the best with 3C-SiC and PSt. The authors concluded that AFM analysis indicated that neural cell interactions with 3C-SiC resulted in the optimal cell viability, morphology and interaction of cells with 3C-SiC surface [1]. Frewin et al. [1] published the results of AFM analysis concerning cellular interaction on graphene. The experiments focused on cytoskeleton organisation and the determination of the number of contact sites, and AFM technology can provide valuable information on the mechanism of cellular adhesion and proliferation on graphene surface. Different methods of graphene preparation, for example, mechanical cleaving, chemical synthesis and chemical vapour deposition (CVD) on metals or epitaxial growth on SiC, not only give graphene different electrical, optical or morphological properties, but also different biocompatibility. For example, the biocompatibility of a single graphene layer produced by CVD on Cu was higher in comparison with SiO₂/Si surfaces studied on human osteoblasts and mesenchymal stem cells [1, 84]. In another study, epitaxially grown graphene films on (0001) 6H-SiC substrates were evaluated in cellular response experiments using AMF analysis. It was found that HaCaT (human keratinocytes) after 72-h culture on graphene and 6H-SiC surfaces exhibited similar morphology to cells cultured on the PSt control. On the other hand, the MTT assay suggested better biocompatibility for 6H-SiC than for the graphene surface. Moreover, different preparation of graphene surfaces (first one without any further surface treatment, and the second one additionally disinfected by immersion in ethanol) resulted in more homogeneous and increased cell adhesion on ethanol-sterilised graphene surface [1]. Our study also confirmed the undeniable value of AMF analysis in the experiment involving the MAC-T cell line seeded on different surfaces (glass, glass coated with poly-D-lysine) (**Figure 7**). In the aforementioned study, surface analysis and cell height analysis clearly exhibited differences in cell growth on the two surface variants [85].

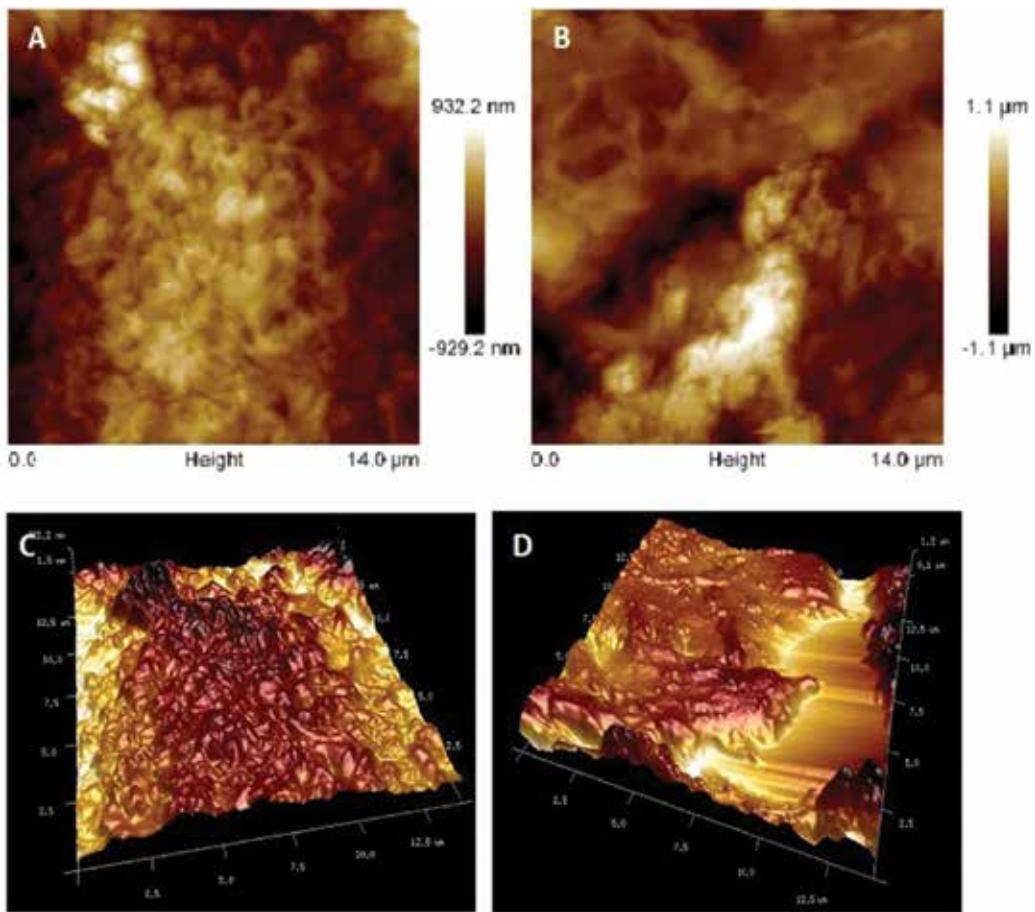


Figure 7. AFM analysis of MAC-T cells: cell height on glass surface (A); cell height on glass coated with poly-D-lysine (B); 3D image of cell growing on glass surface (C); 3D image of cell growing on poly-D-lysine (D) [85].

Another notable study used the AFM technique not only for cell analysis after nanoparticle uptake, but also after exposure to rotating magnetic field (RMF). Observations of MCF-7 cells after 1.5-h incubation in 40 mT magnetic field revealed changes in cell surface, which was rougher with many small pore-like structures in comparison to untreated cells [86].

5. Conclusions

The present overview describes and compares widely used biocompatibility/cytotoxicity assays in nanomaterial studies. Due to the type of nanoparticles and their properties, applicability of popular assays used for engineered nanomaterial screening might be limited. The significant numbers of false-positive or false-negative signals are generated [16]. The tendency of nanoparticles to:

- Interact and photocatalyse assay reagents,
- Create agglomerate in the conditions of in vitro and in vivo environment,
- Create protein layer of several nanometres on nanoparticle surface,
- Degrade and deform in vitro environment,

affect the results obtained in popular assays, thus classic cytotoxicity assays alone are not sufficient to evaluate nanomaterial biocompatibility.

Author details

Magdalena Jedrzejczak-Silicka^{1*} and Ewa Mijowska²

*Address all correspondence to: mjdrzejczak@zut.edu.pl

1 Laboratory of Cytogenetics, West Pomeranian University of Technology, Szczecin, Poland

2 Nanomaterials Physicochemistry Department, West Pomeranian University of Technology, Szczecin, Poland

References

- [1] Frewin CL, Oliverios A, Weeber E, Sadow SE. AFM and cell staining to assess the in vitro biocompatibility of opaque surfaces. In: Frewin CL, editor. *Atomic Force Microscopy Investigations into Biology – From Cell to Protein*. Rijeka: InTech; 2012. pp. 297-324. DOI: 10.5772/37078
- [2] Das S, Mitra S, Khurana SMP, Debnath N. Nanomaterials for biomedical applications. *Frontiers in Life Science*. 2013;7:90-98. DOI: 10.1080/21553769.2013.869510
- [3] Pacheco-Blandino I, Vanner R, Buzea C. Toxicity of nanoparticles. In: Pacheco-Torgal F, Jalali S, Fucic A, editors. *Toxicity of Building Materials*. Cambridge: Woodhead Publishing; 2012. pp. 427-475. DOI: 10.1533/9780857096357
- [4] Buzea C, Pacheco II, Robbie K. Nanomaterials and nanoparticles: Sources and toxicity. *Biointerphases*. 2007;2:MR17-MR71. DOI: 10.1116/1.2815690
- [5] Siafaka PI, Okur NÜ, Karavas E, Bikiaris DN. Surface modified multifunctional and stimuli responsive nanoparticles for drug targeting: Current status and uses. *International Journal of Molecular Science*. 2016;17:1440. DOI: 10.3390/ijms17091440
- [6] Nanotechnology in the Cement Industry – A Patent Analysis [Internet]. 2012. Available from: <https://www.nanowerk.com/spotlight/spotid=28101.php> [Accessed: 2017-09-22]
- [7] Sato K, Hosokawa K, Maeda M. Non-cross-linking gold nanoparticle aggregation as a detection method for single-base substitutions. *Nucleic Acid Research*. 2005;33:e4. DOI: 10.1093/nar/gni007

- [8] Gurr JR, Wang ASS, Chen CH, Jan KY. Ultrafine titanium dioxide particles in the absence of photoactivation can induce oxidative damage to human bronchial epithelial cells. *Toxicology*. 2005;**213**:66-73. DOI: 10.1016/j.tox.2005.05.007
- [9] Long TC, Saleh N, Tilton RD, Lowry GV, Veronesi B. Titanium dioxide (P25) produces reactive oxygen species in immortalized brain microglia (BV2): Implications for nanoparticle neurotoxicity. *Environmental Science and Technology*. 2006;**40**:4346-4352. DOI: 10.1021/es060589n
- [10] Hillaireau H, Couvreur P. Nanocarriers' entry into the cell: Relevance to drug delivery. *Cellular and Molecular Life Science*. 2009;**66**:2873-2896. DOI: 10.1007/s00018-009-0053
- [11] Alkilany AM, Murphy CJ. Toxicity and cellular uptake of gold nanoparticles: What we have learned so far? *Journal of Nanoparticles Research*. 2010;**12**:2313-2333. DOI: 10.1007/s11051-010-9911-8
- [12] Peters A, Veronesi B, Calderon-Garciduenas L, Gehr P, Chen LC, Geiser M, Reed W, Rothen-Rutishauser B, Schurch B, Schulz H. Translocation and potential neurological effects of fine and ultrafine particles—A crucial update. *Particle and Fibre Toxicology*. 2006;**3**:13. DOI: 10.1186/1743-8977-3-13
- [13] Geiser M, Rothen-Rutishauser B, Kapp N, Schurch S, Kreyling W, Schulz H, Semmler M, Im Hof V, Heyder J, Gehr P. Ultrafine particles cross cellular membranes by nonphagocytic mechanism in lungs and in cultured cells. *Environmental Health Perspectives*. 2005;**113**:1555-1560. DOI: 10.1289/ehp.8006
- [14] Sohaebuddin SK, Thevenot PT, Baker D, Eaton JW, Tang L. Nanomaterial cytotoxicity in composition, size, and cell type dependent. *Particle and Fibre Toxicology*. 2010;**7**:22. DOI: 10.1186/1743-8977-7-22
- [15] Schrand AM, Johnson J, Dai L, Hussain SM, Schlager JJ, Zhu L, Hong Y, Ōsawa E. Cytotoxicity and genotoxicity of carbon nanomaterials. In: Webster TJ, editor. *Safety of Nanoparticles*. Springer; 2009. pp. 159-187. DOI: 10.1007/978-0-387-78608-7_8
- [16] Monteiro-Riviere NA, Inman AO, Zhang LW. Limitations and relative utility of screening assays to assess engineering nanoparticle toxicity in a human cell line. *Toxicology and Applied Pharmacology*. 2009;**234**:222-235. DOI: 10.1016/j.taap.2008.09.030
- [17] Zolnik BS, Gonzales-Fernandez A, Sadrieh N, Dobrovolskaia MA. Nanoparticles and the immune system. *Endocrinology*. 2010;**151**:458-465. DOI: 10.1210/en.2009-1082
- [18] Berridge MV, Herst PM, Tan AS. Tetrazolium dyes as tools in cell biology: New insights into their cellular reduction. *Biotechnology Annual Review*. 2005;**11**:127-152. DOI: 10.1016/S1387-2656(05)11004-7
- [19] Ali-Boucetta H, Al-Jamal KT, Kostarelos K. Cytotoxicity assessment of carbon nanotube interaction with cell cultures. In: Hurst SJ, editor. *Biomedical Nanotechnology: Methods and Protocols, Methods in Molecular Biology*. New York: Springer; 2011. pp. 299-312. DOI: 10.1007/978-1-61779-052-2_19

- [20] Ciofani G, Danti S, D'Alessandro D, Moscato S, Menciasci A. Assessing cytotoxicity of boron nitride nanotubes: Interference with the MTT assay. *Biochemical and Biophysical Research Communications*. 2010;**394**:405-410. DOI: 10.1016/j.bbrc.2010.03.035
- [21] Al-Jamal KT, Kostarelos K. Assessment of cellular uptake and cytotoxicity of carbon nanotubes using flow cytometry. In: Balasubramanian K, Burghard M, editors. *Carbon Nanotubes: Methods and Protocols*. Stuttgart: Humana Press; 2010. pp. 123-134. DOI: 10.1007/978-1-60761-579-8_11
- [22] Monteiro-Riviere NA, Inman AO. Challenges for assessing carbon nanomaterial toxicity to the skin. *Carbon*. 2006;**44**:1070-1078. DOI: 10.1016/j.carbon.2005.11.004
- [23] Wörle-Knirsch JM, Pulsmap K, Krug HF. Oops they did it again! Carbon nanotubes hoax scientists in viability assays. *Nano Letters*. 2006;**6**:1261-1268. DOI: 10.1021/nl060177c
- [24] Lupu AR, Popescu T. The noncellular reduction of MTT tetrazolium salt by TiO₂ nanoparticles and its implication for cytotoxicity assays. *Toxicology in Vitro*. 2013;**27**:1445-1450. DOI: 10.1016/j.tiv.2013.03.006
- [25] Popescu T, Lupu AR, Raditoiu V, Purcar V, Teodorescu VS. On the photocatalytic reduction of MTT tetrazolium salt on the surface of TiO₂ nanoparticles: Formazan production kinetics and mechanism. *Journal of Colloid and Interface Science*. 2015;**457**:108-120. DOI: 10.1016/j.jcis.2015.07.005
- [26] Casey A, Herzog E, Davoren M, Lyng FM, Byrne HJ, Chambers G. Spectroscopic analysis confirms the interactions between single walled carbon nanotubes and various dyes commonly used to assess cytotoxicity. *Carbon*. 2007;**45**:1425-1432. DOI: 10.1016/j.carbon.2007.03.033
- [27] Casey A, Davoren M, Herzog E, Lyng FM, Byrne HJ, Chambers G. Probing the interaction of single walled carbon nanotubes within cell culture medium as a precursor to toxicity testing. *Carbon*. 2007;**45**:34-40. DOI: 10.1016/j.carbon.2006.08.009
- [28] Jiao G, He X, Li X, Qiu J, Xu H, Zhang N, Liu S. Limitations of MTT and CCK-8 assay for evaluation of graphene cytotoxicity. *RSC Advances*. 2015;**5**:532-540. DOI: 10.1039/C5RA08958A
- [29] Han X, Gelein R, Corson N, Wade-Mercer P, Jiang J, Biswas P, Finkelstein JN, Elder A, Oberdörster G. Validation of an LDH assay for assessing nanoparticle toxicity. *Toxicology*. 2011;**287**:99-104. DOI: 10.1016/j.tox.2011.06.011
- [30] Wang G, Zhang J, Dewilde AH, Pal AK, Bello D, Therrien JM, Braunhut SJ, Marx KA. Understanding and correcting for carbon nanotube interferences with a commercial LDH cytotoxicity assay. *Toxicology*. 2012;**299**:99-111. DOI: 10.1016/j.tox.2012.05.012
- [31] Smith SM, Wunder MB, Norris DA, Shellman YG. A simple protocol for using a LDH-based cytotoxicity assay to assess the effects of death and growth inhibition at the same time. *PLoS One*. 2011;(11):e26908. DOI: 10.1371/journal.pone.0026908

- [32] Chan FK-M, Moriwaki K, De Rosa MJ. Detection of necrosis by release of lactate dehydrogenase (LDH) activity. *Methods in Molecular Biology*. 2013;**979**:65-70. DOI: 10.1007/978-1-62703-290-2_7
- [33] Herzog E, Casey A, Lyng FM, Chambers G, Byrne HJ, Davoren M. A new approach to the toxicity testing of carbon-based nanomaterials—The clonogenic assay. *Toxicology Letters*. 2007;**174**:49-60. DOI: 10.1016/j.toxlet.2007.08.009
- [34] Gräfe C, Weidner A, Lühe BC, Schacher FH, Clement JH, Dutz S. Intentional formation of a protein corona on nanoparticles: Serum concentration affects protein corona mass, surface charge, and nanoparticle-cell interaction. *International Journal of Biochemistry & Cell Biology*. 2016;**75**:196-202. DOI: 10.1016/j.biocel.2015.11.005
- [35] Palchetti S, Colapicchioni V, Digiacomo L, Caracciolo G, Pozzi D, Capriotti AL, La Barbera G, Laganà A. The protein corona of circulating PEGylated liposomes. *Biochimica et Biophysica Acta*. 2016;**1858**:189-196. DOI: 10.1016/j.bbamem.2015.11.012
- [36] Del Pino P, Pelaz B, Zhang Q, Maffre P, Nienhaus GU, Parak WJ. Protein corona formation around nanoparticles—From the past to the future. *Materials Horizons*. 2014;**1**:301-313. DOI: 10.1039/C3MH00106G
- [37] Zhang Y, Wu C, Guo S, Zhang J. Interactions of graphene and graphene oxide with proteins and peptides. *Nanotechnology Review*. 2013;**2**:27-45. DOI: 10.1515/ntrev-2012-0078
- [38] Vesaratchanon S, Nikolov A, Wasan DT. Sedimentation in nano-colloidal dispersions: Effects of collective interactions and particle charge. *Advances in Colloid and Interface Science*. 2007;**134-135**:268-278. DOI: 10.1016/j.cis.2007.04.026
- [39] Díaz B, Sánchez-Espinel C, Arruebo M, Faro J, de Miguel E, Magadán S, Yagüe C, Fernández-Pacheco R, Ibarra MR, Santamaría J, González-Fernández A. Assessing methods for blood cell cytotoxicity responses to inorganic nanoparticles and nanoparticles aggregates. *Small*. 2008;**4**:2025-2034. DOI: 10.1002/smll.200800199
- [40] Fraczek-Szczypta A, Menaszek E, Blazewicz S. Some observation on carbon nanotubes susceptibility to cell phagocytosis. *Journal of Nanomaterials*. 2011:1-8. ID 473516. DOI: 10.1155/2011/473516
- [41] Bagwe RP, Hillierd LR, Tan W. Surface modification of silica nanoparticles to reduce aggregation and nonspecific binding. *Langmuir*. 2006;**22**:4357-4362. DOI: 10.1021/la052797j
- [42] Mahmoudi M, Lynch L, Ejtehadi MR, Monopoli MP, Bombell FB, Laurent S. Protein-nanoparticle interactions: Opportunities and challenges. *Chemical Reviews*. 2011;**111**:5610-5637. DOI: 10.1021/cr100440g
- [43] Rahman M, Laurent S, Tawil N, Yahia L, Mahmoudi M, editors. Nanoparticle and protein corona. In: *Protein-Nanoparticle Interactions. The Bio-Nano Interface, Springer Series in Biophysics*. Berlin: Springer; 2013. pp. 21-44. DOI: 10.1007/978-3-642-37555-2_2
- [44] Mirshafiee V, Mahmoudi M, Lou K, Cheng J, Kraft ML. Protein corona significantly reduces active targeting yield. *Chemical Communications*. 2013;**49**:2557-2559. DOI: 10.1039/c3cc37307j

- [45] Fleischer CC, Payne CK. Nanoparticle-cell interactions: Molecular structure of the protein corona and cellular outcomes. *Accounts of Chemical Research*. 2014;**47**:2651-2659. DOI: 10.1021/ar500190q
- [46] Pederzoli F, Tosi G, Vandelli MA, Belletti D, Forni F, Ruozi B. Protein corona and nanoparticles: How can we investigate on? *WIREs Nanomed Nanotechnology*. 2017;**9**: e1467. DOI: 10.1002/wnan.1467
- [47] Mahon E, Salvati A, BaldelliBombelli I, Lynch I, Dawson KA. Designing the nanoparticle-biomolecule interface for targeting and therapeutic delivery. *Journal of Controlled Release*. 2012;**161**:164-174. DOI: 10.1016/j.jconrel.2012.04.009
- [48] Davoren M, Herzog E, Casey A, Cottineau B, Chambers G, Byrne HJ, Lyng FM. In vitro toxicity evaluation of single walled carbon nanotubes on human A549 lung cells. *Toxicology in Vitro*. 2007;**21**:438-448. DOI: 10.1016/j.tiv.2006.10.007
- [49] Tenzer S, Docter D, Kuharev J, Musyanovych A, Fetz V, Hecht R, Schlenk F, Fischer D, Kiouptsi K, Reinhardt C, Landfester K, Schild H, Maskos M, Knauer SK. Rapid formation of plasma protein corona critically affects nanoparticle pathophysiology. *Nature Nanotechnology*. 2013;**8**:772-781. DOI: 10.1038/nnano.2013.181
- [50] Maiorano G, Sabella S, Sorce B, Brunetti V, Malvindi MA, Cingolani R, Pompa PP. Effects of cell culture media on the dynamic formation of protein-nanoparticle complexes and influence on the cellular response. *ACS Nanotechnology*. 2010;**4**:7481-7491. DOI: 10.1021/nn101557e
- [51] Ritz S, Schöttle S, Kotman N, Baier G, Musyanovych A, Kukarev J, Landfester K, Schild H, Jahn O, Tenzer S, Mailänder V. Protein corona of nanoparticles: Distinct proteins regulate the cellular uptake. *Biomacromolecules*. 2015;**16**:1311-1321. DOI: 10.1021/acs.biomac.5b00108
- [52] Urbas K, Jedrzejczak-Silicka M, Rakoczy R, Zaborski D, Mijowska E. Effect of GO-Fe₃O₄ and rotating magnetic field on cellular metabolic activity of mammalian cells. *Journal of Biomaterials Applications*. 2016;**30**:1392-1406. DOI: 10.1177/0885328216628762
- [53] Gunawan C, Lim M, Marquis CP, Amal R. Nanaoparticle-protein corona complexes govern the biological fates and function of nanoparticles. *Journal of Materials Chemistry B*. 2014;**2**:2060-2083. DOI: 10.1039/C3TB21526A
- [54] Lesniak A, Fenaroli F, Monopoli MP, Åberg C, Dawson KA, Salvati A. Effects of the presence or absence of a protein corona on silica nanoparticle uptake and impact on cells. *ACS Nano*. 2012;**6**:5845-5857. DOI: 10.1021/nn300223w
- [55] Sacchetti C, Motamedchaboki K, Magrini A, Palmieri G, Mattei M, Barnardini S, Rosato N, Bottini N, Bottini M. Surface polyethylene glycol conformation influences the protein corona of polyethylene glycol-modified single-walled carbon nanotubes: Potential implications on biological performance. *ACS Nano*. 2013;**7**:1974-1989. DOI: 10.1021/nn400409h
- [56] Gaucher G, Asahina K, Wang J, Leroux JC. Effect of poly(N-vinyl-pyrrolidone)-block-poly(D,L-lactide) as coating agent on the opsonisation, phagocytosis, and pharmacokinetics of biodegradable nanoparticles. *Biomacromolecules*. 2009;**10**:408-416. DOI: 10.1021/bm801178f

- [57] Zhao Y, Wang L, Wang Q, Tang W, She Z, Deng Y. Repeated injection of PEGylated solid lipid nanoparticles induces accelerated blood clearance in mice and beagles. *International Journal of Nanomedicine*. 2012;**7**:2891-2900. DOI: 10.2147/IJN.S30943
- [58] Mijowska E, Cendrowski K, Brylak M, Konicki W. Sandwich-like mesoporous silica flakes for anticancer drug transport-synthesis, characterization and kinetics release study. *Colloids and Surfaces B: Biointerfaces*. 2015;**136**:119-125. DOI: 10.1016/j.colsurfb.2015.09.007
- [59] Peruzynska M, Szelong S, Trzeciak K, Kurzawski M, Cendrowski K, Brylak M, Roginska D, Piotrowska K, Mijowska E, Drozdziak M. In vitro and in vivo evaluation of sandwich-like mesoporous silica nanoflakes as promising anticancer drug delivery system. *International Journal of Pharmaceutics*. 2016;**506**:458-468. DOI: 10.1016/j.ijpharm.2016.03.041
- [60] Pelmenschikov A, Leszczynski J, Pettersson LGM. Mechanism of dissolution of neutral silica surfaces: Including effect of self-healing. *The Journal of Physical Chemistry A*. 2012;**24**:1462-1471. DOI: 10.1021/jp011820g
- [61] Yamada H, Urata C, Aoyama Y, Osada S, Yamauchi Y, Kuroda K. Preparation of colloidal mesoporous silica nanoparticles with different diameters and their unique degradation behaviour in static aqueous systems. *Chemistry of Materials*. 2012;**(8)**:1462-1471. DOI: 10.1021/cm3001688
- [62] Chen K, Zhang J, Gu H. Dissolution from inside: A unique degradation behaviour of core-shell magnetic mesoporous silica nanoparticles and the effect of polyethyleneimine coating. *Journal of Materials Chemistry*. 2012;**22**:22005-22012. DOI: 10.1039/c2jm34364a
- [63] Augustyniak A, Cendrowski K, Nawrotek P, Brylak M, Mijowska E. Investigating the interaction between *Streptomyces* sp. and titania/silica nanospheres. *Water Air Soil Pollution*. 2016;**227**:230. DOI: 10.4172/2157-7439.1000182
- [64] Biolog2. Phenotype MicroArrays for Mammalian Cells [Internet]. 2013. Available from: <http://www.biolog.com/pdf/pmmlit/00A%20046rA%20PM-M%20brochure.pdf> [Accessed: 2017-09-06]
- [65] Larson B, Rieger L, Travis J, Wiater L. Label-Free Phenotype MicroArrays™ Analysis of Cellular Energetic and Apoptotic Activity using Microplate Reading and Phase Contrast Imaging [Internet]. 2015. Available from: <https://www.biotek.com/resources/presentations/label-free-phenotype-microarray-analysis-of-cellular-energetics-and-apoptotic-activity-using-microplate-reading-and-phase-contrast-imaging/> [Accessed: 2017-08-21]
- [66] Biolog1. Phenotype MicroArrays™ PM-M TXO1 MicroPlate™ for Measuring Chemosensitivity Phenotypes of Mammalian Cells and for Sensitively Detecting Mitochondrial Toxicity. [Internet]. 2010. Available from: <http://www.biolog.com/pdf/pmmlit/00P%20219%20PMM%20Tox1%20MicroPlate%20100707.pdf> [Accessed: 2017-09-06]
- [67] Biolog3. Phenotype MicroArrays for Mammalian Cells (PM-M) [Internet]. 2017. Available form: http://www.biolog.com/products-static/phenotype_mammalian_cells_overview.php [Accessed: 2017-09-06]

- [68] Bochner BR, Siri M, Hunag RH, Noble S, Lei XH, Clemons PA, Wagner BK. Assay of the multiple energy-producing pathways of mammalian cells. *PLoS One*. 2011;**6**:e18147. DOI: 10.1371/journal.pone.0018147
- [69] Žigon P, Mrak-Pojjšak K, Lakota K, Terčelj M, Čučnik S, Tomsie M, Sodin-Semrl S. Metabolic fingerprints of human primary endothelial and fibroblast cells. *Metabolomics*. 2016;**12**:92. DOI: 10.1007/s11306-016-1024-7
- [70] Parmar N, Wetton N, Alvarado S, Kennedy S. Profiling of human normal and cancer cell lines using phenotype microarray analysis. *FASEB Journal*. 2014;**28**:613.5
- [71] Martinez-Reyes I, Diebold LP, Kong H, Scheiber M, Huang H, Hensley CT, Mehta MM, Wang T, Santos JH, Woychnik R, Dufour E, Spelbrink JN, Weinberg SE, Zhao Y, DeBerardinis RJ, Chandel NS. TCA cycle and mitochondrial membrane potential are necessary for diverse biological functions. *Molecular Cell*. 2016;**61**:199-209. DOI: 10.1016/j.molcel.2015.12.002
- [72] Wiater LA, Naoble S, Bochner BR. Profiling Toxic Chemical with a New Liver Cell-based Assay [Internet]. 2017. Available from: http://www.biolog.com/pdf/pmmlit/Poster_AASLD_2011_PM-M_Tox1_Assay.pdf [Accessed: 2017-09-06]
- [73] Bochner BR. New technologies to assess genotype–phenotype relationships. *Nature Reviews Genetics*. 2003;**4**:309-314. DOI: 10.1038/nrg1046
- [74] Nierode GJ, Perea BC, McFarland SK, Pascoal JF, Clark DS, Schaffer DV, Dordick JS. High-throughput toxicity and phenotypic screening of 3D human neural progenitor cell culture on a microarray chip platform. *Stem Cell Reports*. 2016;**7**:970-982. DOI: 10.1016/j.stemcr.2016.10.001
- [75] xCelligence. xCelligence RTCA DP Instrument. Flexible Real-Time Cell Monitoring [Internet]. 2014. Available from: <https://www.aceabio.com/products/rtca-dp/> [Accessed: 2016-10-09]
- [76] Phase Holographic Imaging. Holomonitor Application Note on Label-free Cell Motility. [Internet]. 2015. Available from: <http://www.phiab.se/reports/2014/CellMotilityAppNotePHI-140919.pdf> [Accessed: 2016-03-20]
- [77] Székács I, Fejes Á, Klátyik T, Patkó D, Pomóthy J, Mörtl M, Horváth R, Madarász E, Dervas B, Székács A. Environmental and toxicological impacts of glyphosate with its formulating adjuvant. *International Journal of Biological Veterinary Agricultural and Food Engineering*. 2014;**8**:219-224
- [78] Peter B, Nador J, Juhasz K, Dobos A, Korosi L, Székács I, Patko D, Horváth R. Incubator proof miniaturized holomonitor to in situ monitor cancer cells expose to green tea polyphenol and preosteoblast cells adhering on nanostructure titanate surfaces: Validity of the measured parameters and their corrections. *Journal of Biomedical Optics*. 2015;**20**:067002. DOI: 10.1117/1.JBO.20.6.067002
- [79] El-Schich Z, Kamlund S, Janickie B, Alm K, Gjørloff Wingren A. Holography: The usefulness of digital holographic microscopy for clinical diagnostics. In: Naydenova I,

- Nazarova D, Babeva T, editors. *Holographic Materials and Optical Systems*. Rijeka: InTech; 2017. pp. 319-333. DOI: 10.5772/63255
- [80] Kim K, Yoon J, Shin S, Lee SY, Yang SA, Park YK. Optical diffraction tomography techniques for the study of cell pathophysiology. *Journal of Biomedical Photonics & Engineering*. 2016;**2**:1-16. DOI: 10.18287/JBPE16.02.020201
- [81] Mölder A, Sebesta M, Gustafssoni M, Gisselson L, Gjörlöf Wingren A, Alm K. Non-invasive, label-free cell counting and quantitative analysis of adherent cells using digital holography. *Journal of Microscopy*. 2008;**232**:240-247. DOI: 10.1111/j.1365-2818.2008.02095.x
- [82] Lajkó E, Spring S, Láng O, Ingebrandt S, Mezö G, Köhidai L. Impedance-based analysis and holographic phase imaging of the GnRH-III-based drug-targeting in melanoma cells. In: *Impedance-Based Cellular Assays (IBCA'16)*; 9-12 August 2016; Regensburg, Germany. p. T20
- [83] Dudziak M. Opracowanie syntezy wytwarzania nanostruktur złota i heksagonalnego azotku boru do zastosowań biomedycznych [Thesis]. Szczecin: West Pomeranian University of Technology; 2017
- [84] Kalbac M, Kalbacova M, Broz A, Kong J. Graphene substrates promote adherence of human osteoblast and mesenchymal stromal cell. *Carbon*. 2010;**48**:4323-4329. DOI: 10.1016/j.carbon.2010.07.045
- [85] Matusiak P. Określenie właściwości mechanicznych komórek MAC-T za pomocą AFM [Thesis]. Szczecin: West Pomeranian University of Technology; 2014
- [86] Liu D, Wang L, Wang Z, Cuschieri A. Magnetoporation and magnetolysis of cancer cells via carbon nanotubes induced by rotating magnetic fields. *Nano Letters*. 2012;**12**:5117-5121. DOI: 10.1021/nl301928z

Review of *In vitro* Toxicity of Nanoparticles and Nanorods: Part 1

Jose Efrain Perez, Nouf Alsharif,
Aldo Isaac Martínez Banderas, Basmah Othman,
Jasmeen Merzaban, Timothy Ravasi and
Jürgen Kosel

Additional information is available at the end of the chapter

<http://dx.doi.org/10.5772/intechopen.76365>

Abstract

The specific use of engineered nanostructures in biomedical applications has become very attractive, due to their ability to interface and target specific cells and tissues to execute their functions. Additionally, there is continuous progress in research on new nanostructures with unique optical, magnetic, catalytic, and electrochemical properties that can be exploited for therapeutic or diagnostic methods. On the other hand, as nanostructures become widely used in many different applications, the unspecific exposure of humans to them is also unavoidable. Therefore, studying and understanding the toxicity of such materials is of increasing importance. Previously published reviews regarding the toxicological effects of nanostructures focuses mostly on the cytotoxicity of nanoparticles and their internalization, activated signaling pathways, and cellular response. Here, the most recent studies on the *in vitro* cytotoxicity of NPs, nanowires, and nanorods for biomedical applications are reviewed and divided into two parts. The first part considers nonmagnetic metallic and magnetic nanostructures. While part 2 covers carbon structures and semiconductors. The factors influencing the toxicity of these nanostructures are elaborated, to help elucidating the effects of these nanomaterials on cells, which is a prerequisite for their safe clinical use.

Keywords: nanoparticles, nanowires, nanorods, biocompatibility, cytotoxicity, nanomedicine

1. Introduction

Nanostructured materials are defined as possessing one of their dimensions in the range of 1–100 nm, according to the American Society for Testing and Materials (ASTM) international

standards definition [1]. For nanoparticles (NPs), which can be of more or less spherical or cubical shape, two dimensions are required to be within this range. In contrast, the shape of nanorods (NRs) is in one dimension much larger than in the others. For a small aspect ratio (<10), both their length and diameter are in the nanoscale, whereas NRs with a large aspect ratio (>10) only have their diameter within this scale, and are often called “nanowires” (NWs). Nanostructures within this specific size scale show unique size-dependent optical, magnetic, catalytic, and electrochemical properties, among others, as well as high surface to volume ratios. Moreover, their shape, surface chemistry, and chemical composition can be used to tailor specific properties, making nanostructures highly versatile for different applications [2, 3].

The size scale of nanostructures is within the range of several biomolecules, such as proteins and antibodies, allowing specific interactions to occur between them. This, when coupled with the high surface to volume ratios and tunable sizes and properties, makes nanostructures prime candidates for biomedical applications such as imaging, drug delivery, and therapy [4–6]. Examples of applications include the use of NPs as magnetic resonance imaging (MRI) contrast agents [7, 8], tissue engineering [9–11], as well as the recent focus on hyperthermia and cancer cell eradication with the use of NPs and NRs [12–17]. Such applications, if they are aimed for a clinical setting, ultimately require a direct NP/NR exposure in the form of ingestion or intravenous delivery into the body. Naturally, there is a rigorous testing required before any new drug formulation is approved for the clinical use in order to ensure their safety and effectiveness. Currently, very few NP-based drugs have been approved by the Food and Drug Administration and are commercially available. Examples include GastroMARK, used as an MRI contrast agent to enhance the delineation of the bowel, and ferumoxytol, an iron-replacement formulation approved for adults with chronic kidney disease with an iron deficiency [18].

Within this scope, biocompatibility and cytotoxicity data are of paramount importance to evaluate the potential of nanostructures for biomedical applications. Nanostructures are normally engineered to interface and target specific cells or tissues to execute their functions, raising questions about their toxicological effects. For instance, there are several characteristics involved in the toxicity of fiber-like nanomaterials, such as shape, length, chemical composition, agglomeration, and purity, making them suitable to fit the “fiber toxicological paradigm” according to the World Health Organization (WHO) criteria used to describe the toxicity of asbestos fibers [19]. Further, nanostructures are usually tuned for biocompatibility on top of the desired biomedical function, with the most relevant aspects that influence their toxicity being the material [20], size and shape [21], surface charge [22], and surface functionalization [23]. *In vitro* studies, while not able to give a complete insight into the biocompatibility of nanostructures, have a high importance, due to their easy implementation, and provide valuable cytotoxicology data regarding the safety of the use of nanostructures in biomedical applications. Previously published reviews regarding the biosafety of nanostructures include that of Lewinski et al. [24] and Zhao et al. [25]. The former focuses mostly on the cytotoxicity of NPs of different materials, whereas the latter is a more in depth review of the internalization, activated signaling pathways, and cellular response of different kinds of NPs.

Here, we review relevant studies assessing the *in vitro* cytotoxicity of both nanoparticles (NPs) and nanowires (NWs)/nanorods (NRs) with the potential to be used in biomedical applications. Due to their prevalence within the applied nanomaterials in biomedicine, this review

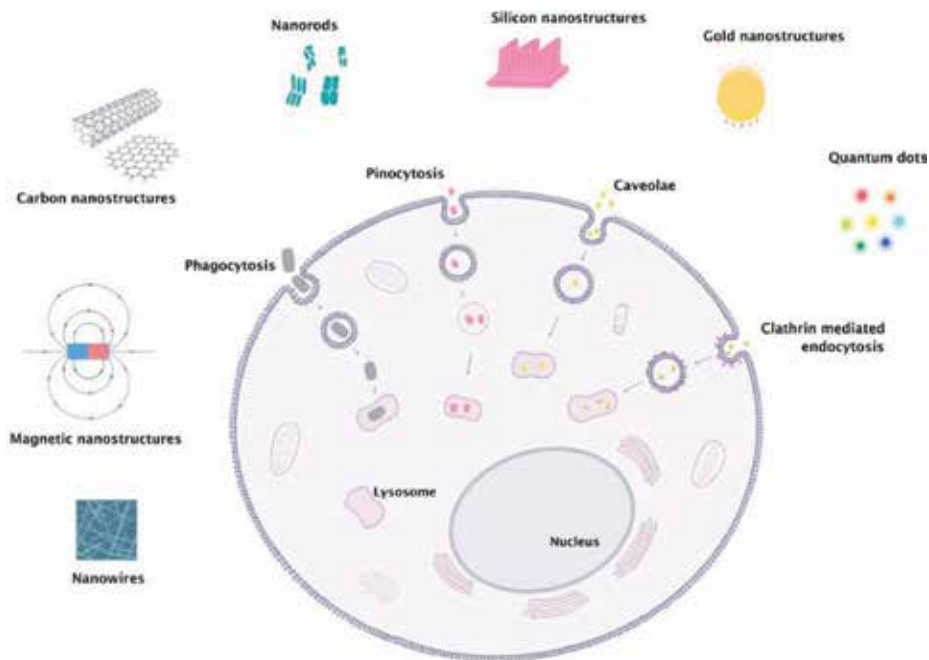


Figure 1. Schematic of the pathways for intracellular uptake of different materials and structures.

covers various materials from four different classes (on Scopus almost 50% of all publications related to cytotoxicity, since the year 2000, fall within these materials) that are typically considered in the context of nanomaterials for biomedical applications. The first part of this review covers nonmagnetic metals and magnetic materials, while the second part covers carbon structures and semiconductors. An overview of the materials and structures covered, together with the various intracellular uptake mechanisms, is given in **Figure 1**.

2. Nonmagnetic metallic nanostructures

2.1. Gold nanoparticles

Gold (Au) NPs are some of the most heavily used nanostructures in biomedical applications, most notably in medical imaging and therapy. The absorbance and fluorescence of Au NPs are higher than that of bulk Au and they can be finely tuned from the visible spectrum to the near infrared by changing their size and morphology [26]. Au can also readily bind different kinds of functionalizing molecules, giving them great versatility [27]. These properties make Au nanostructures popular candidates for X-ray-based imaging and radiotherapy, as well as photothermal therapy, when coupled to their ability to transform absorbed light into heat [26–30].

Two of the first cytotoxicity studies with Au NPs were performed by Tkachenko et al. [31]. In their first approach, they found that NPs conjugated with bovine serum albumin (BSA) and different peptides could enter the cell cytoplasm via an energy-dependent, receptor-mediated

endocytosis pathway, with a decrease in cell viability of only around 5%, using the lactate dehydrogenase (LDH) colorimetric assay. The following year, they tested the same principle in three different cell lines and found that the uptake of Au NPs, as well as their ultimate fate (endosomal or nuclear), was cell dependent [32]. Later, Goodman et al. tested the effects of cationic and anionic Au NPs in the metabolic activity of red blood COS-1 cells, and showed that the former are more cytotoxic, probably due to them being drawn by the cell membrane's negative charge and then taken up [33]. A different approach using human leukemic K562 cells was performed by Connor et al. using different surface modifiers and the 3-(4,5-dimethylthiazol-2-yl)-2,5-diphenyltetrazolium bromide (MTT) assay, concluding that, despite the Au fabrication precursor being cytotoxic, Au NPs are inherently not, even though they are internalized and engulfed in endocytic vesicles [34]. This last finding was also confirmed by Chan and colleagues, who reported a size-dependent, clathrin-mediated uptake of citric acid, and transferrin-coated NPs in HeLa cells (**Figure 2**) [35, 36]. Similarly, size-dependence cytotoxicity was subsequently reported by Pan et al. [37] They showed that fibroblasts, epithelial cells, macrophages, and melanoma cells incubated with small (1.4 nm) Au NPs for 2 days have an IC_{50} ranging from 30 to 56 μM , whereas the same cells can tolerate concentrations 60-fold higher, when changing the particle diameter to 15 nm. The same group then went on to confirm the size-dependent cytotoxicity of Au NPs coated with TPPMS, now extending their findings to elucidate a necrotic death pathway in HeLa cells, due to oxidative stress, intracellular formation of reactive oxygen species (ROS) and a compromised mitochondrial activity [38].

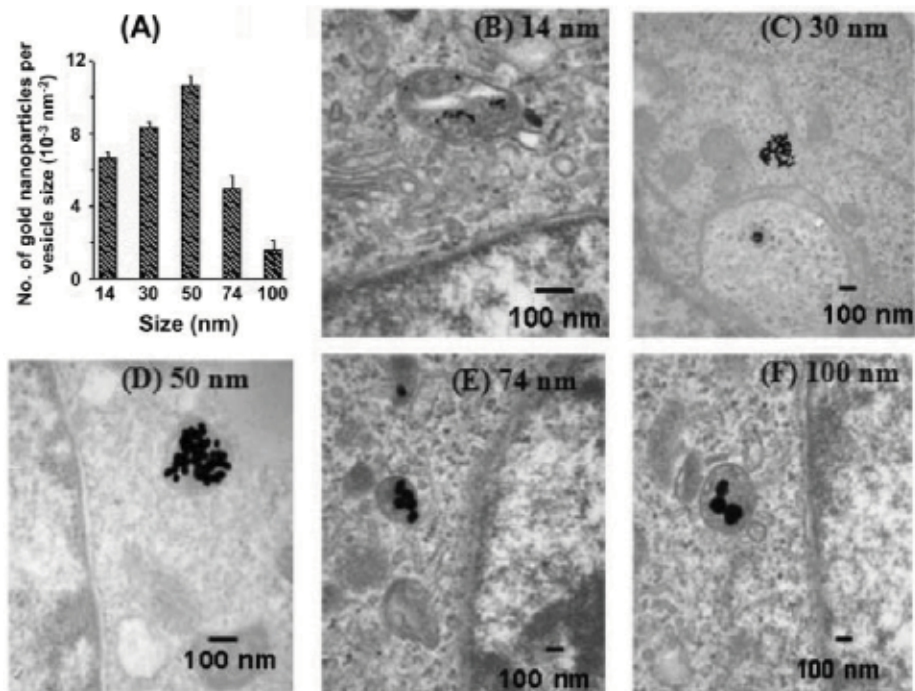


Figure 2. Size-dependent uptake of Au NPs of different sizes in HeLa cells at different positions from B-F, as observed by TEM. While (A) Quantify the number of each Au NPs per vesicle. Adapted with permission from Chithrani et al. [35]. Copyright 2006 American Chemical Society.

The cytotoxicity of Au NPs has also been tested in other relevant cell lines, such as the alveolar type II-like A549 and NCIH441 [39]. Using a combination of metabolic activity, cell proliferation, and release of LDH assays, it was determined that 9.5 nm Au NPs, though internalized and stored in endocytic vesicles, do not have an effect on either of the cell lines' metabolic activity. A 50% decrease in cell proliferation was detected for A549 cells after 24 hours of exposure, decreasing further as time progressed. A mild dose-dependent LDH release was also reported for 24 and 48 hours for Au NP concentrations up to 0.7 mM, although after 72 hours, the release was significantly higher for this concentration, at around 35 and 90% for A549 and NCHIH441 cells, respectively. Macrophages have also been subjected to cytotoxicity assessments using Au NPs [40]. The results in this case are particularly relevant, due to their shedding light on a potential immunological response. Au NPs of three different sizes (2–4, 5–7, and 20–40 nm) were tested in macrophage J774 A1 cells at two concentrations, 1 and 10 ppm. Whereas only the small and medium-sized NPs produced a slight decrease in cell proliferation for the lower concentration, NPs of all three sizes decreased cell proliferation to around 30–40% for the 10 ppm concentration. Au NPs were shown to be inside vesicles in the cytoplasm, as was reported for human leukemic [34], HeLa [35], and alveolar type II-like cells [39]. Additionally, it was reported that Au NPs upregulate the expression of interleukin-1 (IL-1), interleukin-6 (IL-6), and tumor necrosis factor (TNF- α). This data show that macrophages, being one of the principal immune effector cells, activate a pro-inflammatory response, when in the presence of Au NPs of either size.

Cho et al. looked closely at the effects of different surface functional groups on the uptake and cell membrane adsorption of Au NPs by breast cancer SK-BR-3 cells [41]. They tested Au NPs of two sizes (15 and 45 nm) with three different surface groups: poly(ethylene glycol) (PEG), anti-HER2, and poly(allylamine hydrochloride) (PAH). The smaller NPs were found to be more readily internalized than the larger ones, in contrast with previous findings [35, 36]. The PAH-modified NPs showed the greatest amount of internalization, followed by anti-HER2 and then PEG NPs. Using inductively coupled plasma mass spectrometry (ICP-MS) and an etching method to remove the NPs adsorbed to the cell membrane [42], they were able to distinguish between internalized nanoparticles to those that remained attached to the cell membrane and found that PEG-modified NPs had the lowest adsorption rate, thereby internalizing most of the NPs that came in contact with the cells. PAH-modified NPs had a very strong affinity to the cell membrane, probably due to their electrostatic interactions.

A more recent study compared NPs of 10, 25, and 50 nm and found that larger NPs are more readily taken up by NRK cells [43]. It was also reported that Au NPs enter the cells through endocytosis, ultimately accumulating in lysosomes and impairing their degradation capacity through alkalinization: Au NPs cause the dissociation of the V1 protein from the acidification-regulator complex H⁺(V)-ATPase, down-regulating its activity. The impairment of lysosomal function thus reduced the turnover of autophagosomes, carriers of intracellular content to their final degradation in lysosomes, leading to their accumulation in the cell cytoplasm.

2.2. Gold nanorods and nanowires

Gold NRs and NWs, unlike NPs, possess a transverse and a dominant longitudinal plasmon [44]. This intense absorption band is near the infrared region, which biological tissue hardly absorbs, thus making these Au nanostructures attractive in the biomedical field. Early

cytotoxicity data showed that HeLa cells incubated with PEG-stabilized NRs at concentrations up to 0.5 mM survived with more than 90% viability after 24 hours, as per MTT assay [45]. Takahashi et al. observed similar viability effects under the same conditions, but using NRs modified with phosphatidylcholine [46]. Chithrani et al. reported that an increased uptake was observed for NRs in terms of the number of particles per cell with NRs with smaller aspect ratios coated with citric acid ligands [35] and transferrin [36]. Similarly, NRs of varying surface charges provided by layers of polyelectrolyte coatings seem to maintain a cell viability of around 90%, with an increased cellular uptake observed with NRs with a positive surface charge [47]. These results were later confirmed using NRs coated with the polyelectrolytes polyacrylic acid (PAA) and PAH, with human colon cancer HT-29 cells showing 90% viability after incubation with 0.4 nM Au NRs with either coating [48]. Cell growth was also reported not to be impaired, when compared with control cells, although higher internalization numbers were found for PAH-coated NRs compared to PAA ones. This is in agreement with previous findings [47]: positively charged particles (PAH-coated) are more readily taken up, when compared to negatively charged ones (PAA-coated), possibly due to the cell membrane's negative charge attracting the positively charged particles, leading to a higher membrane adsorption, as was observed with Au NPs [33, 41].

More recent studies have continued the analysis of the toxicological properties of Au NRs with a higher aspect ratio, or Au NWs, as they provide enhanced properties such as absorption and scattering, due to their increase in length [49]. One of the first approaches aimed to compare the cytotoxic effects of Au NRs with Au NWs with an aspect ratio 10 times larger [50]. Both instances of particles were coated either with tannic acid (TA) or carboxylated PEG (PEG-COOH) and the cytotoxicity to human keratinocyte cells was evaluated using the (3-(4,5-dimethylthiazol-2-yl)-5-(3-carboxymethoxyphenyl)-2-(4-sulfophenyl)-2H-tetrazolium) (MTS) assay, an indicator of mitochondrial metabolic activity similar to the MTT assay. Following the same trend as previous cytotoxic data with surface-modified Au NRs, both TA and PEG-COOH-coated Au NRs showed a cell viability of up to 90% after 24 hours of incubation and for concentrations as high as 100 $\mu\text{g}/\text{mL}$; however, in the case of Au NWs, TA decreased the cell viability to around 70% at the 50 $\mu\text{g}/\text{mL}$ concentration, whereas PEG-COOH-Au NWs maintained the viability above the 90% mark. These results indicate that, as Au NRs, Au NWs show very low cytotoxic potential, though specific surface coatings may elicit a toxic response. The authors also reported an increased uptake for Au NWs, when compared with NR independent of the surface coating. However, the values are reported in mass of Au per cell, which could be explained by the amount of material, due to the increase in size, and not be a clear representation of the amount of particles internalized.

2.3. Silver nanoparticles and nanowires

Silver (Ag) NPs have proven themselves greatly useful for their antimicrobial activity [51] and they are widely used in therapeutics and as a treatment for burns [52]. Naturally, a plethora of toxicity assessment studies has been carried out in order to understand the potential side effects of these nanostructures. The first cytotoxicity studies observed the effects of NPs on metabolic activity and membrane damage through LDH leakage, as well as the dependence

of the generation of ROS on particle size and the evaluation of the inflammatory response [53–55]. In all three studies, a dose-dependent decrease in mitochondrial metabolic activity and an increase in LDH leakage were reported for Ag NPs of 15 nm in rat liver BRL 3A cells, C18-4 germline stem cells, and macrophages for doses up to 75 $\mu\text{g}/\text{mL}$. Changes in cell morphology and uptake of NPs were also reported, with low levels of apoptosis. Interestingly, larger NPs (55 nm) induced a lesser cytotoxic response in macrophages, a result that can be attributed to the larger agglomerates not being easily internalized. Additionally, Ag NPs significantly impacted ROS generation and the release of inflammatory mediators including TNF- α , MIP-2, and IL-1 β in macrophages for doses starting at 5 $\mu\text{g}/\text{mL}$. In contrast, Yen et al. reported no upregulation of the pro-inflammatory genes TNF- α , IL-1, and IL-6, though the doses tested were considerably higher [40].

It was later confirmed by Miura et al. that the ROS-related genes ho-1 and mt-2A are upregulated in HeLa cells [56], further cementing its role in the cytotoxic response. On the other hand, Autrup and co-workers showed that polyvinylpyrrolidone (PVP)-coated Ag NPs of 70 nm in diameter seemed to elicit both an apoptotic and necrotic response in THP-1 monocytes [57] and human alveolar A549 cells [58]. Although necrosis was markedly higher, the effect could be a progression from an early apoptotic stage to a late apoptotic/necrotic one.

Other parameters, such as genotoxicity, have also been studied. Using human lung fibroblast IMR-90 cells and glioblastoma U251 cells as test models, AshaRani et al. concluded that starch-coated Ag NPs (6–20 nm in size) are taken up and reside inside the mitochondria and nucleus and, on top of generating ROS and reducing the metabolic activity and cell viability (Figure 3), they also reduced the ATP content of the cells and induced DNA damage and chromosomal aberrations in a dose-dependent manner. The latter resulted in cell cycle arrest in the G₂/M phase with no significant cell death observed, possibly due to the repair of DNA damage [59]. On the other hand, RAW 264.7 macrophage cells exposed to increase concentrations of 70 nm Ag NPs showed a significant increase in TNF- α , protein, and gene levels. The secretion of nitric oxide, a second messenger in the inflammatory response, as well as

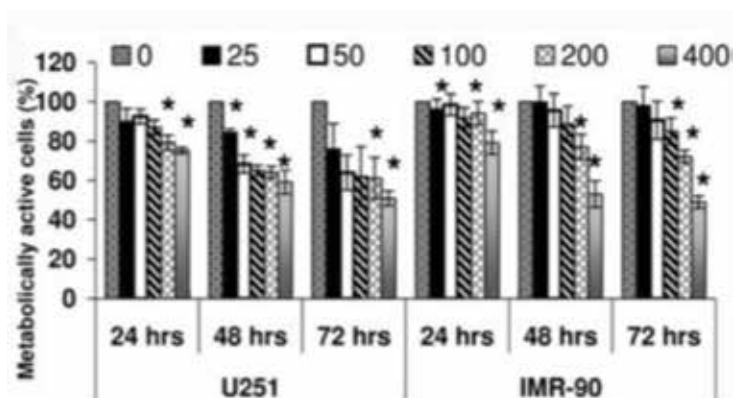


Figure 3. Cytotoxicity of Ag NPs on U251 glioblastoma and IMR-90 fibroblast cells. Different concentrations of NPs with sizes ranging from 6 to 20 nm in diameter were cocultured with the cells for incubation times up to 72 hours. Adapted with permission from AshaRani et al. [59]. Copyright 2009 American Chemical Society.

the gene expression of matrix metalloproteinases (MMPs) MMP-3, MMP-11, and MMP-19, which play a key role in extracellular matrix degradation and can be activated through ROS were also reported [60]. Further, another parameter that has been observed is the effect of Ag NPs of different sizes on the differentiation of embryonic stem cells [61]. Differentiation into cardiomyocytes was inhibited in a dose-dependent manner, with Ag NPs of 20 nm having a stronger effect compared to larger ones.

In recent studies, it has been proposed that the intracellular release of Ag ions from the NPs is one of the causes of their cytotoxicity. Singh et al. showed that, after being taken up through scavenger receptor-mediated phagocytosis in macrophages, intracellular dissolution of Ag NPs had a 50 times faster rate than in water, at around 5% of the total dose being dissolved [62]. It was suggested that Ag ions are a cytotoxic response initiator in human lung BEAS-2B cells [63].

Ag NW cytotoxicity, on the other hand, has not been extensively studied. In a comparative study of Ag NWs with a diameter of around 100 nm and lengths of 3, 5, 10, 14 and 28 μm , it was found that only the wires with a length of 28 μm could elicit a significant decrease in cell proliferation and membrane instability in THP-1 cells [64]. Using light microscopy and back-scattered electron imaging, it was also proven that NWs of 14 and 28 μm are not properly internalized, resulting in a frustrated phagocytosis, or an inability to engulf its target, which is in turn an initiator of the inflammatory response. In a different approach, red blood cells exposed to Ag NWs of 2 μm in length and a diameter of 40 nm were confirmed to suffer structural changes, aggregation, and hemolysis in a dose-dependent manner [65].

3. Magnetic nanostructures

3.1. Magnetic nanoparticles

Magnetic NPs are usually made of a magnetic core bound within a shell that allows them to be functionalized with relevant ligands and gives them stability in solution [66]. Their main advantage is their ability to be manipulated using an external magnetic field, making them attractive for different biomedical applications. These include cell labeling and MRI contrast agents [67, 68], targeted drug delivery [69, 70], and cancer cell eradication [71, 72]. Iron oxide NPs such as magnetite (Fe_3O_4) and maghemite ($\gamma\text{-Fe}_2\text{O}_3$) are the most widely used magnetic NPs [73]. Sufficiently small Fe oxide NPs exhibit superparamagnetism: NPs become magnetized under an external magnetic field, but loose do not possess any remanent magnetization once the field is removed [74]. Superparamagnetic Fe oxide NPs (SPIONs) can be manipulated and guided by a magnetic field without losing the stable colloidal suspension, when there is no field applied, a quality that is attractive for biomedical applications.

3.2. Superparamagnetic iron oxide nanoparticles

Initial cytotoxicity studies compared the cytotoxic effects of bare magnetite NPs with PEG-coated ones in primary human fibroblast hTERT-BJ1 cells, and found that, whereas cells treated with 40–50 nm PEG-coated NPs for 24 hours remained 100% viable for concentrations

as high as 1 mg/mL, uncoated, 10–15 nm NPs reduced the viability to around 70% at a concentration of 250 µg/mL [75]. Similar results were observed with pullulan-coated and uncoated NPs within the same size range [76]. There, it was also shown that bare NPs significantly reduce cell attachment and disrupt the distribution of actin filaments and microtubules, while also being taken up at a higher rate compared to the coated ones. Uncoated NPs were also reported to have cytotoxic effects only at higher doses (100–250 µg/mL) in terms of cell viability and LDH leakage in rat liver BRL 3A cells [53]. In agreement with these findings, hydroxy-tetramethylammonium-coated SPIONs at higher concentrations (23 mM) did not induce a reduction in viability of kidney COS-7 cells, though the time of incubation tested was only of 4 hours [77].

Ma et al. studied the uptake of 30 nm aminosilane-coated NPs by human lung cancer SPC-A1 and human lung WI-38 cells and found that the intracellular Fe content was 15 times higher for the cancerous cells compared to normal counterparts [78]. As with other NPs, they are likely endocytosed through phagocytosis and found within endosomes and lysosomes. Human monocytes-macrophages were also found to endocytose SPIONs and retained them inside lysosomes, remaining highly viable with no apparent activation of pro-inflammatory cytokines for up to 14 days following the incubation with 0.4 mg/mL SPIONs [79].

Using bare 20–30 nm magnetite NPs, Karlsson et al. tested other parameters of cytotoxicity in the human alveolar A549 cells, such as DNA damage and intracellular ROS [80]. No DNA damage or intracellular ROS were found for doses up to 40 µg/cm², although a slight oxidative DNA lesion was found at this dose. In contrast, another study showed that uncoated SPIONs elicited a significant level of apoptosis on mouse fibroblasts (L929), whereas PVA-coated ones did not show a loss of cell viability, apoptosis, necrosis, or cell cycle arrest for up to 72 hours of incubation and concentrations up to 200 mM [81]. However, an increase in the concentration to 400 mM did induce apoptosis and cell cycle arrest, possibly due to DNA damage through oxidative stress. Naqvi et al. obtained similar results for Tween 80-coated NPs in macrophage J774 A1 cells: >95% cell viability for low concentrations (25–200 µg/mL) and low incubation times, with a decrease to 55–65% for higher concentrations (300–500 µg/mL) associated to an apoptotic death pathway through ROS generation [82].

In contrast to previous findings, both citric acid and dextran-coated NPs were found to produce a dose-dependent cytotoxicity in human umbilical vein endothelial cells (HUVECs) [83]. Concentrations as low as 0.1 nM decreased the cell viability for both NPs to around 80% after 24 hours and increasing the value to 20 nM would decrease the cell viability to less than 15%. Additionally, as shown by Soenen et al. [84], actin filaments and microtubules appeared disrupted, thinner, and less organized and vinculin adhesion points were diminished. Further, NPs also reduced the migration and vasculogenesis capabilities of HUVECs. Similar results regarding cell attachment and cytoskeleton morphology were also reported in a multiparametric study with NPs with different coatings on various cell lines [84].

With an aim to understand the differences in cytotoxicity between the charges provided by different coatings on SPIONs, a study showed that when different functional groups were added in order to provide either a positive or negative charge on SPIONs, cell viability and cell membrane integrity remained above 85% up to 24 hours for doses as high as 1000 ppm

on L929 fibroblasts for all the coatings tested [85]. As observed for other types of NPs, the positively charged NPs were more readily taken up than negatively charged ones. Similarly, ROS generation was not significantly different. However, the positively charged and highest negatively charged NPs showed DNA damage starting from concentrations of 200 ppm. In agreement with this, another study using HCM (heart), BE-2-C (brain), and 293T (kidney) cell lines reported similar results [86]. There, bare, positively, and negatively charged NPs all showed a dose-dependent response for doses up to 36 mM, with positively charged NPs being more cytotoxic for the three cell lines, suggesting a cell-specific response. Gene expression analysis showed that genes that were mainly altered were those related to apoptosis, cell cycle, and cell proliferative responses, most probably due to ROS.

More recent studies have focused on looking at other parameters to better understand the cytotoxic response. A size-dependent response was observed for uncoated NPs of 5 and 30 nm, with only the latter inducing a significant increase in ROS generation, whereas dextran-coated and PEG-coated did not have an effect on ROS levels [87]. Khan et al., on the other hand, studied the effects of SPIONs on autophagy, a homeostasis mechanism used to degrade proteins and organelles for multiple functions [88]. They proved that ROS induces autophagy through the mTOR pathway only on human alveolar cancer A549 cells, and not on normal human lung fibroblast IMR-90 cells, while the authors attributed the autophagy to be involved with cell death. Lastly, Singh et al. observed a different cytotoxic response and uptake related to the Fe redox state (magnetite vs. maghemite) in human lymphoblastoid MCL-5 cells [89]. While no significant difference was found between these two states in terms of uptake, a decrease in the serum concentration drastically increased the uptake for dextran-coated maghemite NPs and this specific kind of NPs was the only one reported to elicit a genotoxic response.

3.3. Magnetic nanowires

Magnetic NWs possess tunable lengths and diameters and can be functionalized to provide specific targeting and biocompatibility. Depending on the fabrication method and its parameters, as well as precursor materials, the magnetic properties of NWs can be finely modulated [66, 90]. Magnetic NWs have anisotropic structures with high aspect ratios, which allow them to exert torques when under a magnetic field [91]. Additionally, they possess higher magnetization values per unit of volume when compared to NPs, allowing them to exert larger forces [92]. These qualities have made magnetic NWs prime candidates for different biomedical applications, including cell separation and guidance [91–93], targeted drug delivery [94, 95], and cell eradication [15, 16, 96, 97].

The cytotoxicity of Fe NWs was first characterized by Song et al. on HeLa cells [98]. Using uncoated NWs of <math><10\ \mu\text{m}</math> in length and 50 nm in diameter, they determined that Fe NWs have no significant effect on the cell viability and proliferation for concentrations up to 10,000 NWs per cell and for incubation times up to 72 hours. Fe NWs were internalized either as single NW, bundles or as aggregates, mainly localizing in the cytoplasm and inside vesicles, but not inside cell nuclei. Later, Safi et al. proved the same intracellular distribution in fibroblast NIH/3T3 cells using maghemite NWs of <math><15\ \mu\text{m}</math> and identified such vesicles as late

endosomal or lysosomal endosomes (**Figure 4**) [99]. It was concluded that NWs are degraded by cells and cut into shorter pieces, possibly by the decrease in pH occurring in lysosomal compartments [100]. Along with no significant decrease in cell viability, no ROS were found after 4 hours of incubation for doses up to 170 NWs per cell. In a recent study, NWs with iron core and iron oxide shell were compared to pure iron NWs and tested on HCT 116 cells. The experiments confirmed the high cell viability values found for iron NWs before and revealed even higher values for the core/shell NWs [101]. An additional advantage of the core/shell NWs is the possibility to tune their magnetic properties to the specific requirements of various applications.

Studies with Ni NWs first showed a similar distribution to that of Fe NWs: Ni NWs of 20 μm in length and 200 nm in diameter activated cell membrane receptors associated with metalloproteins, thereby being internalized, triggering lysosomal function in the process and localizing inside them around the cell nucleus [102]. Lamellipodium extensions, due to cell tethering and re-alignment, were also a consequence of Ni NW internalization, possibly due to a cell stiffening response. The same group then studied the biocompatibility of Ni NWs on human monocyte THP-1 cells using high content analysis [103]. Measuring cell viability

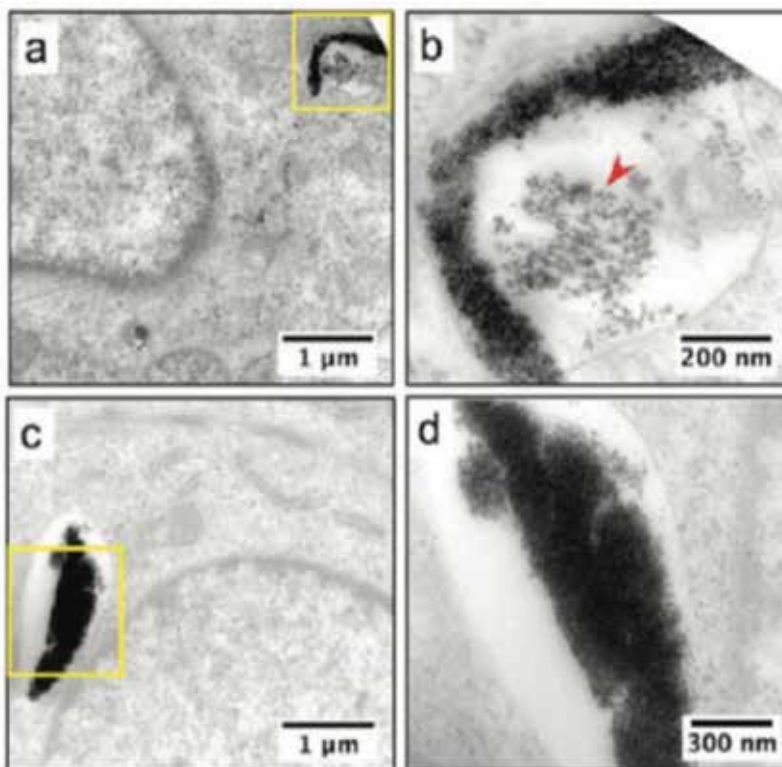


Figure 4. NIH/3T3 fibroblasts incubated with maghemite ($\gamma\text{-Fe}_2\text{O}_3$) NWs during 24 hours. The NWs were found inside membrane-bound compartments, identified as late endosomal or lysosomal endosomes, b) and d) are zoomed images from a) and b) respectively. Adapted with permission from Safi et al. [99]. Copyright 2011 American Chemical Society.

and membrane permeability, they found Ni NWs to be nontoxic for low incubation times (<10 hours) and concentrations (<100 NWs per cell). Hossain and Kleve then investigated the effects of Ni NWs on human pancreatic adenocarcinoma Panc-1 cells [104]. Using NWs of around 6.5 μm in length and 215 nm in diameter, a dose-dependent cytotoxic response was shown, including ROS generation and the induction of apoptosis and cell cycle arrest in the G_0/G_1 phase. A similar response was then reported for HeLa cells, along with mitochondrial membrane depolarization [105].

We reported the cytotoxicity of Ni NWs in human fibroblast WI-38 cells [106] and human colorectal carcinoma HCT 116 cells [107]. Whereas WI-38 cells showed no significant decrease of cell viability up to doses of 120 $\mu\text{g}/\text{mL}$ for 24 hours of incubation and the viability of HCT 116 cells decreased significantly at the same incubation time for doses as low as 5 $\mu\text{g}/\text{mL}$. For both cell lines, NWs were internalized and appeared in the cytosol inside membrane-bound compartments, possibly lysosomes, as shown previously [102], with the internalization in HCT 116 cells taking place through the phagocytosis pathway. Apoptosis was also confirmed to be the cell death pathway, which would later progress into secondary necrosis and induce cell membrane instability and LDH leakage. Lastly, it was also confirmed that Ni^{2+} is released intracellularly following NW uptake, due to the acidic pH inside the lysosomes. Although the percentage of this intracellular dissolution is low compared to the total dose, it is plausible that the leached Ni^{2+} contributes to the cytotoxic effects observed. It should be mentioned that Au-coated Ni NWs showed an improved biocompatibility, possibly due to the Au reducing the degree of dissolution, while also providing a functionalization layer [108, 109]. Similarly, we have reported the stabilization of Fe NWs by coating with a poly(MPC) homopolymer in order to increase dispersion and biocompatibility [110].

4. Conclusion

Recent studies on the *in vitro* cytotoxicity of nonmagnetic and magnetic structures in biomedical applications were reviewed, taking into account nanoparticles and nanowires/nanorods. A summary of the results of representative studies is provided in **Table 1**.

Comparisons between the cytotoxicities of those different nanomaterials are generally difficult to make, due to the vast range of methods, concentrations, dimensions, cell lines, etc. For instance, the concentrations reported in the different studies were typically evaluated using either ICP or cryogenic TEM. However, the concentration or dose of the nanomaterial plays a significant role in the cytotoxic response as well as the biomedical applications.

While the concentrations and exposure times are critical factors, the toxicity of these nanostructures is also material dependent. These relations can be seen in **Figure 5**, which presents the average values reported for the cell viabilities (ignoring differences in concentrations, incubation times, etc.), when exposed to the nanomaterials in the studies covered in **Table 1**. Fe nanomaterials showed higher cell viabilities than Au ones.

Nanostructure type	Surface coating	Nanostructure concentration	Average size	Cell line	Cell viability	Viability test	References
Au NPs	BSA	–	20 nm	HepG2	95%	LDH assay	[31]
Au NPs	–	1 and 10 ppm	2–4, 5–7 and 20–40 nm diameter	J774 A1 macrophages	Cell proliferation decreased to 30–40% for all three sizes at 10 ppm	Multisizer quantification	[40]
Au NRs	PEG	0.5 mM	65 nm length and 11 nm width	HeLa cells	>90%	MTT assay	[45]
Ag NWs	–	4 µg/cm ²	100 nm diameter and 28 µm length	THP-1 cells	Significant decrease in cell proliferation and increase of membrane instability	Alamar Blue, LDH assay	[64]
SPIONs	PEG	1 mg/mL for 40–50 nm NPs, 250 µg/mL for 10–15 nm NPs	40–50 nm diameter, 10–15 nm diameter	hTERT-BJ1	100% for 40–50 nm NPs, 70% for 10–15 nm NPs	MTT assay	[75]
SPIONs	–	100–250 µg/mL	47 nm	BRL 3A rat liver cells	70%	MTT, LDH assay	[53]
Fe NWs	–	10,000 NWs per cell	10 µm length and 50 nm diameter	HeLa cells	No significant effect	MTT assay	[98]
Ni NWs	–	5 µg/mL	5.4 µm length and 33 nm diameter	HCT 116 cells	<80%	MTT, LDH assay	[107]

Table 1. Summary of *in vitro* cytotoxicity studies with different kinds of nanoparticles (NPs) and nanowires (NWs), NWs with aspect ratio < 10 are often called nanorods (NR), SPION referred to superparamagnetic iron oxide NPs.

In addition, the particle size plays a major role in the cytotoxic properties of the nanostructure, whereby both the cellular uptake efficiency and pathway are affected, with smaller particles being internalized faster than larger ones.

The induction of ROS after dissolving the nanostructures in the lysosomes was shown to be the primary underlying cause of the toxicity in several cases, leading to cell death through the apoptotic pathway, due to ROS generation and mitochondrial damage. The acidic condition inside the lysosome increases the digestion of the particles, enhancing the release of ions that

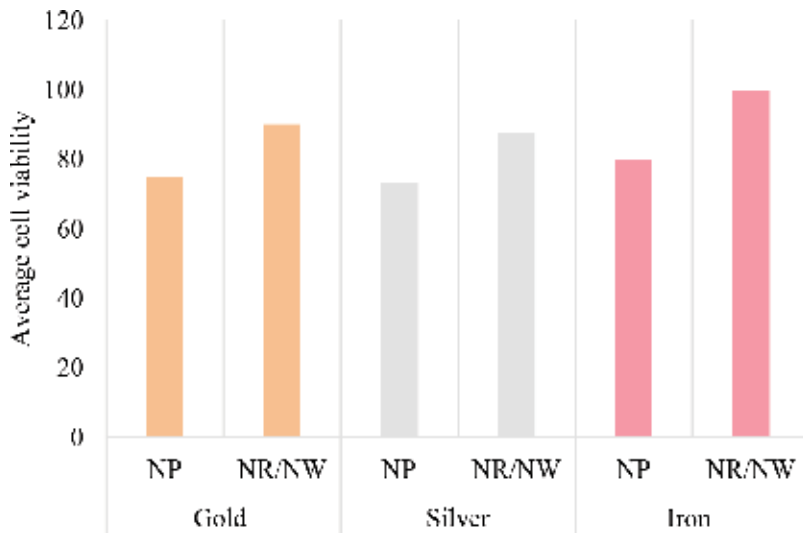


Figure 5. Average cell viability when exposed to nanomaterials reported in **Table 1**, considering nanoparticles (NP), nanorods (NR), and nanowires (NW).

affect the viability of the cells. However, the oxidation of Fe nanostructures did not decrease the cell viability.

Adding a coating to the nanostructure typically affected both the toxicity and the surface charge of the nanostructure, where cationic surfaces are more toxic than anionic. For instance, coating Au with TA coating led to the decrease of the cell viability to around 70%, whereas with a PEG coating, the viability was maintained above 90%.

The cytotoxicity of the nanomaterial depends also on the nanostructure's shape. In this regard, several advantages have been reported for NWs over NPs. For instance, they enhance the drug-loading capacity, due to their large surface area. Moreover, magnetic NWs, due to their higher magnetization, can be better manipulated by the use of the magnetic field than NPs. An interesting observation from **Figure 5** is that NWs/NRs are, on average, less cytotoxic than NPs. This was attributed to the increased interaction of the nanomaterial with the cells, due to the large surface area.

While all these studies contributed to obtain a better picture of the cytotoxicity of nanomaterials and the underlying mechanisms, it is a persisting issue that a consistent measurement and reporting system will be needed for future studies. This will not only enable performing more accurate comparisons of the toxicological characteristics of nanostructures but also to better evaluate the potential of using them for biomedical applications.

Acknowledgements

Research reported in this publication was supported by the King Abdullah University of Science and Technology (KAUST). Policy: <https://www.intechopen.com/authorship-policy.html>.

Author details

Jose Efrain Perez^{1,2}, Nouf Alsharif^{1,2}, Aldo Isaac Martínez Banderas^{1,2}, Basmah Othman¹, Jasmine Merzaban¹, Timothy Ravasi¹ and Jürgen Kosel^{2*}

*Address all correspondence to: jurgen.kosel@kaust.edu.sa

1 Division of Biological and Environmental Sciences and Engineering, King Abdullah University of Science and Technology, Thuwal, Kingdom of Saudi Arabia

2 Division of Computer, Electrical and Mathematical Sciences and Engineering, King Abdullah University of Science and Technology, Thuwal, Kingdom of Saudi Arabia

References

- [1] ASTM International. Standard Terminology Relating to Nanotechnology [Internet]. 2012. Available from: <https://www.astm.org/Standards/E2456.htm> [Accessed: March 15, 2018]
- [2] Sanvicens N, Marco MP. Mint: Multifunctional nanoparticles – properties and prospects for their use in human medicine. *Trends in Biotechnology*. 2008;**26**:425-433. DOI: 10.1016/j.tibtech.2008.04.005
- [3] Sau TK, Rogach AL, Jäckel F, Klar TA, Feldmann J. Mint: Properties and applications of colloidal nonspherical noble metal nanoparticles. *Advanced Materials*. 2010;**22**:1805-1825. DOI: 10.1002/adma.200902557
- [4] Brigger I, Dubernet C, Couvreur P. Mint: Nanoparticles in cancer therapy and diagnosis. *Advanced Drug Delivery Reviews*. 2002;**54**:631-651. DOI: 10.1016/S0169-409X(02)00044-3
- [5] Doane TL, Burda C. Mint: The unique role of nanoparticles in nanomedicine: Imaging, drug delivery and therapy. *Chemical Society Reviews*. 2012;**41**:2885. DOI: 10.1039/c2cs15260f
- [6] Parveen S, Misra R, Sahoo SK. Mint: Anoparticles: A boon to drug delivery, therapeutics, diagnostics and imaging. *Nanomedicine: Nanotechnology, Biology, and Medicine*. 2012;**8**:147-166. DOI: 10.1016/j.nano.2011.05.016
- [7] Li L, Jiang W, Luo K, Song H, Lan F, Wu Y, Gu Z. Mint: Superparamagnetic iron oxide nanoparticles as MRI contrast agents for non-invasive stem cell labeling and tracking. *Theranostics*. 2013;**3**:595-615. DOI: 10.7150/thno.5366
- [8] Xie H, Zhu Y, Jiang W, Zhou Q, Yang H, Gu N, Zhang Y, Xu H, Xu H, Yang X. Mint: Lactoferrin-conjugated superparamagnetic iron oxide nanoparticles as a specific MRI contrast agent for detection of brain glioma *in vivo*. *Biomaterials*. 2011;**32**:495-502. DOI: 10.1016/j.biomaterials.2010.09.024
- [9] Kuo S-W, Lin H-I, Ho JH-C, Shih Y-RV, Chen H-F, Yen T-J, Lee OK. Mint: Regulation of the fate of human mesenchymal stem cells by mechanical and stereo-topographical

- cues provided by silicon nanowires. *Biomaterials*. 2012;**33**:5013-5022. DOI: 10.1016/j.biomaterials.2012.03.080
- [10] Liu D, Yi C, Wang K, Fong CC, Wang Z, Lo PK, Sun D, Yang M. Mint: Reorganization of cytoskeleton and transient activation of Ca²⁺ channels in mesenchymal stem cells cultured on silicon nanowire arrays. *ACS Applied Materials and Interfaces*. 2013;**5**:13295-13304. DOI: 10.1021/am404276r
- [11] Liu D, Yi C, Fong C-C, Jin Q, Wang Z, Yu W-K, Sun D, Zhao J, Yang M. Mint: Activation of multiple signaling pathways during the differentiation of mesenchymal stem cells cultured in a silicon nanowire microenvironment. *Nanomedicine: Nanotechnology, Biology, and Medicine*. 2014;**10**:1-11. DOI: 10.1016/j.nano.2014.02.003
- [12] Laurent S, Dutz S, Häfeli UO, Mahmoudi M. Mint: Magnetic fluid hyperthermia: Focus on superparamagnetic iron oxide nanoparticles. *Advances in Colloid and Interface Science*. 2011;**166**:8-23. DOI: 10.1016/j.cis.2011.04.003
- [13] Cherukuri P, Glazer ES, Curley SA. Mint: Targeted hyperthermia using metal nanoparticles. *Advanced Drug Delivery Reviews*. 2010;**62**:339-345. DOI: 10.1016/j.addr.2009.11.006
- [14] Su Y, Wei X, Peng F, Zhong Y, Lu Y, Su S, Xu T, Lee ST, He Y. Mint: Gold nanoparticles-decorated silicon nanowires as highly efficient near-infrared hyperthermia agents for cancer cells destruction. *Nano Letters*. 2012;**12**:1845-1850. DOI: 10.1021/nl204203t
- [15] Fung AO, Kapadia V, Pierstorff E, Ho D, Chen Y. Mint: Induction of cell death by magnetic actuation of nickel nanowires internalized by fibroblasts. *Journal of Physical Chemistry C*. 2008;**112**:15085-15088. DOI: 10.1021/jp806187r
- [16] Contreras MF, Sougrat R, Zaher A, Ravasi T, Kosel J. Mint: Non-chemotoxic induction of cancer cell death using magnetic nanowires. *International Journal of Nanomedicine*. Jan. 2015;**10**:2141-2153. DOI: 10.2147/IJN.S77081
- [17] Dreaden EC, Mwakwari SC, Austin LA, Kieffer MJ, Oyelere AK, El-Sayed MA. Mint: Small molecule-gold nanorod conjugates selectively target and induce macrophage cytotoxicity towards breast cancer cells. *Small*. 2012;**8**:2819-2822. DOI: 10.1002/smll.201200333
- [18] Cortajarena AL, Ortega D, Ocampo SM, Gonzalez-García A, Couleaud P, Miranda R, Belda-Iniesta C, Ayuso-Sacido A. Mint: Engineering iron oxide nanoparticles for clinical settings. *Nanobiomedicine*. 2014;**1**:2. DOI: 10.5772/58841. DOI: 10.5772/58841
- [19] Liu Y, Zhao Y, Sun B, Chen C. Mint: Understanding the toxicity of carbon nanotubes. *Accounts of Chemical Research*. 2013;**46**:702-713. DOI: 10.1021/ar300028m
- [20] Kong B, Seog JH, Graham LM, Lee SB. Mint: Experimental considerations on the cytotoxicity of nanoparticles. *Nanomedicine*. 2011;**6**:929-941. DOI: 10.2217/nnm.11.77
- [21] Gratton SE, Ropp P, Pohlhaus PD, Luft JC, Madden VJ, Napier ME, JM DS. Mint: The effect of particle design on cellular internalization pathways. *Proceedings of the National Academy of Sciences of the United States of America*. 2008;**105**:11613-11618. DOI: 10.1073/pnas.0801763105

- [22] Fröhlich E. Mint: The role of surface charge in cellular uptake and cytotoxicity of medical nanoparticles. *International Journal of Nanomedicine*. 2012;**7**:5577-5591. DOI: 10.2147/IJN.S36111
- [23] Kim ST, Saha K, Kim C, Rotello VM. Mint: The role of surface functionality in determining nanoparticle cytotoxicity. *Accounts of Chemical Research*. 2013;**46**:681-691. DOI: 10.1021/ar3000647
- [24] Lewinski N, Colvin V, Drezek R. Mint: Cytotoxicity of nanoparticles. *Small (Weinheim an der Bergstrasse, Germany)*. 2008;**4**:26-49. DOI: 10.1002/smll.200700595
- [25] Zhao F, Zhao Y, Liu Y, Chang X, Chen C, Zhao Y. Mint: Cellular uptake, intracellular trafficking, and cytotoxicity of nanomaterials. *Small*. 2011;**7**:1322-1337. DOI: 10.1002/smll.201100001
- [26] Mieszawska AJ, Mulder WJM, Fayad ZA, Cormode DP. Mint: Multifunctional gold nanoparticles for diagnosis and therapy of disease. *Molecular Pharmaceutics*. 2013;**10**:831-847. DOI: 10.1021/mp3005885
- [27] Dreaden EC, Alkilany AM, Huang X, Murphy CJ, El-Sayed M. Mint: The golden age: Gold nanoparticles for biomedicine. *Chemical Society Reviews*. 2012;**41**:2740. DOI: 10.1039/c1cs15237h
- [28] Dykman L, Khlebtsov N. Mint: Gold nanoparticles in biomedical applications: Recent advances and perspectives. *Chemical Society Reviews*. 2012;**41**:2256. DOI: 10.1039/c1cs15166e
- [29] Hainfeld JF, Slatkin DN, Focella TM, Smilowitz HM. Mint: Gold nanoparticles: A new X-ray contrast agent. *The British Journal of Radiology*. 2006;**79**:248-253. DOI: 10.1259/bjr/13169882
- [30] Jain S, Hirst DG, O'Sullivan JM. Mint: Gold nanoparticles as novel agents for cancer therapy. *British Journal of Radiology*. 2012;**85**:101-113. DOI: 10.1259/bjr/59448833
- [31] Tkachenko AG, Xie H, Coleman D, Glomm W, Ryan J, Anderson MF, Franzen S, Feldheim DL. Mint: Multifunctional gold nanoparticle-peptide complexes for nuclear targeting. *Journal of the American Chemical Society*. 2003;**125**:4700-4701. DOI: 10.1021/ja0296935
- [32] Tkachenko AG, Xie H, Liu Y, Coleman D, Ryan J, Glomm WR, Shipton MK, Franzen S, Feldheim DL. Mint: Cellular trajectories of peptide-modified gold particle complexes: Comparison of nuclear localization signals and peptide transduction domains. *Bioconjugate Chemistry*. 2004;**15**:482-490. DOI: 10.1021/bc034189q
- [33] Goodman CM, McCusker CD, Yilmaz T, Rotello VM. Mint: Toxicity of gold nanoparticles functionalized with cationic and anionic side chains. *Bioconjugate Chemistry*. 2004;**15**:897-900. DOI: 10.1021/bc049951i
- [34] Connor EE, Mwamuka J, Gole A, Murphy CJ, Wyatt MD. Mint: Gold nanoparticles are taken up by human cells but do not cause acute cytotoxicity. *Small*. 2005;**1**:325-327. DOI: 10.1002/smll.200400093

- [35] Chithrani BD, Ghazani AA, WCW C. Mint: Determining the size and shape dependence of gold nanoparticle uptake into mammalian cells. *Nano Letters*. 2006;**6**:662-668. DOI: 10.1021/nl052396o
- [36] Chithrani BD, WCW C. Mint: Elucidating the mechanism of cellular uptake and removal of protein-coated gold nanoparticles of different sizes and shapes. *Nano Letters*. 2007;**7**: 1542-1550. DOI: 10.1021/nl070363y
- [37] Pan Y, Neuss S, Leifert A, Fischler M, Wen F, Simon U, Schmid G, Brandau W, Jahnke-Dechent W. Mint: Size-dependent cytotoxicity of gold nanoparticles. *Small*. 2007;**3**:1941-1949. DOI: 10.1002/smll.200700378
- [38] Pan Y, Leifert A, Ruau D, Neuss S, Bornemann J, Schmid G, Brandau W, Simon U, Jahnke-Dechent W. Mint: Gold nanoparticles of diameter 1.4 nm trigger necrosis by oxidative stress and mitochondrial damage. *Small*. 2009;**5**:2067-2076. DOI: 10.1002/smll.200900466
- [39] Uboldi C, Bonacchi D, Lorenzi G, Hermanns MI, Pohl C, Baldi G, Unger RE, Kirkpatrick CJ. Mint: Gold nanoparticles induce cytotoxicity in the alveolar type-II cell lines A549 and NCIH441. *Particle and Fibre Toxicology*. 2009;**6**:18. DOI: 10.1186/1743-8977-6-18
- [40] Yen H-J, Hsu S-H, Tsai C-L. Mint: Cytotoxicity and immunological response of gold and silver nanoparticles of different sizes. *Small*. 2009;**5**:1553-1561. DOI: 10.1002/smll.200900126
- [41] Cho EC, Au L, Zhang Q, Xia Y. Mint: The effects of size, shape, and surface functional group of gold nanostructures on their adsorption and internalization by cells. *Small*. 2010;**6**:517-522. DOI: 10.1002/smll.200901622
- [42] Cho EC, Xie J, Wurm PA, Xia Y. Mint: Understanding the role of surface charges in cellular adsorption versus internalization by selectively removing gold nanoparticles on the cell surface with a I 2/KI etchant. *Nano Letters*. 2009;**9**:1080-1084. DOI: 10.1021/nl803487r
- [43] Ma X, Wu Y, Jin S, Tian Y, Zhang X, Zhao Y, Yu L, Liang XJ. Mint: Gold nanoparticles induce autophagosome accumulation through size-dependent nanoparticle uptake and lysosome impairment. *ACS Nano*. 2011;**5**:8629-8639. DOI: 10.1021/nn202155y
- [44] Chang S-S, Lee C-L, CRC W. Mint: Gold nanorods: Electrochemical synthesis and optical properties. *The Journal of Physical Chemistry B*. 1997;**101**:6661-6664. DOI: 10.1021/jp971656q
- [45] Niidome T, Yamagata M, Okamoto Y, Akiyama Y, Takahashi H, Kawano T, Katayama Y, Niidome Y. PEG-modified gold nanorods with a stealth character for *in vivo* applications. *Journal of Controlled Release*. 2006;**114**:343-347. DOI: 10.1016/j.jconrel.2006.06.017
- [46] Takahashi H, Niidome Y, Niidome T, Kaneko K, Kawasaki H, Yamada S. Mint: Modification of gold nanorods using phosphatidylcholine to reduce cytotoxicity. *Langmuir*. 2006;**22**:2-5. DOI: 10.1021/la0520029
- [47] Hauck TS, Ghazani A, WCW C. Mint: Assessing the effect of surface chemistry on gold nanorod uptake, toxicity, and gene expression in mammalian cells. *Small (Weinheim an der Bergstrasse, Germany)*. 2008;**4**:153-159. DOI: 10.1002/smll.200700217

- [48] Alkilany AM, Nagaria PK, Hexel CR, Shaw TJ, Murphy CJ, Wyatt MD. Mint: Cellular uptake and cytotoxicity of gold nanorods: Molecular origin of cytotoxicity and surface effects. *Small*. 2009;**5**:701-708. DOI: 10.1002/sml.200801546
- [49] Lee KS, El-Sayed MA. Mint: Dependence of the enhanced optical scattering efficiency relative to that of absorption for gold metal nanorods on aspect ratio, size, end-cap shape, and medium refractive index. *Journal of Physical Chemistry B*. 2005;**109**:20331-20338. DOI: 10.1021/jp054385p
- [50] Debrosse MC, Comfort KK, Untener EA, Comfort DA, Hussain SM. Mint: High aspect ratio gold nanorods displayed augmented cellular internalization and surface chemistry mediated cytotoxicity. *Materials Science and Engineering C*. 2013;**33**:4094-4100. DOI: 10.1016/j.msec.2013.05.056
- [51] Morones JR, Elechiguerra JL, Camacho A, Holt K, Kouri JB, Ramírez JT, Yacaman MJ. Mint: The bactericidal effect of silver nanoparticles. *Nanotechnology*. 2005;**16**:2346-2353. DOI: 10.1088/0957-4484/16/10/059
- [52] Chaloupka K, Malam Y, Seifalian AM. Mint: Nanosilver as a new generation of nano-product in biomedical applications. *Trends in Biotechnology*. 2010;**28**:580-588. DOI: 10.1016/j.tibtech.2010.07.006
- [53] Hussain SM, Hess KL, Gearhart JM, Geiss KT, Schlager JJ. Mint: *In vitro* toxicity of nanoparticles in BRL 3A rat liver cells. *Toxicology In Vitro*. 2005;**19**:975-983. DOI: 10.1016/j.tiv.2005.06.034
- [54] Braydich-Stolle L, Hussain S, Schlager JJ, Hofmann MC. Mint: *In vitro* cytotoxicity of nanoparticles in mammalian germline stem cells. *Toxicological Sciences*. 2005;**88**:412-419. DOI: 10.1093/toxsci/kfi256
- [55] Carlson C, Hussein SM, Schrand AM, Braydich-Stolle LK, Hess KL, Jones RL, Schlager JJ. Mint: Unique cellular interaction of silver nanoparticles: Size-dependent generation of reactive oxygen species. *Journal of Physical Chemistry B*. 2008;**112**:13608-13619. DOI: 10.1021/jp712087m
- [56] Miura N, Shinohara Y. Mint: Cytotoxic effect and apoptosis induction by silver nanoparticles in HeLa cells. *Biochemical and Biophysical Research Communications*. 2009;**390**:733-737. DOI: 10.1016/j.bbrc.2009.10.039
- [57] Foldbjerg R, Olesen P, Hougaard M, Dang DA, Hoffmann HJ, Autrup H. Mint: PVP-coated silver nanoparticles and silver ions induce reactive oxygen species, apoptosis and necrosis in THP-1 monocytes. *Toxicology Letters*. 2009;**190**:156-162. DOI: 10.1016/j.toxlet.2009.07.009
- [58] Foldbjerg R, Dang DA, Autrup H. Mint: Cytotoxicity and genotoxicity of silver nanoparticles in the human lung cancer cell line, A549. *Archives of Toxicology*. 2011;**85**:743-750. DOI: 10.1007/s00204-010-0545-5
- [59] AshaRani PV, Mun GLK, Hande MP, Valiyaveetil S. Mint: Cytotoxicity and genotoxicity of silver nanoparticles in human cells. *ACS Nano*. 2009;**3**:279-290. DOI: 10.1021/nn800596w

- [60] Park EJ, Yi J, Kim Y, Choi K, Park K. Mint: Silver nanoparticles induce cytotoxicity by a Trojan-horse type mechanism. *Toxicology in Vitro*. 2010;**24**:872-878. DOI: 10.1016/j.tiv.2009.12.001
- [61] Park MVDZ, Neigh AM, Vermeulen JP, de la Fonteyne LJJ, Verharen HW, Briedé JJ, van Loveren H, de Jong WH. Mint: The effect of particle size on the cytotoxicity, inflammation, developmental toxicity and genotoxicity of silver nanoparticles. *Biomaterials*. 2011;**32**:9810-9817. DOI: 10.1016/j.biomaterials.2011.08.085
- [62] Singh RP, Ramarao P. Mint: Cellular uptake, intracellular trafficking and cytotoxicity of silver nanoparticles. *Toxicology Letters*. 2012;**213**:249-259. DOI: 10.1016/j.toxlet.2012.07.009
- [63] Gliga AR, Skoglund S, Wallinder IO, Fadeel B, Karlsson HL. Mint: Size-dependent cytotoxicity of silver nanoparticles in human lung cells: The role of cellular uptake, agglomeration and Ag release. *Particle and Fibre Toxicology*. 2014;**11**:11. DOI: 10.1186/1743-8977-11-11
- [64] Schinwald A, Donaldson K. Mint: Use of back-scatter electron signals to visualise cell/nanowires interactions *in vitro* and *in vivo*; frustrated phagocytosis of long fibres in macrophages and compartmentalisation in mesothelial cells *in vivo*. *Particle and Fibre Toxicology*. 2012;**9**:34. DOI: 10.1186/1743-8977-9-34
- [65] Kim MJ, Shin S. Mint: Toxic effects of silver nanoparticles and nanowires on erythrocyte rheology. *Food and Chemical Toxicology*. 2014;**67**:80-86. DOI: 10.1016/j.fct.2014.02.006
- [66] Varadan VK, Chen L, Xie J. *Nanomedicine: Design and Applications of Magnetic Nanomaterials, Nanosensors and Nanosystems*. 1st ed. West Sussex, UK: Wiley; 2008. DOI: 10.1002/9780470715611
- [67] Wilhelm C, Gazeau F. Mint: Universal cell labelling with anionic magnetic nanoparticles. *Biomaterials*. 2008;**29**:3161-3174. DOI: 10.1016/j.biomaterials.2008.04.016
- [68] Weissleder R, Cheng HC, Bogdanova A, Bogdanov A. Mint: Magnetically labeled cells can be detected by MR imaging. *Journal of Magnetic Resonance Imaging*. 1997;**7**:258-263. DOI: 10.1002/jmri.1880070140
- [69] Jurgons R, Seliger C, Hilpert A, Trahms L, Odenbach S, Alexiou C. Mint: Drug loaded magnetic nanoparticles for cancer therapy. *Journal of Physics: Condensed Matter*. 2006;**18**:2893-2902. DOI: 10.1088/0953-8984/18/38/S24
- [70] Chertok B, Moffat BA, David AE, Yu F, Bergemann C, Ross BD, Yang VC. Mint: Iron oxide nanoparticles as a drug delivery vehicle for MRI monitored magnetic targeting of brain tumors. *Biomaterials*. 2008;**29**:487-496. DOI: 10.1016/j.biomaterials.2007.08.050
- [71] Yu MK, Jeong YY, Park J, Park S, Kim JW, Min JJ, Kim K, Jon S. Mint: Drug-loaded superparamagnetic iron oxide nanoparticles for combined cancer imaging and therapy *in vivo*. *Angewandte Chemie (International Ed. in English)*. Jan. 2008;**47**:5362-5365. DOI: 10.1002/anie.200800857

- [72] Gonzales-Weimuller M, Zeisberger M, Krishnan KM. Mint: Size-dependant heating rates of iron oxide nanoparticles for magnetic fluid hyperthermia. *Journal of Magnetism and Magnetic Materials*. 2009;**321**:1947-1950. DOI: 10.1016/j.jmmm.2008.12.017
- [73] Mahmoudi M, Sant S, Wang B, Laurent S, Sen T. Mint: Superparamagnetic iron oxide nanoparticles (SPIONs): Development, surface modification and applications in chemotherapy. *Advanced Drug Delivery Reviews*. 2011;**63**:24-46. DOI: 10.1016/j.addr.2010.05.006
- [74] Neuberger T, Schöpf B, Hofmann H, Hofmann M, Von Rechenberg B. Mint: Superparamagnetic nanoparticles for biomedical applications: Possibilities and limitations of a new drug delivery system. *Journal of Magnetism and Magnetic Materials*. 2005;**293**:483-496. DOI: 10.1016/j.jmmm.2005.01.064
- [75] Gupta AK, Wells S. Mint: Surface-modified superparamagnetic nanoparticles for drug delivery: Preparation, characterization, and cytotoxicity studies. *IEEE Transactions on Nanobioscience*. 2004;**3**:66-73. DOI: 10.1109/TNB.2003.820277
- [76] Gupta AK, Gupta M. Mint: Cytotoxicity suppression and cellular uptake enhancement of surface modified magnetic nanoparticles. *Biomaterials*. 2005;**26**:1565-1573. DOI: 10.1016/j.biomaterials.2004.05.022
- [77] Cheng FY, Su CH, Yang YS, Yeh CS, Tsai CY, Wu CL, Wu MT, Bin Shieh D. Mint: Characterization of aqueous dispersions of Fe₃O₄ nanoparticles and their biomedical applications. *Biomaterials*. 2005;**26**:729-738. DOI: 10.1016/j.biomaterials.2004.03.016
- [78] Ma YJ, Gu HC. Mint: Study on the endocytosis and the internalization mechanism of aminosilane-coated Fe₃O₄ nanoparticles *in vitro*. *Journal of Materials Science: Materials in Medicine*. 2007;**18**:2145-2149. DOI: 10.1007/s10856-007-3015-8
- [79] Müller K, Skepper JN, Posfai M, Trivedi R, Howarth S, Corot C, Lancelot E, Thompson PW, Brown AP, Gillard JH. Mint: Effect of ultrasmall superparamagnetic iron oxide nanoparticles (Ferumoxtran-10) on human monocyte-macrophages *in vitro*. *Biomaterials*. 2007;**28**:1629-1642. DOI: 10.1016/j.biomaterials.2006.12.003
- [80] Karlsson HL, Cronholm P, Gustafsson J, Möller L. Mint: Copper oxide nanoparticles are highly toxic: A comparison between metal oxide nanoparticles and carbon nanotubes. *Chemical Research in Toxicology*. 2008;**21**:1726-1732. DOI: 10.1021/tx800064j
- [81] Mahmoudi M, Simchi A, Imani M. Mint: Cytotoxicity of uncoated and polyvinyl alcohol coated superparamagnetic iron oxide nanoparticles. *Journal of Physical Chemistry C*. 2009;**113**:9573-9580. DOI: 10.1021/jp9001516
- [82] Naqvi S, Samim M, Abdin MZ, Ahmed FJ, Maitra AN, Prashant CK, Dinda AK. Mint: Concentration-dependent toxicity of iron oxide nanoparticles mediated by increased oxidative stress. *International Journal of Nanomedicine*. 2010;**5**:983-989. DOI: 10.2147/IJN.S13244
- [83] Wu X, Tan Y, Mao H, Zhang M. Mint: Toxic effects of iron oxide nanoparticles on human umbilical vein endothelial cells. *International Journal of Nanomedicine*. 2010;**5**:385-399. DOI: 10.2147/IJN.S10458

- [84] Soenen SJH, Himmelreich U, Nuytten N, De Cuyper M. Mint: Cytotoxic effects of iron oxide nanoparticles and implications for safety in cell labelling. *Biomaterials*. 2011;**32**: 195-205. DOI: 10.1016/j.biomaterials.2010.08.075
- [85] Hong SC, Lee JH, Lee J, Kim HY, Park JY, Cho J, Lee J, Han DW. Mint: Subtle cytotoxicity and genotoxicity differences in superparamagnetic iron oxide nanoparticles coated with various functional groups. *International Journal of Nanomedicine*. 2011;**6**:3219-3231. DOI: 10.2147/IJN.S26355
- [86] Mahmoudi M, Laurent S, Shokrgozar MA, Hosseinkhani M. Mint: Toxicity evaluations of superparamagnetic iron oxide nanoparticles: Cell "vision" versus physicochemical properties of nanoparticles. *ACS Nano*. 2011;**5**:7263-7276. DOI: 10.1021/nn2021088
- [87] Yu M, Huang S, Yu KJ, Clyne AM. Mint: Dextran and polymer polyethylene glycol (PEG) coating reduce both 5 and 30 nm iron oxide nanoparticle cytotoxicity in 2D and 3D cell culture. *International Journal of Molecular Sciences*. 2012;**13**:5554-5570. DOI: 10.3390/ijms13055554
- [88] Khan MI, Mohammad A, Patil G, Naqvi SAH, Chauhan LKS, Ahmad I. Mint: Induction of ROS, mitochondrial damage and autophagy in lung epithelial cancer cells by iron oxide nanoparticles. *Biomaterials*. 2012;**33**:1477-1488. DOI: 10.1016/j.biomaterials.2011.10.080
- [89] Singh N, Jenkins GJS, Nelson BC, Marquis BJ, Maffei TGG, Brown AP, Williams PM, Wright CJ, Doak SH. Mint: The role of iron redox state in the genotoxicity of ultra-fine superparamagnetic iron oxide nanoparticles. *Biomaterials*. 2012;**33**:163-170. DOI: 10.1016/j.biomaterials.2011.09.087
- [90] Sun L, Hao Y, Chien C-L, Searson PC. Mint: Tuning the properties of magnetic nanowires. *IBM Journal of Research and Development*. 2005;**49**:79-102. DOI: 10.1147/rd.491.0079
- [91] Hultgren A, Tanase M, Chen CS, Reich DH. Mint: High-yield cell separations using magnetic nanowires. *IEEE Transactions on Magnetics*. 2004;**40**:2988-2990. DOI: 10.1109/TMAG.2004.830406
- [92] Hultgren A, Tanase M, Felton EJ, Bhadriraju K, Salem AK, Chen CS, Reich DH. Mint: Optimization of yield in magnetic cell separations using nickel nanowires of different lengths. *Biotechnology Progress*. 2005;**21**:509-515. DOI: 10.1021/bp049734w
- [93] Johansson F, Jonsson M, Alm K, Kanje M. Mint: Cell guidance by magnetic nanowires. *Experimental Cell Research*. 2010;**316**:688-694. DOI: 10.1016/j.yexcr.2009.12.016
- [94] Zhang L, Petit T, Lu Y, Kratochvil BE, Peyer KE, Pei R, Lou J, Nelson BJ. Mint: Controlled propulsion and cargo transport of rotating nickel nanowires near a patterned solid surface. *ACS Nano*. 2010;**4**:6228-6234. DOI: 10.1021/nn101861n
- [95] Zhang L, Petit T, Peyer KE, Nelson BJ. Mint: Targeted cargo delivery using a rotating nickel nanowire. *Nanomedicine: Nanotechnology, Biology, and Medicine*. 2012;**8**:1074-1080. DOI: 10.1016/j.nano.2012.03.002

- [96] Choi DS, Park J, Kim S, Gracias DH, Cho MK, Kim YK, Fung A, Lee SE, Chen Y, Khanal S, Baral S, Kim JH. Mint: Hyperthermia with magnetic nanowires for inactivating living cells. *Journal of Nanoscience and Nanotechnology*. 2008;**8**:2323-2327. DOI: 10.1166/jnn.2008.273
- [97] Choi DS, Hopkins X, Kringel R, Park J, Jeon IT, Kim YK. Mint: Magnetically driven spinning nanowires as effective materials for eradicating living cells. *Journal of Applied Physics*. 2012;**111**:109-112. DOI: 10.1063/1.3678437
- [98] Song MM, Song WJ, Bi H, Wang J, Wu WL, Sun J, Yu M. Mint: Cytotoxicity and cellular uptake of iron nanowires. *Biomaterials*. 2010;**31**:1509-1517. DOI: 10.1016/j.biomaterials.2009.11.034
- [99] Safi M, Yan M, Guedeau-Boudeville MA, Conjeaud H, Garnier-Thibaud V, Boggetto N, Baeza-Squiban A, Niedergang F, Averbeck D, Berret JF. Mint: Interactions between magnetic nanowires and living cells: Uptake, toxicity, and degradation. *ACS Nano*. 2011;**5**:5354-5364. DOI: 10.1021/nn201121e
- [100] Margineanu MB, Julfakyan K, Sommer C, Perez JE, Contreras MF, Khashab N, Kosel J, Ravasi T. Mint: Semi-automated quantification of living cells with internalized nanostructures. *Journal of Nanobiotechnology*. 2016;**14**:4. DOI: 10.1186/s12951-015-0153-x
- [101] Ivanov YP, Alfadhel A, Alnassar M, Perez JE, Vazquez M, Chuvilin A, Kosel J. Mint: Tunable magnetic nanowires for biomedical and harsh environment applications. *Scientific Reports*. Apr 2016;**6**:24189. DOI: 10.1038/srep24189
- [102] Prina-Mello A, Diao Z, Coey JMD. Mint: Internalization of ferromagnetic nanowires by different living cells. *Journal of Nanobiotechnology*. 2006;**4**:9. DOI: 10.1186/1477-3155-4-9
- [103] Byrne F, Prina-Mello A, Whelan A, Mohamed BM, Davies A, Gun'ko YK, Coey JMD, Volkov Y. Mint: High content analysis of the biocompatibility of nickel nanowires. *Journal of Magnetism and Magnetic Materials*. 2009;**321**:1341-1345. DOI: 10.1016/j.jmmm.2009.02.035
- [104] Hossain MZ, Kleve MG. Mint: Nickel nanowires induced and reactive oxygen species mediated apoptosis in human pancreatic adenocarcinoma cells. *International Journal of Nanomedicine*. 2011;**6**:1475-1485. DOI: 10.2147/IJN.S21697\nijn-6-1475[pii]
- [105] Ma C, Song M, Zhang Y, Yan M, Zhang M, Bi H. Mint: Nickel nanowires induce cell cycle arrest and apoptosis by generation of reactive oxygen species in HeLa cells. *Toxicology Reports*. 2014;**1**:114-121. DOI: 10.1016/j.toxrep.2014.04.008
- [106] Felix LP, Perez JE, Contreras MF, Ravasi T, Kosel J. Mint: Cytotoxic effects of nickel nanowires in human fibroblasts. *Toxicology Reports*. 2016;**3**:373-380. DOI: 10.1016/j.toxrep.2016.03.004
- [107] Perez JE, Contreras MF, Vilanova E, Felix LP, Margineanu MB, Luongo G, Porter AE, Dunlop IE, Ravasi T, Kosel J. Mint: Cytotoxicity and intracellular dissolution of nickel nanowires. *Nanotoxicology*. 2015:1-38. DOI: 10.3109/17435390.2015.1132343

- [108] Jeon IT, Cho MK, Cho JW, An BH, Wu JH, Kringel R, Choi DS, Kim YK. Ni-Au core-shell nanowires: Synthesis, microstructures, biofunctionalization, and the toxicological effects on pancreatic cancer cells. *Journal of Materials Chemistry*. 2011;**21**:12089. DOI: 10.1039/c1jm11143d
- [109] Pondman KM, Maijenburg W, Celikkol FB, Pathan A, Kishore U, Ten HB, Ten Elshof JE, Ten Haken B. Mint: Au coated Ni nanowires with tuneable dimensions for biomedical applications. *Journal of Materials Chemistry B*. 2013;**1**:6129. DOI: 10.1039/c3tb20808g
- [110] Luongo G, Campagnolo P, Perez JE, Kosel J, Georgiou TK, Regoutz A, Payne DJ, Stevens MM, Ryan MP, Porter AE, Dunlop IE. Mint: Scalable high-affinity stabilization of magnetic iron oxide nanostructures by a biocompatible antifouling homopolymer. *ACS Applied Materials & Interfaces*. Nov. 2017;**9**:40059-40069. DOI: 10.1021/acsami.7b12290

Review of In Vitro Toxicity of Nanoparticles and Nanorods—Part 2

Jose E. Perez, Nouf Alsharif,
Aldo I. Martínez-Banderas, Basmah Othman,
Jasmeen Merzaban, Timothy Ravasi and
Jürgen Kosel

Additional information is available at the end of the chapter

<http://dx.doi.org/10.5772/intechopen.78616>

Abstract

The specific use of engineered nanostructures in biomedical applications has become very attractive, due to their ability to interface and target specific cells and tissues to execute their functions. Additionally, there is continuous progress in research on new nanostructures with unique optical, magnetic, catalytic and electrochemical properties that can be exploited for therapeutic or diagnostic methods. On the other hand, as nanostructures become widely used in many different applications, the unspecific exposure of humans to them is also unavoidable. Therefore, studying and understanding the toxicity of such materials are of increasing importance. Previously published reviews regarding the toxicological effects of nanostructures focus mostly on the cytotoxicity of nanoparticles and their internalization, activated signaling pathways and cellular response. Here, the most recent studies on the in-vitro cytotoxicity of NPs, nanowires and nanorods for biomedical applications are reviewed and divided into two parts. The first part considers nonmagnetic metallic and magnetic nanostructures, while, the second part covers carbon structures and semiconductors. The factors influencing the toxicity of these nanostructures are elaborated to help elucidate the effects of these nanomaterials on cells, which is a prerequisite for their safe clinical use.

Keywords: nanoparticles, nanowires, nanorods, biocompatibility, cytotoxicity, nanomedicine

1. Introduction

Nanostructured materials are defined as possessing one of their dimensions ranging from 1 to 100 nm, according to the American Society for Testing and Materials (ASTM) international standards definition [1]. For nanoparticles (NPs), which can be of more or less spherical or cubical shape, two dimensions are required to be within this range. In contrast, the shape of nanorods (NRs) is in one dimension much larger than in the others. For a small aspect ratio (<10) both their length and diameter are in the nanoscale, whereas NRs with a large aspect ratio (>10) only have their diameter within this scale, and they are often called “nanowires” (NWs). Nanostructures within this specific size scale show unique size-dependent optical, magnetic, catalytic and electrochemical properties, among others, as well as high surface to volume ratios. Moreover, their shape, surface chemistry and chemical composition can be used to tailor-specific properties, making nanostructures highly versatile for different applications [2, 3].

The size scale of nanostructures is within the range of several biomolecules, such as proteins and antibodies, allowing specific interactions to occur between them. This, when coupled with the high surface to volume ratios and tunable sizes and properties, makes nanostructures prime candidates for biomedical applications such as imaging, drug delivery and therapy [4–6]. Examples of applications include the use of NPs as magnetic resonance imaging (MRI) contrast agents [7, 8], tissue engineering [9–11], as well as the recent focus on hyperthermia and cancer cell eradication with the use of NPs and NRs [12–17]. Such applications, if they are aimed for a clinical setting, ultimately require a direct NP/NR exposure in the form of ingestion or intravenous delivery into the body. Naturally, there is a rigorous testing required before any new drug formulation is approved for clinical use in order to ensure their safety and effectiveness. Currently, very few NPs-based drugs have been approved by the Food and Drug Administration and are commercially available. Examples include GastroMARK, used as an MRI contrast agent to enhance the delineation of the bowel, and ferumoxytol, an iron-replacement formulation approved for adults with chronic kidney disease with an iron deficiency [18].

Within this scope, biocompatibility and cytotoxicity data are of paramount importance to evaluate the potential of nanostructures for biomedical applications. Nanostructures are normally engineered to interface and target-specific cells or tissues to execute their functions, raising questions about their toxicological effects. For instance, there are several characteristics involved in the toxicity of fiber-like nanomaterials, such as shape, length, chemical composition, agglomeration and purity, making them suitable to fit the “fiber toxicological paradigm” according to the World Health Organization (WHO) criteria used to describe the toxicity of asbestos fibers [19]. Further, nanostructures are usually tuned for biocompatibility on top of the desired biomedical function, with the most relevant aspects that influence their toxicity being the material [20], size and shape [21], surface charge [22] and surface functionalization [23]. *In vitro* studies, while not able to give a complete insight into the biocompatibility of nanostructures, have a high importance, due to their easy implementation, and provide valuable cytotoxicology data regarding the safety of the use of nanostructures in biomedical applications. Previously published reviews regarding the biosafety of nanostructures include that of Lewinski et al. [24] and Zhao et al. [25]. The former focuses mostly on the cytotoxicity of

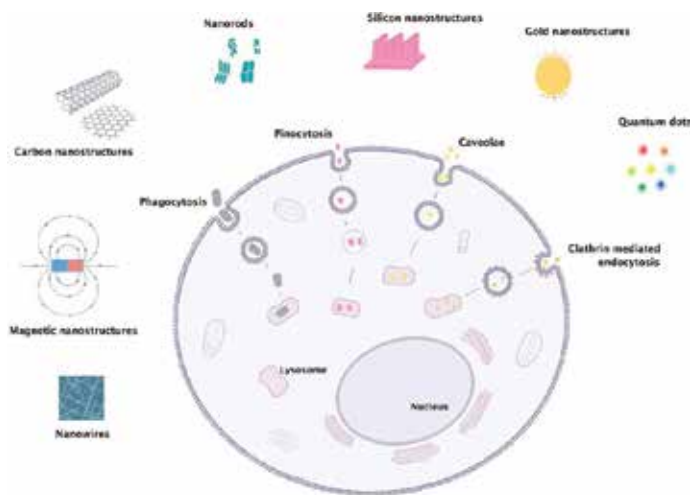


Figure 1. Schematic of the pathways for intracellular uptake of different materials and structures.

NPs of different materials, as well as carbon nanotubes (CNTs), whereas the latter is a more in-depth review of the internalization, activated signaling pathways and cellular response of different kinds of NPs.

Here, we review relevant studies assessing the *in vitro* cytotoxicity of both nanoparticles (NPs) and nanowires (NWs)/nanorods (NRs) with the potential to be used in biomedical applications. Due to their prevalence within the applied nanomaterials in biomedicine, this chapter covers various materials from four different classes (on Scopus almost 50% of all publications related to cytotoxicity, since the year 2000, fall within these materials) that are typically considered in the context of nanomaterials for biomedical applications. The first part of this chapter covers nonmagnetic metals and magnetic materials, while the second part covers carbon structures and semiconductors. An overview of the materials and structures covered, together with the various intracellular uptake mechanisms, is given in **Figure 1**.

2. Carbon nanostructures

Carbon nanostructures include a broad diversity of carbon allotropes that differ from pristine diamond and graphite. Carbon has been used in many technological applications, exploiting its capability of forming networks composed exclusively of C-atoms with the same electronic configuration or hybridizing configurations sp^3 -, sp^2 - and sp -, expanding the possible allotropes that can be constructed [26]. Since the synthesis of the first carbon nanostructures, such as fullerene C_{60} (0D) [27] and CNTs (1D) [28] (**Figure 2**), there has been a tremendous effort for understanding the properties of these nanomaterials and for exploring the broad range of applications in which they can be used. Carbon-based nanomaterials (CNMs) have created a great deal of interest in various applications such as optical imaging [29], drug and gene delivery [30], and nanotherapeutics [31, 32] due to their excellent mechanical, optical and electrical

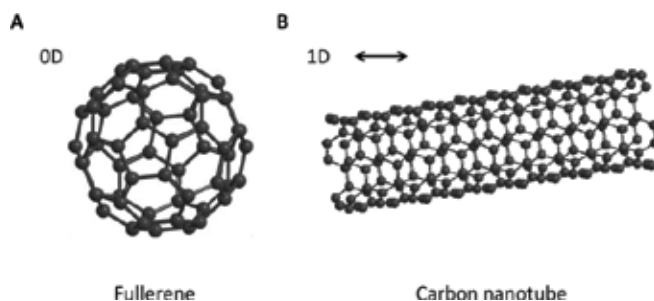


Figure 2. Chemical structure of representative carbon-based nanomaterials. Structure of fullerene C_{60} (A) and carbon nanotube (B).

properties [33–35], as well as due to their ability to translocate through the cell membrane or be internalized via energy-dependent endocytic pathways [36]. Similarly, CNMs possess an extraordinary ability to be loaded with drugs or different chemical agents that are either attached to the surface or, in the case of CNTs, they can be packed into the interior cores [37].

These widespread applications of CNMs are also accompanied by increasing concerns regarding their interactions with tissues, cells, and biomolecules as well as degradation pathways, and at a macroscale, the potential deleterious effects on human health and the environment.

2.1. Fullerene C_{60}

The structure of fullerene C_{60} , which has a van der Waals diameter of approximately 1 nm, is formed from 60 carbon atoms arranged in a spherical, cage-like structure consisting of 60 vertices, 12 pentagonal faces and 20 hexagonal faces [38]. Fullerenes and their derivatives are probably the most extensively studied NPs with several properties and applications including MRI [39], drug delivery [40, 41], photodynamic therapy (PDT) [40] and photothermal therapy (PTT) [42].

Although fullerenes are generally hydrophobic molecules, many strategies have been developed for improving their solubilization in water that is, synthesized water-soluble derivatives of fullerenes by chemical modifications through the addition of functional groups such as hydroxyl-, carboxyl-, amino- and alkyl-groups and other side-chain/cyclic moieties to the C_{60} structure [43]. The different methods employed to increase C_{60} water solubility profoundly influence the physiochemical properties and the toxicological effects of these compounds, raising uncertainties about the possible consequences on human health and potential medical uses [44]. Nakagawa et al. studied the effects of the hydroxylated fullerenes (fullerenols) $C_{60}(\text{OH})_{24}$ and $C_{60}(\text{OH})_{12}$ 0.125 mM in rat hepatocytes, observing a concentration and time-dependent cell death accompanied by mitochondrial dysfunction, with $C_{60}(\text{OH})_{24}$ found to be more cytotoxic with almost 100% of cell death after 30 min. The authors concluded that the toxic effects of fullerenols may depend on the number of hydroxyl groups [38]. $C_{60}(\text{OH})_{24}$ at a concentration of 0.1 mM caused cell blebbing, loss of cellular ATP and lipid peroxidation in rat hepatocytes [45]. Similarly, the cytotoxic effects of fullerene C_{60} and the derivatives $C_{60}(\text{OH})_2$, $C_{60}(\text{OH})_{6-12}$, $C_{60}(\text{OH})_{12}$ and $C_{60}(\text{OH})_{36}$, were evaluated in three different types of liver cells:

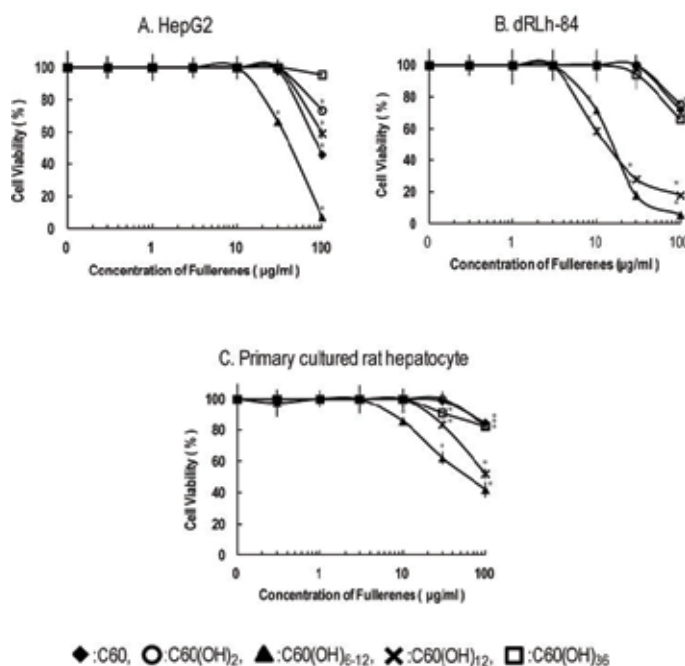


Figure 3. Cytotoxicity of fullerene and hydroxylated fullerenes in liver cells. HepG2 (A); dRLh-84 (B); and primary cultured rat hepatocytes (C) were exposed to C₆₀, C₆₀(OH)₂, C₆₀(OH)_{6–12}, C₆₀(OH)₁₂ and C₆₀(OH)₃₆ for 3 days. Data are represented as mean ± SD (n = 3). (*) statistically significant from control (p < 0.05). Adapted from Shimizu et al. [46]. Copyright 2013 by the authors. Licensee MDPI, Basel, Switzerland. CC BY 3.0.

dRLh-84, HepG2 and rat hepatocytes as shown in **Figure 3** [46]. C₆₀(OH)_{6–12} and C₆₀(OH)₁₂ were found to induce cytotoxic effects after 3 days of exposure in dRLh-84 cells at a concentration of 10 µg/mL reducing the cell viability 30 and 40%, respectively, in the form of inhibition of mitochondrial activity. Similarly, to Nakawaga’s findings, these results indicate that the number of hydroxyl groups on C₆₀(OH)_x contributes to the cytotoxic potential and mitochondrial damage.

Other fullerene derivatives have also been tested for cytotoxic effects in human epithelial HEp-2 cells, such as C₆₀-PVP, C₆₀-NO₂-proline and sodium salt of polycarboxylic C₆₀ [47]. However, the PVP and NO₂-proline derivatives did not have an effect on cell viability, and the sodium salt of polycarboxylic derivative induced a drastic decrease in cell number of about 80% at a concentration around 0.1 mg/mL.

Further, the molecular mechanisms underlying the cytotoxic effects of two similar fullerene derivatives (C₆₀-1,3-dipolar cycloaddition of azomethine ylides) on human MCF-7 cells were analyzed by RNA-seq-based gene expression [44]. It was found that whereas one derivative had a negligible effect, the addition of an extra trifluoroacetate group induced a significant, time-dependent alteration of gene expression, mainly in biological processes involving protein synthesis, cell cycle progression and cell adhesion, with the authors suggesting an inhibition effect of the mTOR pathway.

In a recent study performed by Canape et al., C_{60} fullerenes were covalently functionalized with PEG of various sizes, Full-PEG2000, Full-PEG5000 and Full-PEG10000, and viability was studied on a variety of cell lines 24 h after exposure, evaluating mitochondrial activity, cell membrane integrity and hemolysis [48]. However, all the tested compounds were found to reduce, to some extent, the cellular metabolic activity, only two affected the cell membrane integrity, and none induced hemolysis. It was concluded that fullerenes C_{60} functionalized with higher molecular weight PEGs possess a higher biocompatibility and that side toxicity can be alleviated using proper surface coating. Together, all these findings support that the surface functionalization of fullerenes plays an important role with regard to their interaction with biological systems.

The interaction of CNMs with lipid membranes is of great interest because biological activity requires crossing or breaking lipid membranes. In a study concerning the interaction of fullerenes with the lipid bilayer and the possibility of fullerene crossing it, it was observed that hydrophobic molecules of C_{60} were localized within the inner part of the membrane, whereas hydrophilic $C_{60}(\text{OH})_n$ fullereneols molecules were adsorbed on the heads of membrane phospholipids [49], where they can interact with membrane proteins, such as ATPases and influence their activity [50, 51]. Similarly, Raouf et al. showed that the internalization of a water-soluble derivatized C_{60} malonodiserinolamide takes place through multiple energy-dependent pathways, and they escape endocytotic vesicles to eventually localize and accumulate in the nucleus through the nuclear pore complex [41].

2.2. Single-walled carbon nanotubes

CNTs are classified in single-walled carbon nanotubes (SWCNTs) and multiwalled carbon nanotubes (MWCNTs). The first ones are formed from a single layer of graphene (0.4–10 nm in diameter), whereas the second ones consist of multiple concentric cylinders of graphene with increasing diameters (10–100 nm) [52]. The length of CNTs can range from nanometers to centimeters [53], and they possess unique physical and chemical properties such as a lightweight, high tensile strength, high electrical and thermal conductivities, unique optical properties and extreme chemical stability, as well as high surface-to-volume ratios with reactive surface chemistries. Such properties have made CNTs an interesting material for biomedical applications, where they have been used as drug, protein and nucleic acid delivery tools [54–56], cancer cell destruction [57, 64, 91], diagnostics [59] and as noninvasive and highly sensitive imaging aids [31, 58]. Naturally, biosafety concerns of CNTs are rapidly emerging with numerous reports indicating their potential hazards to the public health.

The graphene sheets can be wrapped in a variety of ways that are denoted by a pair of indices (n , m), which define both the diameter and the chirality of SWCNTs, which can be either metallic (M) or semiconducting (S). As synthesized, SWNTs have a wide range of diameters and chiral angles, which leads to a polydisperse sample of discrete properties [59, 60]. SWCNTs possess small diameters and the large aspect ratios that render them ideal one-dimensional quantum wires that elicit different biological behavior compared to spherical NPs, when introduced in biological systems [26]. The cytotoxicity of pristine SWCNTs and

SWCNTs functionalized with PEG has been evaluated with neuronal PC12 cells at the biochemical, cellular and gene expression levels by Zhang et al. [61]. Cytotoxicity increased with the concentration, whereby SWCNT-PEGs exhibited less cytotoxic potency than bare SWCNTs at the highest concentration tested by reducing the cell viability in approximately 70 and 50%, respectively (Figure 4). Morphological changes appeared in PC12 cells treated with both SWCNTs and SWCNTs-PEG as shown in Figure 5. Cells exposed to SWCNTs showed an elongated shape, which was related to higher toxic effects induced by the untreated CNTs. ROS were generated as a function of both concentration and surface coating after exposure, whereas gene expression analysis showed that the genes involved in oxidoreductases and antioxidant activity, nucleic acid or lipid metabolism and mitochondria dysfunction were highly altered. Interestingly, alteration of the genes was also surface coating-dependent. The authors concluded that surface functionalization of SWCNTs decreases the ROS-mediated toxicological response *in vitro*, corroborating the relevance of surface functionalization in the interaction between nanostructures and biological systems. Likewise, proteins such as type I

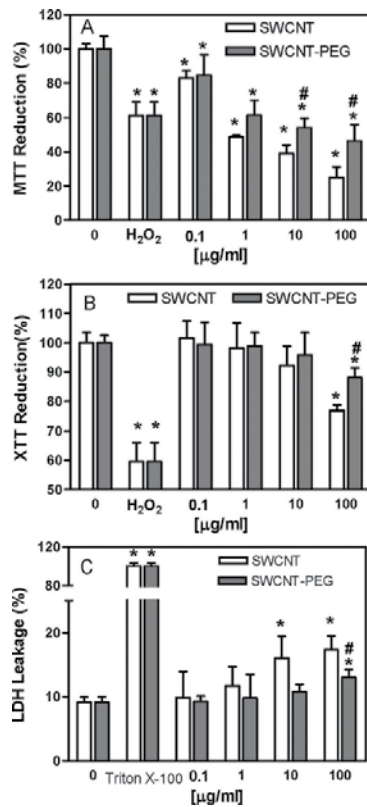


Figure 4. Cytotoxic effect of SWCNTs and SWCNTs-PEG in PC12 cells. Mitochondrial toxicity and membrane damage of neuronal cells incubated with different concentrations of pristine SWCNTs and PEG-coated SWCNTs for 24 h evaluated by MTT (A), XTT (B) and LDH (C) assays. Data are expressed as mean± standard error (n = 3). (*) statistically significant from control; (#) indicates statistically significant within the same concentration group (p < 0.05). Adapted with permission from Zhang et al. [61]. Copyright 2011 American Chemical Society.

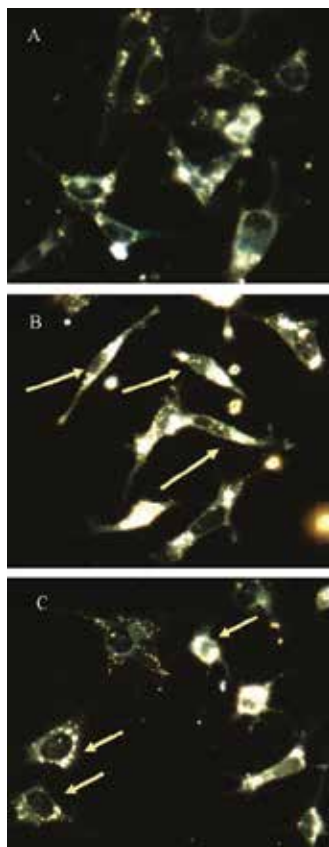


Figure 5. Morphological changes of PC12 cells after 24 h incubation with SWCNTs and SWCNTs-PEG. (A) Normal morphology of the PC12 cells. (B) PC12 cells incubated with SWCNTs present a spindle shape (arrows). (C) SWCNT-PEGs inhibit the dendrite growth (arrows). Adapted with permission from Zhang et al. [61]. Copyright 2011 American Chemical Society.

collagen have shown great potential as surface coating agents in SWCNTs, showing no obvious negative cellular effects and with a high level of internalization taking place through adsorption by the extracellular matrix in bovine articular chondrocytes [62].

Avti et al. showed that SWCNTs synthesized using Gd^{3+} NPs as catalysts induced no structural damage to NIH/3T3 fibroblasts or decreased their viability at concentrations between 1 and 10 $\mu\text{g}/\text{mL}$ [53]. In contrast, highly pure SWCNTs triggered similar amounts of pulmonary fibrosis-related compounds interleukin 1 β (IL-1 β) and transforming growth factor (TGF- β 1) in THP-1 and BEAS-2B pulmonary cells without affecting cell viability [63]. Similarly, Di Giorgio et al. studied the cyto- and genotoxic effects, as well as the inflammatory response and ROS production, of SWCNTs on the mouse macrophage cell line RAW 264.7 [64]. There, the authors reported that SWCNTs induced ROS release, cell ultrastructural damage, necrosis and chromosomal aberrations, but did not cause an inflammatory response.

2.3. Multiwalled carbon nanotubes

MWCNTs are defined as a nested coaxial array of SWCNTs, each nanotube being formed by a graphene sheet rolled into a cylinder of nanometer size diameter [65].

It has been postulated that MWCNTs can provide an innovative and promising alternative to conventional drug formulations for cancer therapy, as they can be conjugated with various bioactive molecules such as drugs, surfactants, diagnostic agents and antibodies in order to target receptors that are overexpressed in cancer cells [66–68].

The generation of carboxyl groups by oxidation on the surface of CNTs is one of the most used strategies for introducing hydrophilic moieties onto the CNT hydrophobic surface and in order to conquer a lack of solubility and to improve their biocompatibility [69–71]. Thus, Liu et al. have studied the effects of carboxylated c-MWCNTs on the human normal liver cell line L02 and found a reduction in the toxicity, when compared to pristine MWCNTs with a reduction of around 60% of cell viability at the highest concentration tested after 72 h and concluded that this effect is probably due to a reduced activation of the mitochondria mediated apoptotic pathway [72]. Moreover, as charged entities, c-MWCNTs bind to proteins in the bloodstream through noncovalent interactions to form a protein corona. De Paoli et al. have characterized the interactions of c-MWCNTs with common human proteins such as albumin, fibrinogen, γ -immunoglobulins and histone H1 and found that the association of proteins to c-MWCNTs depends on the protein's charge, size and structural flexibility and that it affects the agglomeration state and charge of the CNTs [73].

As with SWCNTs, molecules can be covalently and noncovalently attached to the surface of MWCNTs [74]. The main disadvantage of noncovalent attachment is the lack of biomolecule specificity upon adsorption, which affects the CNTs dispersion stability by replacing the functional surface coating with proteins and molecules contained in all physiological fluids (cell culture media or blood) [65]. Heister et al. have compared five types of CNTs, varying in their dimensions and surface properties, for a multidimensional analysis of dispersion stability and their toxicity toward cancer cells (**Figure 6**), from which it was emphasized that the covalent link between PEG and oxidized MWCNTs leads to stable dispersion and biocompatibility in various biological environments [65].

It has been proposed that the metal impurities trapped inside the MWCNTs may be responsible for their toxicity that partially occurs through the generation of ROS [75]. Fe impurities trapped inside the MWCNTs may be partially responsible for neurotoxicity, as postulated by Meng et al., who investigated and compared the effects of two kinds of MWCNTs with different concentrations of Fe impurities in rat pheochromocytoma PC-12 cells [76]. They found that the exposure to Fe MWCNTs can reduce cell viability up to 80% after 72 h exposure and increase cytoskeletal disruption of undifferentiated PC-12 cells, diminish the ability to form mature neurites and then adversely influence the neuronal dopaminergic phenotype in NGF-treated cells.

Additionally, MWCNTs have been shown to affect the immune system. Pescatori et al. used a whole-genome expression approach to assess whether functionalized MWCNTs could stimulate

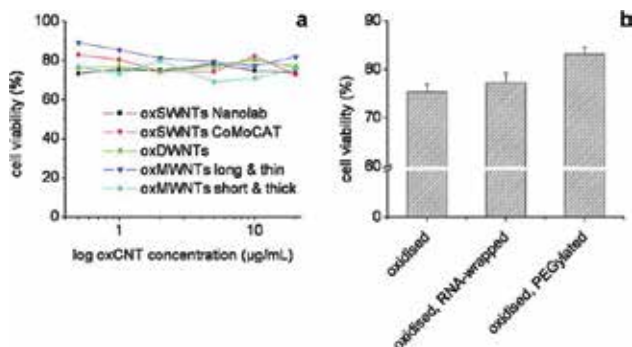


Figure 6. MTT cytotoxicity assay on WiDr human colon cancer cells after being incubated for 96 h with various samples of oxCNTs. No dose-dependent cytotoxicity is observed at this concentration as shown in the range dose-response curves for the five different types of CNTs, displaying (A). Cell viability percentage plot for Nanolab oxidized SWNTs with different surface functionalizations, where PEGylation results in a statistically significant enhancement in cell viability. The cells control correlates with 100% cell viability. Adapted with permission from Heister et al. [74]. Copyright 2010 American Chemical Society.

distinct molecular changes in immune cells, with transcriptomic changes analyzed in human immune cells THP1, a monocytic cell line, Jurkat cells and a T lymphocyte cell line [77]. They found a cell-specific action on monocytes for three types of MWCNTs, which specifically enhanced innate immunity activation mechanisms. The pathways activated are functionally relevant and critical for the development of an effective inflammatory response.

3. Semiconductors

3.1. Titanium dioxide nanoparticles and nanowires

A comprehensive review of the numerous biomedical applications of titanium dioxide (TiO₂) throughout the years was published by Yin et al. [78]. In summary, mostly due to their low cost, strong optical absorption and high chemical stability, TiO₂ NPs have shown great potential in applications such as photodynamic cancer therapy, drug delivery, cell imaging and biosensors, among others.

One of the initial cytotoxicity studies with TiO₂ NPs was performed on human dermal microvascular endothelial cells [79]. There, it was shown that NPs with an average diameter of 70 nm at a dose of 50 µg/mL caused a minor pro-inflammatory response in the form of an increase in the levels of IL-8. Later, a study with mouse fibroblast L929 cells exposed to TiO₂ NPs was conducted by Jin et al. [80]. For 3–600 µg/mL doses, cells appeared to shrink and became round in culture, with a dose-dependent reduction of cell metabolic activity, LDH release and ROS generation. Chromatin fragmentation was also reported, indicating possible DNA damage (Figure 7). It was also found that both human neural astrocyte-like U87 cells and human fibroblast HFF-1 cells exposed to 25 nm TiO₂ NPs for 48 h had a decrease in cell survival for doses up to 100 µg/mL, with cell death reported as a combination of apoptosis and necrosis [81]. On the other hand, BEAS-2B cells underwent cell death

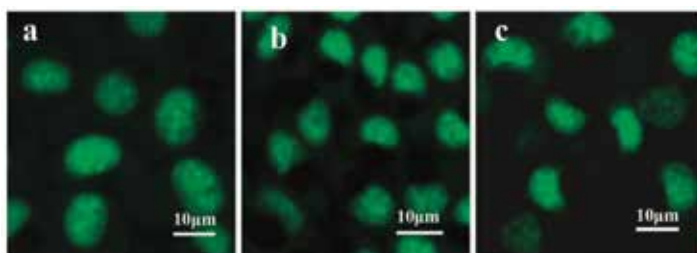


Figure 7. DNA-binding acridine orange staining of L929 mouse fibroblast cells. (A) Control cells with no TiO₂ NPs show normal green nuclei with an organized cellular structure; (B) Cells cultured with 30 µg/mL of TiO₂ NPs show weakly condensed chromatin; and (C) Cells cultured with 600 µg/mL of TiO₂ NPs show fragmented chromatin, an indicator of necrosis. Adapted with permission from Jin et al. [80]. Copyright 2008 American Chemical Society.

through apoptosis, triggered by the activation of caspase-3 and chromatin condensation through ROS [82].

Although the size of single TiO₂ NPs reported by Jin et al. was of 5 nm [80], they were clustered in 20–30 nm aggregates, an effect that could enhance cytotoxicity. It was later shown that there is a correlation between the cytotoxicity of TiO₂ NPs and their aggregate size, as larger aggregates (600 vs. 166 nm) elicited a stronger decrease in cell viability, as well as the expression of genes related to stress and inflammation [83]. In contrast, TiO₂ NPs of 12 nm in diameter aggregated in 450 nm clusters and only at higher doses slightly decreased the viability of glomerular mesangial IP5 and epithelial proximal HK-2 cells, suggesting specific cell responses [84]. Additionally, although ROS was generated in the presence of TiO₂ NPs, the cells were able to maintain their antioxidant potential, thereby showing no oxidative stress.

Cellular uptake studies with 30 nm TiO₂ NPs have been carried out in human amnion epithelial WISH cells using transmission electron microscopy (TEM), with images showing most of the particles localized either inside vesicles or freely in the cytoplasm [85]. In addition to the already mentioned cytotoxic response, WISH cells experience an oxidative response due to ROS accumulation, as well as DNA double strand breaks and cell cycle arrest.

Cytotoxicity data of TiO₂ NWs are scarce, with only a handful of studies published. Magrez et al. observed that TiO₂-based NWs of 5 µm in length and 75 nm in length had a negative impact on the cell proliferation and cell viability of H596 human lung tumor cells in a dose-dependent manner and for concentrations up to 2 µg/mL [86]. NWs were observed to reside in the periphery of the nuclei, which were often enlarged and lobulated or fragmented. In another study, H₂Ti₃O₇ NWs at a dose of 10 µg/mL induced the generation of cell debris in eight different cell lines, which the authors associated with an increase in autophagosome-like vacuoles in the cytosol [87].

3.2. Zinc oxide nanoparticles and nanowires

Zinc is a biologically active element that plays a role in different processes, such as the immune system, cell metabolism, cell proliferation, enzymatic function and gene expression, among

others [88, 89]. Due to these biological functions of zinc, coupled with initial biocompatibility studies [90], ease of fabrication and relevant properties [91], zinc oxide (ZnO) nanostructures have been proposed as suitors for several biomedical applications, including cancer cell therapy [92, 93], drug delivery [94, 95] and imaging [96]. However, possible undesirable effects of the interactions between ZnO nanostructures and biological systems could arise and cause a toxicological response. Additionally, ZnO nanostructures are known to dissolve under acidic conditions. The phase-solubility diagram of ZnO [97] indicates that ZnO NPs will dissolve at a pH value below 6.7 at physiological temperature, and they will rapidly dissolve in the acidic pH of the lysosomes (pH 5.7) after their uptake [98]. Zinc oxide NPs can dissolve in an aqueous media to form hydrated Zn^{2+} , which is enhanced in acidic pH as well as in the presence of biological components, such as amino acids and peptides [99]. A review on studies published between the years 2009 and 2011 on the toxicity of ZnO NPs to mammalian cells was reported by Vandebriel et al. [100]. They concluded that the induction of oxidative stress is the most important and the most likely mechanism underlying ZnO NP toxicity.

Initial cytotoxicity studies in human T lymphocytes showed a significant decrease in cell viability only for concentrations higher than 5 mM using ZnO NPs of 13 nm in diameter [101]. It was then found that ZnO NPs preferentially kill cancerous human T lymphocytes compared to normal ones via ROS and apoptosis [92]. Similarly, NPs of the same size were tested against human lung BEAS-2B cells and RAW 264.7 macrophages, and a dose and time-dependent cytotoxicity was found in both cases for doses up to 50 $\mu\text{g}/\text{mL}$ and incubation times of 16 h [99]. Moreover, the ZnO NPs were reported to induce the generation of ROS, as well as the activation of the pro-inflammatory marker TNF- α and the pro-inflammatory pathway Jun kinase, as well as intracellular calcium release, a major oxidative stress response. Finally, ZnO NPs were found to reside in caveolae in the case of BEAS-2B cells, whereas in the RAW 264.7 cells, they resided inside lysosomes, with intracellular dissolution and release of Zn^{2+} shown in both cases. In a different study, ZnO NPs also impaired the survival of human neural astrocyte-like U87 cells in a dose-dependent manner [81].

The degree of cytotoxicity of ZnO NPs also depends on their size, as shown by Hanley et al. [102]. Using 4, 13 and 20 nm NPs, they determined an inverse relationship between nanoparticle size and cytotoxicity in terms of cell viability and ROS generation in immune cells. Among these, monocytes were the most sensitive to the ZnO NPs, whereas lymphocytes were the most resistant, as reported previously [101]. In contrast, glomerular mesangial IP5 cells showed a similar dose-dependent decrease in cell viability for ZnO NPs of both <100 nm and >1 μm , along with the generation of ROS [84]. The cell viability of neural stem cells appeared to be indifferent of NP size [103]. In a different work, a differential cytotoxic response was reported, when comparing the effects of 20–30 nm ZnO NPs in human myeloblastic leukemic HL60 cells and normal peripheral blood mononuclear cells (PBMCs) [104]. For concentrations up to 1000 $\mu\text{g}/\text{mL}$, PBMCs maintained a steadily high viable cell population, whereas a dose of 50 $\mu\text{g}/\text{mL}$ was enough to bring the cell viability of HL60 cells down to 50%. DNA fragmentation analysis and annexin V staining confirmed that cell death was through the apoptosis pathway. The potent tumor suppressor that regulates the cell cycle and prevents DNA damage, p53 [105], is believed to be a molecular master switch toward apoptosis, and reports show that the p53 pathway was activated in BJ cells (skin fibroblasts) upon ZnO NPs treatment with a concomitant decrease in cell proliferation [106].

The liver, playing a major role in human metabolism, may be a target organ for NPs after they enter into the body. As such, it is an important toxicity evaluation method. Similarly, to previous results, Sharma et al. found that human liver HepG2 cells had a dose-dependent response to ZnO NPs at doses up to 20 $\mu\text{g}/\text{mL}$ and for exposure times from 12 to 24 h [107]. Cell death was also shown as being through the apoptotic pathway, due to ROS generation, oxidative stress and mitochondrial and DNA damage. Taken together, all these results suggest that the cytotoxic response to ZnO NPs is dependent on the target cell tissue as well as on changes in NP dimensions.

Kao et al. observed the effects of ZnO NPs of <50 nm in the homeostasis of intracellular Zn^{2+} in human leukemia Jurkat cells and human lung carcinoma H1355 cells and found an increase in the concentration of cytosolic and mitochondrial Zn^{2+} , most probably due to NP dissolution [108], as shown previously [86]. Caspase-3 activation, mitochondrial membrane depolarization and LDH release were also reported, which suggests an apoptotic death pathway due to mitochondrial dysfunction. In a more recent study, the intracellular concentration of Zn^{2+} of breast cancer MDA-MB-231 cells was also increased after treatment with ZnO NPs, leading to the generation of ROS, damage to the cell membrane and mitochondria and culminating in apoptosis [109].

Limited literature exists regarding the biocompatibility of ZnO NWs, but similar cytotoxicity effects as those of NPs were shown by Li et al. using HeLa cells and connective tissue L-929 cells [110]. Although the NWs used were rather large (200 μm in length and 1 μm in diameter), both cell lines seemed to maintain their viability for concentrations up to 10 $\mu\text{g}/\text{mL}$ and exposure times of 24 h. Similar viability data were then reported for NWs of 10 μm in length and 327 nm in diameter at the same dose in human macrophages (**Figure 8**) [111]. There, too, it

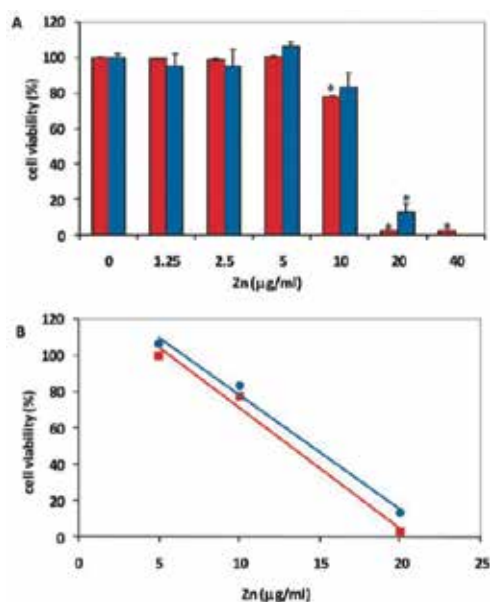


Figure 8. Cytotoxicity of ZnO NWs on HMM human monocyte macrophages. Cell viability was assessed using the neutral red assay, with the red bars denoting doses of Zn in the form of ZnCl_2 or ZnO NWs, respectively. Adapted with permission from Müller et al. [111]. Copyright 2010 American Chemical Society.

was found that an intracellular increase of Zn^{2+} precedes cell death, indicating the intracellular dissolution of the ZnO NWs after uptake [112–120].

3.3. Silicon nanoparticles

Coated silicon nanoparticles (Si NPs) have attracted both a great deal of concern and attention, especially in biomedical applications such as disease diagnosis, tumor cell tracking, imaging, drug delivery and gene therapy [121, 122]. They have been widely studied for such applications because of their active surface state and high suspension ability [121, 123, 124]. However, there are some recent reports that limit the use of Si NPs because of potential side effects on the cells, when using them in such a scale and in high concentrations [125].

One of the first studies on Si NPs focused on their cellular uptake [123]. Si NPs were coated with a fluorone dyes called Rhodamine 6G isothiocyanate (RITC), the fluorescence signal of which indicated uptake. NPs of 50 nm diameter at a dose of 80 $\mu\text{g}/\text{mL}$ were accumulated in the cytoplasm of HeLa cells after 4 h of incubation at 37°C, while the uptake was reduced by 80% at 4°C. A year later, Lin et al. focused on the toxicity effect of the size, concentration and exposure time of Si NPs on human lung cancer cells (calveolar carcinoma-derived cells) [126]. The cell viability decreased significantly as a function of both nanoparticle dosage (10–100 $\mu\text{g}/\text{mL}$) and exposure time (24, 48 and 72 h). However, the cytotoxicity of two different sizes of Si NPs (15 and 46 nm) did not show a significant difference.

A different study compared the cytotoxicity of a variety of sizes of Si NPs (19, 43, 68 and 498 nm) at 100 $\mu\text{g}/\text{mL}$ [127]. After 4 h of incubation with human liver HepG2 cells, it was noticed that the cytotoxicity of Si NPs is size-dependent (i.e., the smaller size the higher cytotoxicity). The live cells were counted by a cell-counting kit (CCK-8). Further, Sahu et al. proved that Si NPs (10–20 nm) are much more toxic than micro-sized ones (0.5–10 μm) for a concentration range of 5–500 $\mu\text{g}/\text{mL}$, after exposing them to human lung epithelial (L-132) and human monocytes (THP-1) for 24 h [128]. The cellular uptake efficiency and pathway of different sized NPs has also been confirmed to be size-dependent, with smaller particles (55 nm) being internalized faster than larger ones (307 nm) [129]. The largest NPs (307 nm) internalized through clathrin-coated pits, whereas medium ones (167 nm) internalized through clathrin-coated vesicles and the smallest (55 nm) were internalized through an energy independent pathway. Despite differences in their internalization pathway, all three sizes showed a high-level of biocompatibility.

In a similar approach as the one of Lin et al., the cytotoxic effects of increasing concentrations of Si NPs (0, 25, 50, 100 and 200 $\mu\text{g}/\text{mL}$) on HepG2 cells were analyzed in terms of ROS level, mitochondrial membrane potential and apoptotic rate. All three tests showed that the level of toxicity of the NPs increases while increasing the concentration from 25 to 100 $\mu\text{g}/\text{ml}$. Additionally, it was shown that the expressions of the apoptotic genes cytC and Caspase-3 were up-regulated with increasing NP concentrations. Additionally, the downregulation of the antiapoptotic Bcl-2 gene and upregulation of the genes p53 and BAX have also been reported [129, 130].

Other approaches have focused on cell-dependent cytotoxicity and surface charge [131]. Kim et al. found that NIH/3T3 fibroblasts appear to be more susceptible to Si NPs in terms of cell

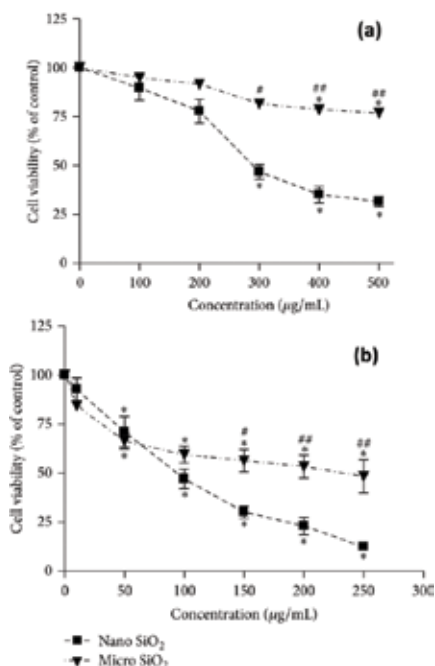


Figure 9. Cytotoxicity of SiO₂ particle is size, concentration and cell-dependent in (a) L-132 cells and (b) THP-1 cells. Results were mean ± SEM of three independent experiments each carried out in triplicate, in comparison to untreated controls. Adapted with permission from Sahu et al. [128]. Copyright 2016 Hindawi Publishing Corporation.

viability, when compared to A549 and HepG2 cells [132]. On the other hand, positively charged (NH₂-coated Si NPs) displayed higher cytotoxicity than negatively charged ones (COOH-coated NPs) in human adenocarcinoma Caco-2 and rat alveolar macrophage NR8383 cells [133]. However, the opposite has also been suggested for HaCaT keratinocyte cells [134]. A summary of the viability dependences on the Si NPs' size, concentration and cell type is shown in **Figure 9** [128].

3.4. Silicon NWs

Si NWs show several advantages over Si NPs. For instance, they tend to not agglomerate in solution compared to Si NPs [135] and they enhance the drug-loading capacity due to their high surface area [136, 137]. However, it has been indicated that Si NWs have more toxic effects to macrophages cells at lower concentrations compared to Si NPs due to the large surface area, which increase the interaction and induce the cell death [138]. Naturally, the concentration of Si NWs plays a role on cell viability. Si NWs of 2 µm long, 55 nm diameter were co-cultured with HeLa and Hep-2 cells at different concentrations [138]. While no toxicity was found on either cell line for concentrations below 190 µg/ml, the cells died and released 75% of their contents into the supernatant at high concentrations (1900 µg/ml) after 72 h of incubation. Zhang et al. used amino-modified (APTES), folate-functionalized Si NWs to study cell interactions [139]. The NWs lengths were between 2.5 and 8.0 µm, with a concentration of

100 µg/mL. It was found that the length of NWs affected the internalization, with NWs longer than 5 µm being more difficult to be internalized, due to geometrical restrictions.

3.5. Quantum dots

Semiconductor quantum dots (QDs) are light-emitting particles that have broad excitation spectra, long fluorescence lifetimes compared to traditional fluorescent probes and are more resistant to photobleaching [140, 141]. Also, they can easily be conjugated to proteins [140], which makes them excellent choices for bioimaging [142–146] and other biomedical applications [141, 147, 148]. Tsoi et al. summarized the toxicity of QDs by two mechanisms: degradation with the release of free cadmium (Cd) and generation of ROS [149]. Each design of QD is a unique combination and has its own physicochemical properties that may influence its biological activity and toxicity. As a result, tremendous research efforts have been devoted to produce high quality QDs by optimizing synthetic procedures, as well as functionalizing their surface in order to enhance biocompatibility [142, 150].

An early study by Derfus et al. demonstrated that CdSe-core QDs oxidized and degraded, releasing Cd ions which induced cell death [151]. When CdSe QDs were exposed to a UV-light for 1, 2, 4 and 8 h and then incubated with hepatocytes, it showed a 6, 42, 83 and 97% decrease in the cells' viability, respectively [143]. Cd is a known carcinogen with potential damage to the renal, skeletal, pulmonary and reproductive systems [152]. Interestingly, Chen et al. showed that the cell viability of HEK293 cells treated with 37.5 nM of 5 nm CdTe QDs was not significantly altered, compared to the control (i.e., untreated cells) after 3 days of incubation [153]. However, high concentrations (300–600 nM) of QDs completely inhibited cell growth from the very beginning. The cytotoxicity of QDs has also been linked to the generation of ROS, which in turn damages cellular proteins, lipids and DNA [149]. The p53 gene was also shown to be inhibited by CdTe QDs, leading to apoptosis and cell death [150].

Tracking the QDs internalization pathways could help explain their toxicological properties. To this end, microscopy studies showed that QDs localize within cellular endosomes and lysosomes, exposing them to an acidic or oxidative microenvironment [149]. It was determined that the hypochlorous acid present in phagocytic cells oxidized polymer-encapsulated CdS and ZnS-capped CdSe QDs, releasing cadmium, zinc, sulfur and selenium into the cytoplasm. Some studies have suggested that the QDs toxicity might derive from multiple factors including the environment and the QDs physicochemical characteristics (such as size, shape and surface chemistry). A surface coating with a ZnS shell [149] or BSA corona [150] reduced the QDs toxicity. In addition, polymeric coatings (i.e., phospholipid-PEG) and inorganic coatings (e.g., Si) can prevent the release of Cd into the biological media [142]. In a different approach, Soenen et al. studied cell viability using Cd-free QDs (ZnSe/ZnS and InP/ZnS QDs) at concentrations ranging from 0 to 100 nM [154]. Cytotoxic effects were observed starting from 60 nM for ZnSe to 80 nM for InP QDs. Further, no increase in cytotoxicity was reported up to 7 days after the initial cell labeling compared to normal QDs due to the absence of Cd.

4. Conclusion

Recent studies on the in-vitro cytotoxicity of carbon structure and semiconductors in biomedical applications were reviewed, taking into account nanoparticles and nanowires/nanorods. A summary of the results of representative studies is provided in **Table 1**.

Comparisons between the cytotoxicities of those different nanomaterials are generally difficult to make due to the vast range of methods, concentrations, dimensions, cell lines etc. For instance, the concentrations reported in the different studies were typically evaluated using either ICP or Cryogenic TEM. However, the concentration or dose of the nanomaterial plays a significant role in the cytotoxic response as well as the biomedical applications. Similarly, the reported toxicology of the nanomaterials depends on their interaction with the assay. For example, carbon nanostructures interact with the MTT-formazan crystals but not with XTT or INT reagents.

While the concentrations and exposure times are critical factors, the toxicity of these nanostructures is also material-dependent. These relations can be seen in **Figure 10**, which presents the average values reported for the cell viabilities (ignoring differences in concentrations, incubation times etc.), when exposed to the nanomaterials in the studies covered in **Table 1**. ZnO NPs showed the highest toxicity, while the lowest has been reported for silicon.

In addition, the particle size plays a major role in the cytotoxic properties of the nanostructure, whereby both the cellular uptake efficiency and pathway are affected, with smaller particles being internalized faster than the larger ones.

The induction of ROS after dissolving the nanostructures in the lysosomes was shown to be the primary underlying cause of the toxicity in several cases, leading to cell death through the apoptotic pathway, due to ROS generation and mitochondrial damage. The acidic condition inside the lysosome increases the digestion of the particles, enhancing the release of ions that affect the viability of the cells. This is a particularly relevant issue in case of CdSe-core QDs, which release Cd ions upon oxidation, leading to fast cell death.

Adding a coating to the nanostructure typically affected both the toxicity and the surface charge of the nanostructure, where cationic surfaces are more toxic than anionic. For instance, the toxicity of QDs was reduced by adding a BSA corona, and the release of Cd was prevented by the addition of polymeric and inorganic coatings. The type of the coatings was shown to affect the cell viability differently.

The cytotoxicity of the nanomaterial depends also on the nanostructure's shape. In this regard, several advantages have been reported for NWs over NPs. For instance, they enhance the drug-loading capacity due to their large surface area. An interesting observation from **Figure 10** is that NWs/NRs are, on average, less cytotoxic than NPs, with titanium dioxide being the only exception. However, one study has shown that the large surface area of Si NWs has a more toxic effect at lower concentrations compared to NPs. This was attributed to the increased interaction of the nanomaterial with the cells due to the large surface area.

Nanostructure type	Surface coating	Nanostructure concentration	Average size	Cell line	Cell viability	Viability test	Reference
C ₆₀	Pristine, C ₆₀ (OH) ₁₂ , C ₆₀ (OH) ₂₄	0.125 mM/1 h	N/A	rat hepatocytes	80% for pristine, C ₆₀ (OH) ₁₂ and 60% for C ₆₀ (OH) ₂₄	Trypan blue/microscopy, MPP, GSH	[35]
C ₆₀	C ₆₀ -alanine, -NO ₂ , -PVP, -NO ₂ -proline, sodium salt of a polycarboxylic derivative	0.001–0.2 mg/mL for C ₆₀ ^o NO ₂ -proline and 0.016–0.2 mg/mL for all others/48 h	N/A	HEp-2 cells	No cytotoxicity except for the sodium salt of a polycarboxylic derivative with 20% viability at 0.01 mg/mL	Crystal violet/optical density	[44]
C ₆₀	PEG of various sizes	0.03–1 mg/mL/24 h	N/A	HepG2, NHDF, Caco2, HUVEC, U937, J774 A1	Maximum inhibition at 1 mg/ml of Full-PEG2000 for J774 (41%) and U937 (62%).	MTT, LDH assays	[45]
SWCNTs	Pristine and PEG	0.1–100 µg/mL/24 h	0.7–1.6 nm diameter, 0.2–3 µm length	PC12 cells	30 and 50% viability in MTT at highest concentration, respectively. Higher values for XTT and 10–20% LDH leakage	MTT, XTT, LDH, DCF, GSH assays	[58]
SWCNTs	Collagen	15 µg/mL/4 h to 15 days.	0.7–1.6 nm diameter, N/A	BACs	No cytotoxicity	WST-1 assay, Live/dead	[59]
SWCNTs	Gd-NPs as catalysis and PEG	50–100 µg/mL/12–48 h	N/A	NIH/3 T3 fibroblasts	70% viability at highest concentration and time exposure	Trypan blue/microscopy, Live/dead	[55]
MWCNTs	Pristine, COOH	12.5–200 µg/mL/24, 48 and 72 h	10–20 nm diameter, 10–30 µm length	human normal liver cell line L02	60 and 80% viability at highest concentration and time exposure, respectively	CellTiter-GloV® assay	[68]
MWCNTs	3 and 23% of Fe impurities	5–60 µg/mL/24, 48 and 72 h	2–50 nm diameter, 50 µm length	PC12 cells	70 and 20% viability at highest concentration and time exposure, respectively	CCK-8	[73]
TiO ₂ NPs	–	600 µg/mL	5 nm diameter	L929 mouse fibroblast cells	<70%	MTT assay	[107]

Nanostructure type	Surface coating	Nanostructure concentration	Average size	Cell line	Cell viability	Viability test	Reference
ZnO NPs	—	10 mM	13 nm diameter	Human T lymphocytes	40%	Propidium iodide staining	[110]
SiO ₂ NPs	—	50 µg/mL	10–20 nm	monocytes (THP-1) cells	71%	MTT assay	[124]
Si NPs	Coated with negatively charged (COOH)	3 mg/ml	1.6 nm	Rat alveolar macrophage NR8383 cells	No cytotoxicity	MTT assay	[132]
Si NPs	Coated with positively charged (NH ₂)	0–100 mg/ml	3.9 nm	Rat alveolar macrophage NR8383 cells	The EC50 values = 0.38 µg/ml	MTT assay	[129]
Si NPs	—	160 µg/ml	7 nm	HepG2 cells	~98%	MTT assay	[136]
Si NPs	—	160 µg/ml	20 nm	HepG2 cells	~72%	MTT assay	[153]
Si NPs	—	160 µg/ml	50 nm	HepG2 cells	~49%	MTT assay	[156]
Si NWs	—	<190 µg/ml	2 µm long, 55 nm diameter	HeLa and Hep-2 cells	75%	MTT assay	[152]
Si NWs	—	1 µg/ml	500 nm long, 100 nm diameter	breast cancer cells line (MCF-7/ADR)	90%	MTT assay	[154]
Si NW arrays	—	—	5 µm long, 20–100 nm diameter	HeLa cells	98%	MTT assay	[155]
Si NW arrays	Coated with AgNPs	—	5 µm long, 20–100 nm diameter	HeLa cells	80%	MTT assay	[156]
Si NW arrays	Coated with Cu NPs	—	5 µm long, 20–100 nm diameter	HeLa cells	~50%	MTT assay	[156]

Nanostructure type	Surface coating	Nanostructure concentration	Average size	Cell line	Cell viability	Viability test	Reference
CdSe QDs	Oxidation for 0 h, 1 h, 2 h and 4 h	62.5 µg/mL	7 nm	Hepatocyte cells	100, 98.55 and 21%, respectively	MTT assay	[152]
CdTe QDs	—	37.5 and 75 nM	5 nm	HEK293 cells	~87 and ~67%	MTT assay	[154]
ZnSe QDs	Cd-free	60 nM	1–10 nm	HUVEC cells	~77%	Alamar Blue assay	[155]
InP QDs	Cd-free	80 nM	1–10 nm	HUVEC cells	~78%	Alamar Blue assay	[155]

Table 1. Summary of in-vitro cytotoxicity studies with different kinds of nanoparticles (NPs) and nanowires (NWs) and nanorods (NR). SWCNT the abbreviation of single-walled carbon nanotube, MWCNT for multiwalled carbon nanotube and QD for quantum dots.

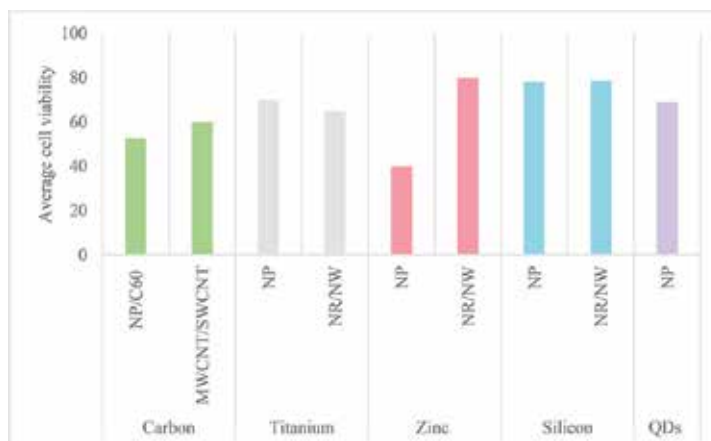


Figure 10. Average cell viability when exposed to nanomaterials reported in **Table 1**, considering nanoparticles (NP), nanorods (NR), nanowires (NW), Fullerene (C₆₀), single-walled carbon nanotubes (SWCNT), multiwalled carbon nanotubes (MWCNT) and Quantum Dots (QDs).

While all these studies contributed to obtain a better picture of the cytotoxicity of nanomaterials and the underlying mechanisms, it is a persisting issue that a consistent measurement and reporting system will be needed for future studies. This will not only enable performing more accurate comparisons of the toxicological characteristics of nanostructures, but also to better evaluate the potential of using them for biomedical applications.

Acknowledgements

Research reported in this publication was supported by the King Abdullah University of Science and Technology (KAUST).

Policy: <https://www.intechopen.com/authorship-policy.html>.

Author details

Jose E. Perez^{1,2}, Nouf Alsharif^{1,2}, Aldo I. Martínez-Banderas^{1,2}, Basmah Othman¹, Jasmine Merzaban¹, Timothy Ravasi¹ and Jürgen Kosel^{2*}

*Address all correspondence to: jurgen.kosel@kaust.edu.sa

1 Division of Biological and Environmental Sciences and Engineering, King Abdullah University of Science and Technology, Thuwal, Kingdom of Saudi Arabia

2 Division of Computer, Electrical and Mathematical Sciences and Engineering, King Abdullah University of Science and Technology, Thuwal, Kingdom of Saudi Arabia

References

- [1] ASTM International. Standard Terminology Relating to Nanotechnology [Internet]. 2012. Available from: <https://www.astm.org/Standards/E2456.htm> [Accessed: March 15, 2018]
- [2] Sanvicens N, Marco MP. Multifunctional nanoparticles—Properties and prospects for their use in human medicine. *Trends in Biotechnology*. 2008;**26**:425-433. DOI: 10.1016/j.tibtech.2008.04.005
- [3] Sau TK, Rogach AL, Jäckel F, Klar TA, Feldmann J. Properties and applications of colloidal nonspherical noble metal nanoparticles. *Advanced Materials*. 2010;**22**:1805-1825. DOI: 10.1002/adma.200902557
- [4] Brigger I, Dubernet C, Couvreur P. Nanoparticles in cancer therapy and diagnosis. *Advanced Drug Delivery Reviews*. 2002;**54**:631-651. DOI: 10.1016/S0169-409X(02)00044-3
- [5] Doane TL, Burda C. The unique role of nanoparticles in nanomedicine: Imaging, drug delivery and therapy. *Chemical Society Reviews*. 2012;**41**:2885. DOI: 10.1039/c2cs15260f
- [6] Parveen S, Misra R, Sahoo SK. Anoparticles: A boon to drug delivery, therapeutics, diagnostics and imaging. *Nanomedicine: Nanotechnology, Biology and Medicine*. 2012; **8**:147-166. DOI: 10.1016/j.nano.2011.05.016
- [7] Li L, Jiang W, Luo K, Song H, Lan F, Wu Y, Gu Z. Superparamagnetic iron oxide nanoparticles as MRI contrast agents for non-invasive stem cell labeling and tracking. *Theranostics*. 2013;**3**:595-615. DOI: 10.7150/thno.5366
- [8] Xie H, Zhu Y, Jiang W, Zhou Q, Yang H, Gu N, Zhang Y, Xu H, Xu H, Yang X. Lactoferrin-conjugated superparamagnetic iron oxide nanoparticles as a specific MRI contrast agent for detection of brain glioma *in vivo*. *Biomaterials*. 2011;**32**:495-502. DOI: 10.1016/j.biomaterials.2010.09.024
- [9] Kuo S-W, Lin H-I, Ho JH-C, Shih Y-R V, Chen H-F, Yen T-J, Lee OK. Regulation of the fate of human mesenchymal stem cells by mechanical and stereo-topographical cues provided by silicon nanowires. *Biomaterials*. 2012;**33**:5013-5022. DOI: 10.1016/j.biomaterials.2012.03.080
- [10] Liu D, Yi C, Wang K, Fong CC, Wang Z, Lo PK, Sun D, Yang M. Reorganization of cytoskeleton and transient activation of Ca⁺² channels in mesenchymal stem cells cultured on silicon nanowire arrays. *ACS Applied Materials & Interfaces*. 2013;**5**:13295-13304. DOI: 10.1021/am404276r
- [11] Liu D, Yi C, Fong C-C, Jin Q, Wang Z, Yu W-K, Sun D, Zhao J, Yang M. Activation of multiple signaling pathways during the differentiation of mesenchymal stem cells cultured in a silicon nanowire microenvironment. *Nanomedicine: Nanotechnology, Biology and Medicine*. 2014:1-11. DOI: 10.1016/j.nano.2014.02.003
- [12] Laurent S, Dutz S, Häfeli UO, Mahmoudi M. Magnetic fluid hyperthermia: Focus on superparamagnetic iron oxide nanoparticles. *Advances in Colloid and Interface Science*. 2011;**166**:8-23. DOI: 10.1016/j.cis.2011.04.003

- [13] Cherukuri P, Glazer ES, Curley SA. Targeted hyperthermia using metal nanoparticles. *Advanced Drug Delivery Reviews*. 2010;**62**:339-345. DOI: 10.1016/j.addr.2009.11.006
- [14] Su Y, Wei X, Peng F, Zhong Y, Lu Y, Su S, Xu T, Lee ST, He Y. Gold nanoparticles-decorated silicon nanowires as highly efficient near-infrared hyperthermia agents for cancer cells destruction. *Nano Letters*. 2012;**12**:1845-1850. DOI: 10.1021/nl204203t
- [15] Fung AO, Kapadia V, Pierstorff E, Ho D, Chen Y. Induction of cell death by magnetic actuation of nickel nanowires internalized by fibroblasts. *Journal of Physical Chemistry C*. 2008;**112**:15085-15088. DOI: 10.1021/jp806187r
- [16] Contreras MF, Sougrat R, Zaher A, Ravasi T, Kosel J. Non-chemotoxic induction of cancer cell death using magnetic nanowires. *International Journal of Nanomedicine*. 2015;**10**: 2141-2153. DOI: 10.2147/IJN.S77081
- [17] Dreaden EC, Mwakwari SC, Austin LA, Kieffer MJ, Oyelere AK, El-Sayed MA. Small molecule-gold nanorod conjugates selectively target and induce macrophage cytotoxicity towards breast cancer cells. *Small*. 2012;**8**:2819-2822. DOI: 10.1002/smll.201200333
- [18] Cortajarena AL, Ortega D, Ocampo SM, Gonzalez-García A, Couleaud P, Miranda R, Belda-Iniesta C, Ayuso-Sacido A. Engineering iron oxide nanoparticles for clinical settings. *Nano*. 2014;**1**. DOI: 10.5772/58841
- [19] Liu Y, Zhao Y, Sun B, Chen C. Understanding the toxicity of carbon nanotubes. *Accounts of Chemical Research*. 2013;**46**:702-713. DOI: 10.1021/ar300028m
- [20] Kong B, Seog JH, Graham LM, Lee SB. Experimental considerations on the cytotoxicity of nanoparticles. *Nanomedicine*. 2011;**6**:929-941. DOI: 10.2217/nmm.11.77
- [21] Gratton SE, Ropp P, Pohlhaus PD, Luft JC, Madden VJ, Napier ME, JM DS. The effect of particle design on cellular internalization pathways. *Proceedings of the National Academy of Sciences of the United States of America*. 2008;**105**:11613-11618. DOI: 10.1073/pnas.0801763105
- [22] Fröhlich E. The role of surface charge in cellular uptake and cytotoxicity of medical nanoparticles. *International Journal of Nanomedicine*. 2012;**7**:5577-5591. DOI: 10.2147/IJN.S36111
- [23] Kim ST, Saha K, Kim C, Rotello VM. The role of surface functionality in determining nanoparticle cytotoxicity. *Accounts of Chemical Research*. 2013;**46**:681-691. DOI: 10.1021/ar3000647
- [24] Lewinski N, Colvin V, Drezek R. Cytotoxicity of nanoparticles. *Small (Weinheim an der Bergstrasse, Germany)*. 2008;**4**:26-49. DOI: 10.1002/smll.200700595
- [25] Zhao F, Zhao Y, Liu Y, Chang X, Chen C, Zhao Y. Cellular uptake, intracellular trafficking, and cytotoxicity of nanomaterials. *Small*. 2011;**7**:1322-1337. DOI: 10.1002/smll.201100001
- [26] Martin N, Guldi DM, Echegoyen L. Carbon nanostructures—Introducing the latest web themed issue. *Chemical Communications*. 2011;**47**:604-605. DOI: 10.1039/c0cc90122a

- [27] Kroto HW, Heath JR, O'Brien SC, Curl RF, Smalley RE. C60: Buckminsterfullerene. *Nature*. 1985;**318**:162-163. DOI: 10.1038/318162a0
- [28] Iijima S. Helical microtubules of graphitic carbon. *Nature*. 1991;**354**:56-58. DOI: 10.1038/354056a0
- [29] Kurkina T, Balasubramanian K. Towards in vitro molecular diagnostics using nanostructures. *Cellular and Molecular Life Sciences*. 2012;**69**:373-388. DOI: 10.1007/s00018-011-0855-7
- [30] Prakash S, Malhotra M, Shao W, Tomaro-Duchesneau C, Abbasi S. Polymeric nanohybrids and functionalized carbon nanotubes as drug delivery carriers for cancer therapy. *Advanced Drug Delivery Reviews*. 2011;**63**:1340-1351. DOI: 10.1016/j.addr.2011.06.013
- [31] Liang F, Chen B. A review on biomedical applications of single-walled carbon nanotubes. *Current Medicinal Chemistry*. 2010;**17**:10-24. DOI: 10.2174/092986710789957742
- [32] Zhu L, Schrand AM, Voevodin AA, Chang DW, Dai LM, Hussain SM. Assessment of human lung macrophages after exposure to multi-walled carbon nanotubes. Part II. DNA damage. *Nanoscience and Nanotechnology Letters*. 2011;**3**:94-98. DOI: 10.1166/nl.2011.1126
- [33] Iancu C, Mocan L. Advances in cancer therapy through the use of carbon nanotube-mediated targeted hyperthermia. *International Journal of Nanomedicine*. 2011;**6**:2543. DOI: 10.2147/ijn.s27335
- [34] Tarakanov AO, Goncharova LB, Tarakanov YA. Carbon nanotubes towards medicinal biochips. *Wiley Interdisciplinary Reviews. Nanomedicine and Nanobiotechnology*. 2010;**2**:1-10. DOI: 10.1002/wnan.69
- [35] Hartman KB, Wilson LJ. Carbon nanostructures as a new high-performance platform for MR molecular imaging. In: Chan WCW, editor. *Handbook of Bio Applications of Nanoparticles*. Berlin: Springer-Verlag; 2007. pp. 74-84. DOI: 10.1007/978-0-387-76713-0
- [36] Lacerda L, Russier J, Pastorin G, Herrero MA, Venturelli E, Dumortier H, Al-Jamal KT, Prato M, Kostarelos K, Bianco A. Translocation mechanisms of chemically functionalised carbon nanotubes across plasma membranes. *Biomaterials*. 2012;**33**:3334-3343. DOI: 10.1016/j.biomaterials.2012.01.024
- [37] Wong BS, Yoong SL, Jagusiak A, Panczyk T, Ho HK, Ang WH, Pastorin G. Carbon nanotubes for delivery of small molecule drugs. *Advanced Drug Delivery Reviews*. 2013;**65**:1964-2015. DOI: 10.1016/j.addr.2013.08.005
- [38] Nakagawa Y, Suzuki T, Ishii H, Nakae D, Ogata A. Cytotoxic effects of hydroxylated fullerenes on isolated rat hepatocytes via mitochondrial dysfunction. *Archives of Toxicology*. 2011;**85**:1429-1440. DOI: 10.1007/s00204-011-0688-z
- [39] Kato H, Kanazawa Y, Okumura M, Taninaka A, Yokawa T, Shinohara H. Lanthanoid Endohedral Metallofullerenols for MRI contrast agents. *Journal of the American Chemical Society*. 2003;**125**:4391-4397. DOI: 10.1021/ja027555+

- [40] Fan J, Fang G, Zeng F, Wang X, Wu S. Water-dispersible fullerene aggregates as a targeted anticancer prodrug with both chemo- and photodynamic therapeutic actions. *Small*. 2013;**9**:613-621. DOI: 10.1002/sml.201201456
- [41] Raouf M, Mackeyev Y, Cheney MA, Wilson LJ, Curley SA. Internalization of C60 fullerenes into cancer cells with accumulation in the nucleus via the nuclear pore complex. *Biomaterials*. 2012;**33**:2952-2960. DOI: 10.1016/j.biomaterials.2011.12.043
- [42] Krishna V, Stevens N, Koopman B, Moudgil B. Optical heating and rapid transformation of functionalized fullerenes. *Nature Nanotechnology*. 2010;**5**:330-334. DOI: 10.1038/nnano.2010.35
- [43] Borm PJA, Robbins D, Haubold S, Kuhlbusch T, Fissan H, Donaldson K, Schins R, Stone V, Kreyling W, Lademann J, Krutmann J, Warheit D, Oberdorster E. The potential risks of nanomaterials: A review carried out for ECETOC. *Particle and Fibre Toxicology*. 2006;**3**:1-35. DOI: 10.1186/1743-8977-3-11
- [44] Lucafò M, Gerdol M, Pallavicini A, Pacor S, Zorzet S, Da Ros T, Prato M, Sava G. Profiling the molecular mechanism of fullerene cytotoxicity on tumor cells by RNA-seq. *Toxicology*. 2013;**314**:183-192. DOI: 10.1016/j.tox.2013.10.001
- [45] Nakagawa Y, Suzuki T, Nakajima K, Inomata A, Ogata A, Nakae D. Effects of N-acetyl-L-cysteine on target sites of hydroxylated fullerene-induced cytotoxicity in isolated rat hepatocytes. *Archives of Toxicology*. 2014;**88**:115-126. DOI: 10.1007/s00204-013-1096-3
- [46] Shimizu K, Kubota R, Kobayashi N, Tahara M, Sugimoto N, Nishimura T, Ikarashi Y. Cytotoxic effects of hydroxylated fullerenes in three types of liver cells. *Materials*. 2013;**6**:2713-2722. DOI: 10.3390/ma6072713
- [47] Bobylev AG, Okuneva AD, Bobyleva LG, Fadeeva IS, Fadeev RS, Salmov NN, Podlubnaya ZA. Study of cytotoxicity of fullerene C-60 derivatives. *Biofizika*. 2012;**57**:746-750. DOI: 10.1134/S0006350912050041
- [48] Canape C, Foillard S, Bonafe R, Maiocchi A, Doris E. Comparative assessment of the in vitro toxicity of some functionalized carbon nanotubes and fullerenes. *RSC Advances*. 2015;**5**:68446-68453. DOI: 10.1039/C5RA11489F
- [49] Monticelli L, Salonen E, Ke PC, Vattulainen I. Effects of carbon nanoparticles on lipid membranes: A molecular simulation perspective. *Soft Matter*. 2009;**5**:4433-4445. DOI: 10.1039/B912310E
- [50] Mohandas N, Gallagher PG. Red cell membrane: Past, present, and future. *Blood*. 2008;**112**:3939-3948. DOI: 10.1182/blood-2008-07-161166
- [51] Grebowski J, Krokosz A, Puchala M. Membrane fluidity and activity of membrane ATPases in human erythrocytes under the influence of polyhydroxylated fullerene. *Biochimica et Biophysica Acta-Biomembranes*. 2013;**1828**:241-248. DOI: 10.1016/j.bbamem.2012.09.008

- [52] Pantarotto D, Singh R, McCarthy D, Erhardt M, Briand J-P, Prato M, Kostarelos K, Bianco A. Functionalized carbon nanotubes for plasmid DNA gene delivery. *Angewandte Chemie, International Edition*. 2004;**43**:5242-5246. DOI: 10.1002/anie.200460437
- [53] Dai H. Carbon nanotubes: Synthesis, integration, and properties. *Accounts of Chemical Research*. 2002;**35**:1035-1044. DOI: 10.1021/ar0101640
- [54] Prakash S, Kulamarva AG. Recent advances in drug delivery: Potential and limitations of carbon nanotubes. *Recent Patents on Drug Delivery & Formulation*. 2007;**1**:214-221. DOI: 10.2174/187221107782331601
- [55] Prato M, Kostarelos K, Bianco A. Functionalized carbon nanotubes in drug design and discovery. *Accounts of Chemical Research*. 2008;**41**:60-68. DOI: 10.1021/ar700089b
- [56] Mo Y, Wang H, Liu J, Lan Y, Guo R, Zhang Y, Xue W, Zhang Y. Controlled release and targeted delivery to cancer cells of doxorubicin from polysaccharide-functionalised single-walled carbon nanotubes. *Journal of Materials Chemistry B*. 2015;**3**:1846-1855. DOI: 10.1039/C4TB02123A
- [57] Madani SY, Naderi N, Dissanayake O, Tan A, Seifalian AM. A new era of cancer treatment: Carbon nanotubes as drug delivery tools. *International Journal of Nanomedicine*. 2011;**6**:2963-2979. DOI: 10.2147/ijn.s16923
- [58] Avti PK, Caparelli ED, Sitharaman B. Cytotoxicity, cytocompatibility, cell-labeling efficiency, and in vitro cellular magnetic resonance imaging of gadolinium-catalyzed single-walled carbon nanotubes. *Journal of Biomedical Materials Research. Part A*. 2013;**101**:3580-3591. DOI: 10.1002/jbm.a.34643
- [59] Arnold MS, Green AA, Hulvat JF, Stupp SI, Hersam MC. Sorting carbon nanotubes by electronic structure using density differentiation. *Nature Nanotechnology*. 2006;**1**:60-65. DOI: 10.1038/nnano.2006.52
- [60] Charlier J-C, Blase X, Roche S. Electronic and transport properties of nanotubes. *Reviews of Modern Physics*. 2007;**79**:677-732. DOI: 10.1103/RevModPhys.79.677
- [61] Zhang Y, Xu Y, Li Z, Chen T, Lantz SM, Howard PC, Paule MG, Slikker W, Watanabe F, Mustafa T, Biris AS, Ali SF. Mechanistic toxicity evaluation of uncoated and PEGylated single-walled carbon nanotubes in neuronal PC12 cells. *ACS Nano*. 2011;**5**:7020-7033. DOI: 10.1021/nn2016259
- [62] Mao H, Kawazoe N, Chen G. Uptake and intracellular distribution of collagen-functionalized single-walled carbon nanotubes. *Biomaterials*. 2013;**34**:2472-2479. DOI: 10.1016/j.biomaterials.2013.01.002
- [63] Wang X, Mansukhani ND, Guiney LM, Lee J-H, Li R, Sun B, Liao Y-P, Chang CH, Ji Z, Xia T, Hersam MC, Nel AE. Toxicological profiling of highly purified metallic and semiconducting single-walled carbon nanotubes in the rodent lung and *E. coli*. *ACS Nano*. 2016;**10**:6008-6019. DOI: 10.1021/acsnano.6b01560

- [64] Di Giorgio ML, Bucchianico, Di S, Ragnelli AM, Aimola P, Santucci S, Poma A. Effects of single and multi walled carbon nanotubes on macrophages: Cyto and genotoxicity and electron microscopy. *Mutation Research, Genetic Toxicology and Environmental Mutagenesis*. 2011;**722**:20-31. DOI: 10.1016/j.mrgentox.2011.02.008
- [65] Dresselhaus MS, Endo M. Relation of carbon nanotubes to other carbon materials. In: Dresselhaus A, Dresselhaus G, Avouris P, editors. *Handbook of Carbon Nanotubes Synthesis, Structure, Properties, and Applications*. Berlin, Heidelberg: Springer; 2001. pp. 11-28. DOI: 10.1007/3-540-39947-x_2
- [66] Datir SR, Das M, Singh RP, Jain S. Hyaluronate tethered, “smart” multiwalled carbon nanotubes for tumor-targeted delivery of doxorubicin. *Bioconjugate Chemistry*. 2012;**23**: 2201-2213. DOI: 10.1021/bc300248t
- [67] Das M, Datir SR, Singh RP, Jain S. Augmented anticancer activity of a targeted, intracellularly activatable, theranostic nanomedicine based on fluorescent and radiolabeled, methotrexate-folic acid-multiwalled carbon nanotube conjugate. *Molecular Pharmaceutics*. 2013; **10**:2543-2557. DOI: 10.1021/mp300701e
- [68] Arya N, Arora A, Vasu KS, Sood AK, Katti DS. Combination of single walled carbon nanotubes/graphene oxide with paclitaxel: A reactive oxygen species mediated synergism for treatment of lung cancer. *Nanoscale*. 2013;**5**:2818-2829. DOI: 10.1039/C3NR33190C
- [69] Bianco A, Kostarelos K, Prato M. Applications of carbon nanotubes in drug delivery. *Current Opinion in Chemical Biology*. 2005;**9**:674-679. DOI: 10.1016/j.cbpa.2005.10.005
- [70] Wu W, Wieckowski S, Pastorin G, Benincasa M, Klumpp C, Briand J-P, Gennaro R, Prato M, Bianco A. Targeted delivery of Amphotericin B to cells by using functionalized carbon nanotubes. *Angewandte Chemie, International Edition*. 2005;**44**:6358-6362. DOI: 10.1002/anie.200501613
- [71] Liu Z, Dong X, Song L, Zhang H, Liu L, Zhu D, Song C, Leng X. Carboxylation of multiwalled carbon nanotube enhanced its biocompatibility with L02 cells through decreased activation of mitochondrial apoptotic pathway. *Journal of Biomedical Materials Research Part A*. 2014;**102**:665-673. DOI: 10.1002/jbm.a.34729
- [72] De Paoli SH, Diduch LL, Tegegn TZ, Orecna M, Strader MB, Karnaukhova E, Bonevich JE, Holada K, Simak J. The effect of protein corona composition on the interaction of carbon nanotubes with human blood platelets. *Biomaterials*. 2014;**35**:6182-6194. DOI: 10.1016/j.biomaterials.2014.04.067
- [73] Wenrong Y, Pall T, Gooding JJ, Simon PR, Filip B. Carbon nanotubes for biological and biomedical applications. *Nanotechnology*. 2007;**18**:412001. DOI: 10.1088/0957-4484/18/41/412001
- [74] Heister E, Lamprecht C, Neves V, Tilmaciu C, Datas L, Flahaut E, Soula B, Hinterdorfer P, Coley HM, Silva SRP, McFadden J. Higher dispersion efficacy of functionalized carbon nanotubes in chemical and biological environments. *ACS Nano*. 2010;**4**:2615-2626. DOI: 10.1021/nn100069k

- [75] Smart SK, Cassady AI, Lu GQ, Martin DJ. The biocompatibility of carbon nanotubes. *Carbon*. 2006;**44**:1034-1047. DOI: 10.1016/j.carbon.2005.10.011
- [76] Meng L, Jiang A, Chen R, Li C, Wang L, Qu Y, Wang P, Zhao Y, Chen C. Inhibitory effects of multiwall carbon nanotubes with high iron impurity on viability and neuronal differentiation in cultured PC12 cells. *Toxicology*. 2013;**313**:49-58. DOI: 10.1016/j.tox.2012.11.011
- [77] Pescatori M, Bedognetti D, Venturelli E, Ménard-Moyon C, Bernardini C, Muresu E, Piana A, Maida G, Manetti R, Sgarrella F, Bianco A, Delogu LG. Functionalized carbon nanotubes as immunomodulator systems. *Biomaterials*. 2013;**34**:4395-4403. DOI: 10.1016/j.biomaterials.2013.02.052
- [78] Yin ZF, Wu L, Yang HG, Su YH. Recent progress in biomedical applications of titanium dioxide. *Physical Chemistry Chemical Physics (PCCP)*. 2013;**15**:4844-4858. DOI: 10.1039/c3cp43938k
- [79] Peters K, Unger RE, Kirkpatrick CJ, Gatti AM, Monari E. Effects of nano-scaled particles on endothelial cell function in vitro: Studies on viability, proliferation and inflammation. *Journal of Materials Science: Materials in Medicine*. 2004;**15**:321-325
- [80] Jin CY, Zhu BS, Wang XF, Lu QH. Cytotoxicity of titanium dioxide nanoparticles in mouse fibroblast cells. *Chemical Research in Toxicology*. 2008;**21**:1871-1877. DOI: 10.1021/tx800179f
- [81] Lai JCK, Lai MB, Jandhyam S, Dukhande VV, Bhushan A, Daniels CK, Leung SW. Exposure to titanium dioxide and other metallic oxide nanoparticles induces cytotoxicity on human neural cells and fibroblasts. *International Journal of Nanomedicine*. 2008;**3**:533-545. DOI: 10.2147/IJN.S3234
- [82] Park E-J, Yi J, Chung K-H, Ryu D-Y, Choi J, Park K. Oxidative stress and apoptosis induced by titanium dioxide nanoparticles in cultured BEAS-2B cells. *Toxicology Letters*. 2008;**180**:222-229. DOI: 10.1016/j.toxlet.2008.06.869
- [83] Okuda-Shimazaki J, Takaku S, Kanehira K, Sonezaki S, Taniguchi A. Effects of titanium dioxide nanoparticle aggregate size on gene expression. *International Journal of Molecular Sciences*. Jun. 2010;**11**:2383-2392. DOI: 10.3390/ijms11062383
- [84] Pujalté I, Passagne I, Brouillaud B, Tréguer M, Durand E, Ohayon-Courtès C, L'Azou B. Cytotoxicity and oxidative stress induced by different metallic nanoparticles on human kidney cells. *Particle and Fibre Toxicology*. 2011;**8**:10. DOI: 10.1186/1743-8977-8-10
- [85] Saquib Q, Al-Khedhairi AA, Siddiqui MA, Abou-Tarboush FM, Azam A, Musarrat J. Titanium dioxide nanoparticles induced cytotoxicity, oxidative stress and DNA damage in human amnion epithelial (WISH) cells. *Toxicology in Vitro*. 2012;**26**:351-361. DOI: 10.1016/j.tiv.2011.12.011
- [86] Magrez A, Horváth L, Smajda R, Salicio V, Pasquier N, Forró L, Schwaller B. Cellular toxicity of TiO₂-based nanofilaments. *ACS Nano*. 2009;**3**:2274-2280. DOI: 10.1021/nn9002067
- [87] Park EJ, Shim HW, Lee GH, Kim JH, Kim DW. Comparison of toxicity between the different-type TiO₂ nanowires *in vivo* and *in vitro*. *Archives of Toxicology*. 2013;**87**:1219-1230. DOI: 10.1007/s00204-013-1019-3

- [88] Vallee BL, Falchuk KH. The biochemical basis of zinc physiology. *Physiological Reviews*. 1993;**73**:79-105. DOI: 10.1152/physrev.1993.73.1.79
- [89] Shankar AH, Prasad AS. Zinc and immune function: The biological basis of altered resistance to infection. *American Journal of Clinical Nutrition*. 1998;**68**:447S-463S
- [90] Zhou J, Xu N, Wang ZL. Dissolving behavior and stability of ZnO wires in biofluids: A study on biodegradability and biocompatibility of ZnO nanostructures. *Advanced Materials*. 2006;**18**:2432-2435. DOI: 10.1002/adma.200600200
- [91] Wang ZL. Zinc oxide nanostructures: Growth, properties and applications. *Journal of Physics. Condensed Matter*. 2004;**16**:R829-R858. DOI: 10.1088/0953-8984/16/25/R01
- [92] Hanley C, Layne J, Punnoose A, Reddy KM, Coombs I, Coombs A, Feris K, Wingett D. Preferential killing of cancer cells and activated human T cells using ZnO nanoparticles. *Nanotechnology*. 2008;**19**:295103. DOI: 10.1088/0957-4484/19/29/295103
- [93] Javed Akhtar M, Ahamed M, Kumar S, Majeed Khan M, Ahmad J, Alrokayan SA. Zinc oxide nanoparticles selectively induce apoptosis in human cancer cells through reactive oxygen species. *International Journal of Nanomedicine*. 2012;**7**:845-857. DOI: 10.2147/IJN.S29129
- [94] Zhang H, Chen B, Jiang H, Wang C, Wang H, Wang X. A strategy for ZnO nanorod mediated multi-mode cancer treatment. *Biomaterials*. 2011;**32**:1906-1914. DOI: 10.1016/j.biomaterials.2010.11.027
- [95] Mitra S, Subia B, Patra P, Chandra S, Debnath N, Das S, Banerjee R, Kundu SC, Pramanik P, Goswami A. Porous ZnO nanorod for targeted delivery of doxorubicin: in vitro and *in vivo* response for therapeutic applications. *Journal of Materials Chemistry*. 2012;**22**:24145-24154. DOI: 10.1039/C2JM35013K
- [96] Hong H, Shi J, Yang Y, Zhang Y, Engle JW, Nickles RJ, Wang X, Cai W. Cancer-targeted optical imaging with fluorescent zinc oxide nanowires. *Nano Letters*. 2011;**11**:3744-3750. DOI: 10.1021/nl201782m
- [97] Peulon S, Lincot D. Mechanistic study of cathodic electrodeposition of zinc oxide and zinc hydroxychloride films from oxygenated aqueous zinc chloride solutions. *Journal of the Electrochemical Society*. 1998;**145**:864-874. DOI: 10.1149/1.1838359
- [98] Franklin NM, Rogers NJ, Apte SC, Batley GE, Gadd GE, Casey PS. Comparative toxicity of nanoparticulate ZnO, bulk ZnO, and ZnCl₂ to a freshwater microalga (*Pseudokirchneriella subcapitata*): The importance of particle solubility. *Environmental Science & Technology*. 2007;**41**:8484-8490. DOI: 10.1021/es071445r
- [99] Xia T, Kovoichich M, Liang M, Mädler L, Gilbert B, Shi H, Yeh JI, Zink JI, Nel AE. Comparison of the mechanism of toxicity of zinc oxide and cerium oxide nanoparticles based on dissolution and oxidative stress properties. *ACS Nano*. 2008;**2**:2121-2134. DOI: 10.1021/nn800511k
- [100] Vandebriel RJ, De Jong WH. A review of mammalian toxicity of ZnO nanoparticles. *Nanotechnology, Science and Applications*. 2012;**5**:61-71. DOI: 10.2147/NSA.S23932

- [101] Reddy KM, Feris K, Bell J, Wingett DG, Hanley C, Punnoose A. Selective toxicity of zinc oxide nanoparticles to prokaryotic and eukaryotic systems. *Applied Physics Letters*. 2007;**90**:213902-1–213902-3. DOI: 10.1063/1.2742324
- [102] Hanley C, Thurber A, Hanna C, Punnoose A, Zhang J, Wingett DG. The influences of cell type and ZnO nanoparticle size on immune cell cytotoxicity and cytokine induction. *Nanoscale Research Letters*. 2009;**4**:1409-1420. DOI: 10.1007/s11671-009-9413-8
- [103] Deng X, Luan Q, Chen W, Wang Y, Wu M, Zhang H, Jiao Z. Nanosized zinc oxide particles induce neural stem cell apoptosis. *Nanotechnology*. 2009;**20**:115101. DOI: 10.1088/0957-4484/20/11/115101
- [104] Premanathan M, Karthikeyan K, Jeyasubramanian K, Manivannan G. Selective toxicity of ZnO nanoparticles toward Gram-positive bacteria and cancer cells by apoptosis through lipid peroxidation. *Nanomedicine: Nanotechnology, Biology and Medicine*. 2011;**7**:184-192. DOI: 10.1016/j.nano.2010.10.001
- [105] Lane DP. Cancer p53, guardian of the genome. *Nature*. 1992;**358**:15-16. DOI: 10.1038/358015a0
- [106] Ng KW, Khoo SPK, Heng BC, Setyawati MI, Tan EC, Zhao XX, Xiong SJ, Fang WR, Leong DT, Loo JSC. The role of the tumor suppressor p53 pathway in the cellular DNA damage response to zinc oxide nanoparticles. *Biomaterials*. 2011;**32**:8218-8225. DOI: 10.1016/j.biomaterials.2011.07.036
- [107] Sharma V, Anderson D, Dhawan A. Zinc oxide nanoparticles induce oxidative DNA damage and ROS-triggered mitochondria mediated apoptosis in human liver cells (HepG2). *Apoptosis*. 2012;**17**:852-870. DOI: 10.1007/s10495-012-0705-6
- [108] Kao YY, Chiung YM, Chen YC, Cheng TJ, Liu PS. Zinc oxide nanoparticles interfere with zinc ion homeostasis to cause cytotoxicity. *Toxicological Sciences*. 2012;**125**:462-472. DOI: 10.1093/toxsci/kfr319
- [109] Othman BA, Greenwood C, Abuelela AF, Bharath AA, Chen S, Theodorou I, Douglas T, Uchida M, Ryan M, Merzaban JS, Porter AE. Correlative light-electron microscopy shows RGD-targeted ZnO nanoparticles dissolve in the intracellular environment of triple negative breast cancer cells and cause apoptosis with intratumor heterogeneity. *Advanced Healthcare Materials*. 2016;**5**:1310-1325. DOI: 10.1002/adhm.201501012
- [110] Li Z, Yang R, Yu M, Bai F, Li C, Wang ZL. Cellular level biocompatibility and biosafety of ZnO nanowires. *Journal of Physical Chemistry C*. 2008;**112**:20114-20117. DOI: 10.1021/jp808878p
- [111] Müller KH, Kulkarni J, Motskin M, Goode A, Winship P, Skepper JN, Ryan MP, Porter AE. pH-dependent toxicity of high aspect ratio ZnO nanowires in macrophages due to intracellular dissolution. *ACS Nano*. 2010;**4**:6767-6779. DOI: 10.1021/nn101192z
- [112] Gong C, Tao G, Yang L, Liu J, He H, Zhuang Z. The role of reactive oxygen species in silicon dioxide nanoparticle-induced cytotoxicity and DNA damage in HaCaT cells. *Molecular Biology Reports*. 2012;**39**:4915-4925. DOI: 10.1007/s11033-011-1287-z

- [113] Huan C, Shu-Qing S. Silicon nanoparticles: Preparation, properties, and applications. *Chinese Physics B*. 2014;**23**:88102. DOI: 10.1088/1674-1056/23/8/088102
- [114] Xing X, He X, Peng J, Wang K, Tan W. Uptake of silica-coated nanoparticles by HeLa cells. *Journal of Nanoscience and Nanotechnology*. 2005;**5**:1688-1693. DOI: 10.1166/jnn.2005.199
- [115] Yan L, Wang H, Zhang A, Zhao C, Chen Y, Li X. Bright and stable near-infrared pluronic-silica nanoparticles as contrast agents for *in vivo* optical imaging. *Journal of Materials Chemistry B*. 2016;**4**:5560-5566. DOI: 10.1039/C6TB01234E
- [116] Bahadar H, Maqbool F, Niaz K, Abdollahi M. Toxicity of nanoparticles and an overview of current experimental models. *Iranian Biomedical Journal*. 2016;**20**:1. DOI: 10.7508/ibj.2016.01.001
- [117] Lin W, Huang Y, Zhou X-D, Ma Y. *In vitro* toxicity of silica nanoparticles in human lung cancer cells. *Toxicology and Applied Pharmacology*. 2006;**217**:252-259. DOI: 10.1016/j.taap.2006.10.004
- [118] Li Y, Sun L, Jin M, Du Z, Liu X, Guo C, Li Y, Huang P, Sun Z. Size-dependent cytotoxicity of amorphous silica nanoparticles in human hepatoma HepG2 cells. *Toxicology in Vitro*. 2011;**25**:1343-1352. DOI: 10.1016/j.tiv.2011.05.003
- [119] Sahu D, Kannan GM, Tailang M, Vijayaraghavan R. *In vitro* cytotoxicity of nanoparticles: A comparison between particle size and cell type. *Journal of Nanoscience*. 2016;**2016**. DOI: 10.1155/2016/4023852
- [120] Zhu J, Liao L, Zhu L, Zhang P, Guo K, Kong J, Ji C, Liu B. Size -dependent cellular uptake efficiency, mechanism, and cytotoxicity of silica nanoparticles toward HeLa cells. *Talanta*. 2013;**107**:408-415. DOI: 10.1016/j.talanta.2013.01.037
- [121] Lu X, Qian J, Zhou H, Gan Q, Tang W, Lu J, Yuan Y, Liu C. *In vitro* cytotoxicity and induction of apoptosis by silica nanoparticles in human HepG2 hepatoma cells. *International Journal of Nanomedicine*. 2011;**6**:1889-1901. DOI: 10.2147/IJN.S24005
- [122] Ahmad J, Ahamed M, Akhtar MJ, Alrokayan SA, Siddiqui MA, Musarrat J, Al-Khedhairi AA. Apoptosis induction by silica nanoparticles mediated through reactive oxygen species in human liver cell line HepG2. *Toxicology and Applied Pharmacology*. 2012;**259**:160-168. DOI: 10.1016/j.taap.2011.12.020
- [123] Kim I-Y, Joachim E, Choi H, Kim K. Toxicity of silica nanoparticles depends on size, dose, and cell type. *Nanomedicine: Nanotechnology, Biology and Medicine*. 2015;**11**:1407-1416. DOI: 10.1016/j.nano.2015.03.004
- [124] Bhattacharjee S, Rietjens IMCM, Singh MP, Atkins TM, Purkait TK, Xu Z, Regli S, Shukaliak A, Clark RJ, Mitchell BS, Alink GM, Marcelis ATM, Fink MJ, Veinot JGC, Kauzlarich SM, Zuilhof H. Cytotoxicity of surface-functionalized silicon and germanium nanoparticles: The dominant role of surface charges. *Nanoscale*. 2013;**5**:4870. DOI: 10.1039/c3nr34266b

- [125] Park Y-H, Bae HC, Jang Y, Jeong SH, Lee HN, Ryu W-I, Yoo MG, Kim Y-R, Kim M-K, Lee JK. Effect of the size and surface charge of silica nanoparticles on cutaneous toxicity. *Molecular & Cellular Toxicology*. 2013;**9**:67-74. DOI: 10.1007/s13273-013-0010-7
- [126] Julien DC, Richardson CC, Beaux MF, McIlroy DN, Hill RA. *in vitro* proliferating cell models to study cytotoxicity of silica nanowires. *Nanomedicine: Nanotechnology, Biology and Medicine*. 2010;**6**:84-92. DOI: 10.1016/j.nano.2009.03.003
- [127] Peng F, Su Y, Wei X, Lu Y, Zhou Y, Zhong Y, Lee S, He Y. Silicon-nanowire-based nanocarriers with ultrahigh drug-loading capacity for *in vitro* and *in vivo* cancer therapy. *Angewandte Chemie, International Edition*. 2013;**52**:1457-1461. DOI: 10.1002/anie.201206737
- [128] Salata OV. Applications of nanoparticles in biology and medicine. *Journal of Nanobiotechnology*. 2004;**2**:3. DOI: 10.1186/1477-3155-2-3
- [129] Adili A, Crowe S, Beaux MF, Cantrell T, Shapiro PJ, McIlroy DN, Gustin KE. Differential cytotoxicity exhibited by silica nanowires and nanoparticles. *Nanotoxicology*. 2008;**2**:1-8. DOI: 10.1080/17435390701843769
- [130] Zhang W, Tong L, Yang C. Cellular binding and internalization of functionalized silicon nanowires. *Nano Letters*. 2012;**12**:1002-1006. DOI: 10.1021/nl204131n
- [131] Barroso MM. Quantum dots in cell biology. *Journal of Histochemistry and Cytochemistry*. 2011;**59**:237-251. DOI: 10.1369/0022155411398487
- [132] Kairdolf BA, Smith AM, Stokes TH, Wang MD, Young AN, Nie S. Semiconductor quantum dots for bioimaging and biodiagnostic applications. *Annual Review of Analytical Chemistry*. 2013;**6**:143-162. DOI: 10.1146/annurev-anchem-060908-155136
- [133] Du Y, Guo S. Chemically doped fluorescent carbon and graphene quantum dots for bioimaging, sensor, catalytic and photoelectronic applications. *Nanoscale*. 2016;**8**:2532-2543. DOI: 10.1039/C5NR07579C
- [134] Luo PG, Sahu S, Yang S-T, Sonkar SK, Wang J, Wang H, LeCroy GE, Cao L, Sun Y-P. Carbon "quantum" dots for optical bioimaging. *Journal of Materials Chemistry B*. 2013;**1**:2116-2127. DOI: 10.1039/C3TB00018D
- [135] Qian Z, Shan X, Chai L, Ma J, Chen J, Feng H. Si-doped carbon quantum dots: A facile and general preparation strategy, bioimaging application, and multifunctional sensor. *ACS Applied Materials & Interfaces*. 2014;**6**:6797-6805. DOI: 10.1021/am500403n
- [136] Wegner KD, Hildebrandt N. Quantum dots: Bright and versatile *in vitro* and *in vivo* fluorescence imaging biosensors. *Chemical Society Reviews*. 2015;**44**:4792-4834. DOI: 10.1039/C4CS00532E
- [137] Zhang J, Ma Y, Li N, Zhu J, Zhang T, Zhang W, Liu B. Preparation of graphene quantum dots and their application in cell imaging. *Journal of Nanomaterials*. 2016;**2016**. DOI: 10.3109/21691401.2015.1052468

- [138] Bajwa N, Mehra NK, Jain K, Jain NK. Pharmaceutical and biomedical applications of quantum dots. *Artificial Cells, Nanomedicine, Biotechnology*. 2016;**44**:758-768. DOI: 10.3109/21691401.2015.1052468
- [139] Zhou J, Yang Y, Zhang C. Toward biocompatible semiconductor quantum dots: From biosynthesis and bioconjugation to biomedical application. *Chemical Reviews*. 2015;**115**:11669-11717. DOI: 10.1021/acs.chemrev.5b00049
- [140] Tsoi KM, Dai Q, Alman BA, Chan WCW. Are quantum dots toxic? Exploring the discrepancy between cell culture and animal studies. *Accounts of Chemical Research*. 2012;**46**:662-671
- [141] Yong KT, Law W-C, Hu R, Ye L, Liu L, Swihart MT, Prasad PN. Nanotoxicity assessment of quantum dots: From cellular to primate studies. *Chemical Society Reviews*. 2013;**42**:1236-1250. DOI: 10.1039/C2CS35392J
- [142] Derfus AM, Chan WCW, Bhatia SN. Probing the cytotoxicity of semiconductor quantum dots. *Nano Letters*. 2004;**4**:11-18. DOI: 10.1039/C2CS35392J
- [143] Godt J, Scheidig F, Grosse-Siestrup C, Esche V, Brandenburg P, Reich A, Groneberg DA. The toxicity of cadmium and resulting hazards for human health. *Journal of Occupational Medicine and Toxicology*. 2006;**1**:21-22, 2006. DOI: 10.1186/1745-6673-1-22
- [144] Fellahi O, Sarma RK, Das MR, Saikia R, Marcon L, Coffinier Y, Hadjersi T, Maamache M, Boukherroub R. The antimicrobial effect of silicon nanowires decorated with silver and copper nanoparticles. *Nanotechnology*. 2013;**24**. DOI: 10.1088/0957-4484/24/49/495101
- [145] Chen N, He Y, Su Y, Li X, Huang Q, Wang H, Zhang X, Tai R, Fan C. The cytotoxicity of cadmium-based quantum dots. *Biomaterials*. 2012;**33**:1238-1244. DOI: 10.1016/j.biomaterials.2011.10.070
- [146] Soenen SJ, Manshian BB, Aubert T, Himmelreich U, Demeester J, De Smedt SC, Hens Z, and Braeckmans K. Cytotoxicity of cadmium-free quantum dots and their use in cell bioimaging. *Chemical Research in Toxicology*. 2014;**27**:1050-1059. DOI: 10.1021/tx5000975
- [147] Dinan NM, Atyabi F, Rouini M-R, Amini M, Golabchifar A-A, Dinarvand R. Doxorubicin loaded folate-targeted carbon nanotubes: Preparation, cellular internalization, in vitro cytotoxicity and disposition kinetic study in the isolated perfused rat liver. *Materials Science and Engineering*. 2014;**39**:47-55. DOI: <http://dx.doi.org/10.1016/j.msec.2014.01.055>

Edited by Tülay Aşkin Çelik

The book *Cytotoxicity* is aimed to be an essential reading to all medical students, biologists, biochemists and professionals involved in the field of toxicology. This book is a useful and ideal guide for novice researchers interested in learning research methods to study cytotoxic bioactive compounds. The parts of this book describe the replacement and different applications of the cytotoxic agents. All chapters are written by paramount experts in cytotoxicity research. This will hopefully stimulate more research initiatives, funding, and critical insight into the already increasing demand for cytotoxicity researches that have been evidenced worldwide.

Published in London, UK

© 2018 IntechOpen
© OLA Mishchenko / unplash

IntechOpen

